UDK 621.3:(53+54+621+66)(05)(497.1)=00 ISSN 0352-9045

INFORMACIJE MIDEM

Strokovno društvo za mikroelektroniko elektronske sestavne dele in materiale

4·2008

Strokovna revija za mikroelektroniko, elektronske sestavne dele in materiale
Journal of Microelectronics, Electronic Components and Materials

INFORMACIJE MIDEM, LETNIK 38, ŠT. 4(128), LJUBLJANA, december 2008

MIDEM 2008

UDK 621.3:(53+54+621+66)(05)(497.1)=00 ISSN 0352-9045

INFORMACIJE MIDEM 4 ○ 2008

INFORMACIJE MIDEM LETNIK 38, ŠT. 4(128), LJUBLJANA, DECEMBER 2008

INFORMACIJE MIDEM VOLUME 38, NO. 4(128), LJUBLJANA, DECEMBER 2008

Revija izhaja trimesečno (marec, junij, september, december). Izdaja strokovno društvo za mikroelektroniko, elektronske sestavne dele in materiale - MIDEM.
Published quarterly (march, june, september, december) by Society for Microelectronics, Electronic Components and Materials - MIDEM.

Naslov uredništva
Headquarters
Uredništvo Informacije MIDEM
MIDEM pri MIKROIKS
Stegne 11, 1521 Ljubljana, Slovenija
tel.: + 386 (0)1 51 33 768
faks: + 386 (0)1 51 33 771
e-pošta: Iztok.Sorli@guest.arnes.si
http://www.midem-drustvo.si/

Letna naročnina je 100 EUR, cena posamezne številke pa 25 EUR. Člani in sponzorji MIDEM prejemajo Informacije MIDEM brezplačno.
Annual subscription rate is EUR 100, separate issue is EUR 25. MIDEM members and Society sponsors receive Informacije MIDEM for free.

Znanstveni svet za tehnične vede je podal pozitivno mnenje o reviji kot znanstveno-strokovni reviji za mikroelektroniko, elektronske sestavne dele in materiale. Izdajo revije sofinancirajo ARRS in sponzorji društva.
Scientific Council for Technical Sciences of Slovene Research Agency has recognized Informacije MIDEM as scientific Journal for microelectronics, electronic components and materials.
Publishing of the Journal is financed by Slovene Research Agency and by Society sponsors.

Znanstveno-strokovne prispevke objavljene v Informacijah MIDEM zajemamo v podatkovne baze COBISS in INSPEC.

Prispevke iz revije zajema ISI® v naslednje svoje produkte: Sci Search®, Research Alert® in Materials Science Citation Index™

Scientific and professional papers published in Informacije MIDEM are assessed into COBISS and INSPEC databases.

The Journal is indexed by ISI® for Sci Search®, Research Alert® and Material Science Citation Index™

Po mnenju Ministrstva za informiranje št.23/300-92 šteje glasilo Informacije MIDEM med proizvode informativnega značaja.

Grafična priprava in tisk
Printed by
BIRO M, Ljubljana

Naklada
Circulation
1000 izvodov
1000 issues

Poštnina plačana pri pošti 1102 Ljubljana
Slovenia Taxe Percue

UDK621.3:(53+54+621+66), ISSN0352-9045 Informacije MIDEM 38(2008)4, Ljubljana

VSEBINA **CONTENT**

Obnovitev članstva v strokovnem društvu MIDEM in iz tega izhajajoče ugodnosti in obveznosti

Spoštovani,

V svojem več desetletij dolgem obstoju in delovanju smo si prizadevali narediti društvo privlačno in koristno vsem članom.Z delovanjem društva ste se srečali tudi vi in se odločili, da se v društvo včlanite. Življenske poti, zaposlitev in strokovno zanimanje pa se z leti spreminjajo, najrazličnejši dogodki, izzivi in odločitve so vas morda usmerili v povsem druga področja in vaš interes za delovanje ali članstvo v društvu se je z leti močno spremenil, morda izginil. Morda pa vas aktivnosti društva kljub temu še vedno zanimajo, če ne drugače, kot spomin na prijetne čase, ki smo jih skupaj preživeli. Spremenili so se tudi naslovi in način komuniciranja.

Ker je seznam članstva postal dolg, očitno pa je, da mnogi nekdanji člani nimajo več interesa za sodelovanje v društvu, se je Izvršilni odbor društva odločil, da stanje članstva uredi in **vas zato prosi, da izpolnite in nam pošljete obrazec priložen na koncu revije.**

Naj vas ponovno spomnimo na ugodnosti, ki izhajajo iz vašega članstva. Kot član strokovnega društva prejemate revijo »Informacije MIDEM«, povabljeni ste na strokovne konference, kjer lahko predstavite svoje raziskovalne in razvojne dosežke ali srečate stare znance in nove, povabljene predavatelje s področja, ki vas zanima. O svojih dosežkih in problemih lahko poročate v strokovni reviji, ki ima ugleden IMPACT faktor.S svojimi predlogi lahko usmerjate delovanje društva.

Vaša obveza je plačilo članarine 25 EUR na leto. Članarino lahko plačate na transakcijski račun društva pri A-banki : 051008010631192. Pri nakazilu ne pozabite navesti svojega imena!

Upamo, da vas delovanje društva še vedno zanima in da boste članstvo obnovili. Žal pa bomo morali dosedanje člane, ki članstva ne boste obnovili do konca leta 2009, brisati iz seznama članstva.

Prijavnice pošljite na naslov:

MIDEM pri MIKROIKS

Stegne 11

1521 Ljubljana

Ljubljana, december 2008

Izvršilni odbor društva

DEVELOPMENT OF LTCC-MATERIALS AND THEIR APPLICATIONS - AN OVERVIEW

Jaroslaw Kita, Ralf Moos

University of Bayreuth, Functional Materials Lab, Bayreuth, Germany

Key words: LTCC materials, Overview, Sintering, Thick Film Conductors, Applications

Abstract: The first Low Temperature Co-fired Ceramics (LTCC) tapes were developed more than thirty years ago. During the past decades, LTCC have spread around many different fields of application. This contribution gives an overview of the development of new materials used in combination with typical LTCC tapes, as well as on their application for new devices. Besides commercially offered materials like self-constrained tapes, high-k tapes or ferromagnetic tapes, newly developed LTCC compositions and their possible applications are presented and discussed.

Razvoj LTCC materialov in njihova uporaba - pregled

Kjučne besede: LTCC materiali, pregled, sintranje, debeloplastni prevodniki, uporaba

Izvleček: Keramika z nizko temperaturo žganja (LTCC - Low Temperature Co-fired Ceramics) je bila razvita pred več kot tridesetimi leti. V preteklih desetletjih se je njena uporaba razširila na mnoga področja. V tem prispevku podajamo pregled razvoja novih materialov, ki se uporabljajo v kombinaciji s tipičnimi LTCC folijami in aplikacije v novih napravah. Poleg komercialno dostopnih LTCC materialov, kot so na primer folije, ki se med žganjem ne krčijo, folije z visoko dielektričnostjo in feroelektrične folije bomo predstavili in opisali tudi aplikacije novih LTCC folij s posebnimi lastnostmi.

1 Introduction

The origin of LTCC development were needs of a multilayer technology comparable with already existed HTCC but at lower costs with possible application of high conductives that are well known from thick-film technology. Introduction of glass-ceramics compositions allowed decreasing of firing temperature and thus using almost all precious metal pastes (gold, silver, silver-platinum or silver- palladium). Due to cost issues, silver-based inks dominate.

During the past three decades, LTCC was expanded from rather small but profitable military and spacecraft markets into the radio frequency and automotive area. Moreover, besides already industry-established applications, new areas, most of them micro- or mesosystems were investigated. Flexibility and easy processing of unfired tapes as well as ability to construct three-dimensional ceramic devices in one single sintering process opened not only the door for new opportunities but also new requirements occurred.

The development of LTCC-technology can be described from different points of view. In this paper, three ways of LTCC development were considered. First and very important is the development of LTCC materials - tapes and pastes. Second, technological development like novel processing of tapes and pastes or joining of LTCC with other materials. And third, the development of LTCC applications besides radio-frequency applications, like different kind of physical and chemical sensors, chemical micro-reactors and others.

Detailed describing of above-mentioned kinds of LTCC developments would go beyond the scope of this paper. Nevertheless, we show you some, in our opinion, milestones in LTCC-development, a few very interesting ideas of LTCC applications, as well as some trends in R&D of LTCC.

2 Development of LTCC Materials and technology itself

Typical LTCC tapes mostly consist of glass-ceramics composites. Dependent on the ceramic powder content and the sintering mechanism, LTCC tapes can be divided into four groups /1/: "glass-free" ceramics (C), glass-bonded ceramics (GBC), glass ceramic composites (GCC) and glass ceramics (GC).

The low temperature sintering process is well known and well described in the literature (for example in /2/ or /3/. Typical for tape technology is the shrinkage of tapes during firing. The shrinkage differs dependent on material composition, lamination parameters, metallization coverage and firing parameters. For typical LTCC tapes, the shrinkage varies between 12-15% in x-y direction and 18-35% in z-direction. The shrinkage of the substrate, especially in x-y direction, can be disadvantageous for multilayer technology. Therefore, zero-shrinkage methods were introduced.

2.1 Zero-Shrinkage Process

Generally, it is not possible to avoid completely shrinkage of the tapes during firing, due to densification process and sintering viscosity /4/. At first, methods to join unfired LTCC and ceramics like Tape on Substrate (TOS) or LTCC-on-Metal (LTCC-M) have been introduced. These methods use classical LTCC tapes. The LTCC tapes are laminated on fired ceramics and the solid part prevents shrinking. Therefore, the ceramic part has to be bigger than the LTCC tapes.

In other words, these techniques describe ceramic elements with integrated LTCC, not LTCC structures itself. The newest of such system is called substrate-bonded tape system (SBTS) and was presented by ESL /5/. In the 1990's, the first zero-shrinkage method was introduced. Here, one should notice that not all methods called "zero-shrinkage" cause a zero-shrinking of the whole substrate. These methods are intended (and have been developed) for minimizing shrinking of the substrate in its plane directions.

2.1.1 PAS, PLAS

Pressure Less Assisted Sintering (PLAS) and Pressure Assisted Sintering (PAS) are very similar in use. To avoid shrinkage, in PLAS additional release tapes are introduced. Such release tapes consist of alumina and are laminated on the top and the bottom of the structure. During firing, the structure is "fixed" in x-y direction, since these sacrificial layers shrink at higher temperatures. After firing, the release layers are removed. This simple method has some disadvantages. First, it is impossible to print metallic layers on the top or bottom of the green sample - such elements can only deposited by post-firing. The zero-shrinkage effect is limited by thickness of the sample, i.e., if the sample contains more than 20 layers, the inner layers shrink like typical LTCC materials and some unwanted effects occur.

PAS means that the sample is fired in a special pressure furnace under a low uniaxial pressure, up to 50 kN /6/. Thus, the sample is fixed due to the applied pressure. Similar to PLAS, some shrinkage in homogeneities in z-direction can take place, but pressure adjusting can avoid it, even for samples with a higher number of layers.

Another advantage of PAS or PLAS is that almost all typical LTCC tapes can be used. The quality of zero-shrinkage effect (deformation and stress of structure, shrinkage anisotropy) depends on material chemistry, glass crystallization and microstructures /7/.

Both methods, originally proposed by DuPont have been established in industry a few years ago and at present almost all LTCC foundries offer PAS or PLAS for LTCC manufacturing.

2.1.2 Self-Constrained Sintering (SCS)

In spite of being in industrial application, both above-described methods have disadvantages. It is either technological limitation (PLAS) or additional expenses for new equipment (PAS). In 2002, Heraeus presented the self-constrained tape HL-2000 (a part of the so-called Heralock-System with Ag, Au and Ag/Pd conductors for co-firing) /8-10/. The SCS method requires neither special equipment nor additional release tapes. The self-constrained tape consists of three layers of different compositions. Both outer layers have the same chemical composition, whereas the inner layer, which serves as a locking layer or constraint layer, is different. It sinters at a higher temperature and therefore locks the compound. Laminating and firing conditions as well as electrical properties are very similar to classical LTCC tapes. The shrinkage is only about 0.2 % (shrinkage tolerance ± 0.02%) in x- and y-axes and 32 % in z-axis, respectively /1/. At present, Heralock is the only commercially available SCS system. In 2004, DuPont patented similar layer alignment with two primary layers and constraint layer inside /11/. This tape, however, is at the moment not commercially available. The constrained sintering of multilayer laminate with layers containing CaO-B_2O_3-SiO_2 glass and pure alumina has been reported as well. The x-shrinkage in this case was not as good as for HL2000, but, depending of alumina particles size, in the range of only 2.0% /12/.

2.2 Tapes for special purposes

One advantage of LTCC technology is its possibility to join tapes with different electrical properties. Very interesting are tapes with a high dielectric constant, e or *k* (high *k*-tapes) and ferroelectric tapes. The main issue in this respect is their compatibility with standard LTCC materials and the required low firing temperature below 1000C /13/.

2.2.1 High k-materials

Typical LTCC tapes have k-values in range of 5-9. This relatively low value is required in RF-applications to minimize parasitic capacitances and to increase signal speed. Although for the design of integrated capacitors this mentioned k-value is to low. In 2002, ESL brought a series of dielectric tapes with dielectric constant between 50-250 to the market (412xx-Series /14, 15/). It is an important feature that they can be joined with commercially available standard LTCC products of DuPont or Ferro. The dissipation factor is about 1% and temperature variations are comparable with X7R characteristics. From non-commercial products, different low-temperature tapes based on $CaZrO_3$-$CaTiO_3$ /16/, bismuth-titanate ceramics /17-21/ or zinc-titanate /22, 23/ were investigated. To decrease the firing temperature, different composition of lithium-borosilicate glasses were added to the dielectric composition. Middle dielectric constant compositions ($30 < k < 50$) were obtained with a low temperature coefficient (about 2 ppm/K /22/). Addition of zinc-borosilicate glasses to $BaTiO_3$ enabled to reduce the firing temperature down to 900 C with dielectric constant of about 1000 /19/.

2.2.2 Ferromagnetic materials

Ferroelectric tapes are generally used for buried inductors to increase the inductance of such structures and to save space. Here, ESL offers a magnetic tape with a permeability between 50 and 500. Its permeability value depends strongly on firing temperature. The highest permeability (μ = 1100) was achieved by firing at 1030 C /15/. Unfortunately, typical silver pastes cannot be used as coils material because due to the lower melting point of silver.

Other tested composites contain NiZn ferrites with a permeability of 500 /24/. To lower their sintering temperature, small amounts of AgO were added. Another group reported on tapes of hexaferrites of $BaFe_{12}O_{19}$ /25/ that are compatible with standard LTCC. Low firing temperature was obtained by adding reactive glasses. Here, however a much lower permeability of only about 20 was achieved.

2.3 Photoimageable pastes on LTCC

Thick-film photoimageable conductor and dielectric pastes on alumina have been known for many years (Fodel System from DuPont or KQ-Series from Heraeus) /26/. In the 1990's DuPont introduced Fodel pastes for LTCC /27/. First, silver pastes were presented followed in 2000 by a family of resistor pastes /28/. The advantage of this product is that the photolithographic process can be carried out on unfired materials. In contrast to typical photo-lithography, developing of the structure occurs with environmental friendly 1% Na_2CO_3 solution. At the moment, the minimum line width and space distance is between 30 - 40 µm for conductors /29-30/. First investigations on Fodel microresistors showed that it is possible to produce 50x50 μm^2 resistors with only a small dependence of the sheet resistance on resistor length providing also a good long-term stability /31-32/.

2.4 Development of technological processes

New applications require new technological processes. In the past years, a few achievements in the field of LTCC technology were reported. Here, in our opinion, interesting and promising are advances in laser patterning, construction of channels with the aid of fugitive layers or with by photolithography and integration of fired ceramic materials into unfired LTCC structures.

2.4.1. Laser structuring and application thereof

Structuring of LTCC tapes with laser is not new, but in the last years, new laser machines were introduced bringing improved resolution und repeatability in this field. Typically, for structuring of fired ceramics as well as for green tapes, CO_2-lasers were used. Such lasers can be characterized by a relatively large laser spot diameter and a high laser power. The typical Nd:YAG laser with a wavelength of 1064 nm was used in thick-film technology for resistors trimming. Cutting of ceramics was impossible in this case due to the very low absorption coefficient at this wavelength. However, it was possible to use standard Nd:YAG lasers to structure unfired LTCC tapes /33/. The cut quality was quite good, but in the case of very small structures far from perfection. The application of frequency-tripled Nd:YAG (355 nm) sources with a laser beam diameter of 20 µm could increase resolution and could minimize structure dimensions. Thus, it was possible to cut 50 µm channels in unfired tapes or vias with diameters of 50 µm /34/.

In the case of hot-plate gas sensors, hot-plate beams were as narrow as 260 µm /35/. Another laser application can be the construction of microcapacitors /36/, inductors /37/ and microresistors /38/.

2.4.2. Constructing of channels

The construction of channels in LTCC structures is a suggesting and relatively easy task. The tapes are cut prior to the lamination process. After stacking, lamination, and firing, a three-dimensional channel structure is created. The key-issue by the channel construction (especially by wide channels and cavities) is the sagging of top layers during lamination and/or during the firing processes. To avoid this phenomenon, different methods were proposed. The most popular one is to fill channels or cavities with graphite or carbon black /39-41/. Thus, flat membranes (up to 10 mm diameter) can be fabricated using a ne-sized graphite powder. However, in case of closed channels the depletion of air to oxidize the graphite and the lack of degassing can cause problems with the flatness of such elements.

Another possibility of small channel construction (down to 20 µm wide) is etching of partially fired LTCC ceramics /42/. Here, Riston foil (DuPont) is laminated on a partially fired LTCC structure and after exposure and developing, a channel structure is etched in HF-solution. After etching, the LTCC structure is finally stacked and fired.

2.4.3. Integration of fired ceramics into unfired LTCC structure

Electrical and thermal properties of LTCC tapes are, for some applications, not suitable. Therefore, a method to integrate a ceramic substrate with other thermal and/or electrical properties as standard LTCC tape was proposed /43/.

Generally, such elements are added (joined with the aid of adhesives or glasses) after firing the structure, because of the shrinkage of typical LTCC material. The introduction of mentioned SCS-tapes allowed joining of fired alumina prior firing of LTCC. Additional joining layers should improve adhesion and stability. Small modifications of this method enable integration of aluminum nitride or zirconia ceramics /44/.

3. Innovative LTCC applications

At the very beginning, LTCC applications were rather limited to military and spacecraft area. Due to excellent high frequency properties (low dielectric constant and low dissipation factor), LTCC materials found place in RF-frequency applications. Good thermal and mechanical stability extended the LTCC application area into the automotive sector.

The mentioned areas of LTCC applications are at present standard for LTCC technology. However, in the past ten years new LTCC applications emerged. This includes gas

sensors /45-49/, physical sensors (pressure, force, temperature, etc.) /50-58/, chemical and biochemical devices /59-64/, fluidic structures with mixer and pumps /65-70/ and three-dimensional structures for different purposes /71-73/.

LTCC ceramics are very often used in applications where thermal treatment (heating) is necessary and therefore materials like FR4 or glass cannot be used. In contrast, LTCC technology allows integration of stable heaters and heating of the structure up to 700 C.

The increase of applications is also observed in wide considered bio-applications due to chemical stability, possibility of integration of conductive materials (electrodes) and easy structuring of unfired LTCC materials.

4 Conclusions - Future of LTCC Technology

In this paper, an overview over the development of LTCC technology during the past years is given. It is almost impossible to present all novel LTCC materials and devices in such a short summary. Nevertheless, in our opinion the presented examples can give a good impression on recent progresses in LTCC technology. A growing number of reported applications confirm the advantages of LTCC as well as that LTCC can be applied not only in RF-applications but is also suitable to be used in the microsystems field as well.

The progress in the material development eliminated the barriers and limitations of the first LTCC tapes. The Possibility of fine material processing allows creating small and reliable LTCC parts.

Here should be emphasized that LTCC cannot compete with mass product technologies like PCB. LTCC was not developed for this and nobody thought that LTCC would compete with PCB or polymer techniques, because generally ceramic technologies are expensive (materials high temperature processes, technology park, etc).

Nevertheless, the future of LTCC seems to be very promising, especially in areas where stability and reliability are important. Therefore, next LTCC applications should focus on areas, where using of low-cost materials is prohibitively impossible because of thermal, mechanical or chemical requirements. Thus, LTCC can achieve not really a big but a really profitable market niche.

References

/1/ Rabe T., Schiller W.A., Hochheimer T., Modes C., Kipka A., Zero Shrinkage of LTCC by Self-Constrained Sintering, Int. J. Appl. Ceram. Technol., 2, 2005, p. 374-382, doi: 10.1111/j.1744-7402.2005.02038.x,

/2/ Valant M., Suvorov D., Pullar R.C., Kumaravinothan Sarma, McN. Alford N., A mechanism for low-temperature sintering, J. Europ. Cer. Soc., 26, 2006, pp. 2777-2783, doi:10.1016/j.jeurceramsoc.2005.06. 026

/3/ Kemethmüller S., Hagymasi M., Stiegelschmitt A., Roosen A., Viscous Flow as the Driving Force for the Densification of Low-Temperature Co-Fired Ceramics, J. Am. Ceram. Soc., 90, 2007, p. 64-70, doi: 10.1111/j.1551-2916.2006.01362.x

/4/ Mohanram A., Messing, G.L. Green D.J., Densification and Sintering Viscosity of Low-Temperature Co-Fired Ceramics, J. Am. Cer. Soc., 88, 2005, p. 2681-2689, doi: 10.1111/j.1551-2916.2005.00497.x

/5/ Wahlers R.L., Feingold A.H., Heinz M., Lead Free, Zero Shrink, Substrate Bonded LTCC System, Proc. Int. Symp. On Microel. IMAPS, USA

/6/ Hintz M., Thust H., Polzer E., Generic investigation on 0 - shrinkage processed LTCC, Proc. IMAPS Nordic, Stockholm 2002, p. 243-249

/7/ Mohanram A., Lee S.-H., Messing, G.L. Green D.J.,Green, Constrained Sintering of Low-Temperature Co-Fired Ceramics, J. Am. Cer. Soc., 89, 2006, pp. 1923-1929, doi: 10.1111/j.1551-2916.2006.01079.x

/8/ Barnwell P., Amaya E., Lautzenhiser, F., Wood J., HeraLock TM 2000 Self-constrained LTCC Tape -Benefits and Application, Proc. IMAPS Nordic, Stockholm 2002, pp. 250-256.

/9/ Lautzenhiser F., Amaya E., Hochheimer T.J., Self-constrained low temperature glass-ceramic unfired tape for microelectronics and method for making and using the same, US Patent Application 2003/0087136A1.

/10/ Lautzenhiser F., Amaya E., Barnwell P., Wood J., Microwave module design with Heralock HL2000 LTCC, Proc. 35th International Symposium on Microelectronics, IMAPS 2002, Denver, Colorado, pp. 285-291.

/11/ Tape Composition and Process for Internally Constrained Sintering of Low-Temperature Co-Fired Ceramic, US Patent Application 2004/6776861B1

/12/ Liao C., Jean J., Hung Y., Self-Constrained Sintering of a Multilayer Low-Temperature-Cofired Glass-Ceramics /Alumina Laminate, J. Am. Cer. Soc., 4, 2007, p. 1-4,

/13/ Jantunen H., Hu T., Uusimäki A., Leppävuori S., Tape casting of ferroelectric, dielectric, piezoelectric and ferromagnetic materials, J. Europ. Cer. Soc., 24, 2004, p. 1077-1081, doi:10.1016/S0955-2219(03) 00552-1

/14/ Feingold A.H., Heinz M., Wahlers R.L., Stein M.A., Compliant Dielectric and Magnetic Materials for buried Components, Proc. Int. Symp. On Microel. IMAPS, Denver, USA, 2002

/15/ Feingold A.H. Heinz M., Wahlers R.L., Stein M.A., Materials for Capacitive and Inductive Components Integrated with Commercially Available LTCC Systems, Proc. Int. Symp. On Microel. IMAPS Israel Chapter, 2003

/16/ Choi Y., Park J.-H., Park J.-H., Park J.-G., Middle-permittivity LTCC dielectric compositions with adjustable temperature coefficient, Mat. Let., 58, 2004, p. 3102-3106, doi:10.1016/j.matlet.2004.05. 049

/17/ Choi Y., Park J., Ko W., Park J.-W., Nahm S., Park J.-G., Low Temperature Sintering of $BaTi_4O_9$-Based Middle-k Dielectric Compo-sition for LTCC Applications, J. Electrocer., 14, 2005, p. 157-162,

/18/ Choi Y., Park J.-H., Park J.-H., Nahm S., Park J.-G., Middle- and high-permittivity dielectric compositions for low-temperature co-fired ceramics, J Europ. Cer. Soc., 27, 2007, p. 2017-2024, doi:10.1016/j. jeurceramsoc.2006.05.104

/19/ Hsiang H.-I, Hsi C.-S., Huang C.-C., Shen-Li Fu, Sintering behavior and dielectric properties of $BaTiO_3$ ceramics with glass addition for internal capacitor of LTCC, J. Alloys and Comp., 459, 2008, p. 307-310

/20/ Zou D., Zhang Q., Yang H., Li S., Low temperature sintering and microwave dielectric properties of $Ba_2Ti_3Nb_4O_{18}$ ceramics for LTCC applications, J. Europ. Cer. Soc., 28, 2008, p. 2777-2782, doi:10. 1016/j.jeurceramsoc.2008. 04.021

/21/ Higuchi Y., Sugimoto Y., Harada J., Tamura H., LTCC system with new high-e_r and high-Q material co-fired with conventional

low-ε_r base material for wireless communications, J. Europ. Cer. Soc., 27, 2007, p. 2785-2788, doi:10.1016/ j.jeurceramsoc.2006.11.048

/22/ Zhang Q.L., Yang H., Zou J.L., Wang H.P, Sintering and microwave dielectric properties of LTCC-zinc titanate multilayers, Mat. Letters, 59, 2005, p. 880-884, doi:10.1016/j.matlet.2004. 11.036

/23/ Yue Z., Yan J., Zhao F., Gui Z., Li L., Low-temperature sintering and microwave dielectric properties of $ZnTiO_3$-based LTCC materials, J. Electrocer. online, 2007, doi:10.1007/s10832-007-9096-4,

/24/ Hong S.H., Park J.H., Choa Y.H, Kim J., Magnetic properties and sintering characteristics of NiZn(Ag, Cu) ferrite for LTCC applications, J. Magnetism and Magnetic Mat., 290-291, 2005, p. 1559-1562, doi:10. 1016/j.jmmm.2004. 11.242,

/25/ Matz R., Götsch D., Karmazin D., Männer R. Siessegger B., Low temperature cofirable MnZn ferrite for power electronic applications, J. Electrocer. online, 2007, doi:10.1007/s10832-007-9334-9

/26/ Karmazin R., Dernovsek O., Ilkov N., Wersing W., Roosen A., Hagymasi M., New LTCC-hexaferrites by using reaction bonded glass ceramics, J. Europ. Cer. Soc., 25, 2005, p. 2029-2032, doi:10.1016/j. jeurceramsoc.2005.03.064

/27/ Weng Y.L., Ollivier P.J., Skurski M.A., Photoformed thick Im materials and their application to ne feature Circuitry, Proc. of the 2000 Int. Conf. on High-Density Interc. and System Packag., Denver, 2000, p. 579-84

/28/ Skurski M.A., Smith M.A., Draudt R.R., Amey D.I., Horowitz M.J., Champ M.J., Photoimageable Silver Cofireable Conductor Compatible With 951 Green TapeTM, Proc. Proc. Int. Symp. On Microel. IMAPS, San Diego, USA 1998,

/29/ Bacher R.J., Wang Y.L., Skurski M.A., Crumpton J.C., Nair K.M., Next Generation Ceramic Multilayer Systems, Proc. Int. Symp. On Microel. IMAPS 2000, Boston, USA

/30/ Kautio K., Properties of High Definition Photoimaged Conductors in LTCC, Proc. 38th IMAPS Nordic 2002 Conference, Stockholm, p. 227-232,

/31/ Weber J., Röthlingshöfer W., Goebel U., Innovative Anwendungen der LTCC-Technologie im Automobilbau, Conf. „Folien- und Multilayer-technologie", 10. April 2003, Berlin (in German),

/32/ Dziedzic A. et al. Electrical and stability properties and ultrasonic microscope characterisation of low temp-erature co-red resistors, Microelectr. Reliab., 2001, 41, p. 669-76

/33/ Dziedzic A., Rebenklau L., Golonka L.J., Wolter K.-J., Fodel microresistors--processing and basic electrical properties, Microelec. Rel., 43, 2003, p. 377-383, doi:10.1016/S0026-2714(02) 00346-3

/34/ Kita J., Dziedzic A., Golonka L.J., Non-conventional Application of Laser in Thick-film Technology - Preliminary Results, Proc. 23rd International Spring Seminar on Electronics Technology ISEE'2000, Balatonfüred, Hungary, pp. 219-223,

/35/ Gollner E., Kita J., Moos R., Frequency-tripled Nd:YAG-laser in thick-film and LTTC applications, Proc. XXX Int. Conf. IMAPS Poland Chapter, Krakow, Poland, 2006, p.147-152

/36/ Kita J., Rettig F., Moos R., Drüe K.-H., Thust H., Hot Plate Gas Sensors – Are Ceramics Better?, Int. J. Appl. Cer. Techn., 2, 2005, p. 383-389, doi: 10.1111/ j.1744-7402.2005.02037.x

/37/ Miś E., Dziedzic A., Piasecki T., Kita J., Moos R., Geometrical, electrical and stability properties of thick-Im and LTCC microcapacitors, Microel. International, 25, 2008, p. 37-41

/38/ Bąk M., Dudek M., Dziedzic A., Kita J., Chosen electrical and stability properties of laser-shaped thick-film and LTCC inductors, Proc. ESTC 2008 Conference (will be published)

/39/ Nowak D., Józenków T., Dziedzic A., Kita J., Miniaturization of Thick-Film and LTCC Resistors by Laser-Shaping, Proc. IMAPS-CPMT Conference, Pultusk, Poland, 2008 (will be published)

/40/ Birol H., Maeder T., Ryser P., Processing of Graphite-Based Sacrificial Layer for Microfabrication of Low Temperature Co-fired Ceramics (LTCC), Sens. and Act. A, 130-131, 2006, p. 560-567

/41/ Birol H., Maeder T., Ryser P., Application of graphite-based sacrificial layers for fabrication of LTCC (low temperature co-fired ceramic) membranes and micro-channels, J. Micromech. Microeng., 17, 2007, p. 50-60

/42/ Espinoza-Vallejos P., Zhong, J., Gongora-Rubio M., Sola-Laguna L., Santiago-Aviles J., The Measurement and Control of Sagging in Meso electromechanical LTCC Structures and Systems, Proc. Mat. Research Soc. Symp., Warrendale, USA, 1998, p. 73-79

/43/ Espinoza-Vallejos P., Santiago-Aviles J., Photolitho-graphic Feature Fabrication of LTCC, Int. J. Microcirc. and Electron. Packag., 23, 2000, p.286-9

/44/ Moos R. Kita J., Integration von bereits gebrannten Substratkeramikem mit LTCC-Folien, DE Patent Application 2006, DE102006021432A1,

/45/ Kita J., Rettig F., Moos R., Integration of Fired Ceramics on LTCC Structures - Feasibility Study, Proc. EMPS 2006, 4th Europ. Microel. and Packag. Symp., Terme Catez, Slovenia, 2006, p.51-55

/46/ Teterycz H., Kita J., Bauer, R. Golonka L.J., Licznerski B.W., Nitsch K., Wisniewski K., New design of an SnO_2 gas sensor on low temperature cofiring ceramics, Sens. and Act. B, 47, 1998, p. 100-103, doi:10.1016/S0925-4005(98)00008-2

/47/ Rettig F., Moos R., Ceramic meso hot-plates for gas sensors, Sensors and Actuators B: Chemical, 103, 2004, p. 91-97, doi:10.1016/j.snb.2004.04. 040

/48/ Bansky J., Pietrikova A., Urbancik J., Unconventional Application of Low Temperature Co-fired Ceramics in Thick-Film Gas Sensors, Proc. Int. Symp. On Microel. IMAPS Poland Chapter, Polanczyk, 2001

/49/ Kita J., Dziedzic A., Friedel K., Golonka L.J., Janus P., Szeloch R., Surface temperature distribution analysis in sensors with buried heater made in LTCC technology, Proc. 13th European Microel. & Pack. Conf., Strasbourg (France), 2001, p. 123-128

/50/ Pisarkiewicz T., Sutor A., Maziarz W., Thust H., Thelemann T., Thin Film Gas Sensor on Low Temperature Co-fired Ceramics, Proc. European Microelectronics Packaging and Interconnection Symposium, Prague 2000, p. 399-403

/51/ Slosarcik S., Zivcak J., Bauer R., Molcanyi T., Gmiterko A., Mracik M., Podprocky T., Pressure Sensor in LTCC Multilayer Technology for Medical Application, Proc. 22nd Int. Spring Sem. On Electron. Technol., Dresden, Germany, 1993, p.111-115

/52/ Khanna P. K., Hornbostel B., Grimme R., Schäfer W., Dorner J., Miniature pressure sensor and micromachined actuator structure based on low-temperature-cofired ceramics and piezoelectric material, Mat. Chemistry and Physics, 87, 2004, p. 173-178, doi:10.1016/ j.matchemphys.2004.05.021

/53/ Meijerink M.G.H., Nieuwkoop E., Veninga E.P., Meuwissen M.H.H., Tijdink M.W.W.J., Capacitive pressure sensor in post-processing on LTCC substrates, Sens. and Act. A, 123-124, 2005, p. 234-239, doi:10.1016/j.sna.2005.04.026

/54/ Hrovat M., Belavic D., Bencan A., Bernard J., Holc J., Cilensek J., Smetana W., Homolka H., Reicher R., Golonka L., Dziedzic A., Kita J., Thick-film resistors on various substrates as sensing elements for strain-gauge applications, Sens. and Act. A, 107, 2003, p. 261-272, doi:10.1016/j.sna.2003.07.003

/55/ Lynch H., Park J., Espinoza-Valejos P.A., Santiago-Aviles J.J., Sola-Laguna L., Meso-Scale Pressure Trasducer Utilizing Low Temperature Co-Fired Ceramic Tapes, Proc. Int. Symp. On Microel. IMAPS, USA

/56/ Golonka L.J., Dziedzic, Roguszczak H., Tankiewicz S., Terech D., Novel technological and constructional solutions of pressure sensors made in LTCC technology, Proc. of SPIE, 2000, vol. 4516, p.10-14,

/57/ Birol H., Maeder T., Nadzeyka I., Boers M., Ryser P., Fabrication of a millinewton force sensor using low temperature co-fired ceramic (LTCC) technology, Sens. and Act. A, 134, 2007, p. 334-338, doi:10.1016/j.sna.2006.05.025

/58/ Hrovat M., Belavič D., Kita J., Cilenšek J., Golonka L., Dziedzic A., Thick-film temperature sensors on alumina and LTCC substrates, J. Europ. Cer. Soc., 25, 2005, pp. 3443-3450, doi:10.1016/j.jeurceramsoc.2004.09. 027

/59/ Hrovat M., Belavič D., Kita J., Holc J., Cilenšek J., Golonka L., A. Dziedzic, Thick-film PTC thermistors and LTCC structures: The dependence of the electrical and microstructural characteristics on the firing temperature, J. Europ. Cer. Soc., 27, 2007, pp. 2237-2243, doi:10.1016/j.jeurceramsoc.2006.08.005

/60/ Martínez-Cisneros C.S., Ibáñez-García N., Valdés F., Alonso J., LTCC microflow analyzers with monolithic integration of thermal control, Sens. and Act. A, 138, 2007, p. 63-70, doi:10.1016/ j.sna.2007. 04.059

/61/ Goldbach M., Axthelm H., Keusgen M., LTCC-based microchips for the electrochemical detection of phenolic compounds, Sens. and Act. B, 120, 2006, p. 346-351, doi:10.1016/j.snb. 2006.01.047

/62/ Wang X., Zhu J., Bau H., Gorte R.J, Fabrication of Micro-Reactors Using Tape-Casting Methods, Cat. Letters, 77, 2001, p. 173-177, doi: 10.1023/ A:1013236306883

/63/ Baker A., Lanagan M., Randall C., Semouchkina E., Semouchkin G., Rajab K.Z., Eitel R., Mittra R., Rhee S., Geggier, P. Duschl C., Fuhr G., Integration Concepts for the Fabrication of LTCC Structures, Int. J. Appl. Cer. Techn., 2, 2005, p. 514-520, doi:10. 1111/j.1744-7402.2005.02052.x

/64/ Achmann S., Hämmerle M., Kita J., Moos R., Miniaturized Low Temperature Co-red Ceramics (LTCC) Biosensor for Amperometric Gas Sensing, Sens. And Act. B, 2008, *in Press*, doi:10.1016/ j.snb.2008.07.024

/65/ Gongora-Rubio M.R., Kofuji S.T., Seabra A.C. Hernandez E., Simoes E.W., Fontes M., Verdonck P., LTCC Sensors for Environmental Monitoring System, Proc. Ceram. Intercon. and Ceram. Packag. Conf. CICMT 2005

/66/ Chaudhary A., van Amerom F.H.W., Short R.T., Bhansali S., Fabrication and testing of a miniature cylindrical ion trap mass spectrometer constructed from low temperature co-fired ceramics, International J. Mass Spectr., 251, 2006, p. 32-39, doi:10.1016/j. ijms.2005.12.013

/67/ Jihua Zhong, Mingqiang Yi, Haim H. Bau, Magneto hydrodynamic (MHD) pump fabricated with ceramic tapes, Sens. and Act. A, 96, 2002, p. 59-66, doi:10.1016/S0924-4247(01)00764-6

/68/ Aguilar Z. P., Arumugam P., Fritsch I., Study of magnetohydrodynamic driven flow through LTCC channel with self-contained electrodes, J. Electroanal. Chem., 591, 2006, p. 201-209, doi:10.1016/j. jelechem.2006.04.019

/69/ Santiago-Aviles J.J., Gongora-Rubio M., Espinoza-Vallejos P., Sola-Laguna L., Sensors, Actuators and Other Non-Packaging Applications of LTCC Tapes, Proc. Ceram. Intercon. & Ceram. Packag. Conf. CICMT, Denver, USA, 2004, p. 07-12

/70/ Gongora-Rubio M., Sola-Laguna L. Smith M., Santiago-Aviles J.J., A Meso-scale Electromagneti-cally Actuated Normally Closed Valve Realized on LTCC Technology, Proc. of SPIE, Conf. on Microfluidic Device and Systems II, Santa Clara, USA, 1999, vol. SPIE 3877, pp. 230-239,

/71/ Rebenklau L., Wolter K.-J., Howitz S., Realization of Hybrid Microfluidic Systems Using Standard LTCC Process, Proc. 50th ECTC IEEE Conf., Las Vegas, USA, 2000, p. 1696-1700,

/72/ Peterson K.A., Rohde S.B., Walker C.A., Patel K.D., Turner T.S., Nordquist C.D., Microsystem Integration with new Techniques in LTCC, Proc. Ceram. Interconn. and Ceram. Packag. Conf. CICMT - Baltimore, 2004

/73/ Li J., Ananthasuresh G.K., Three-dimensional Low-Temperature Co-fired Ceramic Shells for Miniature System Applications, J. Micromech. Microeng., 12, 2002, p. 198-203

Jaroslaw Kita, Ralf Moos
University of Bayreuth, Functional Materials Lab
Universitätsstr. 30, D-95447 Bayreuth, Germany
E-mail: Jaroslaw.Kita@Uni-Bayreuth.de

Prispelo (Arrived): 17.09.2008 *Sprejeto (Accepted): 15.12.2008*

UDK621.3:(53+54+621+66), ISSN0352-9045 Informacije MIDEM 38(2008)4, Ljubljana

SILICON PHOTOMULTIPLIER: A NOVEL TYPE OF PHOTO-DETECTOR WITH SINGLE PHOTON DETECTION CAPABILITY

Giorgio Umberto Pignatel

Dept. of Electronic and Information Engineering DIEI, Perugia, Italy

Key words: silicon photomultiplier, single photon, avalanche breakdown, Geiger mode, photodetector

Abstract: Silicon Photo-Multiplier (SiPM) is a novel type of avalanche photon detector which operates in Geiger mode. It allows great advancement in photon detection and is a good candidate for replacing traditional photomultiplier tubes (PMTs). In this paper the current status of development of a research project founded by the Italian National Institute for Nuclear Physics (INFN) will be presented, in the framework of the DASIPM collaboration which involves several Universities and the Center for Scientific and Technological Research (FBKirst, Trento, Italy). Recent advancements in SIPM technology will be presented, along with some preliminary results and a discussion about possible exploitations in medical and astroparticle physics applications.

Silicijeva fotopomnoževalka: nov tip fotodetektorja s sposobnostjo detekcije posameznega fotona

Kjučne besede: silicijeva fotopomnoževalka, posamezni foton, plazoviti preboj, Geigerjev način, fotodetektor

Izvleček: Silicijeva fotopomnoževalka (SiPM) je nov tip plazovitega prebojnega fotodetektorja, ki deluje v Geigerjevem načinu. Nova fotopomnoževalka predstavlja velik napredek pri detekciji fotona in je dober kandidat za nadomestitev tradicionalne fotomultiplikacijske cevi (PMT). V prispevku bo predstavljen trenutni položaj na projektu, ki je podprt od Italijanskega nacionalnega instituta za nuklearno fiziko (INFN) v okviru sodelovanja DASIPM, ki vključuje nekatere univerze ter Center za znanstvene in tehnološke raziskave (FBKirst, Trento, Italy). Predstavljeni bodo novi dosežki na področju SIPM tehnologije, skupaj z nekaterimi preliminarnimi rezultati ter obravnavo možnih aplikacij v medicini in astrofiziki.

1 Introduction

Efficient detectors for low-light level (LLL) and photon counting applications are today required in a large variety of fields including astroparticle physics, nuclear medicine and high-energy physics. For such experiments, photon detectors typically employed are vacuum photon detectors, i.e., photomultiplier tubes—PMT, micro-channel plate photo-multipliers—MCP, hybrid photodetectors—HPD /1-3/. The main advantages of such devices are high internal gain (10^6–10^7), very good timing resolution (tens or hundreds of ps) and good single photoelectron resolution. However, these devices have low quantum efficiency limited by the photocathode materials, high operation voltages, they are sensitive to magnetic fields and the vacuum technology used for their fabrication confers them a bulky shape and sensitivity to handling.

The search for new photon detectors which can over-come the drawbacks of vacuum photon detectors has lead to the development of solid state photon detectors (PN or PIN photodiodes, avalanche photodiodes—APD and avalanche photodiodes operating in linear Geiger-mode—GAPD or SPAD) /4, 5/. These solid-state devices have important advantages over the vacuum ones, namely higher quantum efficiency, lower operation voltages, insensitivity to the magnetic fields and robustness and compactness. The step-by-step evolution of solid-state photon detectors was mainly determined by their internal gain: a PIN has no gain, an APD has a gain of few hundreds and the GAPD gain is 10^5–10^6. A gain comparable with that of the vacuum photon detectors allowed the GAPD to achieve single-photon sensitivity and to be used in LLL applications (~10^7 photons/mm^2/sec).

Essentially, a GAPD is a p–n junction that operates above the breakdown voltage. At this bias, the electric field is so high that a single charge carrier injected into the depletion layer can trigger a selfsustaining avalanche (so-called Geiger breakdown). The Geiger breakdown mechanism in avalanche diodes was studied several years ago /6, 7/ and important progresses on suitable quenching circuits al. /8/. However, a GAPD has the disadvantage that it acts as a binary device, having a standardized output signal independent of the number of incident photons. A new structure called Silicon Photo- /9–10/ overcome this inherent limitation bringing together on the same substrate many micro-cells connected in parallel, in which each micro-cell is a GAPD in series with its integrated quenching resistor. Therefore, the SiPM acts as an analog device with an output signal representing the sum of the signals from all fired micro-cells and it becomes a suitable solid-state device for LLL detection and photon counting applications, including the detection of the space radiation in astroparticle physics, medical imaging in nuclear medicine, and calorimetry in high-energy physics /11, 12/.

At the beginning of 2005, within collaboration between the Italian National Institute for Nuclear Physics (INFN) and the Center for Scientific and Technological Research of Trento, Italy (FBK-irst), a 3-year project aimed at the development of silicon photomultipliers was launched. Within

this project, the role of FBK-irst was the technological development and the electrical characterization of silicon photomultipliers, whereas the role of INFN was mainly focused on the application of such devices, with special emphasis on Calorimetry, time-of-flight (TOF) measurements, and PositronEmission Tomography (PET).

In this paper the FBK-irst activity in developingand producing SiPMs will be reviewed, and theongoing activity of the DASIPM collaboration /13/:"Development and Applications of Silicon Photo-Multipliers" - which involves the Universities ofPisa, Perugia, Trento, Bologna and Bari - will bereported.

2 Detector description

Fig.1 shows the picture of a SiPM device. It is composed by a matrix of 25x25 photo-diode cells with an area of 40x40 μm^2 covering a surface of 1x1mm^2. The device is realized on a low-resistivityp+-type substrate (500μm thick).

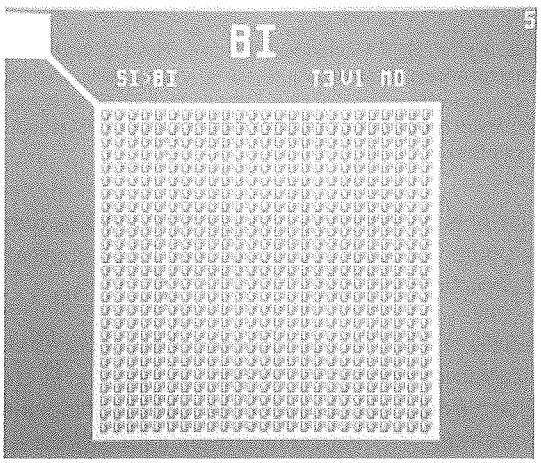

Fig. 1: Photograph of the first prototype of SiPMfrom FBK-irst.

The structure of each diode consists of an asymmetric shallow junction (n+p) implanted in a thin (~4μm) lowly doped p-type epitaxial layer. The junction is created by an Arsenic implantation and is located at about 100nm from the top silicon surface.The breakdown voltage value is fixed by a further Boron implantation. The doping profiles and the dielectric layers deposited on the silicon surface are designed to enhance the photon-detection efficiency in the short wavelength region (420-450nm) /14/. It must be emphasized that each micro-pixel has about 6Pm wide dead area along the edges which is needed to accommodate the structures for the reduction of the lateral fields (guard rings) and for the electrooptical isolation (V-groove, fig.2).

A simple equivalent circuit of the SiPM is shownin fig.3. A reverse bias voltage (Vbias) is applied to all junctions through the common substrate electrode to deplete the epi-layer and the induced current is read on the resistor side electrode.

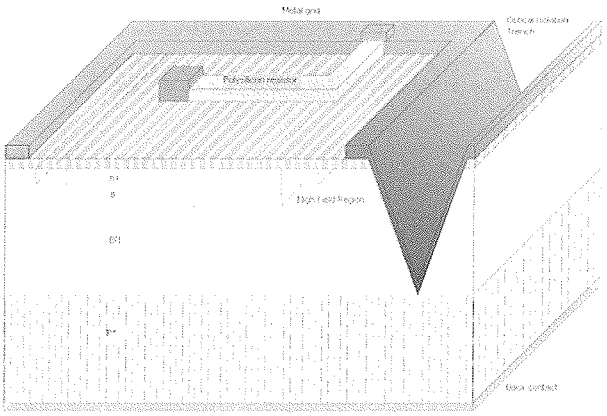

Fig. 2: Schematic of a single GAPD cell.

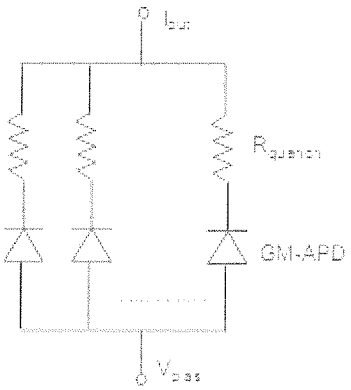

Fig. 3: Simplified equivalent circuit of a SiPM.

2.1 Principle of operation

When the diodes are biased (VB) at few volts above breakdown (VBD) the electric field in the junction region is so high that any carrier, generated either thermally or by photons and drifted in that region, may trigger a self-sustaining avalanche breakdown. While a swift current pulse grows to a macroscopic level in a very short time (~500ps) it flows through a series resistor RQ which limits the current to about 10μA and develops a voltage drop which quenches the avalanche by reducing the bias voltage. Thereafter the original over-voltage ($\Delta V=V_B-V_{DB}$) isexponentially recovered within a time constant $R_Q x C_D$. At room temperature the rate of thermally generated carriers is of the order of 0.1-1.0MHz/mm2 (dark-count rate) and that represents the limitin gfactor (noise level) of the device.

3 Detector characterization

This section reports the characterization of the single micro-pixel. It is divided in two parts describing the static and the dynamic functional characteristics, respectively.

3.1 Static Characterization

Several information concerning the behavior of the SiPM can be inferred from static I-V measurements

3.1.1 Forward characteristic

The forward I-V characteristic of a single micro-cellor a whole SiPM allows us to extract the value of the quenching resistor RQ.

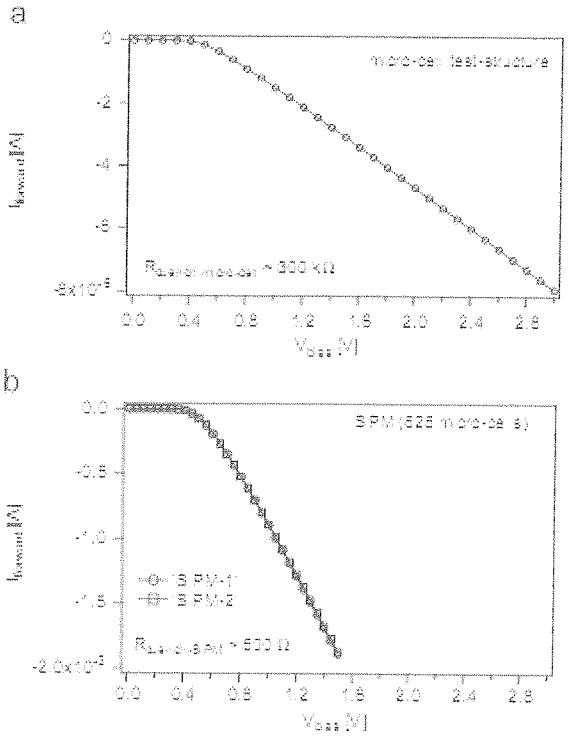

Fig. 4. I-V forward characteristics of (a) a single micro-cell test structure and (b) two SiP

For example, for the device reported in fig.1, the value of the quenching resistor extracted from the forward characteristics of the micro-cell test structure is of 300kΩ, whereas for the SiPM a value of ~500Ω has been determined (see Figs. 4a and 4b), in good agreement with the expected value (RSiPM =Rmicro-cell / Nmicro-cell, with Nmicro-cell=625)/14/.

Measurements have been repeated on a statistically meaningful number of devices on each wafer, showing a very good uniformity of the resistance values and confirming the reliability of the polysilicon technology used for the Rquench fabrication.

3.1.2 Reverse characteristic

The reverse characteristic contains precious information on the functionality of the SiPM. First of all, the breakdown voltage can be extracted. Forexample, in fig.5 /15/ it is clearly visible that V_{BD} is about 31V, with a uniformity which has been estimated to be within ±0.5V from SiPM to SiPM, inspite of the fact that the reverse current above V_{BD} can differ by a factor of about 10 from pixel-to-pixel, as reported in fig.6.

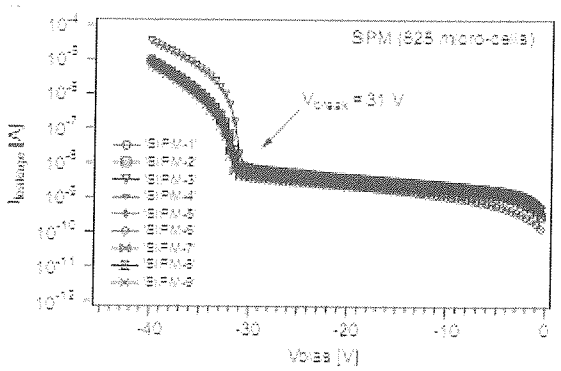

Fig. 5. Reverse I-V characteristics of 9 SiPM taken from the same wafer.

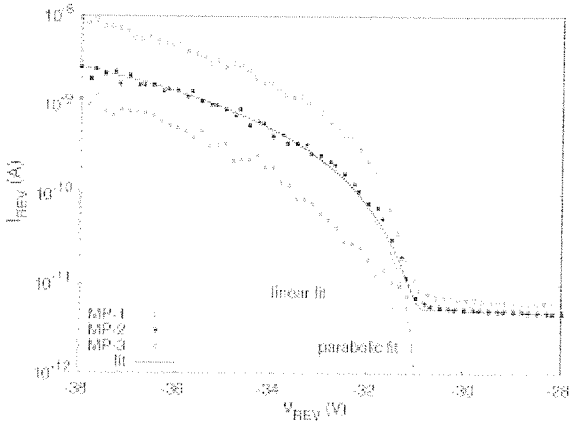

Fig. 6. Close view of the I-V reverse characteristic of a SiPM around breakdown. The reverse current of two micro-pixels multiplied by 625 is shown as well.

Concerning the current level below the breakdown, that is determined by the carriers generated both in the bulk as well as on the surface of the depleted region around the junction. Fortunately, the latter do not contribute to the dark-count rate, as it is orders of magnitude lower than that predicted by the measured current level.

Concerning the current behavior above breakdown, it is interesting to note that it follows a parabolic law up to voltages of several Volts above breakdown. This behavior can be explained considering that the DC current flowing through the GAPD in this region (above breakdown) is given by the average charge generated from spontaneous (thermally generated) breakdown in 1s. In an ideal device, this value is given by the charge contained in one pulse (Q) timesthe number of pulses per second (dark count rate).

$$I_{DC} = Q \times DCR$$

The first term represents the gain $G = Q/e$ of the GAPD since it is the number of carriers generated by a single carrier triggering the avalanche. The I-V curve is parabolic because, as it will be shown in thefollowing sections, both the gain and the dark countrate grow linearly with the bias voltage.

3.2 Dynamic Characterization

The signal coming from the micro-pixel is expected to show a very fast leading edge, determined both by the avalanche spreading and by the discharge of the diode capacitance C_D through the series resistance R_S (which includes the resistance of the neutral region of the semiconductor and the space-charge of the avalanche junction), and a slow exponential decay, determined by the time constant

$$\tau = R_Q \times C_D$$

C_D can be estimated from the geometry of the microcell applying the parallel-plate capacitance equation. Considering a 4μm thick epitaxial layer and a device area of 40x40μm, an indicative value is 50fF/pixel gives a recovery time constant of 17ns. A slightly longer recovery time can be expected, taking into account the parasitic capacitance CQ of the polysilicon quenching resistor which lies on top of the photo-diode area.

3.2.1 Dark pulse measurements

Several information on the dynamic characteristic of a SiPM can be inferred from simple dark pulse measurements.

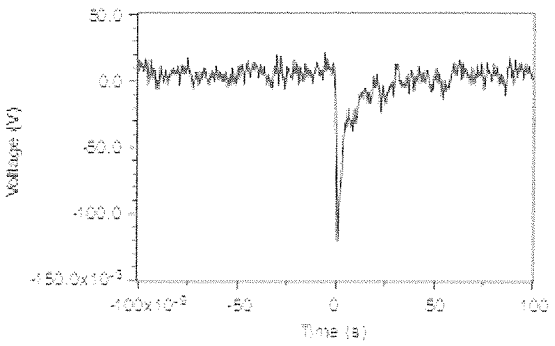

Fig. 7. Dark pulse from a SiPM micro-cell biased at 4V above V_{break}.

Fig.7 shows a typical dark pulse measured with a wide-band digital oscilloscope. A rise time of less than 1ns and a recovery time constant of a 20ns demonstrate the fast timing characteristics of the SiPM signal. The total recovery time, defined as the time needed to recharge the diode to 99% of the bias voltage, is about 80ns, and this parameter determines the maximum allowed photon counting rate.

3.2.2 SiPM's Gain

The Geiger signal from one pixel is determined by the charge ($Q_{PIXEL} = C_{PIXEL} \times \Delta V$) accumulated in the pixel capacitance CD biased at an overvoltage:

$$\Delta V = V_{BIAS} - V_{BD}$$

The overvoltage is of the order of few Volts and C_{pixel} is typically 50fF; so Q_{pixel} is of the order of 150fC or 10^6 electrons. One pixel signal on 50Ω load resistor corresponds to a pulse amplitude of ~ 1mV which can be detected by a wide-band oscilloscopeeven without a preamplifier near the detector. A direct measurement of Q_{pixel} can be obtained integrating the pulse signal.

Fig.8 shows the *spectra* obtained integrating the pulses reported in Fig.7 for an integration time of 100ns (which includes the whole signal) at different bias voltages.

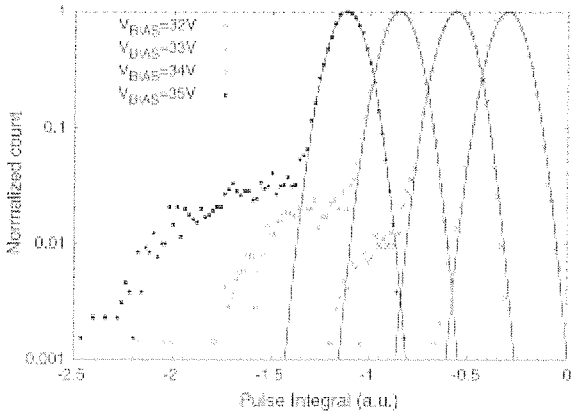

Fig. 8. Spectra of the signal charge (integration time 100ns) at four bias voltages.

Each distribution has a dominant peak that can be very well fitted by a Gaussian distribution. The centroid of the Gaussian is the most probable charge generated in one pulse and grows linearly with the bias voltage, in contrast to the exponential voltage dependence of the gain of APDs. The variance of the Gaussian is determined by two contributions: the noise introduced by the read-out system and the fluctuations of the GAPD gain. The tail in thedistribution of Fig.8 is due to multiple events which occur in the 100ns integration time.

The linear dependence of the gain with bias voltage is clearly visible in Fig.9 showing the charge expressed in number of carriers as a function of the bias voltage along with a linear fit.

The intercept with the x-axis corresponds very well to the breakdown voltage value that was previously extracted from the I-V characteristics. The slope is proportional to the capacitance of the micro-cell, which, as expected, is about 50 fF.

3.2.3 After pulsing

The pulse reported in Fig.7 represents the ideal case in which a single event is detected in the observation time slot. In practice, while acquiring a SiPM signal, there is a certain probability that a secondary pulse is emitted after a short time. This phenomenon is called "after-pulsing" and is attributed to the release of carriers which have beentrapped in the band-gap of the semiconductor during the main avalanche, and which are re-emitted after a characteristic decay time, and then can trigger a second breakdown /16/

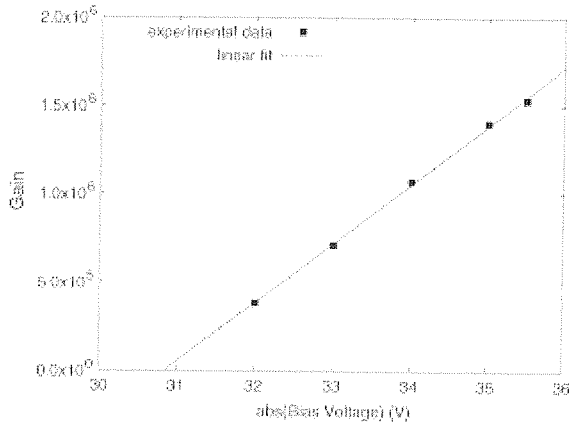

Fig. 9. Gain of the GAPD as a function of the bias voltage.

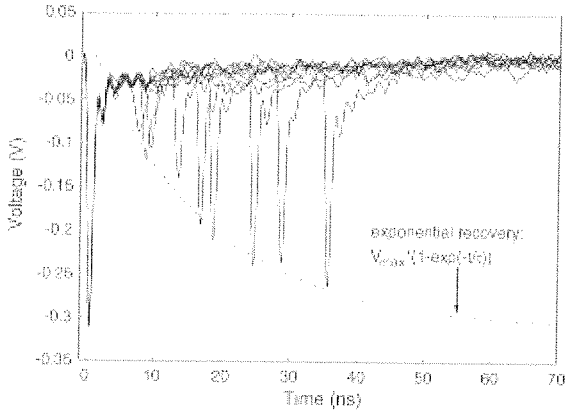

Fig. 10. Collection of pulses presenting an after-pulse event (V_{bias} = 35V).

A collection of such events is reported in fig.10/15/. The main pulses are exactly overlaid at time 0, whereas the secondary pulses are randomly distributed after the primary. The height of the second pulse depends on the relative position (intime) with respect to the first one, because the diode voltage is still slowly increasing towards V_{BIAS} andconsequently the gain changes according to the plot in Fig.9. It is interesting to note that, from the convolution of the secondary pulse peak (dashed line), a recovery time constant consistent with the previously reported $R_Q C_D$ can be extracted.

3.2.4 Cross-talk

Another contribution to the "noise" of a SiPM is cross-talk. Since a SiPM is composed of hundreds (or even thousands) of pixels, there is a certain probability that an avalanche breakdown generated in one pixel can trigger the avalanche in another, adjacent pixel. It has been shown /17/ that this phenomenon is due to infrared optical photons which are emitted during the main avalanche and reach the adjacent pixels not only in the horizontal plain, but also by reflection from the back side of the device. The emission probability of optical photons from hot carriers in an avalanche breakdown was estimated tobe $3x10^{-5}$ /16/; therefore, it can be argued that a 30 optical photons are emitted per pulse with a gain of 10^6. An optical cross-talk coefficient $K_{2/1}$ can be defined as the probability for a second pixel to be-fired. It has been shown that this coefficient is linearly dependent on the gain and can vary from a few per cent up to 35% /18/. Since the velocity of optical photons in Silicon is ~ 100μm/ps, the optical cross-talk is seen at the output of a SiPM as a single pulse with amplitude 2x, 3x, ...etc.

Fig.11 is an example of the output signal from a SiPM which exhibits single pulses, after-pulses, and cross-talk.

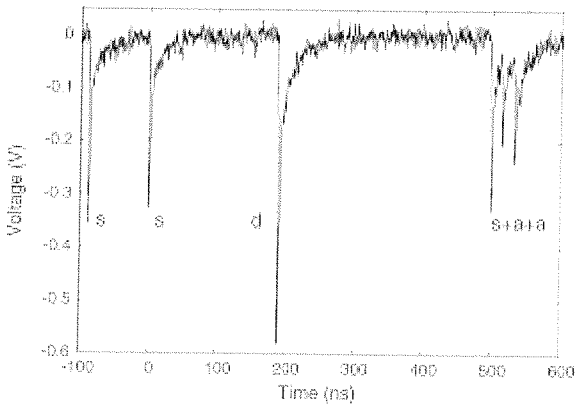

Fig.11. Output signal from a SiPM presenting single pulses (s), double pulses (d), and after-pulses (a).

The cross-talk effect is visible as a tail in the spectra of a signal charge, as reported in Fig.8. From inspection of fig.8 it can be argued that, for FBK-irst SiPMs, the cross-talk is less than 5%.

3.2.5 Dark Count Rate

The dark count rate can be measured either with a digital oscilloscope with counting capability, or with a counter inserted after a pulse-height discriminator. Due to the short rise time of the pulses and to their good stability, it is not necessary to use a constant fraction discriminator.

Fig.12 shows the measurement of a SiPM dark count rate as a function of pulse amplitude (threshold level) at room temperature.

The dark count rate for a threshold of 1 photoelectron (p.e.) level varies between 1 and 3MHz for ΔV values from 1.5 to 3.5V. At 3 p.e. level the dark count is just few kHz at ΔV=1.5V and ~1 kHz at 3.5 V.

That means that DCR is a limiting factor for single photon detection, but not for low-light level illumination, when the number of hitting photons is > 3 or 4.

4 SiPM parameters

The performance of a Silicon Photomultiplier is affected by two important parameters: photon detection efficiency (PDE) and Linearity (dynamic range).

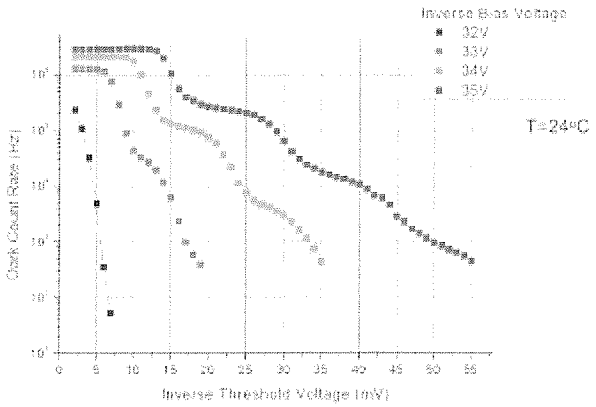

Fig.12. SiPM dark count rate as a function of puls eamplitude (threshold) for different bias voltages.

4.1 Photon detection efficiency – PDE

PDE can be defined as the probability that an incident photon generates a useful output signal. The detection efficiency of a SiPM is given by the product of 3 terms: the quantum efficiency (QE), the probability to initiate an avalanche breakdown (Pa),and the geometrical - or fill - factor (GF).

$$PDE = QE(\lambda) \times Pa(V) \times GF$$

4.1.1 Quantum efficiency – QE(λ)

The quantum efficiency represents the probability for a photon to generate an e-h pair. It is given by the product of 2 factors: the transmittance of the dielectric layer on top of the silicon surface and the intrinsic silicon QE. Both are wavelength dependent. The former can be maximized by implementing an anti-reflective coating (ARC). The second represents the probability for a photon that has crossed the dielectric layer to generate an e-h pair in the active area of the device. In a conventional n+/p/p+ diode, the active layer is roughly limited on top by the undepleted n+ doped layer, whereas on the bottom it is limited by the p+ layer used for the ohmic contactor by the highly doped substrate in case of epitaxial substrates. Indeed, when a pair is generated in those regions, there is a high probability for electrons andholes to recombine by means of Auger or Shockley-Read-Hall (SRH) processes. For short wavelengths, the problem is focused in the top layer. As an example, a 420nm light is almost totally absorbed in the first 500nm of silicon, which, for non-optimized fabrication processes, is usually well inside the undepleted layer.

4.1.2 Avalanche probability – Pa(V)

There is a finite probability that a carrier swept or generated within the space-charge region triggers an avalanche breakdown. In case of a photon generated event, 2 carriers are created travelling in opposite directions. Both contribute to the triggering probability as:

$$Pa = Pe + Ph - PePh$$

where Pe and Ph are the electron and hole avalanche initiation probabilities respectively /19, 20/. These terms depend on the impact ionization coefficients of electrons (α) and holes (β) which are strongly dependent upon the electric field (applied bias voltage). The ionization coefficient for electrons is higher than that for holes (e.g., at $5x10^5$V/cm, α is about twice than β)

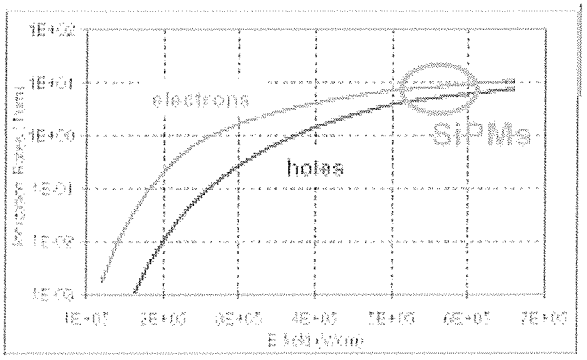

Fig.13. Ionization rates of electrons and holes in silicon /Grant SSE 16, 1973/.

4.1.3 Geometric factor – GF

The ratio between the active area and the total area of the device is a critical issue in SiPMs. The reason is that each GAPD cell is surrounded by a dead region determined by the guard ring and the structure preventing optical cross-talk. Considering that the area of a cell can be very small (of the order of 30x30μm^2) even few microns of dead region around the cell have a detrimental effect on the geometrical efficiency. Presently, the fill factor of FBK-irst SiPM is limited to 0.2-0.33 for cell areas ranging from 30x30μm^2 to 50x50μm^2.

As an example, the PDE of a SiPM with fill factor=0.2 is reported in fig.13 /21/.

The PDE dependence on the bias voltage has to be attributed to the avalanche initiation probability. The dependence on the light wavelength is a mixed contribution from Pa and QE. To separate the two contributions the quantum efficiency of some diodes extracted from the same wafers, which have the same anti-reflecting coating and doping profiles have been measured (see fig.15 from ref /21/).

It is worth while noting that in a conventional n+/p/p+ device structure, there is more chance that the avalanche breakdown is initiated by electrons at long wavelength, and by holes at short wavelength, as the photon absorption length in silicon ranges from 0.01μm to few μm for wavelengths 300nm<λ<700 nm.

4.2 Dynamic range & Linearity

In principle, the dynamic range of a SiPM is equal to the number of micro-pixels contained in a macrocell. Howev-

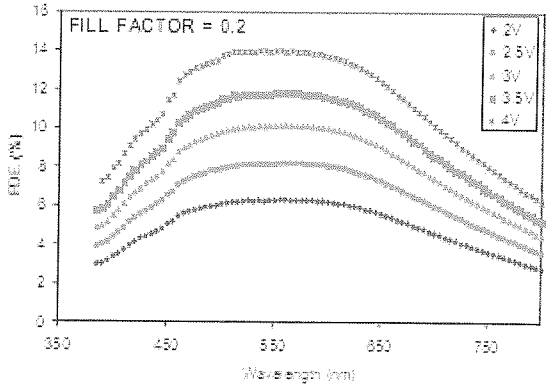

Fig.14. PDE vs wavelength of a SiPM measured at different over-voltages: from 2V to 4V.

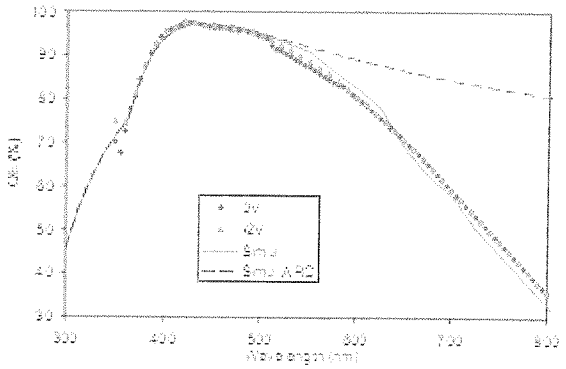

Fig. 15. QE vs wavelength of a 1mm² diode having the same doping profiles and anti-reflecting coating of the SiPM

er, the output signal amplitude is proportional to the number of incident photons only if each micro-cell is hit by a single photon during the recovery time of the micro-cell. When the number of photons increases, there is a certain probability that two or more photons hit the same cell, thus producing the same signal. It can be shown that the dependence of the SiPM signal (N_{SiPM}) on the number of incident photons (N_{ph}) follows a Poisson distribution:

$$N_{SiPM} = N_{cells}\left[1-\exp\left(\frac{N_{ph}\times PDE}{N_{cells}}\right)\right]$$

where N_{cells} is the total number of cells of the SiPM. Fig.15 shows the saturation effect measured on 5FBK-irst SiPMs /22a/.

The linearity of the SiPM response is crucial for energy calibration when the SiPM is coupled to a scintillator which exhibit high light yield (thousands of photons) or long decay time (hundred of ns).

4.3 Temperature dependence

The temperature dependence of the gain of a SiPMis related to the leakage current and the dark count rate of the detector:

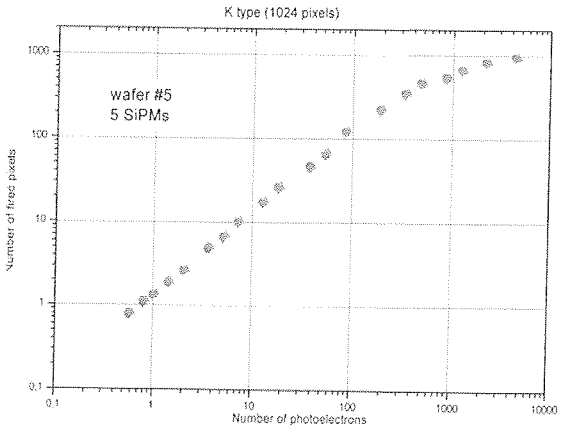

Fig. 16. Non-linear output saturation of 1024 pixel /1.0 mm² FBK-irst SiPMs as a function of incident photon number /22a/

$$G(T) = \frac{I_{leak}(T)}{e\times DCR(T)}$$

where e is the electron charge and I_{leak} is the rms dark current. A picture of such dependence is reported in fig.16 /23/. It has been shown that the gain is linear with the over voltage (V_{OV}) independently of the temperature. However, if the bias voltage is kept constant, an effective variation of the gain is observed, as reported in fig.17, due to the fact that the breakdown voltage changes:

$V_{OV}(T) = V_{BIAS} - V_{BD}(T)$

For a pure avalanche process /5,6/, the temperature dependence of the breakdown voltage can be approximated as:

$$V_{BD}(T) = V_{BDO}[1 + \beta(T - T_O)]$$

where V_{BDO} is the breakdown voltage at room temperature (T_O) and β is a linear coefficient.

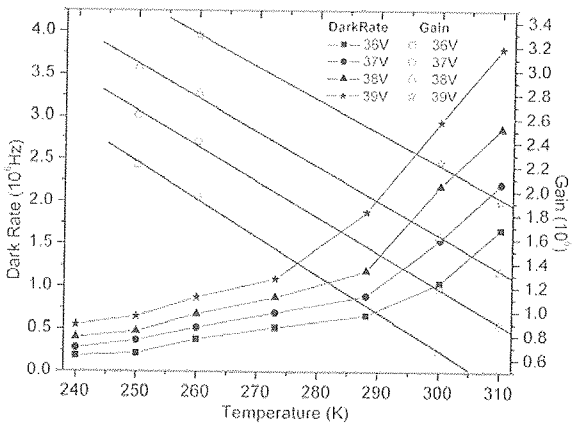

Fig. 17. SiPM gain and dark rate as a function of temperature.

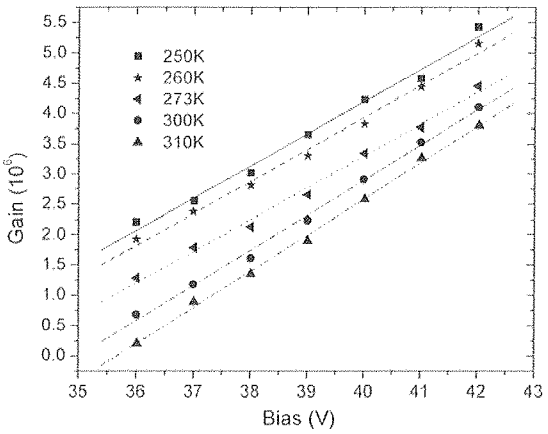

Fig. 18. SiPM gain as a function the bias voltage at different operating temperatures.

For the samples reported in fig.19 this model fit the experimental data for β equal to 2 ± 0.06810^{-3} K^{-1}.

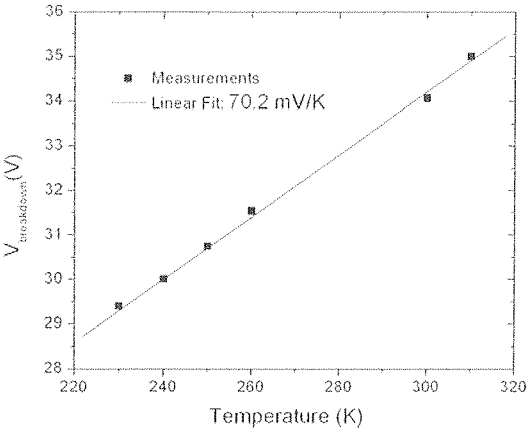

Fig. 19. SiPM breakdown voltage as a function of temperature.

5 Readout electronics

As previously mentioned, the output signal of a SiPM is a short pulse whose amplitude on a 50 Ω load resistor is expected to be of the order of 1mV per fired pixel. Such signal can be displayed on a wide-bandwidth digital oscilloscope, even without amplification, as reported in fig.19.

However, when connected to a threshold discriminator in photon counting or spectroscopy applications, the SiPM signal requires some pre amplification.One possibility is to use a wide-band voltage amplifier; however, as the SiPM behaves like a current pulse generator, a trans-impedance amplifier (TIA) is preferable for keeping the input impedance low and the response time very short.

The use of discrete components for the read-out electronics is convenient for a single photon detector, and eventually for a limited array of photon detectors. However, for applications where a large number of arrays or matrixes of

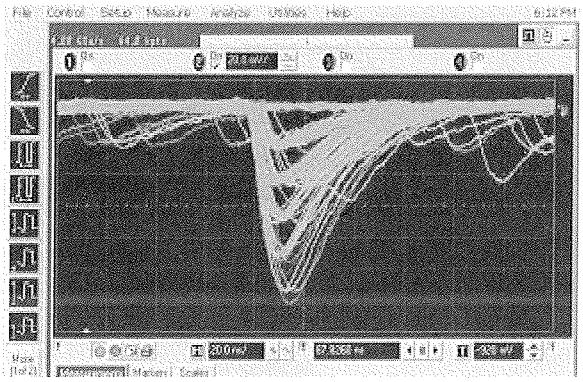

Fig. 20. Example of single photoelectron levels as observed on an oscilloscope (courtesy of SensL)

SiPMs is required,the use of a dedicated reado-ut circuit (ASIC) is mandatory.

In the framework of the DASIPM collaboration, the research unit of Bari is responsible of the design of an innovative read-out chip optimized for the FBK-irst SiPM. Preliminary results have been presented at the Nuclear Science Conferences /24, 25/. First of all, a spice model of the SiPM has been extracted which takes into account internal and external parasitic components /26/. Secondly, a first prototype of a single channel, front-end circuit has been realized in AMS 0.35um CMOS technology which exhibits an input current buffer stage and a current discriminator /27/.

At the present moment there is no read-out chip available on the market specifically designed for SiPM devices. However, it is worth mentioning that in the framework of the international CALICE collaboration for the realization of a Hadrons Calorimeter (HCAL) at the International Linear Collider (ILC, CERN-CH), the electronic group of LAL-Orsay (CNRS-FR) is developing a 36-channel SiPM read-out ASIC called "SPIROC" /28/.

6 Applications

SiPM is a compact, rugged, solid state detector insensitive to magnetic fields /29/. For these reasons it is a good candidate for replacing bulky vacuum photomultiplier tubes (PMTs) in low-light level applications. The number of such applications is enormous in the field of high energy physics (HEP), astroparticle physics, biology, oncology and nuclear medicine. An excellent overview of the potential applications of SiPM in HEP experiments can be found in ref /30/. Biology and oncology applications include protein fluorescence, molecular imaging, and single photon emission computed tomography (SPECT). The DASIPM collaboration is focused on a stroparticle physics and positron emission tomography (PET). Astroparticle physics includes intillating fiber tracking of high energetic particles,time of-flight measurements (TOF), Cerenkov imaging of cosmic rays /22b/. In this section some results concerning gamma-ray spectroscopy from radioac-

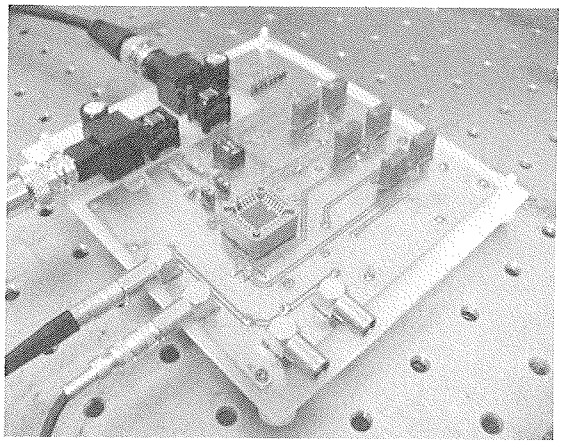

Fig. 21. Evaluation board of the first ASIC prototype

tive sources by means of LSO scintillators coupled to SiPM for PET/MRI and small animal imaging will be reported.

6.1 Energy resolution

At low level of illumination a good resolution is given by the ability of the detector to distinguish between single photo-electrons (s.p.e.).

In fig.21 a s.p.e. spectrum has been obtained illuminating the device with a pulsed LED at very low light intensity. The peaks corresponding to 1 to 9 p.e. can clearly be distinguished, showing the excellent s.p.e. resolution of these devices /31/.

For particle tracking and for PET applications the SiPM is coupled to a scintillator who converts a single high energetic (gamma) photon into a shower of optical photons. The efficiency of the conversion process depends upon the properties of the scintillating materials, i.e., atomic density, light yield, decay time and emission wavelength. Cesiumor Yttrium doped Lutetium Oxyortosilicate (LSO) is a good material for PET, because it has a high density (7.2gr/cm^3), high luminosity (>26000ph/MeV), short decay time (~40ns), and a max emission wavelength of 420nm (blue).

In positron emission tomography the position of the emitting radioactive source is reconstructed from the coincidence of two 0.511MeV gamma photons which are emitted at 180° by positron annihilation.

A spatial resolution of less than 1mm over a distance of several cm can be achieved, provided that the 511KeV spectrum peak can be separated from the low energy tail that is generated by Comptons cattering of gamma photons in living tissue.

Another difficulty is that, while keeping a submillimeter-space resolution, we would like image are latively large area of the body tissue. Finally, the large number of photons emitted by the scintillator can saturate the detector. The solution is a large area detector, or a matrix of many pixilated detectors.

Fig.22 shows a SiPM matrix composed of four (2x2) pixel elements in a common substrate, with a 1mm^2 LYSO scin-

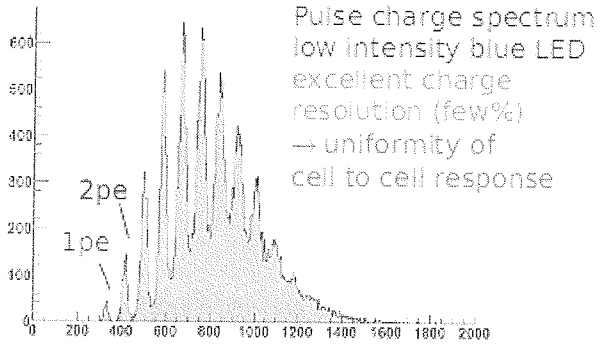

Fig. 22. Single photo electron spectrum. The first peak is the pedestal. The other peaks correspond to 1, 2..p.e.

tillator placed in the middle. Fig.23 shows the ^{22}Na spectrum obtained summing the signal from the four adjacent pixels /32/.

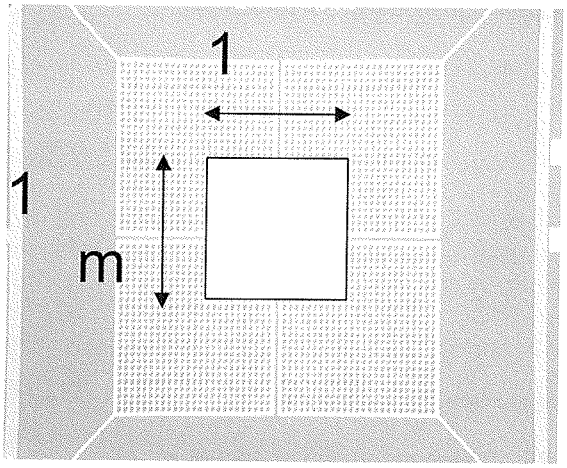

Fig. 23. SiPM matrix of 2x2 pixels with at 1 x 1 x 10mm^3 LSO cubic scintillator placed in the middle

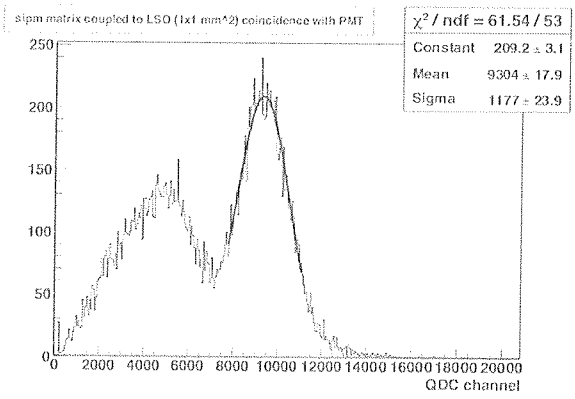

Fig. 24. ^{22}Na energy spectrum obtained as the sum of four adjacent SiPM.

The energy resolution is only 30% FWHM, but the sodium peak is well defined and can easily separated from the Compton tail by setting the threshold of the discriminator above 7000 channels.

A much better resolution of 16% FWHM has been obtained on a 3x3mm^2 SiPM (3200 sub-pixels) coupled to a cubic 3x3x3mm^3 LYSO crystal /33/.

The results obtained so far are very promising, and support the idea that large area detectors can be fabricated to meet the specifications of PET/MRI.

6.2 Timing resolution

The SiPM is a fast detector, and this characteristic can be exploited in TOF or TOF-PET experiments.

6.2.1 Single photon timing resolution

The intrinsic timing resolution of a SiPM has been evaluated at the single photoelectron (p.e.) level, illuminating the device with a pulsed laser with 60 fs pulse width at 80 MHz rate (T=12.34 ns) with less than 100 ps jitter /31/. The time difference between contiguous signals is evaluated and plotted, and there sulting distribution is fitted with a Gaussian function (fig.25, ref /34/).

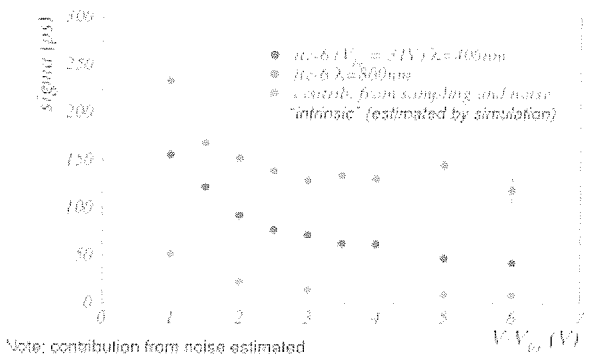

Fig. 25. Timing resolution of a SiPM at single photoelectron level as a function of the overvoltage measured at two different wavelengths

The measurement has been performed with blue light (400±7nm) and red light (800±15nm). An intrinsic timing resolution of ~ 60 ps rms has been measured for blue light at 4V overvoltage. The value for red light is higher, since the photons penetrate deeper in the detector and the carriers drift for a longer time before reaching the avalanche region.

6.2.2 Multi photon timing resolution

When more than 1 p.e. is generated in the SiPM, the timing resolution improves as $1/\sqrt{Npe}$, according to the Poisson statistics. At 15p.e, the timing resolution is ~ 20 ps rms.

6.2.3 Coincidence timing resolution

The time coincidence of events occurring in two different detectors is measured with two discriminators. One select the full energy event and generates the trigger signal; the second generates the coincidence signal that will be em-

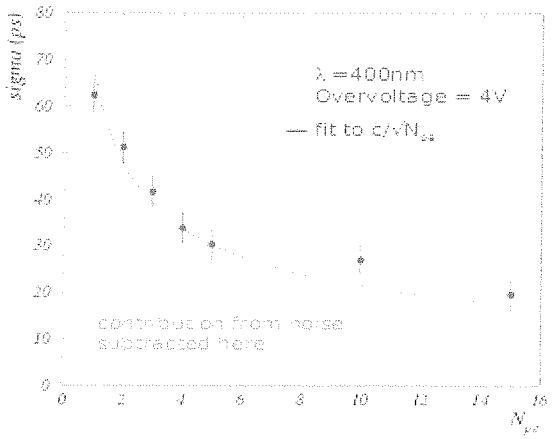

Fig. 26. Timing resolution of a SiPM as a function of photogenerated electrons (Npe)

ployed to estimate the time jitter between the two devices. The time distribution obtained for two LSO crystals coupled to two SiPMs is shown in fig.26.

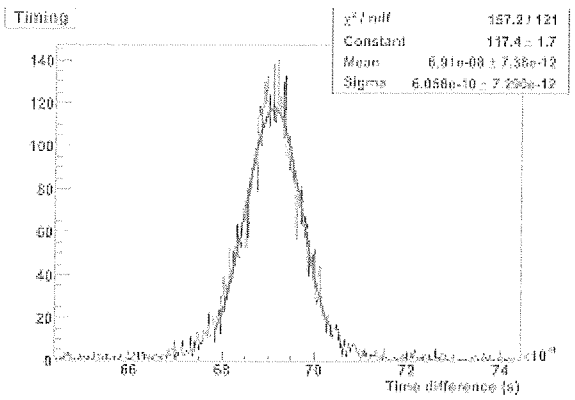

Fig. 27. Coincidence timing resolution of two SiPMs coupled to LSO crystals.

The timing resolution is 600ps sigma (1.4nsFWHM); a value well below the typical 10ns resolving time used in PET.

Finally, fig.26 shows the 511KeV Na spectrum obtained with a 1mm x 1mm x 10mm LSO crystal coupled to a SiPM, operated in coincidence with another device. In these conditions an energy resolution of 21% FWHM was obtained / 33/.

7 Conclusions

Silicon photomultipliers (SiPMs) have undergone a fast development in the last few years and they are currently produced by different manufacturers (Amplification Technologies, id-Quantique, Hamamatsu, Photonique, SensL, Zecotek). Their numerous advantages as compared to other photo detectors, i.e.,high gain, fast timing, compactness, insensitivity to magnetic fields, make them excellent candidates for replacing PMTs and APDs in several applications, in particular for nuclear medicine /11/. In the last year, SiPMs have further improved their characteristics, mainly increasing the photon detection efficiency (PDE) in

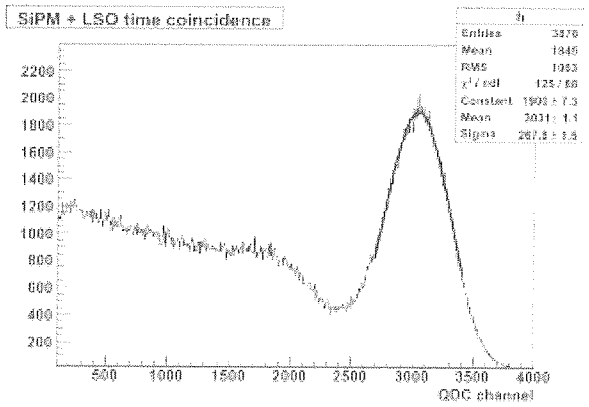

Fig. 28. ^{22}Na (E=511KeV) coincidence spectrumobtained from two SiPM in opposition

the blue region, enlarging the size of the active area and reducing the noise /35/. In the future the technology development will be devoted to the realization of low noise, large area, pixilated detectors /36/. However, it should be emphasized that the exploitation of these detectors will not be possible without a contemporary development of dedicated read-out ASIC chips.

Acknowledgments

I wish to acknowledge Nicoleta Dinu, ClaudioPiemonte (dinu@lal.in2p3.fr - piemonte@fbk.eu) Gabriela Llosa (gabriela.llosa@pi.infn.it) and Marco Petasecca (marcop@uow.edu.au) for helpful discussion and for providing most of the figures reported in this review paper.

References

/1/ K.K.Hamamatsu Photonics, Photomultiplier TubeHandbook, Electron Tube Division, 3rd ed.,2006.

/2/ http://www.electrontubes.com

/3/ http://www.photonis.com,

/4/ K.K. Hamamatsu Photonics, Photodiode TechnicalGuide. http://sales.hamamatsu.com/

/5/ http://www.microphotondevices.com

/6/ K. G. McKay, "Avalanche breakdown in silicon,"Phys. Rev., vol. 94, p.877, 1954.

/7/ M. Singh Tyagi, "Zener and avalanchebreakdown in silicon alloyed p-n junctions" SolidState Electronics, vol. 11, pp. 117-128, 1968.

/8/ F. Zappa et al., "Monolitic active-quencing andactive-reset circuit for single-photon avalanchedetectors", IEEE Journal of Solid-State Circuits,vol.38(7), pp. 1298-1301, 2003

/9/ Z. Sadygov, Russian Patent nr. 2086047 C1,1997.

/10/ V. M. Golovin, et al., Russian Patent nr.1644708, 1999.

/11/ P. Buzhan et al, "Silicon photomultiplier and itspossible applications", Nucl. Instr. Meth A,vol.504, pp. 48-52, 2003

/12/ P. Krizan et al., "Silicon Photomultiplier as adetector of Cherenkov photons", 2007 IEEENucl. Sci. Symposium Conference Record N41-3,pp. 2093-2096, 2007

/13/ http://sipm.itc.it

/14/ N. Dinu et al., "Development of the firstprototypes of silicon photomultiplier (SiPM) atITC-irst", Nucl. Instr. Meth. A, vol.572, pp. 422-426, 2007

/15/ C. Piemonte et al., "Characterization of the firstprototypes of silicon photomultiplier fabricated atITC-irst", IEEE Trans. Nucl. Sci., vol.54, No.1,pp. 236-244, Feb.2007

/16/ A. Lacaita et al., "On the Bremsstralhung originof hot-carrier-induced photons in silicondevices", IEEE Trans. Electron Dev., vol.40, pp.577-582, 1993.

/17/ A. Ingargiola et al., "A new model for opticalcrosstalk in single-photon avalanche diodesarray", 5th Int'l Conference on NewDevelopments in Photodetection, Aix-Les-Bains(France), June 15-20, 2008, electronic fileavailable at http://ndip.in2p3.fr/ndip08/

/18/ B. Dolgoshein, et al., "Large area siliconphotomultipliers: performances and applications",4th Int'l Conference on New Developments inPhotodetection, Beaune (France), June 19-24,2005. Nucl. Instr. and Meth. A 567, pp. 80-82,2005

/19/ W. G. Oldham et al., "Triggering phenomena inavalanche diodes", IEEE Trans. ElectronDevices, vol.ED-19, No.9, pp. 1056-1060, 1972

/20/ . J. McIntyre, "On the avalanche initiationprobability of avalanche diodes above thebreakdown voltage", IEEE Trans. ElectronDevices, vol.ED-20, No.7, pp. 637-641, 1973

/21/ C. Piemonte et al., "New results on thecharacterization of ITC-irst silicon photomultipliers",2006 IEEE Nucl. Sci. Symposium-Conference Record N42-4, pp. 1566-1569, 2006

/22a, 22b/ a) A. Del Guerra, b) R. Battiston, PerugiaWorkshop on Photon Detection, Perugia Italy,June 13-14, 2007 published in: Il NuovoCimento, vol.30-C, No.5, Sept.-Oct.2007.

/23/ M. Petasecca et al., "Thermal and electricalcharacterization of silicon photomultiplier", IEEETrans. Nucl. Sci., vol.55, pp.1686-1690, 2008.

/24/ F. Corsi et al., "Electrical characterization ofsilicon photomultiplier detectors for optimalfront-end design", 2006 IEEE Nucl. Sci.Symposium Conference Record N30-222,pp.1276-1280, 2006

/25/ F. Corsi et al., "Preliminary results from acurrent mode CMOS front-end circuit for siliconphotomultiplier detectors", 2007 IEEE Nucl. Sci.Symposium Conference Record N15-49, pp. 360-365, 2007

/26/ F. Corsi et al., "Modeling a siliconphotomultiplier (SiPM) as a signal source foroptimum front-end design", Nucl. Instr. andMeth. A, vol. 572, pp. 416-418, 2007

/27/ C. Marzocca et al., "Experimental results froman analog front-end channel for siliconphotomultiplier detectors", 2008 IEEE Nucl. Sci.Symposium, Dresden GE, 19-25 Oct. 2008

/28/ C. De la Taille, "SPIROC: Silicon PM ReadoutASIC", 5th Int'l Conference on NewDevelopments in Photodetection, Aix-Les-Bains(France), June 15-20, 2008.http://omega.in2p3.fr

/29/ R. Hawkes et al., "Silicon PhotomultiplierPerformance Tests in Magnetic Resonance PulsedFields", 2007 IEEE Nucl. Sci. Symposium Conf.Record M18-118, pp. 3400-3403, 2007

/30/ D. Renker, "Photo Detectors in High EnergyPhysics", Proceedings of Science: Int'l Workshopon new photon detectors, Kobe (Japan), June 27-29, 2007. http://www-conf.kek.jp/PD07/

/31/ G. Collazuol et al., "Single photon timingresolution and detection efficiency of the IRSTsilicon photo-multipliers" Nucl. Instr. Meth. A,vol.581, pp. 461-464, 2007

/32/ G. Llosa et al., "Silicon photomultipliers andSiPM matrices as photodetectors in nuclearmedicine", 2007 IEEE Nucl. Sci. SymposiumConference Record M14-4, pp. 3220-3223, 2007

/33/ M. Petasecca et al., "Gamma spectroscopyperformance of silicon photomultipliers coupledwith LYSO scintillators", 2008 IEEE Nucl. Sci.Symposium, Dresden GE, 19-25 Oct. 2008

/34/ G. Llosa et al., "Novel silicon photomultipliersfor PET applications", IEEE Trans. Nucl. Sci.,vol.55, pp. 877-881, 2008

/35/ C. Piemonte et al., "Recent developments onsilicon photomultipliers produced at FBK-irst ",2007 IEEE Nucl. Sci. Symposium ConferenceRecord N41-2, pp. 2089-2092, 2007

/36/ N. Dinu et al., "Characterization of a prototypematrix of Silicon PhotoMultipliers (SiPM's)", 5thInt'l Conference on New Developments inPhotodetection, Aix-Les-Bains (France), June 15-20, 2008. http://ndip.in2p3.fr/ndip08/

Giorgio Umberto Pignatel
on behalf of the INFN-DASIPM collaboration
Dept. of Electronic and Information Engineering
DIEI - via G.Duranti 93, 06125 Perugia, Italy
giorgio.pignatel@diei.unipg.it

Prispelo (Arrived): 17.09.2008 *Sprejeto (Accepted): 15.12.2008*

DESIGN OF AN EFFICIENT MICROWAVE PLASMA REACTOR FOR BULK PRODUCTION OF INORGANIC NANOWIRES

Jeong H. Kim, Vivekanand Kumar, Boris Chernomordik, and Mahendra K. Sunkara*

Department of Chemical Engineering, University of Louisville, Louisville, USA

Key words: plasma, atmospheric pressure, microwave, argon, oxygen, nanowire, nanoparticle, metal oxide

Abstract: We report the design of an atmospheric microwave plasma reactor to produce metal oxide nanowires. The reactor has a custom-made tapered waveguide and a 2.45GHz, 3kW (MKS ASTeX) magnetron and power supply unit for generating highly dense microwave plasma. As a result, a high temperature microwave plasma flame inside a quartz tube of 2 in. diameter and 1 ft. length was generated to produce metal oxide nanowires and nanoparticles. High Frequency Structure Simulator (HFSS) software was used to simulate the electric field distribution inside the dielectric tube.

Mikrovalovni plazemski reaktor za učinkovito izdelavo velike količine anorganskih nanožičk

Kjučne besede: plazma, atmosferski tlak, mikrovalovi, argon, kisik, nanožičke, nanodelci, kovinski oksidor

Izvleček: Predstavljamo konstrukcijske rešitve pri razvoju in izdelavi plazemskega reaktorja za proizvodnjo nanožičk kovinskih oksidov. Reaktor značilno deluje pri atmosferskem tlaku. Z razvojem novega posebej prilagojenega valovnega vodnika, magnetrona z največjo močjo 3kW in frekvenco 2.45 GHz in ustreznega močnostnega napajalnika smo uspeli v razelektritveni komori dobiti izredno gosto mikrovalovno plazmo. Znotraj kvarčne cevi s premerom okoli 5 cm in dolžino okoli 0.5 m ustvarimo plamen izredno vroče plazme, v katerem poteka sinteza nanožičk in drugih nanodelcev kovinskih oksidov. Porazdelitev električnega polja smo tudi izračunali z uporabo primerne programske opreme.

1 Introduction

Plasma has been used for various interesting applications particularly with production of nanomaterials /1-5/, quantum dots /6-8/, carbon nanostructures /9-12/, surface treatment /13-18/, decomposition /19-21/, and functional treatment /22-26/. One popular process for producing metal oxide nanowires is plasma-enhanced chemical vapor deposition (PECVD) /27/. Inorganic nanowires are an interesting set of nanostructures with a lot of potential applications in the fields such as solar cells /28/, Li-ion batteries /29/, nano-composites /30-32/, gas sensing /33-35/, and others. In many of these applications, nanowires are needed in large quantities. Thus, an efficient method for bulk production of nanowires is needed. The methods employed so far include catalyst-based Vapor Liquid Solid (VLS) /36/, thermal evaporation /37/, laser ablation /38/, hydrothermal synthesis /39/, sol-gel /40/, electrodeposition, plasma foil oxidation /41-44/ and others. None of these methods, however, are capable of producing nanowires in bulk amounts because they are all based on the use of a substrate or template which limits the amount of material that can be synthesized /45/. A truly bulk production system would require a vertical reactor with the ability to treat the metal powders continuously in gas phase and sweep the reacted species away from the reaction zone.

Design of such a reactor would invariably involve plasma or a combustion flame. The system would also require a fast, high through-put system, direct reaction (without the need of any substrate), highly dense dissociated reactive gases, large volume, and a stable and efficient flame system. An atmospheric system /46-48/ would be less expensive than vacuum, and would likewise be easier and faster to operate. The combustion flame method has been used to produce nanoparticles by completely vaporizing the metal powder /49/. However, it is prone to carbon contamination with the vapor sources-(e.g from oxygen-acetylene (or C_nH_m))-and is not ideal for creating molten metal conditions required for nanowires. The plasma employed in such a reactor could be based on medium frequency (MF), radio frequency (RF), capacitively/inductively coupled plasma (C/ICP), microwave (MW), and direct current (DC) /50-53/. MF, RF, and C/ICP require the use of a co-axial cable, which makes it difficult to produce plasma for bulk production because the cable would melt if high density plasma is obtained.

DC plasma uses electrodes which degrade easily under atmospheric conditions because of presence of oxygen in the gas species. This requires frequent change of electrodes which causes contamination problems /54-55/. To avoid this problem, an electrode-less high temperature plasma can be used to produce metal oxide nanowires under atmospheric pressure. RF uses co-axial cables to generate plasma, which makes it difficult to make large volume, high temperature plasma under atmospheric conditions with low power (1 to 3 kW). RF can also be used at atmospheric conditions for producing nanowires but at higher powers, e.g 30kW /56/.

Microwave energy can be used to generate large volume plasma without electrodes, thus avoiding contamination

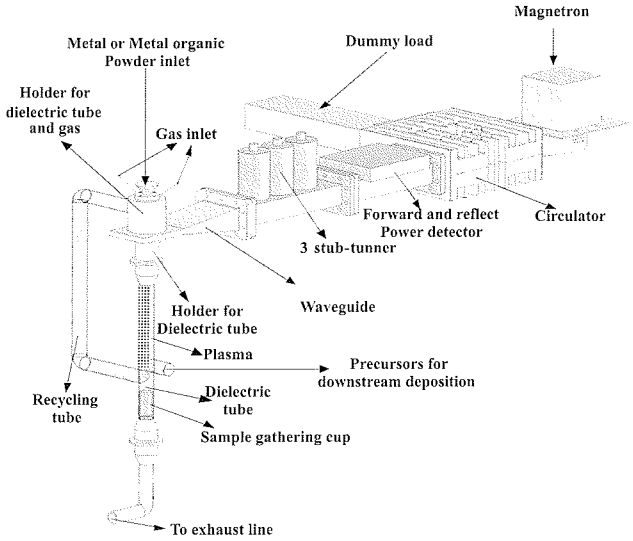

Fig. 1: A simplified schematic of the microwave plasma reactor.

/57/. The low electrical resistance loss, no need of any dielectric substance, low radiation loss, and ability to transfer high power to generate high density atmospheric microwave plasma makes it an ideal solution for high-throughput continuous metal-oxide nanowire synthesis. Therefore, we used a microwave source to produce plasma in this reactor.

2 Experimental and reactor set up

A reactor was designed that could efficiently generate highly dense microwave plasma discharges in a jet like manner confined inside tubes operating at pressures ranging from few Torr to atm. and at powers ranging from 300 W - 3 kW. A simplified schematic of the reactor set-up is shown in Figure 1. The set-up includes a plasma producing source (consisting of magnetron, forward and reflect power detector, dummy load, 3 stub-tuner and a circulator); a custom made waveguide; an entry port for feed source; an entry port for gases; a holder for gases and metal powder inlet; a dielectric tube such as quartz; a sample gathering cup; and an exit port for exhaust gases. The electric field (at 2.45 GHz microwave frequency) produced by magnetron and transported through the rectangular WR284 channels is concentrated in the middle of the dielectric tube in the waveguide which is appropriately designed (discussed later). A microwave plasma head with 3kW MKS Inst. ASTeX power supply and a 2.45GHz magnetron is used. A metallic rod with pointed end is used to ignite the plasma after introducing Ar gas (2 standard liter per minute (slpm)) and is immediately removed. Subsequently the reacting gases (air 8-14 slpm, O_2 500 sccm) are introduced and plasma is stabilized by stub-tuner and the reflected power is tuned to zero. The plasma jet length is about 12-15 in. as shown in the Figure 2. The quartz tube diameter is 1 to 1.5 in. and the length is 3 ft.

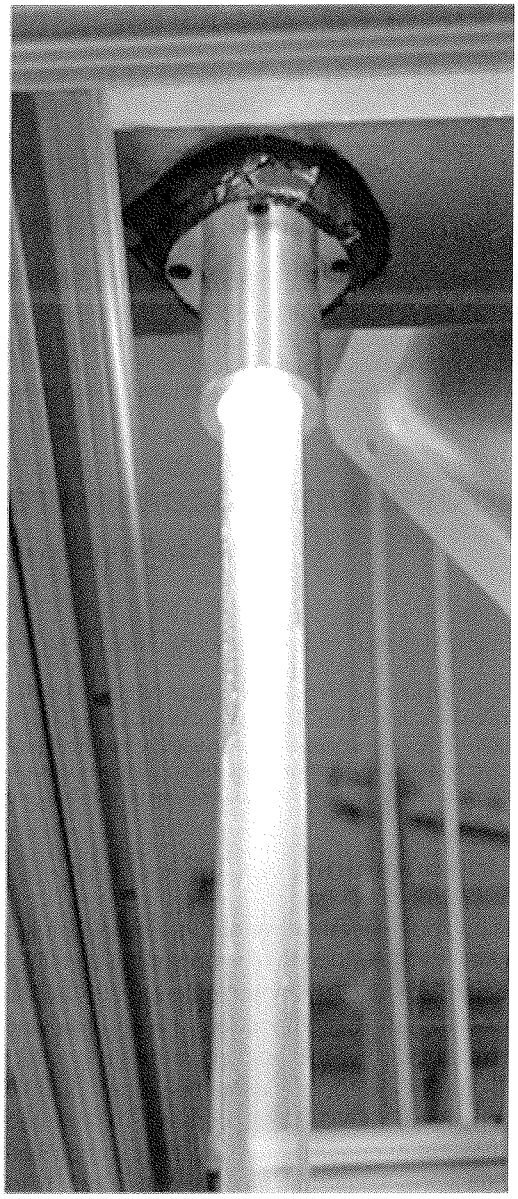

Fig. 2: Photograph of the microwave plasma discharge at 2 kW power.

Various gases are mixed in a single gas line and fed at the top of the reactor at the two diametrically opposite ends of the gas port holder in the gas delivery. Figure 3 shows the schematic of the port for gas delivery system. The gas is delivered tangentially at an angle of 60^0 with the vertical. The angle of the gas inlet produces a helical gas path around the periphery of the dielectric tube with downward momentum when sheath gas is delivered through the gas inlet. By delivering sheath gas (air, 8-14 slpm) via this system, the high density plasma discharge is confined near the center of the tube. Thus, contact of the plasma with the dielectric tube is avoided and the peripherally-confined sheath gas prevents the transmission of heat from the plasma to the dielectric tube. This helps to contain the plasma and to keep the dielectric tube cool during the operation of the reactor for any desired period of time. Air, oxygen, and nitrogen etc. could be used as sheath gases. The die-

lectric tube is important so that the plasma distributes uniformly within the tube. Preferably, the plasma should occupy a large portion of the tube cross section without touching or melting the tube. The desired metal powder (or metal-containing precursor) is delivered into the dielectric tube via gravity feed and is conveyed through the plasma by gravity. The collector is a cup which is attached at the bottom of tube while leaving space for exhaust gases to escape through. The exhaust line is connected to a mechanical pump which also sustains the plasma discharge by maintaining the optimum amount of gases in the reactor. The batch plasma reactor can be converted in to a continuous reactor by recycling partially converted products through recycling tube and combining with incoming feeds as discussed later.

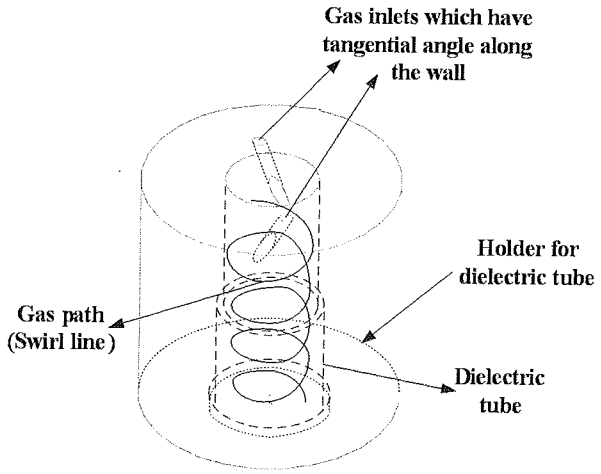

Fig. 3: Schematic showing the gas delivery system at a specified angle.

3 Processing scheme and results

The metal oxide nanowires of tin and zinc were produced using the above mentioned microwave plasma reactor operating at 1000-2000 W and 2.45 GHz in an atmosphere of 8-15 slpm air as sheath gas, and a plasma forming gas of 2-4 slpm argon and 100-700 sccm of oxygen (used as oxidative gas) at atmospheric pressure. In this process, the metal powder is supplied from the top into the microwave plasma jet and the nanowires are collected at the bottom of the tube. Gases and metals react at the center of the quartz tube near the plasma flame head and continue reacting as they fall under gravity along the plasma flame length. The length of the plasma can be varied by changing the gas flow rates or by changing the microwave power. The gas flow rate can be controlled by the mass flow controllers (MFC) and also by the mechanical pump. The products are collected at the bottom of the reactor. Figure 4a and b shows the Scanning Electron Micrographs (Nova Nano-600 Scanning Electron Microscope) of these as-synthesized metal oxide nanowires. From the SEM images we find that all these nanowires are typically 1-10 μm in length and less than 100 nm in diameter. At higher applied powers nanoparticles of alumina were produced using micron-sized Aluminum metal shown in Figure 4c. These nanoparticles are less than 100 nm in size and are uniform in size distribution.

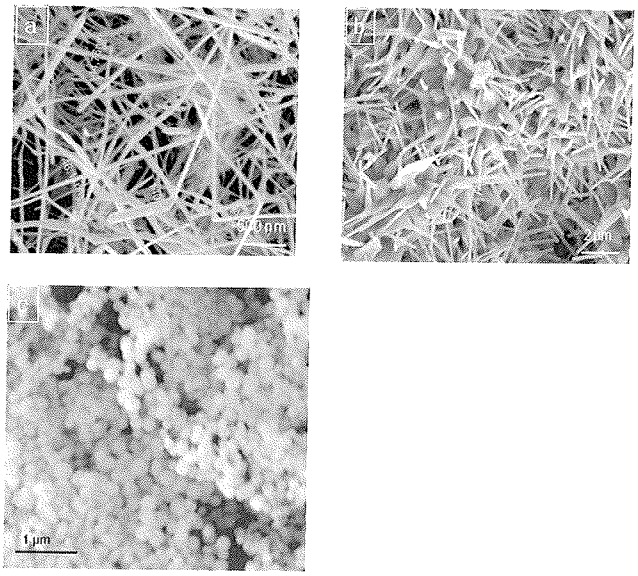

Fig. 4: As-synthesized nanowires of (a) tin oxide, (b) zinc oxide, (c) and nanoparticles of alumina.

3.1 Reactor Simulation and Analysis

The design of the waveguide to concentrate the electric field is a critical factor in this reactor. A perfectly designed waveguide would concentrate the maximum intensity of the electric field at a point where the dielectric break-down of the gases can occur by introducing plasma forming gases to strike the plasma. The design was done by simulating the electric field patterns inside the waveguide. Theoretically, the strongest electric field position is $\lambda/4$. The magnetic field can be ignored in the TE_{10} mode because of lower magnitude compared to the electric field.

For a 2.45 GHz microwave (λ=12.24cm) using WR284 waveguide, where *a* =72.14 mm=2,84 in (*a. is* width of the larger side of rectangular channel), the cut off wavelength $\lambda_c = 2a = 14.43$ cm, the cut off frequency $f_c=c/\lambda_c$=1.6 GHz, λ_g the waveguide wavelength can be calculated using equation (1) /24/:

$$\lambda_g = \frac{\lambda}{\sqrt{1-\left(\frac{f_c}{f}\right)^2}} = \frac{12.24cm}{\sqrt{1-\left(\frac{1.6}{2.45}\right)^2}} = 21.34cm \qquad (1)$$

Electric field intensity simulations were performed for two different waveguide shapes - rectangular and tapered - in a WR284 wave guide as shown in Figure 5. The tapered waveguide was preferred over rectangular one because the maximum electric field intensity is more than doubled (170,000 vs. 80,000 V/m in the two cases). The tapered shape also causes the gradual change in the impedance at the end of waveguide and thus there is no formation of

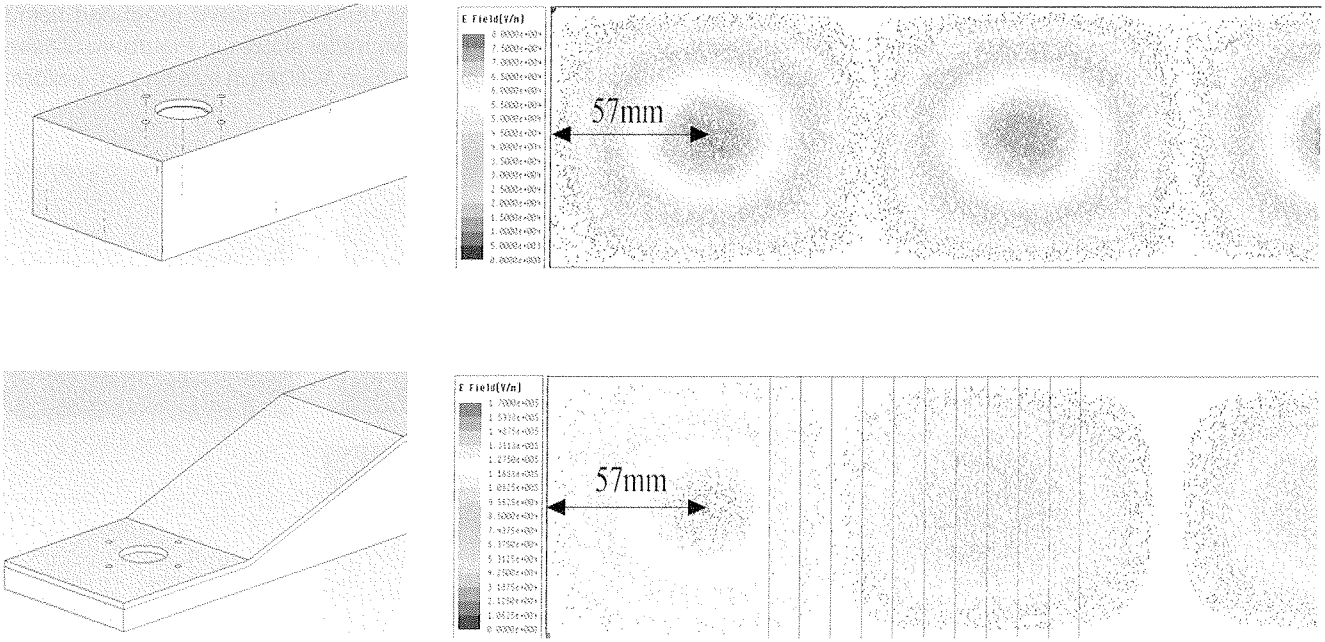

Fig. 5: Rectangular and tapered waveguides and the electric field intensities using them. The top image shows the rectangular and bottom shows the tapered waveguide.

"standing waves" (as in a rectangular waveguide) and hence has higher efficiency. Note that the theoretical $\lambda/4$ in a WR284 waveguide is $\lambda_g/4$ = 53.36 mm whereas the simulated $\lambda_g/4$ = 57 mm, as shown in Fig. 5, slightly differs.

The simulation result for electric field intensities at the shortened end of the tapered waveguide using quartz and ceramic tubes with varying diameters and thickness are shown in Table 1. $\lambda_g/4$, where the electric field is strongest is 53.35mm without a dielectric tube from equation 1. The simulated distance for maximum electric field intensity in a tapered and rectangular waveguide without any tube is 57 mm which differs only slightly from the theoretical value. As shown in Table 1, the maximum field intensity distance ($\lambda_g/4$) increases with larger tube diameters for same thickness of tube and decreases with larger tube thicknesses for the same diameter. Also for the same diameter and thickness the $\lambda_g/4$ distance is lower in the case of a material with higher dielectric constant (e.g. compare the values for 1 in. and 1 mm thick quartz and ceramic tubes).The

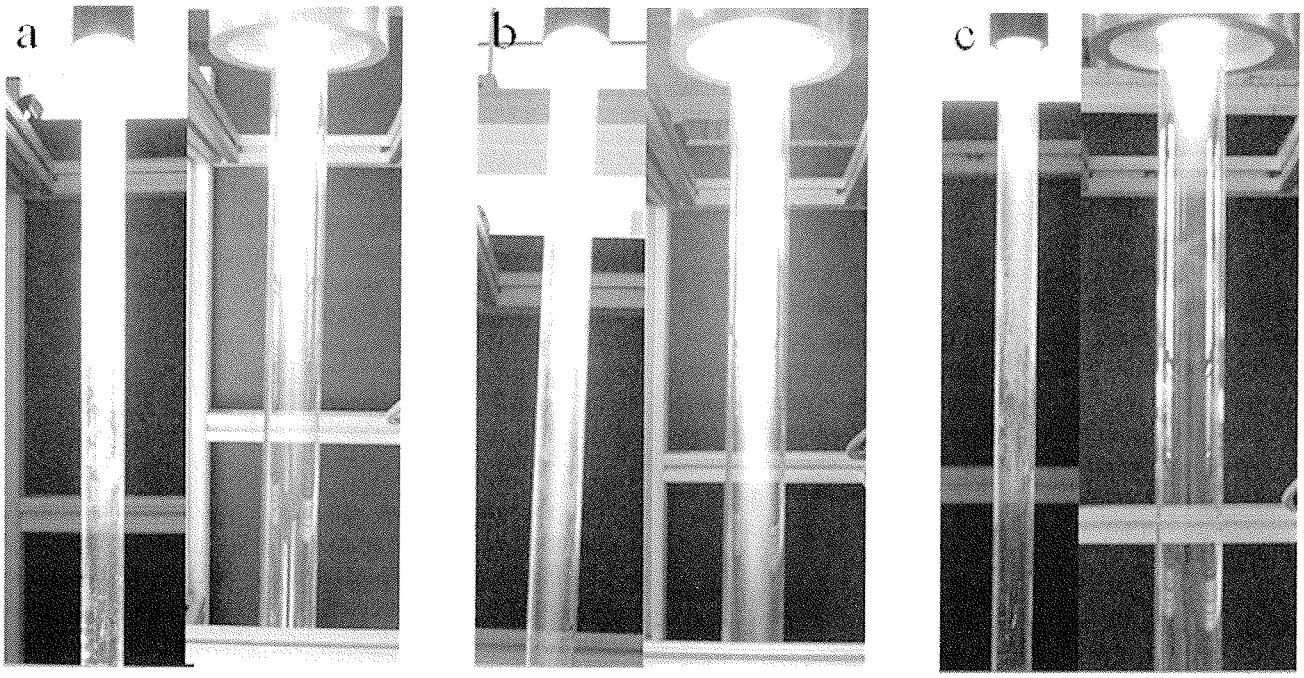

Fig. 6: Plasma discharge inside quartz tube diameters of 1 in (left) and 1.5 in. (right) using (a) air, (b) oxygen, and (c) nitrogen. The applied power and gas flow rate are 1.2 kW and 12 slpm respectively.

effect can possibly be due to the dielectric effect, which acts as the shield of the electrical energy. So, the electric field line is changed with dielectric tube material (dielectric constants for ceramic, quartz and air are 10, 4.2 and 1 respectively) and thickness. Materials with higher dielectric constants and likewise thicker materials show pronounced shielding effects. The waveguide was designed in such a way so that the maximum electric field lines are located at the middle of holes created for the insertion of vertical quartz tube. The tube would melt due to arcing if the maximum electric filed lines are at the periphery of the tube. Thus, the design of waveguide would depend on the diameter and thickness of the dielectric material being used. This principle was used in the design of a waveguide to generate stable and strong plasma flame.

3.2 Other design issues

The design of the microwave plasma reactor involves many issues such as: design of metal powder and gas delivery system, design of waveguide, choice of quartz tube diameter and the reacting gases, plasma flame stabilization, minimization of product deposition on the quartz tube wall, design of bottom product collection system, and product efficiency. Design of wave guide and metal powder and gas delivery system has been explained earlier. An appropriately chosen quartz tube diameter serves many purposes. It avoids the contact of hot plasma flame with the wall of the quartz tube and hence avoids the tube melting. The sheath gas is also important for the purpose of carrying out the reaction.

Table 1: Electric field simulation results for $\lambda g/4$ distances in different materials of different thickness and diameters

Wave guide type used	Theoretical calculation	Rectangular waveguide	Tapered waveguide
Distance mm	53.35	57	57
1 in. quartz tube - tapered waveguide			
Thickness	1mm	3mm	5mm
Distance mm	60.96	55.88	50.8
1.5 in. quartz tube - tapered waveguide			
Thickness	1mm	3mm	5mm
Distance mm	66.55	61.09	58.42
1 in. ceramic tube - tapered waveguide			
Thickness	1mm	3mm	5mm
Distance mm	53.34	31.75	29.08

Figure 6 shows the plasma discharges in two different diameter of quartz tube (1 in and 1.5 in) using air (Figure 6a), oxygen (Figure 6b), and nitrogen (Figure 6c) at 1.2 kW plasma power and 12 slpm gas flow. The flame in 1 in. quartz tube is shown in the left while that in the 1.5 in. is shown in the right of each figure. As evident from Figure 6, a 1 in. tube diameter results in significant closeness of plasma flame with the tube thereby melting the tube with prolonged exposure. The plasma flame is brightest and most reactive using oxygen, diminishes in the air, and is least reactive in nitrogen flame as shown in Figure 6c. The nitrogen plasma flame turns from violet to yellow to white with the increase in applied powder. Hence we chose 1.5 in. tube diameter and air or oxygen as the sheath gas. The choice of sheath gas also depends on the required product. For example, to produce sulfide and nitride compounds, N and S containing gases (e.g. NH_3 and H_2S) need to be introduced in an oxygen free environment. The plasma flame has tendency to overflow at the top of the reactor thereby creating difficulty in pouring the metal powders from the top. The flame can be directed downwards by using a mechanical pump which quickly evacuates feed gases. A significant portion of the product formed goes to waste by depositing on the walls of the quartz tube if the tube diameter is small. Although 1.5 in. quartz tube is barely sufficient for treatment of large amount of metal powders, a 4 in. or higher diameter quartz tube would be appropriate to avoid deposition of products onto the wall. However, striking and maintaining the plasma in a 4 in. diameter tube poses significant challenge and hence we used 1.5 in. tube diameter. Figure 7 shows the schematic and photograph of a product collection system consisting of a quartz cup placed inside a 4 way 4"-2" reducing cross. The gravity falling product impacts the bottom of the cup and also other finer products are entrained by the gas and can be captured by placing a filter paper in the side-way exit for the exhaust out-let.

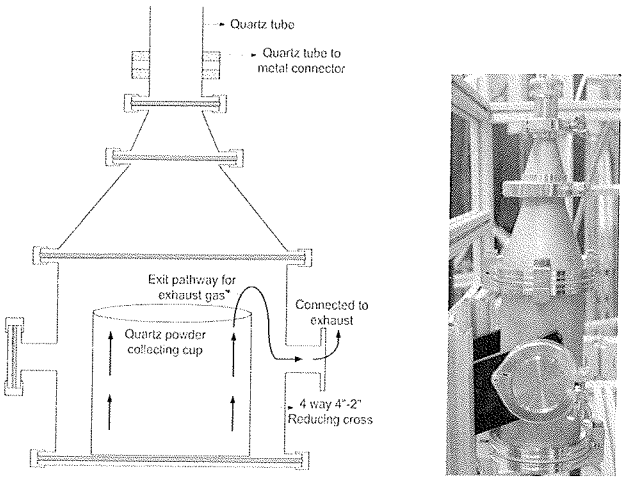

Fig. 7: (a) Schematic and (b) photograph of product collection cup used in the reactor.

The height of the cup should be higher than the height of the side-way exit and also its cross-sectional area should occupy a large portion of the bottom of reducing cross on which it rests. The product efficiency (i.e. % of required nanowires or nanoparticles vs. unreacted or agglomerated materials) can be improved by recycling the product as shown in Figure 8. The recycling system makes use of a cyclone separator and an entraining gas (carrying the un-

reacted and heavier products) forming part of the gases introduced at the top of the reactor. The final product is the outcome of cyclone separation. The recycling system, which makes for a continuous way of producing nanowires, is limited by two parameters: (1) the maximum solid loading in the entraining gas and also (2) the maximum solid which can be treated by the plasma flame. So at steady state these two should be equal and they together with the efficiency with which heavier and finer particles get separated will determine the production rate. Recycling a part of the product not only improves the efficiency but also leads to a continuous production of products.

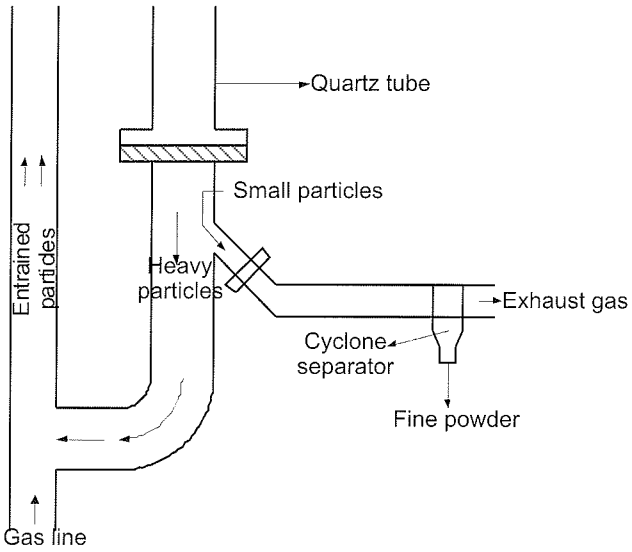

Fig. 8: Schematic of the recycling system.

4 Conclusions

A new microwave plasma reactor was successfully designed to produce highly dense plasma. The waveguide design is the key aspect of this reactor. The design involves several key issues such as gas and metal powder delivery, plasma flame stabilization, product collection cup. Using this reactor metal oxide nanowires and nanoparticles were produced in bulk (kg) quantities.

Acknowledgements

Authors gratefully acknowledge support from US Army Space Missile Defense Command (W9113M-04-C-0024), US Department of Energy (DE-FG02-05ER64071 and DE-FG02-05ER64071) and the U.S. Department of Energy/ Kentucky Rural Energy Consortium (DE-FG36-05G085013A).

References

/1/ K. Ostrikov and A. B. Murphy, J. Phys. D: Appl. Phys., vol. 40, pp. 2223-2241, 2007.

/2/ S. Sharma and M. K. Sunkara, , Nanotechnology, vol. 15, pp. 130-134, 2004.

/3/ K. Ostrikov, Rev. Mod. Phys., vol. 77, no.2, pp. 489-511, 2005.

/4/ E. Tam, I. Levchenko and K. Ostrikov, J. Phys. D: Appl. Phys., vol. 100, no.3, art. no. 036104, 2006.

/5/ U. Cvelbar, K. Ostrikov and M. Mozetic, Nanotechnology, vol. 19, no. 40, art. no. 405605, 2008.

/6/ J. C. Ho, I. Levchenko, and K. Ostrikov, J. Appl. Phys., vol. 101, art. no. 094309, 2007.

/7/ Q.J. Cheng, S. Xu, J.D. Long et al., Appl. Phys. Lett., vol. 90, no. 17, art. no. 173112, 2007.

/8/ I. Levchenko, A.E. Rider, and K. Ostrikov, Appl. Phys. Lett., vol. 90, no. 19, art. no. 193110, 2007.

/9/ K. Ostrikov, Z.L.Tlakatze, P. P. Rutkevych, J. D. Long, S. Xu, I. Denysenko, , Cont. to Plasma Phys., vol. 45, pp. 514-521, 2005.

/10/ I. B. Denysenko, S. Xu, J. D. Long, P. P. Rutkevych, N. A. Azarenkov, and K. Ostrikov, J. Appl. Phys., vol. 95, pp. 2713-2724, 2004.

/11/ I. Levchenko et al., J. Phys. D : Appl. Phys., vol. 41, no. 13, art. no. 132004, 2008.

/12/ I. Denysenko et al., J. Appl. Phys., vol. 104, no. 7, art. no. 073301, 2008.

/13/ U. Cvelbar, S. Pejovnik, M. Mozetic, and A. Zalar, Appl. Surf. Sc., vol. 210, pp. 255-261, 2003.

/14/ J.-H. Kim, G. Liu, and S. H. Kim, J. Mater. Chem., vol. 16, pp. 977-981, 2006.

/15/ C. Canal, F. Gaboriau, S. Villeger et al., Int. J. Pharm., vol. 367, no. 1-2, pp. 155-161, 2009.

/16/ C. Canal, F. Gaboriau, A. Ricard et al., Plasma Chem. Plasma Proces., vol. 27, no.4, pp. 404-413, 2007.

/17/ A. Ricard et al., Plasma Chem. Plasma Proces., vol. 5, no.9, pp. 867-873, 2008.

/18/ C. Canal, R. Molina, P. Erra, and A. Ricard, Eur. Phys. J. Appl. Phys., vol. 36, no. 35-36, 2006.

/19/ J. H. Hsieh and C. Li, Thin Solid Films, vol. 504, pp. 101-103, 2006.

/20/ M. Mafra et al., Key Eng. Mater., vol. 373-374, pp. 421-425, 2008.

/21/ N. Krstulović, I. Labazan, S. Milošević et al, J. Phys. D : Appl. Phys., vol. 39, pp. 3799-3804, 2006.

/22/ T. Vrlinic et al., Surf. Interface Anal., vol. 39, no. 6, pp. 467-481, 2007.

/23/ U. Cvelbar et al., Appl. Surf. Sci., vol. 253, no. 21, pp. 8669-8673, 2007.

/24/ C. Canal, S. Villeger, S. Cousty, B. Rouffet, J.P. Sarrette, P. Erra, A. Ricard, Appl. Surf. Sci., vol. 254, no. 18, pp. 5959-5966, 2008.

/25/ U. Cvelbar Sci., B. Markoli, I. Poberaj, A. Zalar, L. Kosec, and S. Spaic, Appl. Surf. Sci., vol. 253, pp. 1861-1865, 2006.

/26/ A. Vesel et al., Surf. Interface Anal., vol. 40, no.11, pp. 1444-1453, 2008.

/27/ D. Mariotti, H. Lindstrom, A.C. Bose, Nanotechnology, vol. 19, no. 49, 495302, 2008.

/28/ S. Gubbala, V. Chakrapani, V. Kumar, and M. K. Sunkara, Adv. Func. Mater., vol. 18, pp. 2411-2418, 2008.

/29/ P. Meduri, C. Pendyala, V. Kumar, G. U. Sumanasekera, and M. K. Sunkara, Nano Lett., vol. 9, pp. 612-616, 2009.

/30/ S. R. C. Vivekchand, K. C. Kam, G. Gundiah, A. Govindaraj, A. K. Cheetham, and C. N. R. Rao, J. Mater. Chem., vol. 15, pp. 4922-4927, 2005.

/31/ U. Cvelbar, M. Mozetic, and M.Klanjsek Gunde, IEEE Trans. Plasm. Sci., vol. 33, no.2, pp. 236-237, 2005.

/32/ M. Klanjsek Gunde, M. Kunaver at. al., Prog. Ora. Coat, vol. 54, no. 2, pp. 12-16, 2006

/33/ B. Deb, S. Desai, G. U. Sumanasekera, and M. K. Sunkara, Nanotechnology, pp. 285501-285507, 2007.

/34/ U. Cvelbar, K. Ostrikov, A. Drenik, and M. Mozetic, Appl. Phys. Lett., vol. 93, no. 13, art. no. 133505, 2008.

/35/ A. Drenik, U. Cvelbar, K. Ostrikov, and M. Mozetic, J. Appl. Phys.D : Appl. Phys., vol. 41, no. 11, art. no. 115201, 2008.

/36/ R. S. Wagner and W. C. Ellis, Appl. Phys. Lett., vol. 4, pp. 89-90, 1964.

/37/ B. D. Yao, Y. F. Chan, and N. Wang, Appl. Phys. Lett., vol. 81, pp. 757-759, 2002.

/38/ A. M. Morales and C. M. Lieber, Science, vol. 279, pp. 208-211, 1998.

/39/ Z. Li, X. Huang, J. Liu, and H. Ai, Mater. Lett., vol. 62, pp. 2507-2511, 2008.

/40/ M. Zhang, Y. Bando, and K. Wada, J. Mater. Sc. Lett., vol. 20, pp. 167-170, 2001.

/41/ M. Mozetic, U. Cvelbar, M. K. Sunkara, and S. Vaddiraju, Adv. Mater., vol. 17, pp. 2138-2142, 2005.

/42/ U. Cvelbar et al., Small, vol. 4, no.4, pp. 1610-1614, 2008.

/43/ Z.Q. Chen et al., Chem. Mater., vol. 20, no.9, pp. 3224-3228, 2008.

/44/ U. Cvelbar and K. Ostrikov, Cryst. Growth Des., vol.8, no.12, pp. 4347-4349, 2008.

/45/ V. Kumar, J. H. Kim, C. Pendyala, B. Chernomordik, and M. K. Sunkara, J. Phys. Chem. C, vol. 112, pp. 17750-17754, 2008.

/46/ V. Hody et al., Plasma Chem. Plasma Process, vol. 26, no. 3, pp. 251-266, 2006.

/47/ G. Arnoult, R.P. Cardoso, T. Belmonte and G. Henrion, Appl. Phys. Lett., vol. 93, no. 19, art. no. 191507, 2008.

/48/ T. Belmonte, R.P. Cardoso, G. Henrion, and F. Kosior, J. Phys. D: Appl. Phys., vol. 40, no. 23, pp. 7343-7356, 2007.

/49/ J. B. Donnet, H. Oulanti, T. L. Huu, and M. Schmitt, Carbon, vol. 44, pp. 374-380, 2006.

/50/ M. Mozetic, A. Vesel, U. Cvelbar et al., Plasma Chem. Plasma Process., vol. 26, no.2, pp. 236-237.

/51/ M. Mozetic, U. Cvelbar, A. Vesel, et al., J. Appl. Phys., vol. 97, no. 10, art. no. 103308, 2005.

/52/ K.N. Ostrikov, S. Xu, M.Y. Yu, J. Appl. Phys., vol. 88, no. 5, pp. 2268-2271, 2000.

/53/ A. Ricard, F. Gaboriau, and C. Canal, Surf. Coat. Tech., vol. 202, pp. 5220-5224, 2008.

/54/ S.V. Vladimirov et al., Phys. Rev. E, vol. 58, no. 6, pp. 8046-8048, 1998.

/55/ K.N. Ostrikov, M.Y. Yu and H. Sugai, J. Appl. Phys., vol. 86, no.5, pp. 2425-2430, 1999.

/56/ H. Peng, Y. Fangli, B. Liuyang, L. Jinlin, and C. Yunfa, J. Phys. Chem. C, vol. 111, pp. 194-200, 2007.

/57/ R.P. Cardoso, T. Belmonte, P. Keravec, F. Kosior and G. Henrion, J. Phys.D: Appl. Phys., vol. 40, no.5, pp. 1394-1400, 2007.

*Jeong H. Kim, Vivekanand Kumar, Boris Chernomordik, and Mahendra K. Sunkara**
Department of Chemical Engineering, University of Louisville, Louisville, KY 40292
Corresponding Author: mahendra@louisville.edu

Prispelo (Arrived): 17.09.2008 *Sprejeto (Accepted): 15.12.2008*

LOW TEMPERATURE PLASMA TREATMENTS OF TEXTILES

Cristina Canal

Pharmacy and Pharmaceutical Technology Dpt., Faculty of Pharmacy, University of Barcelona, Barcelona, Spain

Key words: plasma, discharge, afterglow, oxygen, functionalization, textile, wool, polyamide

Abstract: Textile finishing is the stage at which their final properties are imparted to fabrics, conferring them with one or many functional properties such as shrink-resistance, water-resistance, softness, antibacterial, etc. At this stage of the textile chain is where a high number of chemicals are used, and often highly polluted wastewaters may be produced, so considering the increasingly strict environmental legislation, low temperature glow discharge plasmas (LTP) have emerged as an environmentally friendly technique for the finishing of textiles. Plasma processes need only small amounts of selected chemicals (if any) and do not produce waste waters or chemical effluents, so the use of plasma processes in textile finishing can reduce its environmental impact. Another advantage of plasma processes is modifying the textile fibre surfaces to a depth of nanometres without altering the bulk properties of the fibres, such as mechanical properties, of relevance in textiles. In the present review work, an overview is given on some outstanding plasma treatments of natural and synthetic fibres. For instance, the effects of plasmas (radiofrequency plasma, microwave post-discharge) on wool fibres and fabrics are shown with respect to their wettability, shrink-resistance, softness and adhesion of polymers. In parallel, the effects of plasma on polyamide 6 fibres and fabrics are shown related to their wettability, ageing properties, post-deposition of biopolymers and dyeability.

Obdelava tekstilnih materialov z nizkotemperaturno plazmo

Kjučne besede: plazma, razelektritev, porazelektritev, kisik, funkcionalizacija, tekstil, volna, poliamid

Izvleček: Zadnja stopnja pri obdelavi tekstilnih materialov določa njihove funkcionalne lastnosti, kamor sodijo na primer odpornost proti krčenju, prepustnost za vodne kapljice in paro, mehkost in morebitna bakteriostatičnost. V zadnji stopnji pri obdelavi tekstilij se običajno uporablja obilo kemikalij. Poleg tega so odpadne vode, ki so posledica spiranja kemikalij pogosto močno onesnažene, zaradi česar se iščejo alternativni postopki obdelave. Zaradi vedno ostrejših okoljskih predpisov se vedno bolj širi uporaba okolju prijaznih tehnik, ki temeljijo na uporabi nizkotemperaturne plinske plazme. Pri plazemskih procesih uporabimo zelo majhne količine kemikalij, pogosto pa njihova uporaba sploh ni potrebna, da bi dosegli določene funkcionalne lastnosti tekstilij. Pri plazemskih tehnologijah tekstilij ni potrebno spirati z vodo, zaradi česar se bistveno zmanjša onesnaževanje okolja. Druga pomembna prednost plazemskih tehnologij je možnost modifikacije zgolj površinske plasti debeline nekaj nanometrov, medtem ko ostanejo siceršnje lastnosti materiala nespremenjene. V pričujočem preglednem članku podajamo pregled najpomembnejših dosežkov na področju plazemske modifikacije naravnih in sintetičnih vlaken. Najboljše lastnosti tekstilij dobimo z uporabo plazme, ki jo generiramo z radiofrekvenčno ali mikrovalovno razelektritvijo, pogosto pa namesto plazme uporabimo porazelektritveni del. V prispevku podrobneje predstavimo vpliv plazemske obdelave na volnena vlakna in tekstil. Prikazujemo spremembo omočljivosti, odpornosti proti krčenju, spremembo mehkobe volnenega blaga in sposobnost površinske vezave polimerov. Prav tako prikazujemo vplive plazemske obdelave na sintenična vlakna in tekstilije izdelane iz poliamida PA-6, kjer poseben poudarek posvečamo pojavu staranja vlaken in tekstila,j pa tudi naknadni depoziciji biopolimerov in barvanju.

1 Introduction

Wool is a natural fibre mainly constituted by keratins. Morphologically, the fibres are formed by cortical and cuticular cells and cell membrane complex. Cuticular cells are located in the outermost part of the fibre, surrounding the cortical cells. The cuticle consists of a layer of flat scales of approximately 1 μm thickness overlapping one another like tiles on a roof (Fig. 1a), and forming a ratchet-like structure, which provokes a directional frictional effect /1/ which has traditionally been considered the main responsible for felting shrinkage of wool fabrics. Felting shrinkage is a process which comprises compacting and entanglement of fibres submitted to mechanical action, friction and pressure in presence of heat and humidity, and accounts for the undesirable and irreversible reduction of the area of the fabrics. From the chemical point of view, the outermost part of cuticle cells is of hydrophobic nature due to the presence of the "Fatty Layer", a thin layer of 18-methyl eicosanoic acid (18-MEA) covalently bound via a thioester linkage to the protein layer of cuticle /2/. It has recently been shown that the presence of this fatty layer on the surface influences the shrinkage behaviour of wool fabrics during aqueous washing /3/.

Polyamide 6 is a chemical fibre, also known as nylon 6 (H-[NH-C_5H_{10}-CO]$_n$-OH), is an aliphatic polyamide obtained through polycondensation reaction of ε-caprolactam. It is characterized by recurring amide groups (-CONH-) in the polymeric chain and amino and carboxylic end groups /4/.

Low temperature glow discharge plasmas (LTP) are considered as an emerging technique in the achievement of wool with shrink-resistant properties by environmentally friendly methods /5/, as well as on the surface modification of textile fibres in general, as they modify the fibre surface to a depth of nanometers, without altering the bulk properties of the fibre. Plasma processes need only small amounts of selected chemicals and do not produce wastewater or chemical effluents, so plasma is efficient, economical, and can reduce the environmental impact caused by the use of chemicals in the textile industry, traditionally extensive in the consumption of water and chemicals. Plasma is a partially ionized gas generated by an electrical discharge, and consists of neutral particles (molecules, ex-

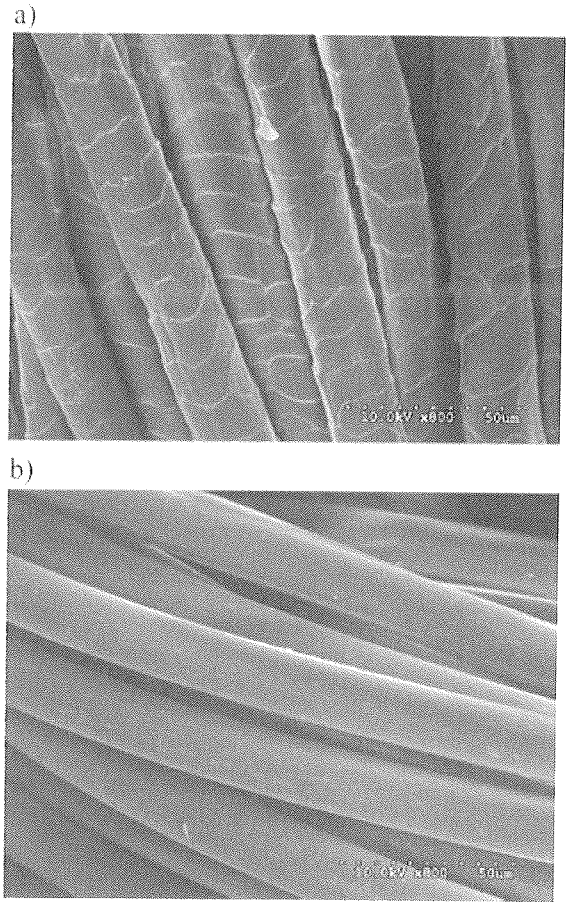

Fig. 1: Morphology of (a) wool and (b) polyamide 6 fibres.

cited atoms, free radicals and metastable particles), charged particles (ions and electrons) and UV and V radiation. Plasma chemistry takes place while the gas remains at relatively low temperatures, close to room temperature /6/. Due to these oxidative processes the wetting properties of the surface of fibres are improved, and therefore the adhesion properties /7,8/. In the plasma discharge, high density of species such as ions, electrons and UV radiation in addition to the active atoms already mentioned, can act on the fibre surface. Such ions disappear by recombination with electrons at the end of the discharge, as well as UV and other excited species, so in the post-discharge only stable atoms are present /9/.

Different kinds of plasmas have been extensively studied /10-23/ and characterized /24-28/ for the synthesis of ordered nanostructures /20-33/, for the engineering of materials /34-37/ and for surface functionalisation /38-51/ for example.

In the present paper an overview is given on the effects of plasma and post-discharge plasma treatments on natural (wool) and chemical fibres (polyamide 6), and its possible combination with different chemical post-treatments for obtaining textiles with different functionalities.

2 Experimental

2.1 Materials

Botany knitted merino wool fabric with a cover factor of 1.22 $tex^{1/2}mm^{-1}$ was used throughout the work. Keratin hair fibers were used as a model for the wool fiber on the determination of contact angle due to their chemical and morphological similarities /52/. Before treatment, fabrics and fibers were washed with a solution of 2 $g.L^{-1}$ of the non-ionic surfactant Cadetram 9M (Comp. Suministros Cades S. A.), at 25°C for 15 min and then thoroughly rinsed with deionized water and dried at ambient temperature.

PA6 microfiber fabrics were used throughout this work and washed with 2 $g.L^{-1}$ of surfactant solution (Nekanil LN) at 95°C for 45 min and then thoroughly rinsed with deionized water and dried at ambient temperature.

PA6 rods (Goodfellow Ltd, UK) of 2 mm diameter were used for the determination of contact angle. Prior to any treatment, they were cleaned by Soxhlet extraction with benzene (Probus, Spain) and acetone (Merck, Germany).

2.2 Methods

A radio-frequency (RF) reactor (Fig. 2) operating at 13.56 MHz was employed /53/ using air, nitrogen or water vapour as plasma gases. The distance between the electrodes was 8.5 cm, and the sample was hung equidistant between the electrodes. During treatments, the pressure and the incident power were kept constant at 100 Pa and 100 W, respectively. This power was uniformly distributed on a 400 cm^2 cathode surface.

A flowing post-discharge (PD) reactor (Fig. 3) was used /54/, composed of a pyrex cylinder of 15 cm of internal diameter (i.d.) and 20 cm height separated 70 cm from

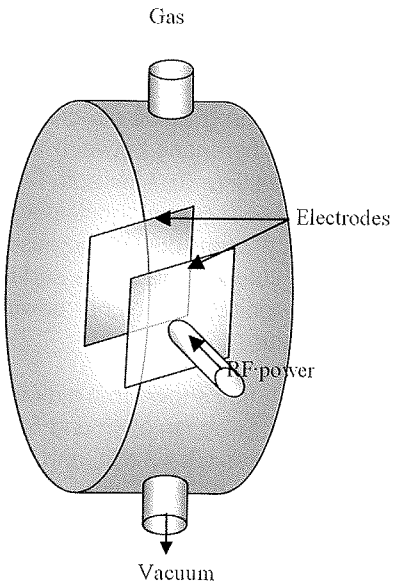

Fig. 2. Schematic description of the stainless steel reaction chamber

the plasma source by a 5 mm i.d. quartz tube. The discharges were generated by a 2.45 GHz microwave source using 60 W of incident power. The discharge tube is sealed to a bent quartz tube of 15 mm i.d. which is connected to the post-discharge reactor. The gas flow rate was set constant at 1 L.min^{-1} and the pressure in the reactor was 533 Pa (4 Torr). The samples were hung vertically in the center of the reactor.

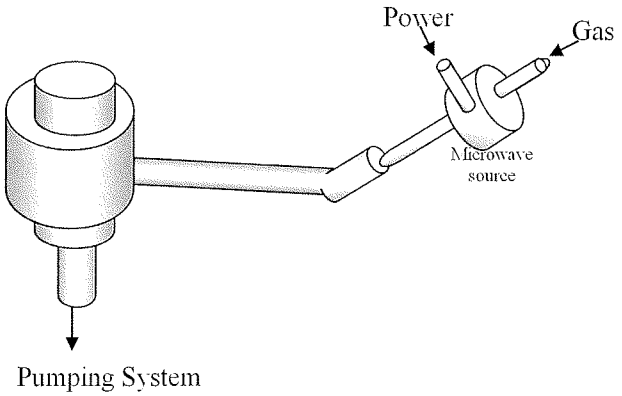

Fig. 3. Scheme of the pyrex post-discharge reaction chamber

Optical emission spectroscopy and catalytic probes was used to characterize post-discharges as described in /55/. Contact angles, X-ray photoelectron spectroscopy, scanning electron microscopy and shrink-resistance methods were carried out as described in /53, 56/.

3 Results and discussion

In the course of different works, we have compared the effects of plasma and post-discharges (PD) on the properties of wool and polyamide 6 fibres and fabrics.

3.1. Effects of plasma on wool

One of the main features characterizing wettability of untreated (UT) wool fibres is their different receding adhesion tension as a function of scale direction (Fig. 4a), attributed to chemical differences between the frontal and the dorsal of the scales (Fig. 5). After both RF plasma and PD (Figs. 4 b and c) with oxygen-containing gases, this feature is no longer present due to increased chemical homogeneity of the cuticle scales. The surface of the fibres becomes hydrophilic, with higher advancing adhesion tension (F/L) values.

Previous studies /57/ had shown that a direct N_2 plasma treatment produced a decrease of around 58° in the contact angle of keratin fibres after 2 min, and thus an important increase in the wettability, while 15 min of N_2 PD resulted in a decrease of 42° /55/. Consequently, both post-discharge plasmas and direct plasmas are efficient for producing hydrophilic wool surfaces, although slightly longer treatment times are required for achieving similar hydrophilicity with PD than with direct discharges.

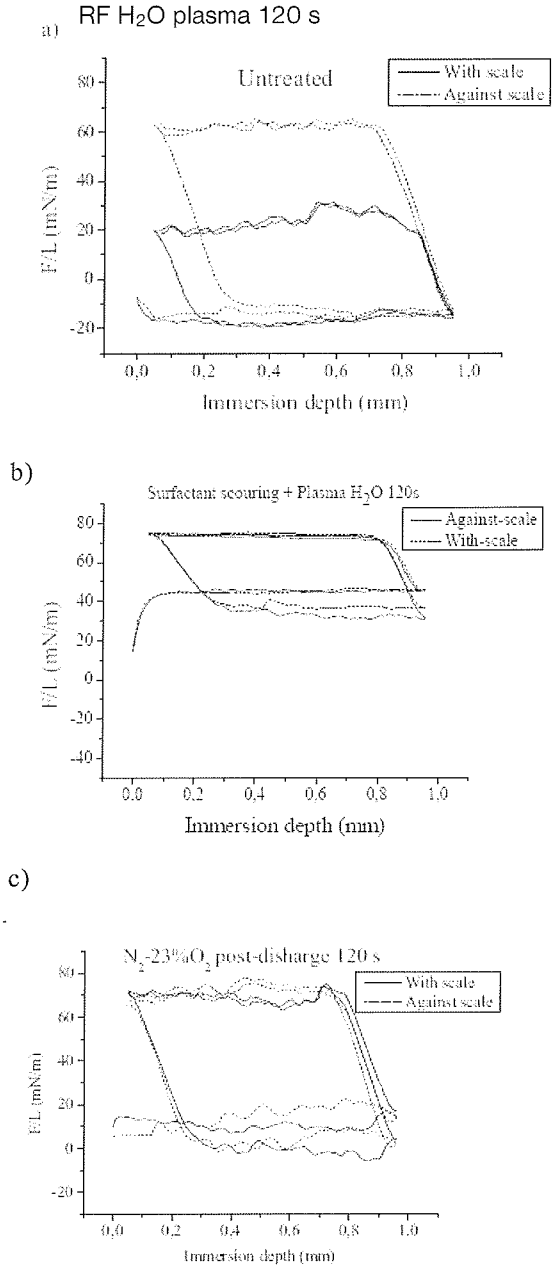

Fig. 4: Adhesion tension wetting hysteresis cycles of UT (a), H_2O RF plasma treated (b) and N_2-23% O_2 PD treated (c) keratin fibres in water.

When the plasma is generated by an oxidative gas, such as air, oxygen or water vapour, the wool fibre surface is oxidized progressively by forming C-OH, C=O, HOC=O groups, and promoting an ablation effect of the fatty layer. Also, the cystine residues of wool are oxidized to cysteic acid residues increasing the anionic groups on the wool fibre surface /52, 54, 58/.

It has been shown that the effects produced by plasma and PD treatments on the surface are mainly due to the neutral atoms of the discharges /54/, as detected by optical emission spectroscopy. The use of catalytic probes for O detection during PD treatment of wool /59/ revealed that the etching process of the fatty layer, which takes place

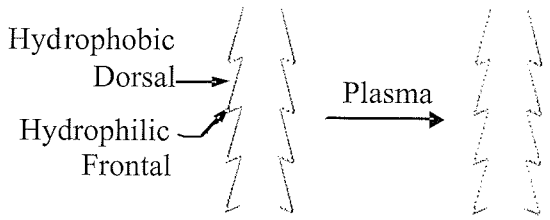

Fig. 5: Schematic representation of the chemical homogeneisation of the dorsal and frontal of the wool cuticle scales by the action of plasma

at the early stages of treatment, represents a great source of consumption of atoms.

Several publications have shown the shrink-resistance effect promoted by plasma on wool fabrics. Comparison (Fig. 6) of the shrink-resistance effect of direct and post-discharge N_2 plasma on wool fabrics /55/ revealed the equivalent effectiveness of both treatments, although to achieve equivalent shrinkage reduction percentages, longer treatment times have to be applied with post-discharge plasma. The slightly longer times required to achieve similar shrinkage reduction percentages (as well as similar contact angles) on N_2 PD treated wool can be explained by the fact that only N atoms are present, while in direct plasmas, the added effect of ions and UV radiation has to be considered.

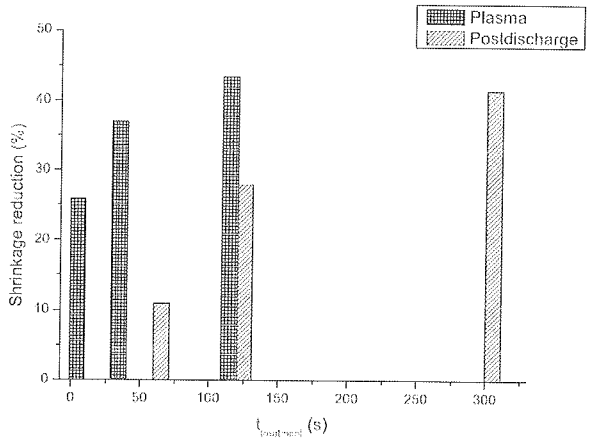

Fig. 6. Comparison of the shrinkage reduction attained by direct plasma treatment or by post-discharge plasma.

Post-application of finishing products on the surface of wool after plasma treatment has been the object of different studies, and its interest lays in the wide number of textile finishes which would benefit from increased adhesion product-fibre, or the possibility of employing lower quantities of chemicals. One of the critical points in plasma treatment of wool is the improvement of handle of the fabrics, which is harsher after the plasma treatment. Given the ageing in wettability observed /60/, it is advisable to carry out such post-treatments as soon as possible after plasma.

Through the application of acid chlorides on UT and RF plasma treated wool it was shown that the presence of the fatty-layer on the surface of UT wool exerts a strong influence on the post-deposition of products /3/. After the oxidation and partial elimination of the fatty-layer through a plasma treatment, post-application of acid chlorides of different chain length revealed a clear relationship between wettability and shrink-resistance (Fig. 7). The higher the wettability, the better the shrink-resistance. In addition, handle evaluation showed, as expected, that the longer the chain length, the better the softness perceived.

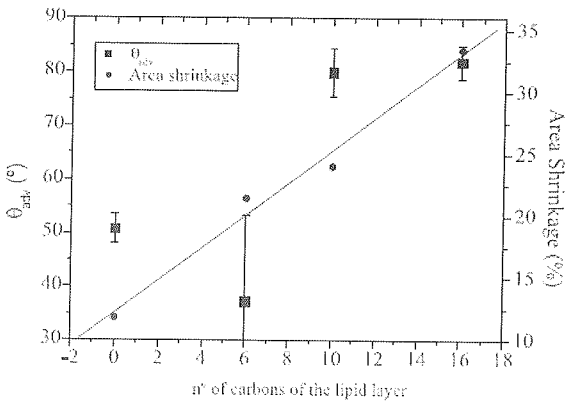

Fig. 7: Relationship between advancing contact angle (Θ_{adv}) and area shrinkage as a function of the number of carbons theoretically present on the surface, playing the role of fatty-layer.

The application of conventional cationic softeners on RF plasma treated wool fabrics reverts in high shrinkage values /60/. The application of certain cationic or polar polysiloxane softeners on H_2O RF plasma-treated wool improves the handle of the fabrics and the deposition of the softener while conserving an acceptable shrink-resistance /56/. A possible mechanism of interaction between the different polysiloxane groups and the surface of untreated (UT) and LTP-treated wool was proposed, as shown in Fig.8.

3.2. Effects of plasma on polyamide 6

Contrarily to wool, untreated polyamide 6 (PA6) is a chemical fibre of hydrophilic nature (see Table 1). As can be seen, when air and nitrogen were used as RF plasma gases, an important increase in the hydrophilicity of polyamide surface was achieved, with very similar advancing contact angle values /61/. The treatment with water vapor plasma was the most effective to generate highly hydrophilic PA6 surfaces, reducing the advancing contact angle to 34.7°.

The ageing process of RF plasma treated PA6 was studied by means of contact angle /61/ as a function of storage time after treatment.

Figure 9 shows an increase in hydrophobicity of the plasma treated PA6 as a function of the time elapsed after plasma treatment, indicating that the concentration of hydrophilic groups on the surface decreases, which could

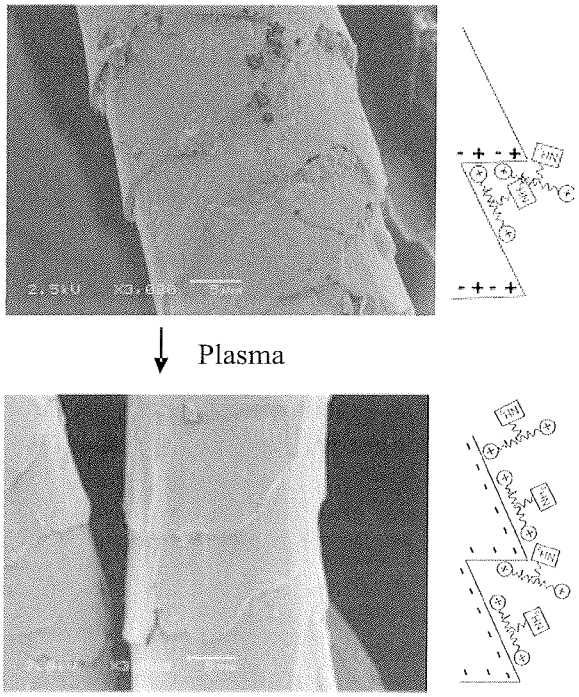

Fig. 8: SEM images and proposed mechanism of interaction between wool (UT - up, and H_2O plasma treated - down) and a cationic polysiloxane.

Table 1. Advancing (Θ_{adv}) contact angle and contact angle hysteresis ($\Delta\Theta$) of PA6 UT and treated for 2 min in plasma or PD of different gases

Treatment	$\theta_{adv} \pm 2.2°$ (°)	$\Delta\theta$ (°)
Untreated	*71.4*	*55.8*
Air RF plasma	53.4	46.2
N_2 RF plasma	49.7	41.3
N_2 post-discharge	*43.3*	*30.1*
H_2O plasma	34.7	26.1
O_2 post-discharge	*45.8*	*28.4*

be due to migrarion or reorientation of these groups towards the bulk phase of PA6 during their storage in air environment. This point was confirmed by immersion of the aged samples in water /61/, which revealed a partial recovery of the wetting properties, or even complete recovery in PA6 treated in oxidizing plasma gases.

Relevant topographical modifications (in general undesirable for textile finishing purposes), are only achieved in relatively aggressive conditions, such as oxygen treatments for long times in both RF plasmas or post-discharges (Fig. 10).

Post-application of finishing products on PA6 can be aimed to different effects, such as improving dye exhaustion or increasing colour intensity (K/S) of dyeings. Chitosan is a polycationic biopolymer which has been applied to fabrics to confer antibacterial properties. In this case, its application was studied to enhance efficiency of dyeings.

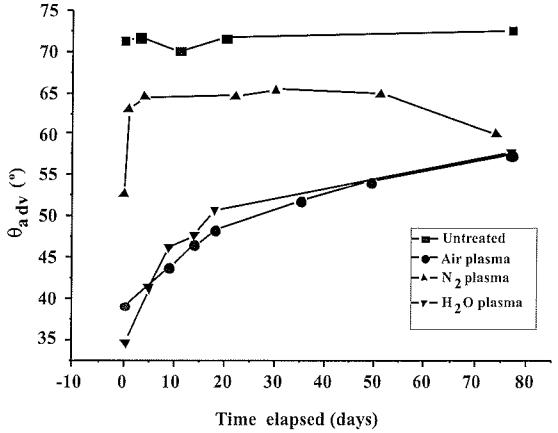

Fig. 9: Evolution of advancing water contact angle as a function of time elapsed after the treatment.

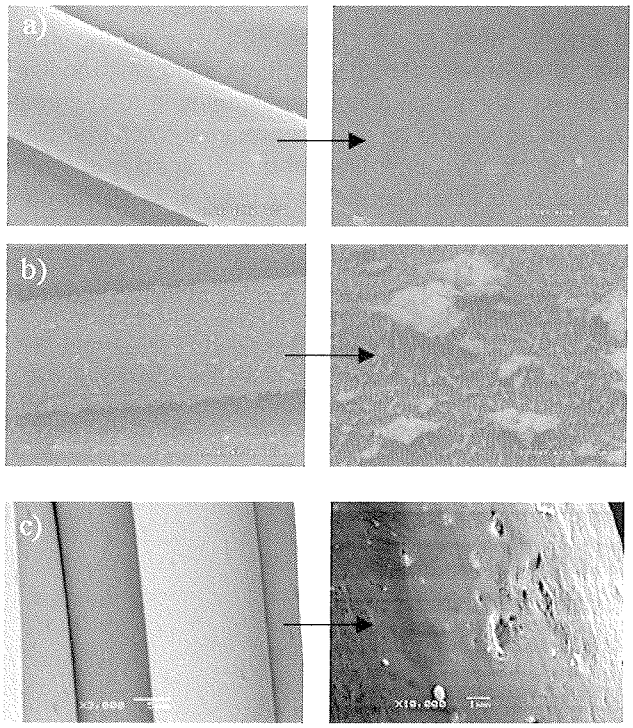

Fig. 10: Scanning Electron Micrographs of PA6 (a) Untreated, (b) 5 min O_2 RF plasma and (c) 15 min O_2 post-discharge treated.

Contact angle results (Fig. 11) showed improved adhesion of chitosan on the surface of H_2O RF plasma-treated PA6.

The presence of chitosan on the surface of the fibres increased colour intensity of the dyeings (Fig. 12), with respect to those only treated with plasma. This is most probably due to the good interaction of the sulfonic groups of the acid dyestuff studied with the amine groups of the chitosan biopolymer deposited on the surface of polyamide 6 fibres.

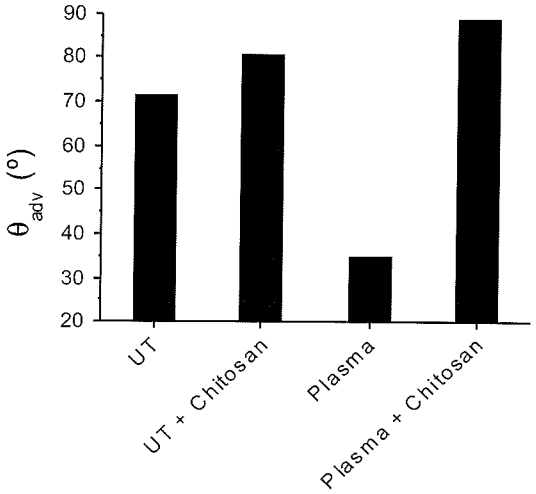

Fig. 11: Advancing contact angle of UT and H_2O RF plasma treated PA6 post-treated with chitosan.

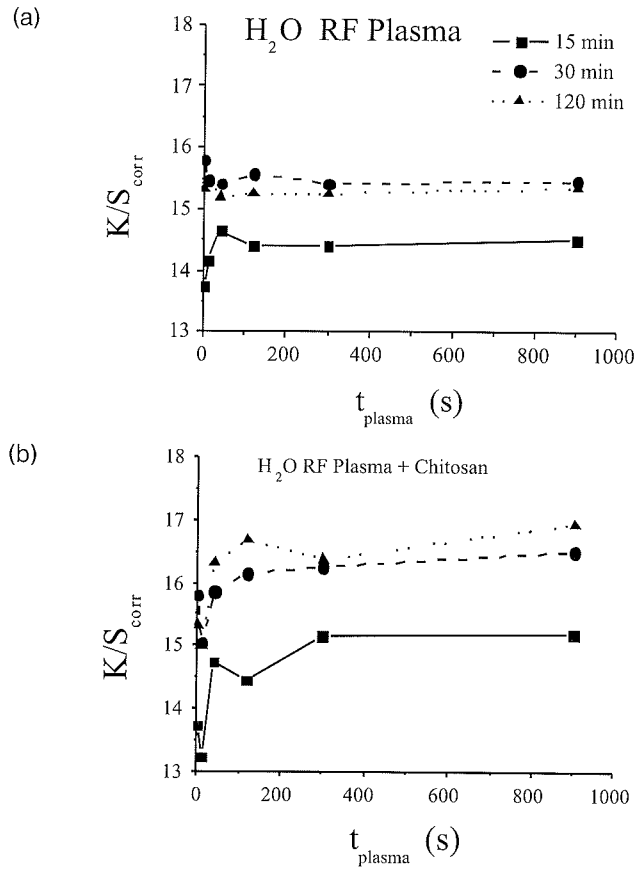

Fig. 12: K/S_{corr} of PA6 fabric treated different times in H_2O plasma (a) and post-treated with chitosan (1.25 g/l) (b) in dyeings with acid dyestuff.

4 Conclusions

Consumers increasingly demand for fabrics with improved properties, and are also more environmentally conscious. In this context plasma treatment of fibers and fabrics provides an alternative technology which allows complying with both requirements.

As reviewed in the paper, plasma and post-discharge treatments improve wool and PA6 wettability, reduce shrink-resistance of wool, and the etching of the fatty-layer on the surface of wool allows control over the wetting properties in the post-application of different finishing products (such as softeners). The ageing of wetting properties is a parameter to control in the post-application of finishing products. The application of a biopolymer on PA6 fabrics has been enhanced by plasma treatments, and it promotes higher colour intensity in dyeing with acid dyes.

Acknowledgments

The authors acknowledge the support of Departament d'Educació i Universitats of Generalitat de Catalunya for the post-doc fellowship of CC.

References

/1/ M. Feughelman, "Mechanical Properties and Structure of Alpha-Keratin Fibres: Wool, Human Hair and Related Fibres", University New South Wales Press, Sydney 1997.

/2/ A. P. Negri, H. J. Cornell, D. E. Rivett "A model for the surface of keratin fibers" Textile Res. J., Vol. 63, pp. 109-115, 1993.

/3/ C.Canal, P.Erra, R.Molina, E.Bertran "Regulation of surface hydrophilicity of plasma treated wool fabrics" Textile Res. J. Vol.77, nş8, pp.559-564, 2007.

/4/ J. Gacén "Fibras de Poliamida" Universitat Politčcnica de Catalunya, Terrassa, 1986.

/5/ IPPC Reference Document on Best Available Techniques for the Textile Industry European Comission, Seville, 2003.

/6/ A. Grill, "Cold Plasma in Materials Fabrication, From Fundamentals to Applications", IEEE Press, New York 1993.

/7/ I. M. Zuchairah, M. T. Pailthorpe, S. K. David, "Effect of Glow Discharge Polymer Treatments on the Shrinkage Behavior and Physical Properties of Wool Fabric"Textile Res. J, Vol. 67, pp. 69-74, 1997.

/8/ P. Erra, R. Molina, D. Jocic, M.R. Julia, A. Cuesta, J.M.D. Tascon, "Shrinkage Properties of Wool Treated with Low Temperature Plasma and Chitosan Biopolymer" Textile Res. J., Vol. 69, pp. 811-815, 1999.

/9/ A. Ricard, "Présentation physique des plasmas hors equilibre" in "Applications Innovantes des Plasmas Hors Equilibre", Ed. Ecrin, Paris, 2004.

/10/ I.B. Denysenko, et al. "Nanopowder management and control of plasma parameters in electronegative SiH4 plasmas" J. Appl. Phys., Vol.94, No. 9, pp.6097-6107, 2003.

/11/ K.N. Ostrikov, M.Y. Yu, S.V. Vladimirov et al. "On the realization of the current-driven dust ion-acoustic instability", Phys. Plasmas Vol. 6, pp.737-740, 1999.

/12/ Ostrikov KN, Yu MY, Azarenkov NA, "Nonlinear effects of ionization on surface waves on a plasma-metal interface", J. Appl. Phys. Vol. 84, No. 8, p.p. 4176-4179, 1998.

/13/ K.N. Ostrikov, M.Y. Yu, "Ion-acoustic surface waves on a dielectric-dusty plasma interface" IEEE Transactions on Plasma Science Vol. 26, no.1, pp. 100-103, 1998.

/14/ K.N. Ostrikov, M.Y. Yu, H. Sugai, "Standing surface waves in a dust-containated large-area planar plasma source" J. Appl. Phys Vol. 86, no. 5, pp. 2425-2430, 1998

/15/ K.N. Ostrikov, M.Y. Yu, H. Sugai "Charging and trapping of macroparticles in near-electrode regions of fluorocarbon plasmas with negative ions" Phys. Plasmas Vol. 8(7), pp. 3490-3497, 2001.

/16/ K.N. Ostrikov, S. Yu, M.Y. Yu "Power transfer and mode transitions in low-frequency inductively coupled plasmas" J. Appl. Phys. Vol. 88, no. 5, pp. 2268-2271, 2000.

/17/ G. Arnoult, R.P. Cardoso, T. Belmonte, G. Henrion "Flow transition in a small scale microwave plasma jet at atmospheric pressure" Appl. Phys Letters Vol. 93, no. 19, art. no. 191507, 2008.

/18/ T. Belmonte, R.P. Cardoso, G. Henrion, F. Kosior "Collisional-radiative modelling of a helium microwave plasma in a resonant cavity" J. Phys. D: Appl. Phys., Vol. 40, no. 23, pp. 7343-7356, 2007.

/19/ M.K. Sunkara, S. Sharma, R. Miranda, et al. "Bulk synthesis of silicon nanowires using a low-temperature vapor-liquid-solid method" Appl. Phys Lett. Vol. 79, no. 10, pp. 1546-1548, 2001.

/20/ S. Vaddiraju, A. Mohite, A. Chin, et al. "Mechanisms of 1D crystal growth in reactive vapor transport: Indium nitride nanowires" Nano Lett. Vol. 5, no. 8, pp. 1625-1631, 2005.

/21/ K.C. Krogman, T. Druffel, M.K. Sunkara "Anti-reflective optical coatings incorporating nanoparticles" Nanotechnol. Vol 16, no. 7, pp. S338-S343, 2005.

/22/ J. Thangala, S. Vaddiraju, R. Bogale, et al. "Large-scale, hot-filament-assisted synthesis of tungsten oxide and related transition metal oxide nanowires" Small Vol. 3, no. 5, pp. 890-896, 2007.

/23/ H. Chandrasekaran, G.U. Sumanasekara, M.K. Sunkara "Rationalization of nanowire synthesis using low-melting point metals" J. Phys. Chem. B Vol. 110, no. 37, pp. 18351-18357, 2006.

/24/ M. Mozetic, et al. "An iron catalytic probe for determination of the O-atom density in an Ar/O-2 afterglow" Plasma Chem. Plasma Process, Vol. 26, no. 2, pp. 103-117, 2006.

/25/ M. Mozetic, U. Cvelbar, A. Vesel, et al. "A diagnostic method for real-time measurements of the density of nitrogen atoms in the postglow of an Ar-N-2 discharge using a catalytic probe" J. Appl. Phys Vol. 97, no. 10, art. no. 103308, 2005.

/26/ U. Cvelbar, M. Mozetic, I. Poberaj, et al. "Characterization of hydrogen plasma with a fiber optics catalytic probe" Thin Solid films Vol. 475, no. 1-2, pp. 12-16, 2005.

/27/ A. Drenik, et al. "Catalytic probes with nanostructured surface for gas/discharge diagnostics: a study of a probe signal behaviour" J. Phys D: Appl. Phys Vol. 41, no. 11, pp. 115201, 2008.

/28/ D. Vujosevic, et al. "Optical emission spectroscopy characterization of oxygen plasma during degradation of Escherichia colif." J. Appl. Phys. Vol. 101, no. 10, art. no. 103305-7, 2007.

/29/ I. Levchenko, et al. "Nanostructures of various dimensionalities from plasma and neutral fluxes" J. Phys D: Appl. Phys., Vol 40, no. 8, pp. 2308-2319, 2007.

/30/ E. Tam, et al. "Deterministic shape control in plasma-aided nanotip assembly" J. Appl. Phys. Vol. 100, no. 3, art. no. 036104, 2006.

/31/ K. Ostrikov, A.B. Murphy "Plasma-aided nanofabrication: where is the cutting edge?" J. Phys. D-Appl. Phys, Vol. 40, no. 8, pp. 2223-2241, 2007.

/32/ Denysenko IB, et al. "Inductively coupled Ar/CH4/H-2 plasmas for low-temperature deposition of ordered carbon nanostructures" J. Appl. Phys., Vol. 95, no. 5, pp. 2713-2724, 2004.

/33/ U. Cvelbar, K. Ostrikov, M. Mozetic " Reactive oxygen plasma-enabled synthesis of nanostructured CdO: tailoring nanostructures through plasma-surface interactions" Nanotechnology, Vol. 19, no. 40, art. no. 405605, 2008.

/34/ Z. Vratnica, et al. "Degradation of bacteria by weakly ionized highly dissociated radio-frequency oxygen plasma" IEEE Trans. Plasma Sci., Vol. 36, no. 4, pp. 1300-1301, 2008.

/35/ U. Cvelbar, K. Ostrikov "Deterministic Surface Growth of Single-Crystalline Iron Oxide Nanostructures in Nonequilibrium Plasma" Crystal Growth & Design, Vol. 8, no. 12, pp. 4347-4349, 2008.

/36/ U. Cvelbar, B. Markoli, I. Poberaj, A. Zalar, L. Kosec, S. Spaic "Formation of functional groups on graphite during oxygen plasma treatment" Appl. Surf. Sci., Vol. 253, no. 4, pp. 1861-1865, 2006.

/37/ N. Krstulovic, I. Labazan, S. Milosevic, U. Cvelbar, A. Vesel, M. Mozetic "Optical emission spectroscopy characterization of oxygen plasma during treatment of a PET foil" J. Phys D- Appl. Phys., Vol. 39, pp. 3799-3804.

/38/ U. Cvelbar, et al. "Oxygen plasma functionalization of poly(p-phenilene sulphide) " Appl. Surf. Sci., Vol. 253, no. 21, pp. 8669-8673, 2007.

/39/ T. Belmonte, C.D. Pintassilgo, T. Czerwiec, et. Al. "Oxygen plasma surface interaction in treatments of polyolefines" Surface Coat. Tech., Vol. 200, no. 1-4, pp. 26-30, 2005.

/40/ M. Mozetic, et al. "A method for the rapid synthesis of large quantities of metal oxide nanowires at low temperatures " Adv. Mat., Vol. 17, pp. 2138-2142, 2005.

/41/ Z.Q. Cheng, et al. "Long-range ordering of oxygen-vacancy planes in alpha-Fe2O3 nanowires and nanobelts"Chem. Mat., Vol. 20, no. 9, pp. 3224-3228, 2008.

/42/ U. Cvelbar, Z.Q. Chen, M.K. Sunkara, et al. "Spontaneous Growth of Superstructure alpha-Fe2O3 Nanowire and Nanobelt Arrays in Reactive Oxygen Plasma", Small, Vol. 4, no. 10, pp. 1616-1614, 2008.

/43/ U. Cvelbar, M. Mozetic "Behaviour of oxygen atoms near the surface of nanostructured Nb2O5" J. Phys. D: Appl. Phys, Vol. 40, no. 8, pp. 2300-2303, 2007.

/44/ U. Cvelbar, M. Mozetic, M. Klanjsek-Gunde, "Selective oxygen plasma etching of coatings" IEEE Transactions Plasma Sci., Vol. 33, no. 2, pp. 236-237, 2005.

/45/ T. Vrlinic, et al. "Rapid surface functionalization of poly(ethersulphone) foils using a highly reactive oxygen-plasma treatment " Surf. Int. Anal., Vol. 39, no. 6, pp. 476-481, 2007.

/46/ U. Cvelbar, M. Mozetic, D. Babic, et al. "Influence of effective pumping speed on oxygen atom density in a plasma post-glow reactor" Vacuum, Vol. 80, no. 8, pp. 904-907, 2006.

/47/ I. Levchenko, K. Ostrikov, M. Keidar, et al. "Modes of nanotube growth in plasmas and reasons for single-walled structure" J. Phys. D: Appl. Phys, Vol. 41, no. 13, 132004, 2008.

/48/ Z. Vratnica, D. Vujosevic, U. Cvelbar, et al. "Degradation of bacteria by weakly ionized highly dissociated radio-frequency oxygen plasma" IEEE Trans. Plasma Sci., Vol. 36, no. 4, pp. 130-1301, 2008.

/49/ U. Cvelbar, B. Markoli, I. Poberaj, A. Zalar, L. Kosec, S. Spaic " Formation of functional groups on graphite during oxygen plasma treatment" Appl. Surf. Sci., Vol. 253, no. 4, pp. 1861-1865, 2006.

/50/ N. Krstulovic, I. Labazan, S. Milosevic, U. Cvelbar, A. Vesel, M. Mozetic "Optical emission spectroscopy characterization of oxygen plasma during treatment of a PET foil" J. Phys., D: Appl. Phys,. Vol. 39, pp. 3799-3804, 2006.

/51/ U. Cvelbar, D. Vujosevic, Z. Vratnica, M. Mozetic "The influence of substrate material on bacteria sterilization in an oxygen plasma glow discharge" J. Phys. D: Appl. Phys., Vol. 39, pp. 3487-3493, 2006.

/52/ R. Molina, P. Jovancic, D. Jocic, E. Bertran, P. Erra, "Surface characterization of keratin fibres treated by water vapour plasma" Surf. Interface Anal., Vol. 35, pp. 128-135, 2003.

/53/ G. Viera, J. Costa, F. J. Compte, E. Garcia-Sanz, J. L. Andujar, E.Bertran, "Accurate electrical measurements for in situ diagnosis of RF discharges in plasma CVD processes" Vacuum, Vol. 53, pp. 1-5, 1999.

/54/ C.Canal, F.Gaboriau, R.Molina, P.Erra, A.Ricard, "Role of the active species of plasmas involved in the modification of textile materials", Plasma Process. Polym. Vol. 4, pp. 445-454, 2007.

/55/ C.Canal, R.Molina, P.Erra, A.Ricard "Effects of N_2 post-discharge plasma treatments on wool fabrics" Eur. Phys. J. Applied Phys. Vol. 36, pp. 35-41, 2006.

/56/ C.Canal, R.Molina, E.Bertran, P.Erra "Polysiloxane softener coatings on plasma-treated wool: study of the surface interactions" Macromol. Mater. Eng., Vol. 292 no. 7, p.p. 817-824, 2007

/57/ R.Molina, P.Jovancic, F.Comelles, E.Bertran, P.Erra "Shrink-resistance and wetting properties of keratin fibres treated by glow discharge" J. Adhesion Sci. Technol., Vol. 16, pp.1469-1485, 2002.

/58/ C.W. Kan, K. Chan, C.W.M. Yuen, M.H. Miao, "Low temperature Plasma on Wool substrates: The Effect of the Nature of the Gas" Textile Res. J., Vol.69, pp. 407-416,1999.

/59/ C. Canal, F. Gaboriau, A. Ricard, M. Mozetic, U. Cvelbar, A. Drenik, "Density of O-atoms in an afterglow reactor during treatment of wool", Plasma Chem. Plasma Process., Vol. 27 no. 4, pp. 404-413, 2007.

/60/ C.Canal, R.Molina, A.Navarro, E.Bertran, P.Erra "Effects of low temperature plasma on wool and wool/nylon blend dyed fabrics" Fibers Polym. Vol. 9 no. 3, pp.293-300, 2008.

/61/ C.Canal, R.Molina, E.Bertrán, P.Erra "Wettability, ageing and recovery process of plasma treated polyamide 6" J. Adhesion Sci.Technol., Vol.13, pp. 1077-1089, 2004.

Cristina Canal
Pharmacy and Pharmaceutical Technology Dpt.,
Faculty of Pharmacy, University of Barcelona (UB),
Avda. Joan XXIII s/n, 08028 Barcelona, Spain.
E-mail: cristinacanal@ub.edu

Prispelo (Arrived): 17.09.2008 *Sprejeto (Accepted): 15.12.2008*

PLASMA FLUORINATION FOR IMPROVING OF THE PERMEABILITY, WETTING, BIOCOMPATIBILITY AND OPTICAL ABSORPTION OF DIFFERENT POLYMERS

Fabienne Poncin-Epaillard*, Dominique Debarnot

PCI, UMR 6120 CNRS-Université du Maine, Le Mans, France

Key words: plasma, tetrafluormethane, flourine, hydrogen, substitution, polymer, epoxy

Abstract: Polymer materials are of great interest for many applications due to their easy processing, mass production and low cost compared to other materials. However, some of their surface properties are poor and must be improved for the selected application. For example, polymers such as unsaturated polyesters, (co)polyolefins are sensitive to water sorption. Reversible phenomena as water diffusion, irreversible phenomena such as chain scissions and chemical degradations can be both at the origin. CF_4 plasma-treated layer improves drastically the barrier effects. Superhydrophobic surfaces, as lotus leaves correspond to hydrophobic surfaces whose water contact angle is higher than 150°. Such surfaces present weak physical properties like optical and mechanical ones but good biocompatibility. Two new different approaches of CF_4 plasma treatment are proposed leading to stable and transparent polymeric superhydrophobic surfaces. Many integrated photonic devices for micro-electro-optical-mechanical system based on epoxy polymer present high optical losses at near-infrared (IR) wavelengths mainly assigned to absorption from vibrational overtones of the carbon-hydrogen bonds. These losses can be reduced by the substitution of hydrogen atoms from C-H bonds with heavier atoms such as fluorine obtained through a plasma fluorination.

Modifikacija polimerov s plazemsko flourinacijo za izboljšanje prepustnosti, omočljivosti, biokompatibilnosti in optičnih lastnosti

Kjučne besede: plazma, tetrafluormetan, fluor, vodik, substitucija, polimer, epoksi

Izvleček: Polimerni materiali so zanimivi za uporabo zaradi preproste obdelave in nizke cene. Nekatere njihove lastnosti pa niso najboljše, zato jih moramo pred uporabo spremeniti. Nekateri polimeri, kamor sodijo tudi nenasičeni poliestri in poliolefini, so občutljivi na absorpcijo vode. V tovrstnih materialih se pojavljajo reverzibilni procesi (na primer difuzija vode) in nereverzibilni procesi (na primer trganje polimernih verig in degradacija polimerov). Obdelava s plinsko plazmo, ki vsebuje plin CF_4, lahko drastično spremeni tovrstne procese. Po obdelavi lahko opazimo izredno povečanje hidrofobnosti materiala, saj lahko kontaktni kot vodne kapljice naraste preko 150°. Takšno stanje površine, ki ga včasih imenujemo pojav lotusovega lista, vodi k zelo dobri biokompatibilnosti materialov. V prispevku prikazujemo dva originalna pristopa k funkcionalizaciji površine polimernih materialov s CF_4 plazmo, ki vodita k stabilni funkcionalizaciji in s tem superhidrofobnosti obdelovancev. Mnoge integrirane optične naprave, ki temeljijo na uporabi epoksi polimerov, imajo visoke optične izgube v bližnjem infrardečem področju, kar razlagamo predvsem z absorpcijo na vezeh ogljika z vodikom. Tovrstne izgube lahko zmanjšamo s substitucijo vodikovih atomov s težjimi atomi, kot so fluorovi. Tovrstno substitucijo najlažje dosežemo s plazemsko flourinacijo.

1 Introduction

Many advances have been made in developing new surface treatments, such as plasma treatment, to modify physical and chemical properties of polymer surface without altering bulk properties /1-7/. One of the applications is dealing with the superhydrophobic surfaces. Natural superhydrophobic surfaces /8-9/ as observed with leaves of plants (lotus) or feathers of some birds, correspond to hydrophobic surface whose water contact angle (Q) is higher than 150° /10/. Such surfaces are sometimes called self-cleaning surfaces since a water flux will push away the particles of dirtiness /9/. Different methods to prepare such surfaces were proposed, some of them devoted to inorganic materials /11/, the other to organic materials /12-16/. The fabrication of inorganic model superhydrophobic surfaces /17-19/ allows studying the influence of the roughness on the water contact angle. Therefore, Si wafers were etched by lithography techniques to produce different topographic structures whose shape depends on the mask used. Then a hydrophobic layer of dimethyldichlorosilane, N-octyldimethylchlorosilane or heptadecafluoro-1,1,2,2-

tetrahydrodimethylchlorosilane was deposited from liquid, vapour or plasma phase /20/. The contact angle increase with the hydrophobic character of the layer depends also on the number of plots but not on their respective heights. Other superhydrophobic model surfaces are synthesized from successive alkyl ketene dimmer (AKD) and dialkyl ketone (DAK) recrystallisations /21,23/. The controlled recrystallization of such compounds allows producing surfaces with a fractal dimension varying from 2.18 to 2.29. Sol-gel techniques /24-27/ have also been developed through the copolymerization of fluoroalkylsilane with different organometallic precursors /28-29/, on aluminium /30-31/, or on titanium dioxide /32/.

Organic superhydrophobic surfaces are obtained when poly(tetrafluoroethylene) (PTFE) /33/ or polystyrene (PS) /18-19,34/ spherical microparticles are dispersed in a hy-

drophobic polymer matrix. Hozumi and coworkers /25,35/ describe the fabrication of superhydrophobic surfaces based on plasma enhanced chemical vapor deposition of organosilanes in presence of oxygen onto silicon wafer. Then in a second step, the fluoroalkylsilane replaces O_2 in the plasma phase and the deposited layer becomes hydrophobic and superhydrophobic. Pulsed plasma of 1H,1H,2H,2H-heptadecafluorodecylacrylate /13/ also leads to the deposition of a fluorinated layer whose chemical structure is close to the monomer vapour and its roughness varies from 0 to 100 ěm depending on the initial roughness of the PTFE substrate /14/. Favia *et al.* /15/ proposed the pulsed RF plasma deposition of tetrafluoroethylene (TFE). Superhydrophobic surfaces composed of juxtaposition of very thin ribbons whose crystallinity is close to PTFE lead to a 150°-165° contact angle. However, this surface structure depends strongly on the plasma parameters (value of the duty cycle in pulsed RF glow discharges fed with TFE). CF_4 plasma surface modification of spin coated polybutadiene onto various substrates leads also to superhydrophobic surfaces (Q = 172%) /16/. Another illustration is given with the sputtering of PTFE onto polypropylene (PP) film /36/; the roughness is due to the PTFE sputtering by Ar+ bombardment but also by the PP degradation during the sputtering. The dissolution of polypropylene in a *p*-xylene/methyl ethyl ketone solution followed by its deposition onto the substrate and the solvents evaporation also leads to a rough hydrophobic surface /37/.

Here, the synthesis in dry medium (plasma) is proposed leading to stable and transparent polymeric superhydrophobic polyethylene surfaces.

Barrier properties for packaging materials have been improved over the years to protect packaged foodstuffs from the oxidation and the moisture. Owing to their favourable performances as efficient barrier materials, ethylene-vinyl alcohol copolymers (EVOH) are used in many applications and therefore are widely used in packaging and protective coating. Among all the new technologies involved in improving the barrier properties of EVOH films, one in particular is often used: the creation of multilayer systems mostly through the plasma technique /38/.

The glycidyl ether of bisphenol A (epoxy-based) polymer whose common name is SU-8, widely used as negative photoresist, has also been studied for micro-electro-optical mechanical system (MEOMS) applications and optical waveguides /39-43/. However, it presents high optical losses at near-infrared (IR) wavelengths mainly assigned to absorption from vibrational overtones of the carbon-hydrogen (C-H) bonds. These losses can be reduced by the substitution of hydrogen atoms of C-H bonds with heavier atoms such as fluorine (F), deuterium (D) or chlorine (Cl) ones /11-14/ thanks to the plasma technique allowing the substitution of hydrogen atoms by fluorine ones.

The chemical and topographic modifications of the polymeric surface induced by plasma treatment were found to be strongly influenced by the type of feed gas and parameters employed. Studied plasma parameters are the discharge power, treatment time and nature of plasma (CF_4 or mixtures of CF_4/H_2), in order to optimize plasma treatment for different applications.

2 Plasma fluorination of polymers

Poly(ethylene-co-vinyl alcohol) and polyethylene films have been modified by CF_4 microwave plasma. The influence of vinyl alcohol comonomer contents on the properties of these materials under CF_4 microwave plasma has been studied by means of surface energies, atomic force microscopy (AFM), secondary ion mass spectroscopy (SIMS) and calorimetric measurements (DSC). The CF_4 plasma treatment improved the hydrophobicity and the roughness of the film surfaces was hardly changed. Lower the vinyl alcohol comonomer content, higher is the increase of the water contact angle value (Table 1).

Table 1: Wettability of CF_4 plasma-treated polymers

Sample	θH_2O	γ^{Sd}	γ^{Sp}	γ^{S}
LLDPE [OH] = 0 mol%	92	26.3	1.2	27.5
LLDPE 50W 15 min	95	21.0	1.1	22.1
EVOH(E) [OH] = 56 mol%	76	32.8	3.8	36.6
EVOH(E) 50W 15 min	98	12.0	3.2	15.2
EVOH(F) [OH] = 68 mol%	72	30.5	7.3	37.8
EVOH(F) 50W 15 min	99	15.9	2.7	18.6
EVOH(S) [OH] = 71 mol%	52	29.3	17.2	46.6
EVOH(S) 50W 15 min	105	12.2	1.5	13.7

The decrease of surface energy of polymeric material, corresponding to an increase of the water contact angle, was associated to a chemical surface modification. XPS analyses of EVOH, polyethylene (Fig. 1) or SU8 plasma-treated surfaces give evidence of fluorinated groups attachment.

Depending on plasma parameters, the chemical surface structure varies from CHF group to the Teflon-like structure. The atomic F/C ratio can reach the value of 0.5 with pure CF_4 plasma treatment. Addition of hydrogen to the CF_4 plasma phase allows to control the fluorine atom density in the plasma phase and therefore to modify the surface fluorination rate. Addition of 10% of hydrogen leads to the lowest polar surface energy of plasma-treated SU8 surface (Fig. 2).

3 Superhydrophobic plasma-fluorinated polymers

Whatever the plasma phase composition is, the elemental composition of the CF_4 plasma-treated polyethylene is associated to the grafting of $CHF-CH_2$, CF, CF_2 and CF_3 functional groups whose proportions depend on plasma parameters. But another side effect of the plasma interaction is observed and corresponds to the surface degradation and roughness. Drastic powers, long durations or oxygen plasma pre-treatment emphasize this phenomenon. The

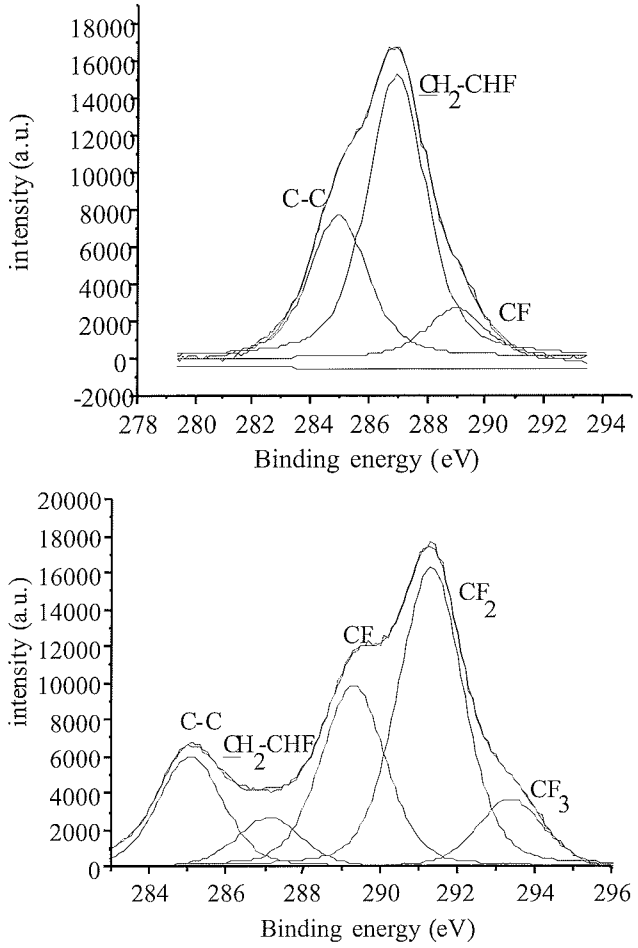

Fig. 1: Plasma-fluorinated HDPE in different conditions.

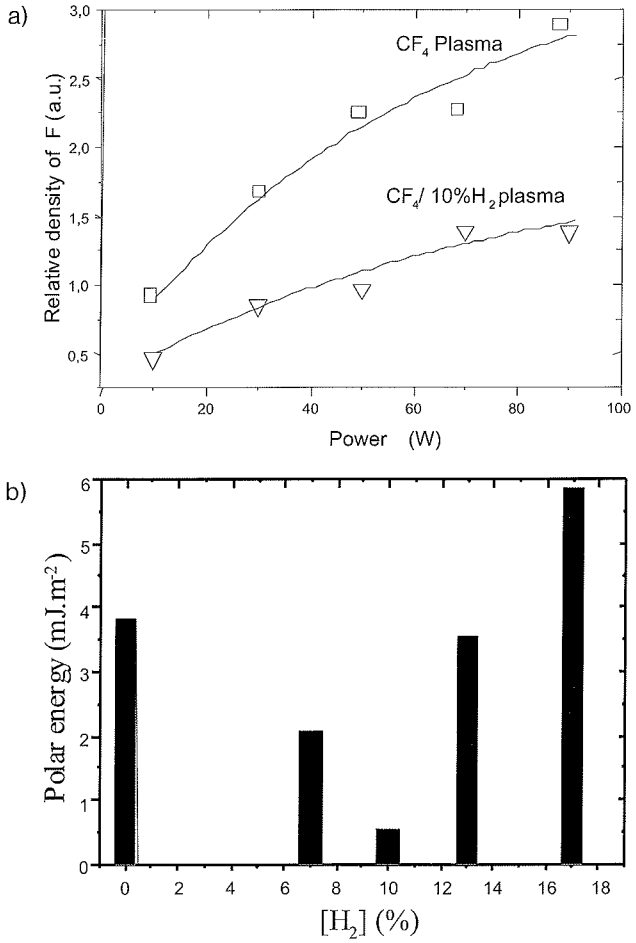

Fig. 2: Dependence of gaseous fluorinated species on discharge power (a), of surface energy of plasma-treated SU8 on hydrogen proportions (b).

combination of surface fluorination and roughness induces the superhydrophobic character appearance (i.e. water contact angle higher than 150°). Beside this evolution, if the discharge power and/or duration are important, the hysteresis of the contact angle becomes smaller. Figure 3 illustrates the domain of roughness leading to polyethylene superhydrophobic surface.

4 Applications of plasma-fluorinated polymers

These plasma-fluorinated surfaces may be used in different domains. The first one is dealing with the biomaterials field. The bioadhesion or the non adhesion of proteins, cells onto the biomaterials is strongly dependent on the nature of the interactions between these two entities. Among them, hydrophobic-hydrophobic and electrostatic ones are the predominant ones. However, in the case of nonadhesion processes, biosurfaces bearing a superhydrophobic character may act as self-cleaning surface towards the biomolecules adhesion. The self-cleaning property implies a fast dynamic de-wetting of a water thin film as shown in Fig. 4.

Another application is dealing with barrier properties and permeability of plasma-treated polymers. If the water permeability coefficient is almost constant after the plasma fluorination of linear low density polyethylene, this coefficient is strongly altered by the surface fluorination of EVOH, especially when the vinyl alcohol content is increasing (Table 2). This barrier effect is also noticed with plasma fluorination of polyamide 12.

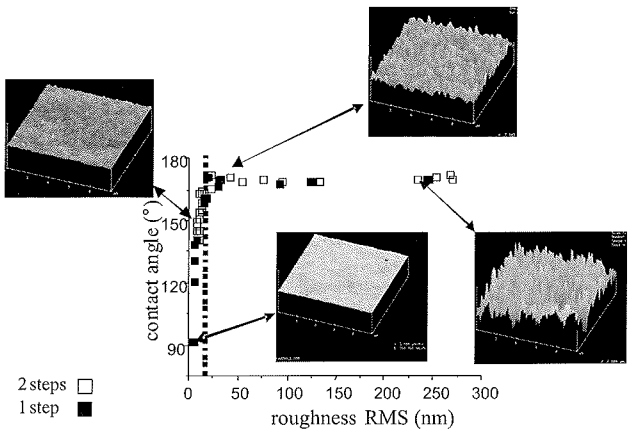

Fig. 3: Dependence of the contact angle versus roughness of plasma-fluorinated polyethylene.

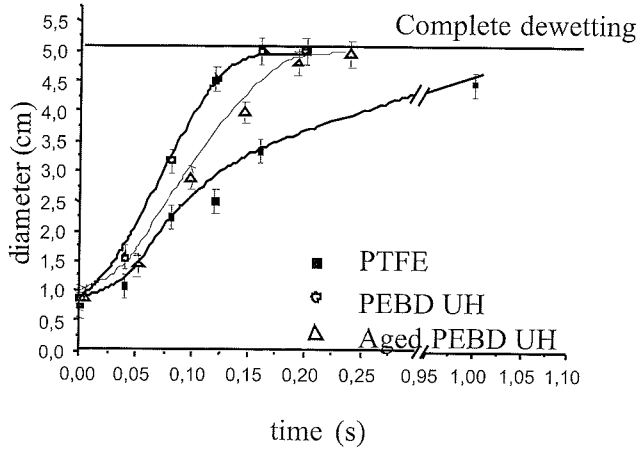

Fig. 4: Dynamic de-wetting of thin water layer onto polymer surfaces.

Table 2: Water permeability of plasma-fluorinated polymers.

Sample	[OH] (mol %)	Thickness (μm)	P (Barr)	γ^S
LLDPE [OH] = 0 mol%	0	55	68	27.5
LLDPE 50W 15 min	0	55	64	22.1
EVOH(E) [OH] = 56 mol%	56	15	241	36.6
EVOH(E) 50W 15 min	56	14	86	15.2
EVOH(F) [OH] = 68 mol%	68	15	222	37.8
EVOH(F) 50W 15 min	68	15	1865	18.6
EVOH(S) [OH] = 71 mol%	76	14	31350	46.6
EVOH(S) 50W 15 min	76	101	17754	13.7

Fluorination, obtained with the CF_4 plasma treatment allows reducing water permeability of the films. The higher hydrophilicity of the base materials, the more water barrier effect of CF_4 plasma treatment is obtained compared to the non-treated materials. However, the very significant enhancement of the water barrier properties of EVOH(S) after plasma treatment was explained not only by the introduction of fluorine groups but an increase of the crystallinity too, so that the diffusivity and solubility of water through the CF_4 plasma treated film were more reduced. The effect of surface modification on water permeability decreased the water uptake at the film surface at the feed side so that the plasticization effect of the hydrophilic films by the sorbed water molecules was decreased during the water vapour permeation.

The last illustration will be given with the decrease of optical losses thanks to the plasma fluorination. The measured propagation loss values of untreated and plasma-treated SU8 single-mode planar waveguides for both transverse electric (TE) and transverse magnetic (TM) polarizations at 632.8, 1304 and 1540 nm are shown in Fig. 5.

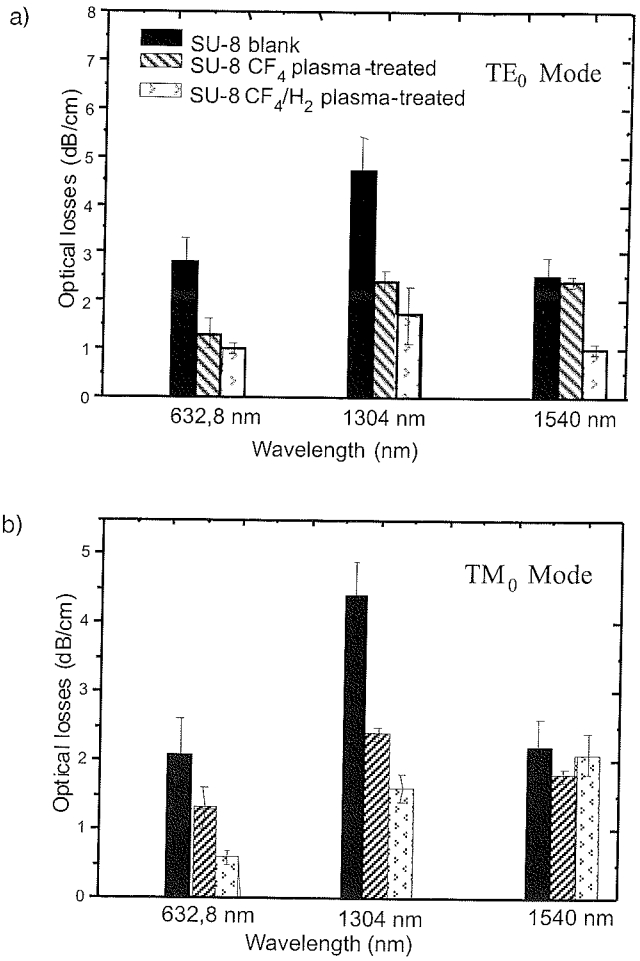

Fig. 5: Optical losses of plasma-fluorinated SU8 waveguide

5 Conclusions

Plasma fluorination of polymers leads to a chemical surface modification through the grafting of fluorinated groups. The appearance of new pendant groups induce a hydrophobic and sometimes a superhydrophobic character leading to specific properties requested in biomaterial, permeation or photonic fields.

References

/1/ F. Poncin-Epaillard, J. C. Brosse, and T. Falher, Macromolecules, vol. 30, pp.4415, 1997.

/2/ J. Fresnais, J. P. Chapel, and F. Poncin-Epaillard, Surf. Coat. Techn., vol. 200, pp. 5296, 2006.

/3/ S. Marais, M. Metayer, M. Labbe, J. M. Valleton, S. Alexandre, J. M. Saiter, F. Poncin-Epaillard, Surf. Coat. Techn., vol. 122, pp. 247, 1999.

/4/ N. Médard, J.-C. Soutif, F. Poncin-Epaillard, Surf. Coat. Techn., vol. 160, pp.197, 2002.

/5/ A. Vesel, I. Junkar, U. Cvelbar, J. Kovac, M. Mozetic, Surf. Int. Anal., vol. 40, no.11, pp. 1444, 2008.

/6/ A. Vesel, M. Mozetic, A. Zalar, Surf. Int. Anal., vol. 40, no.3-4, pp. 661, 2008.

/7/ A. Vesel, M. Mozetic, A. Zalar, Vacuum, vol. 82, no. 2, pp. 248, 2008.

/8/ C. Neinhuis, and W. Barthlott, An. Bot., vol. 79, pp. 667, 1997.

/9/ E. Nun, M. Oles, and B. Schleich, Macromolecular symposium, vol. 187, pp. 677, 2002.

/10/ K. Tadanaga, J. Morinaga, A. Matsuda, and T. Minami, Chem. Mater., vol. 12, pp. 590, 2000.

/11/ T. Nishino, M. Meguro, K. Nakamae, M. Matsushita, and Y. Ueda, Langmuir, vol. 15, pp. 4321, 1999.

/12/ F. Poncin-Epaillard, I. Rouger, J. P. Gilles, and J. P. Grandchamp, J. Macromol. Sci., vol. 31, pp. 1087, 1994.

/13/ S. R.Coulson, I. S. Woodward, J. P. S. Badyal, and S. A. Brewer, C. Willis, Chem. Mater., vol. 12, pp. 2031, 2000.

/14/ S. R. Coulson, I. S. Woodward, J. P. S. Badyal, S. A. Brewer, C. Willis, J. Phys. Chem., vol. 104, pp. 8836, 2000.

/15/ P. Favia, G. Cicala, A. Milella, F. Palumbo, P. Rossini, R. D'Agostino, Surf. Coat. Tech, vol. 169-70, pp. 609, 2003.

/16/ I. S. Woodward, W. C. E. Schofield, V. Roucoules, J. P. S. Badyal, Langmuir, vol. 19, no.8, pp. 3432, 2002.

/17/ R. E. Jonson, Jr. and R. H. Dettre, Adv. Chem. Ser., vol. 43, pp.112, 1964.

/18/ D. Öner and T. J. McCarthy, Langmuir, vol. 16, pp. 7777, 2000.

/19/ W. Chen, A. Y. Fadeev, M. C. Hsieh, D. Öner, J. Youngblood and T. J. McCarthy, Langmuir, vol. 15, pp. 3395, 1999.

/20/ S. Tsuruta, K. Morimoto, T. Hirotsu and H. Suzuki, J. Appl. Phys Part 1, Jpn, vol. 45, pp. 8502, 2006.

/21/ T. Onda, S. Shibuichi, N. Satoh and K. Tsujii, Langmuir, vol. 12, pp. 2125, 1996.

/22/ S. Shibuichi, T. Onda, N. Satoh and K. Tsujii, J. Phys. Chem., vol. 100, pp.19512, 1996.

/23/ F. Iacona, G. Casella, F. La Via, S. Lombardo, V. Raineri and G. Spoto, Microelectronic Eng., vol. 50, pp. 67, 2000.

/24/ A. Hozumi and O. Takai, Thin Solid Films, vol. 334, pp. 54, 1998.

/25/ T. Nakagawa and M. Soga, J. Non-crystalline Solids, vol. 260, pp.167, 1999.

/26/ Y. Li, W. P. Cai, B. Q. Cao, G. T. Duan, F. Q. Sun, C. C. Li and L. C. Jia, Nanotechnology, vol. 17, pp. 238, 2006.

/27/ B. S. Hong, J. H. Han, S. T. Kim, Y. J. Cho, M. S. Park, T. Dolukhanyan and C. Sung, Thin Solid Films, vol. 351, pp. 274, 1999.

/28/ T. Yoneda and T. Morimoto, Thin Solid Films, vol. 351, pp. 279, 1999.

/29/ K. Tadanaga, N. Katata and T. Minami, J. Am. Ceramic Soc., vol. 80, pp. 1040, 1997.

/30/ K. Tadanaga, N. Katata and T. Minami, J. Am. Ceramic Soc., vol. 80, pp. 3213, 1997.

/31/ X. T. Zhang, M. Jin, Z. Liu, S. Nishimoto, H. Saito, T. Murakami and A. Fujishima, Langmuir, vol. 22, pp. 9477, 2006.

/32/ G. Yamauchi, J. D. Miller, H. Saito, K. Takai, T. Ueda, H. Takazawa, H. Yamamoto and S. Nishi, Colloids Surfaces, vol. 116, pp. 125, 1996.

/33/ A. Nakajima, K. Hashimoto and T. Watanabe, Monatsh. Chem.,vol. 132, pp. 31, 2001.

/34/ A. Hozumi, H. Sekoguchi, N. Sugimoto and O. Takai, Trans. Inst. Metal Finishing, vol. 76, pp. 51, 1998.

/35/ J. Youngblood and T. J. McCarthy, Macromolecules, vol. 32, pp. 6800, 1999.

/36/ H. Y. Erbil, A. L. Demirel, Y. Avci and O. Mert, Science, vol. 299, pp. 1377, 2003.

/37/ R. D'Agostino, Plasma Deposition, Treatment and Etching of Polymers, Academic Press, Boston, 1990.

/38/ N. Pelletier, B. Bęche, E. Gaviot, L. Camberlein, N. Grossard, F. Polet, J. Zyss, IEEE Sensors J., vol. 6, no. 3, pp. 565, 2006.

/39/ B. Bęche, N. Pelletier, E. Gaviot, J. Zyss, Opt. Commun., vol. 230, no. 1-3, pp. 91, 2004.

/40/ J. S. Kim, J. W. Kang, J. Kim, J. Jpn. J. Appl. Phys., vol. 42, pp. 1277, 2003.

/41/ B. Bęche, J. F. Jouin, N. Grossard, E. Gaviot, E. Toussaere, J. Zyss, Sens. Act. A, vol. 114, no. 1, pp. 59, 2004.

/42/ N. Pelletier, B. Bęche, N. Tahani, J. Zyss, L. Camberlein, E. Gaviot, Sens. Act. A, vol. 135, pp. 179, 2007.

Fabienne Poncin-Epaillard, Dominique Debarnot
PCI, UMR 6120 CNRS-Université du Maine, avenue O Messiaen 72085 Le Mans France
**Email: Fabienne.poncin-epaillard@univ-lemans.fr*

Prispelo (Arrived): 17.09.2008 *Sprejeto (Accepted): 15.12.2008*

XPS STUDY OF SURFACE MODIFICATION OF DIFFERENT POLYMER MATERIALS BY OXYGEN PLASMA TREATMENT

Alenka Vesel

Jozef Stefan Institute, Ljubljana, Slovenia

Key words: polymer; PES; PET; PPS; PS; PP; PA6; PTFE; cellulose; oxygen; plasma; functionalization; surface activation; surface modification, XPS

Abstract: A review on surface modification of different polymers by treatment in oxygen plasma is presented. The following polymers were studied: polyethyleneterephthalate (PET), polyethersulphone (PES), polyphenylenesulfide (PPS), Nylon 6 polyamide (PA6), polytetrafluoroethylene (PTFE), polystyrene (PS), polypropylene (PP) and cellulose (ink-jet paper and textile). The polymer samples were treated for 3 s in oxygen plasma (glow region) at a pressure of 75 Pa. Plasma was created by RF generator operating at a frequency of 13.56 MHz and a power of 200 W. The chemical changes of the surface of the samples after the plasma treatment were monitored by using X-ray photoelectron spectroscopy (XPS). The results showed that oxygen plasma treatment is an effective tool for surface modification. On all polymer surfaces increased concentrating of oxygen was detected resulting in formation of several new oxygen-containing functional groups. Groups like C-O, C=O and O=C-O were observed. The concentration of the groups which were produced at the same treatment procedure depended on polymer type. The only exception was polymer PTFE where practically no chemical changes were observed.

XPS preiskave modifikacije površine različnih polimerov s kisikovo plazmo

Kjučne besede: polimer; PES; PET; PPS; PS; PP; PA6; PTFE; celuloza; kisik; plazma; funkcionalizacija; aktivacija površine; modifikacija površine, XPS

Izvleček: Podan je pregled plazemske modifikacije površine različnih polimerov. V raziskavah so bili uporabljeni naslednji polimeri: polietilentereftalat (PET), polietersulfon (PES), polifenilensulfid (PPS), Nylon 6 poliamid (PA6), politetrafluoroetilen (PTFE), polistiren (PS), polipropilen (PP) in celuloza (ink-jet papir in tkanina). Vzorce polimerov smo obdelovali v kisikovi plazmi 3 s pri tlaku 75 Pa. Plazmo smo generirali z radiofrekvenčnim generatorjem pri frekvenci 13.56 MHz in moči 200 W. Spremembe v kemijski sestavi površine po obdelavi v plazmi smo spremljali z metodo XPS. Rezultati so pokazali, da je kisikova plazma učinkovita za modifikacijo površinskih lastnosti polimernih materialov. Ugotovili smo, da se je na površini vzorcev močno povečala koncentracija kisika, kar je imelo za posledico nastanek različnih kisikovih funkcionalnih skupin na površini kot so C-O, C=O in O=C-O. Koncentracija posameznih funkcionalnih skupin pri enakih pogojih obdelave polimerov je bila različna za različne tipe polimerov. Edina izjema je bil polimer PTFE, kjer nismo opazili nobenih sprememb na njegovi površini po obdelavi v plazmi.

1 Introduction

Polymer materials are known for their very poor adhesion properties and wettability. Therefore, they must be modified before printing, painting, coating, for improving biocompatibility etc. One of the most promising methods for modifying the surface properties of polymer materials is plasma treatment. Plasma treatment is ecologically suitable method and it is replacing the traditional wet chemical techniques, which can involve harmful chemicals. By treatment in plasma of different gases we can achieve a wide range of surface wettability, from moderate hydrophilicity to significant hydrophobicity. The hydrophobicity can be achieved by a treatment in plasma created in halogens while for achieving the hydrophilicity of the surface it is the best to use oxygen plasma. In some applications especially biological, when we want to coat the substrate with proteins or DNA for example, nitrogen or ammonia plasma is more desirable than oxygen plasma /1/. It should be noted that plasma treatment does not produce one unique functionality on a polymer surface. Typically, a distribution of several different functional groups is produced. Some of the functional groups may be important and some may actually be detrimental. Thus it is desirable to determine which of the functional group is important for a given application and to attempt to shift the distribution in favour of a specific functionality by changing the plasma gas or other plasma parameters /2/. In oxygen plasma different functional groups like C-O, C=O, O=C-O or even more exotic groups can be produced on the surface /2/,/3/.

In the literature there are reported different treatment times used for surface modification of polymers ranging from milliseconds /4/,/5/ to several minutes /6/. At milliseconds of treatment it is difficult to talk about surface functionalization, since the first thing that appears at the polymer surface is just removing of contaminants which may also lead to improved wettability. With further treatment time insertion of oxygen/nitrogen atoms at active sites on the polymer surface appears leading to the formation of various functional groups that change the surface wettability. With prolonged treatment time excessive change scission may appear leading to a layer of low-molecular-weight fragments on the surface /3/.

The main drawback of plasma treated surface is ageing. Functional groups formed on the plasma treated surface are not stable with time, as the surface tends to recover to its untreated state. Thus the surface is loosing its hydrophilic character and becoming hydrophobic. There are two processes which are usually responsible for surface ageing:

the first one is the reorientation of the polar groups into the bulk polymer and the second is the mobility of the small polymer chain segments into the matrix, both leading to different free surface energy. It was also reported that the chain mobility mainly occurs in the amorphous region while the mobility in the crystalline region is fairly limited because of an orderly packed structure. Therefore more crystalline polymers are ageing slower. Since plasma treatment can increase the surface crystallinity due to selective etching of the softer amorphous phase, the polymers treated for longer times are usually ageing slower /3/,/4/,/5/,/7/. This is not always true - too long treatment times may again lead to faster ageing due to overtreatment leading to formation of small fragments loosely bound on the surface. Such surface has a greater tendency to ageing because of migration of small fragments to the bulk.

Here it is worth to mention that plasma treatment affects only first few nanometers of material without changing the bulk properties /8/. The quickest method to check the effect of a plasma treatment on the polymer surface is to determine its wettability by contact angle measurements. But this method does note say anything about the chemical modification of the surface. One of the most powerful techniques for determination of various functional groups that can be created on the polymer surface after being exposed to plasma treatment, is X-ray photoelectron spectroscopy (XPS) /8/,/10/. The interpretation of XPS spectra can be quite difficult. A fundamental problem in polymer surface analysis is the occurrence of charging effects due to the insulating nature of polymer materials. With non-monochromatic source this effect is less pronounced than with monochromatic source. To avoid this effect charge neutralization (gun with a low energy electron flux) must be used. A common convention is to shift unfunctionlized C 1s peak (C-C) to 284.8 eV. In some cases all the carbon atoms are chemically shifted - an example is cellulose, where all carbon atoms are bound to at least one oxygen atom. For these materials a peak which is assigned to hydrocarbon contamination can be used as a reference. But this is not always possible since sometimes this peak is not clearly observable.

In general, polymers are quite stable during typical analysis times. However prolonged exposure to X-rays can produce radiation damage of the sample which can cause the spectrum to change with exposure time. A visual evidence of this is a sample discolouration /11/. For example, this can be very easily observed on paper substrates. Especially halogen containing polymers can be sensitive to X-ray induced sample degradation. The result is a loss of halogen atoms with the exposure time /12/.

2 Experimental

2.1 Plasma modification

Experiments were performed with different polymers including PP, PS, PET, PES; PPS; PA6, PTFE and cellulose materials like ink-jet paper and textile. The samples of these materials were treated in the experimental system shown in Figure 1. The system is pumped with a two-stage oil rotary pump with a pumping speed of 16 m^3/h. The discharge chamber is a Pyrex glass cylinder with a length of 200 mm and an inner diameter of 36 mm. A Pyrex glass tube with an inner diameter of 5 mm and a length of 6 cm leads to the afterglow chamber, which is also a Pyrex glass cylinder, with a length of 400 mm and an inner diameter of 36 mm. The plasma is created inside the discharge chamber with an inductively coupled RF generator, operating at a frequency of 27.12 MHz and an output power of about 200 W. The plasma's parameters are measured with a double Langmuir probe and a catalytic probe. The Langmuir probe is placed into the discharge chamber, while the catalytic probe is mounted in the afterglow chamber. Commercially available oxygen is leaked into the discharge chamber, as shown in Figure 2. The pressure is measured with an absolute vacuum gauge. The pressure is adjusted during continuous pumping using a precise leak valve. During our experiments the pressure was fixed at 75 Pa, where the density of the oxygen atoms was the highest. Using these discharge parameters an oxygen plasma with an ion density of $8x10^{15}$ m^{-3}, an electron temperature of 5 eV, and a density of neutral oxygen atoms of $4x10^{21}$ m^{-3} was obtained.

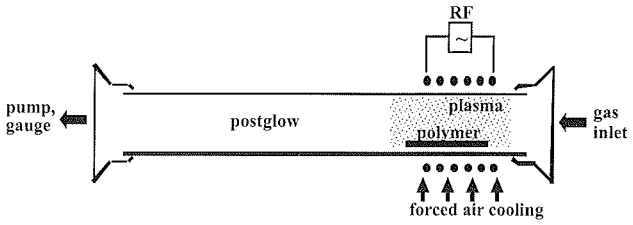

Fig. 1: The plasma chamber.

2.2 XPS characterization

The samples were exposed to air for a few minutes after the plasma treatment and then mounted in the XPS instrument (TFA XPS Physical Electronics) in order to assess the surface of the sample. The base pressure in the XPS analysis chamber was about 6×10^{-10} mbar. The samples were excited with X-rays over a 400-μm spot area with monochromatic Al $K_{\alpha1,2}$ radiation at 1486.6 eV. The photoelectrons were detected with a hemispherical analyzer positioned at an angle of 45° with respect to the normal to the sample surface. The energy resolution was about 0.6 eV. Survey-scan spectra were made at a pass energy of 187.85 eV, while for C1s, S2p, N1s, F1s and O1s individual high-resolution spectra were taken at a pass energy of 23.5 eV and a 0.1-eV step. Since the samples are insulators, we used an additional electron gun to allow for surface neutralization during the measurements. The spectra were fitted using MultiPak v7.3.1 software from Physical Electronics, which was supplied with the spectrometer. The curves were fitted with symmetrical Gauss-Lorentz functions. The peak width (FWHM) was fixed during the fitting process. In this study a C1s (C-C) peak was shifted to 285 eV.

3 Results and discussion

The effect of oxygen plasma treatment of various polymer surfaces was studied. The following polymers were used in the study:

- *only carbon containing polymers*: aliphatic polypropylene PP (Figure 2a) and aromatic polystyrene PS (Figure 2b)
- *oxygen containing polymers*: polyethylene-terephthalate PET (Figure 2c) and cellulose CELL (Figure 2d) like textile and ink-jet paper
- *sulphur containing polymers*: polyphenylenesulfide PPS (Figure 2e) and polyethersulphone PES (Figure 2f)
- *nitrogen containing polymer*: Nylon 6 polyamide PA6 (Figure 2g)
- *halogen containing polymer*: polytetrafluoro-ethylene PTFE (Figure 2h).

3.1 Carbon containing polymers

Carbon containing polymers consist of carbon and hydrogen only. Therefore their XPS spectrum is composed of one peak positioned at a binding energy of 285 eV which corresponds to C-C and C-H bonds. Since there is no oxygen in the original polymer they are very good candidates for studding the effect of oxygen plasma treatment, because it is more easily to observe new peaks due to oxygen incorporation to the surface after plasma treatment. One of such candidates is PP which consists of aliphatic chain containing carbon atoms (Figure 2a). In Figure 3a is shown a comparison of the XPS spectra of the untreated PP surface and PP surface treated for 3 s in oxygen plasma. As already mentioned the C1s spectrum of untreated sample consists of a single peak, while the C1s spectrum after the treatment clearly reveals the new peaks resulting from plasma oxidation. A more detailed understanding of these new species can be obtained using a curve fitting procedure as shown in Figure 3b. Besides the main C1 peak (C-C), there is also a peak C2 which corresponds to C-O bond, peak C3 which corresponds to C=O bond and peak C4 which corresponds to O-C=O bond.

The same is true for the case of plasma treatment of PS (Figure 4a) which is another example of the structurally simple polymer. Here, changes are more pronounced indicating a higher concentration of new functional groups at the surface. In this case not only peaks C2, C3 and C4 are observed, but additional peak C5 appeared as well at a binding energy of 290 eV (Figure 4b) which can correspond to -C(=O)-O-C(=O)- or to -O-C(=O)-O- group at the surface /12/. Also, in Figure 4a is shown a carbon C1s peak of a sample treated for 30 s. We can see that the surface is actually already saturated, since 10-times longer treatment time did not cause any remarkable changes at the surface.

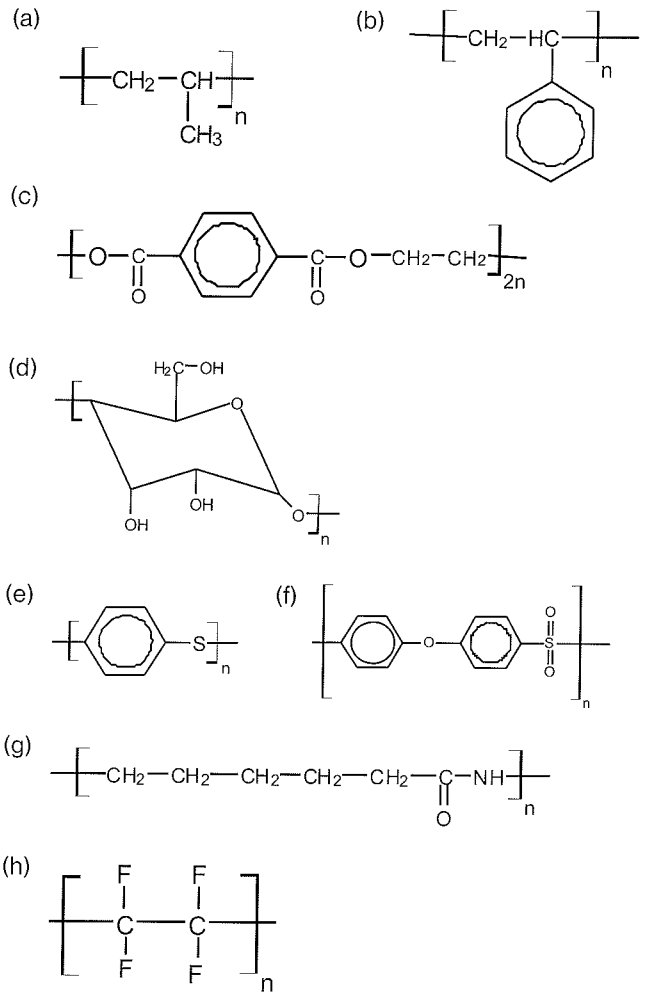

Fig. 2: Structural formulas of polymers used for plasma activation: (a) PP, (b) PS, (c) PET, (d) cellulose, (e) PPS, (f) PES, (g) PA and (h) PTFE.

Another important characteristic of untreated PS in comparison with untreated PP is a small peak at a binding energy of 291 eV - 292 eV (Figure 4a), which is not observed in the case of PP. This peak is due to the π–π^* shake-up transition and it is characteristic of the aromaticity in the phenyl ring. Therefore this peak is observed only at polymers having phenyl rings /2/,/12/. Changes in the intensity of this peak can provide information regarding the extent of ring-opening induced by plasma treatment. In our case, after the plasma treatment the intensity of this peak decreased indicating that plasma caused a destruction of the phenyl ring in PS.

3.2 Oxygen containing polymers

Oxygen containing polymers do not have so simple shape of the XPS spectrum like hydrocarbons. The interpretation of XPS spectra after oxygen plasma treatment of these polymers can be quite complex due to difficulties to distinguish between existing and newly formed oxygen functional groups at the surface. One of the polymers which is very often studied is PET /4/,/5/,/7/,/13/,/14/,/15/. In Figure 5a is shown a carbon peak for an untreated PET sur-

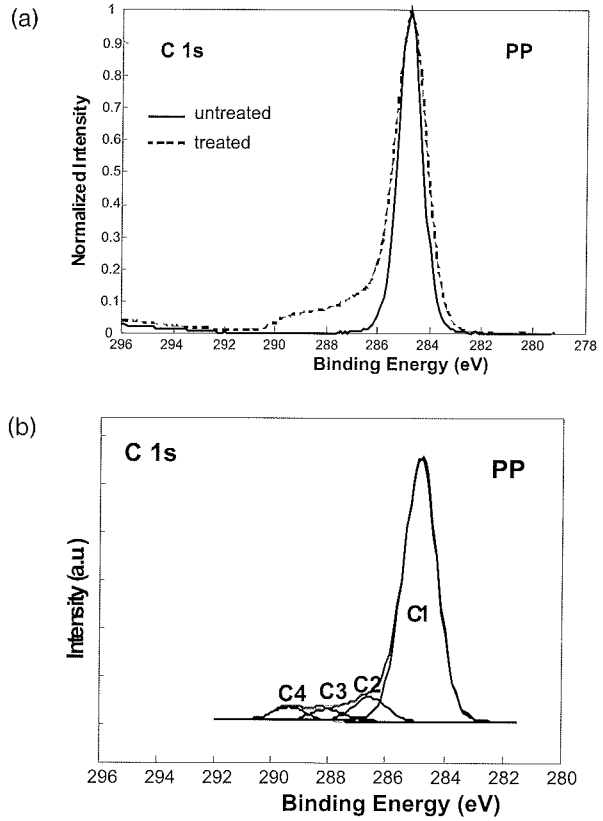

Fig. 3: (a) A comparison of C1s peaks of untreated and treated PP and (b) fitting of C1s peak of treated PP surface.

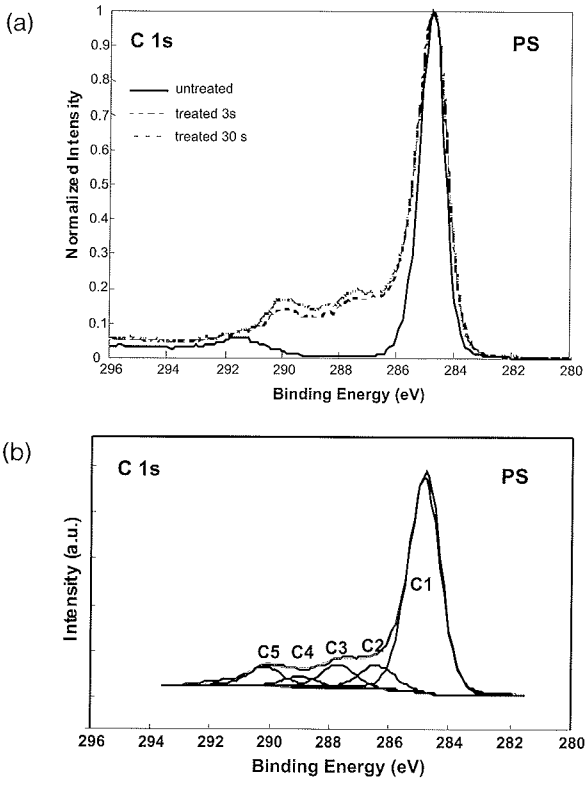

Fig. 4: (a) A comparison of C1s peaks of untreated and treated PS and (b) fitting of C1s peak of treated PS surface.

face. We can observe three peaks: C1 corresponding to C C bonds in phenyl ring, C2 corresponding to C-O bond (eter) and C3 corresponding to O=C-O bond (ester group) (Fig 2c). After the plasma treatment the intensity of the peaks C2 and C3 remarkable increased (Figure 5b) and a new peak C4 is observed due to C=O bond /13/,/14/, /15/,/16/.

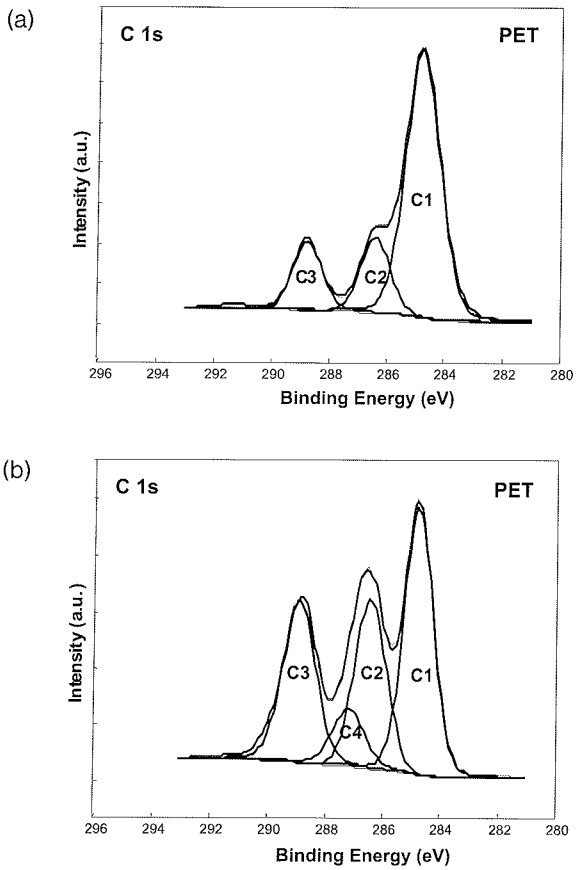

Fig. 5: High-resolution C 1s peak of (a) untreated and (b) treated PET surface.

While in the case of the PET polymer we can still clearly observe changes after oxygen plasma treatment, this is not true for cellulose. In cellulose all carbon atoms are bound to at least one oxygen (Figure 2d): each cellulose unit contains five carbon atoms with a single bond to oxygen C-O (hydroxyl groups) and one carbon atom with two bonds to oxygen O-C-O. Thus, for pure cellulose one would expect just two peaks C2 and C3. In our case for textile (Figure 6a) we observed also the C1 peak, which is often observed on cellulose and is due to the presence of contaminants. After the plasma treatment of textile (Figure 6b), the contribution of C3 peak increased, while the contribution of C2 and C1 peaks decreased. Furthermore, a new peak C4 with a binding energy of 289.2 eV appeared. An increase of the C3 peak is associated with a formation of new functional groups like O-C-O or C=O, while a new peak C4 is attributed to formation of the O=C-O group. Here, it is worth mentioning that, since carbon atoms in the cellulose are bonded to at least one oxygen atom, the

incorporation of new species from plasma can cause the degradation of the molecule. This can be a reason for the decrease of the C2 peak.

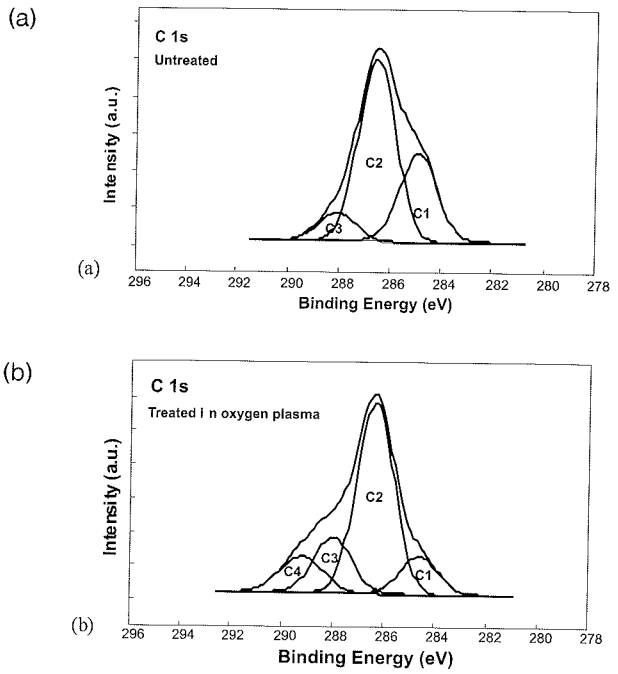

Fig. 6: High-resolution C 1s peak of (a) untreated and (b) treated textile surface.

Interesting is also plasma treatment of paper. At our experiments we used ink-jet paper, which contained about 10 weight % of alkyl ketene dimer (AKD) and few weight % of $CaCO_3$, the rest being cellulose. In the untreated sample (Figure 7a) we see typical spectrum of cellulose. We can not observe the peak due to $CaCO_3$ which is present in the bulk. The situation after 3 s of treatment (Figure 7b) is quite the same as for untreated sample - it is difficult to see any changes, while after 200 s of treatment the situation is much different (Figure 7c). After 200 s of plasma treatment the organic part (cellulose) was burned, while inorganic particles remained. In the XPS spectrum of the ash of this sample we can observe peaks C1, C2, C3 and C4 like in the case of textile and a new peak C5, which is due to carbon atoms in $CaCO_3$. Accordingly, XPS survey-scan measurements showed that Ca concentration was increasing with increasing treatment time /17/. This kind of plasma treatment is also known as plasma ashing and it allows as to detect inorganic material which is present in organic samples in so small quantities, that it is below the detection limit of techniques for surface characterization.

3.3 Sulphur containing polymers

With sulphur containing polymers there is a problem with overlapping of peaks due to C-C bond at a BE of 285 eV and C-S bond at a BE of 285.3 eV /18/,/19/ which are not clearly distinguished. In XPS spectrum of the carbon peak of the untreated PES we can see only 2 peaks (Figure 8a): the larger one C1 at 285 eV and the smaller one

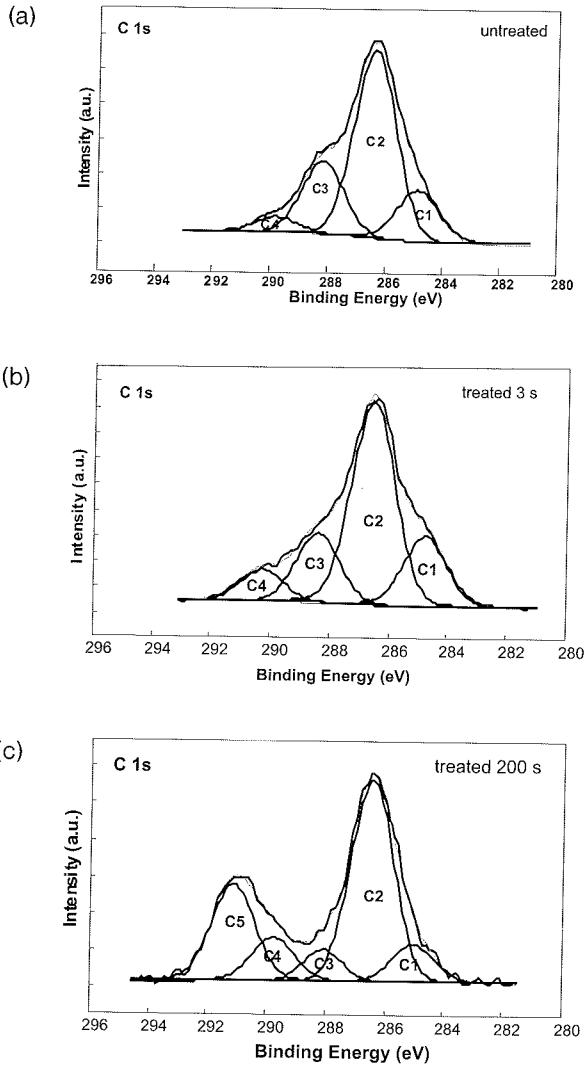

Fig. 7: High-resolution C 1s peak of (a) untreated surface of ink-jet paper, (b) treated for 3s and (c) treated for 200 s.

C2 at 286.5 eV. The larger peak corresponds to a C-C bond, while the smaller peak corresponds to a C-O bond. As already mentioned it is difficult to see the C S peak since it is overlapping with the peak C1. Figure 8b shows XPS spectrum of the carbon C1s peak of the sample treated for 3 s. The carbon peak of the plasma-treated sample is different from the peak of untreated sample. Now, four separate peaks can be observed; namely a new peak C3 due to C=O and a peak C4 due to O=C-O are observed. The peak C2 is enlarged in comparison to the untreated sample /19/.

Of more interest is the plasma activation of polymer PPS. Figure 9a represents the evolution of the C1s peak during oxygen plasma treatment of the PPS polymer. Surprisingly enough, the carbon peak of oxygen plasma treated sample is not much different from the untreated sample. One can therefore conclude that the oxygen-carbon bonds are presented relatively in small concentration. Nevertheless, oxidation of carbon (Figure 9b) resulted in formation of C-O, C=O and O-C=O groups at the surface like in the case

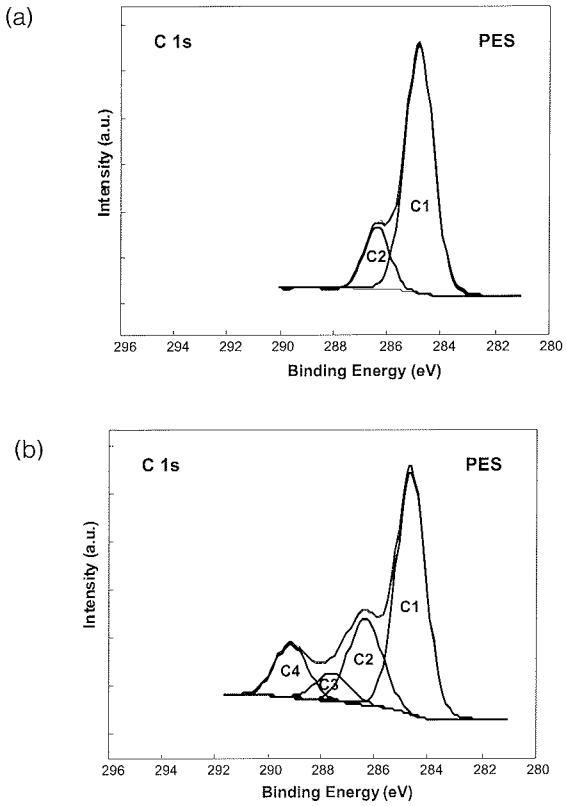

Fig. 8: High-resolution C 1s peak of (a) untreated and (b) treated PES surface.

of PES. But the right mechanism for PPS activation can be deduced from Figure 9c, which represents the high resolution S2p peak. We can see that in this case not only carbon is oxidized but also sulphur /20/. At a beginning sulphur S2p peak (duplet) is positioned at a BE of 163.7 eV corresponding to oxidation state S^{2-} (C-S-C bond). After the oxidation a new broad peak appeared at a BE of about 169 eV. According to the literature, this peak corresponds either to double peaks of S^{4+} or S^{6+}. Namely, the S^{4+} oxidation state is found at 168.2 and 169.4 eV, and S^{6+} at 169.1 and 170.2 eV, respectively. The oxidation state of sulphur therefore changed dramatically after the plasma treatment.

From XPS results of plasma activation of sulphur containing polymers we can conclude that sulphur is more easily oxidized than carbon, like shown in the case of PPS. We can not observe this in the case of polymer PES because sulphur atoms in virgin PES (Figure 2f) are already bounded to oxygen and further binding of oxygen is limited. Prolonged oxygen plasma treatment of PES can cause formation of SO_3^{2-} (leading to polymer degradation) which is desorbed from the surface like shown by Feng at al /18/.

3.4 Nitrogen containing polymers

At plasma treatment of nitrogen-containing polymers we do not observe oxidation of nitrogen like in the case of sulphur-containing polymers. Only carbon atoms are oxidized.

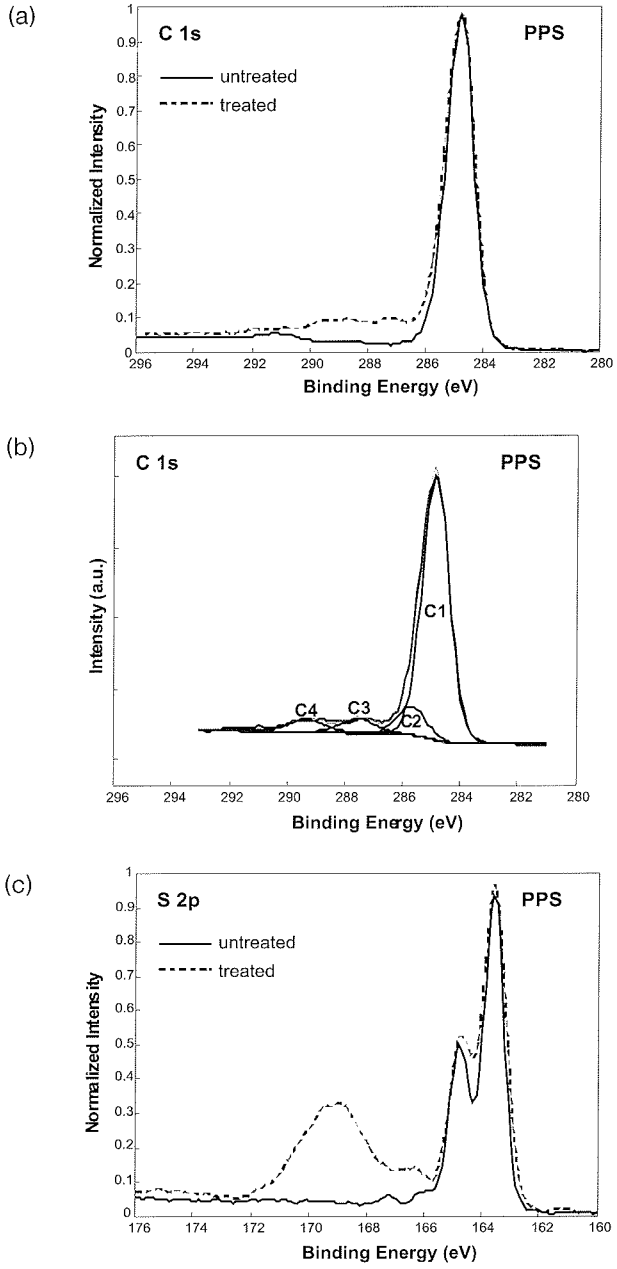

Fig. 9: (a) Comparison of carbon C1s peaks for untreated and treated PPS, (b) fitting of C1s peak of the treated PPS and (c) Comparison of sulphur S 2p peaks for untreated and treated PPS.

One problem associated with nitrogen containing polymers is difficult determination of the exact type and concentration of nitrogen functional groups, since there is a problem with strong overlapping of oxygen- and nitrogen-containing functionalities, because they appear at similar binding energies (Figure10) /12/. Moreover, relevant literature reports different data for binding energies of different nitrogen peaks which are positioned quite close together: C-N (285.5 eV - 286.3 eV), C=N (285.5 eV - 286.6 eV), C≡N (286.7 eV - 287.0 eV) /21/,/22/,/23/,/24/,/25/,/26/ and this makes the interpretation of XPS spectra very difficult.

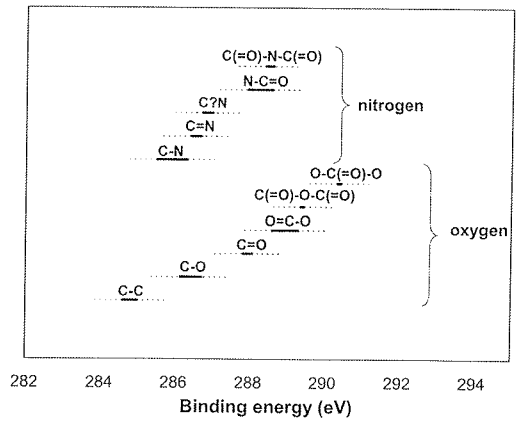

Fig. 10: Expected positions of oxygen and nitrogen functional groups: full line - position of the peak maximum, dotted line - peak width (FWHM).

Also the N1s peak can not give a decisive answer about the nitrogen containing functionalities /27/. The N1s peak is always composed of a single relatively broad symmetric peak that could correspond to different nitrogen states. According to the literature we can find several carbon-nitrogen species (like amines, amides, imides, nitriles, etc.) in the range between 399.1 eV and 400.2 eV /12/,/27/. As reported by Morent at al, it is very difficult to incorporate nitrogen at polymer surfaces /27/. Therefore, he assumed that during plasma treatment only nitrogen singly-bonded to carbon are usually formed on the surface. Amide groups (N-C=O) can be also present at the surface, while the presence of the groups where nitrogen is bounded to oxygen (nitro, oxime and nitrate groups) can be definitively excluded, since they should appear at energies 406-408 eV /12/,/27/ and this is never observed.

An example of plasma treatment of nitrogen-containing polymer PA is shown in Figure 11. Figure 11a shows XPS spectrum of the untreated PA sample. The carbon peak is composed of three peaks; C1 corresponding to C-C bond, C2 at a BE of 286.1 eV corresponding to C-N bond and C3 at a BE of 287.9 eV corresponding to O=C-N bond (amide group). The spectrum of a PA sample treated in plasma (Figure 11b) shows that the peaks C2 and C3 increased, while a new peak C4 appeared as well, corresponding to O=C-O. The increase of C2 component can be explained by formation of C-O groups, which appear at a similar binding energy as C-N group, while the increase of C3 peak can be explained by the formation of C=O group.

3.5 Halogen containing polymers

PTFE is one of the most chemically inert polymers. Therefore it is very difficult to activate its surface by plasma treatment. In Figure 12a is shown a comparison of the carbon peak for untreated and plasma-treated PTFE surface. It can be seen that practically, there is no difference in the shape of XPS spectrum /28/. Also the comparison of the fluorine peaks (Figure 12b) does not show any difference. The survey-scan measurements showed no changes in oxygen concentration at the surface (Table 1).

Table 1: Surface composition of the polymer samples before and after plasma treatment for 3s (PTFE 10 min).

Sample	C	O	N	S	F	Ca	Na	K	O/C
Untreated PA6	76.2	13.1	10.7						0.17
Treated PA6	63.0	25.3	11.7						0.40
Untreated PET	73.4	26.6							0.36
Treated PET	60.0	40.0							0.67
Untreated PES	74.6	20.4		5.0					0.27
Treated PES	57.3	37.8		5.0					0.66
Untreated PTFE	33.3	0.6			66.1				0.02
Treated PTFE	31.7	0.5			67.8				0.02
Untreated textile	64.2	35.8							0.56
Treated textile	49.6	50.4							1.02
Untreated paper	75.3	23.0	1.4			0.4			0.31
Treated paper	48.9	45.2	2.3			2.4	1.2		0.92
Treated paper-ash	29.8	47.6				8.5	2.9	11.2	1.60

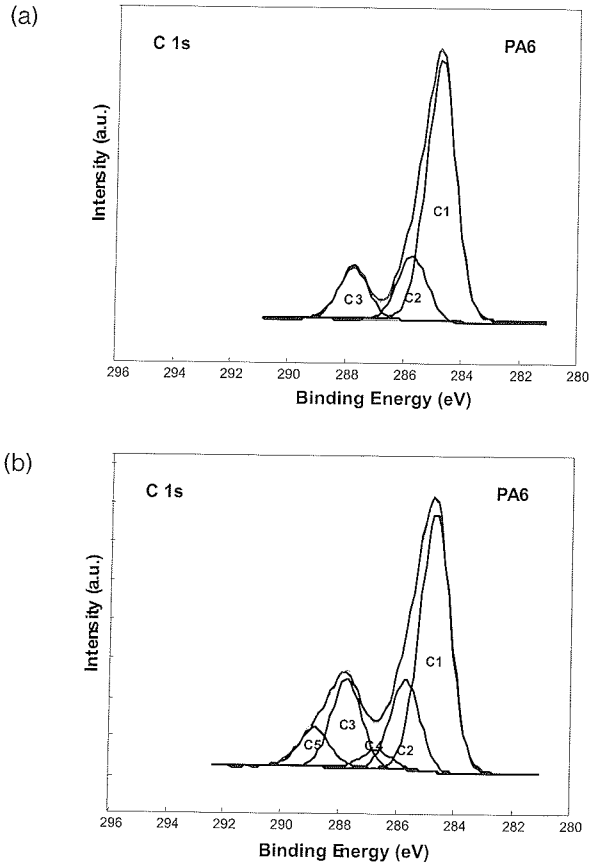

Fig. 11: High-resolution C 1s peak of (a) untreated and (b) treated PA6 surface.

Here the treatment time was 1 minute and not 3 s like at all previous polymers. Even after 10 min of treatment the situation was quite the same. So the plasma treatment seems

to be ineffective in this case. Here it is worth to mention that halogen-containing polymers are known to be sensitive to X-ray exposure, resulting in a decrease in the halogen peak intensity and an increase in the C 1s peak intensity /11/,/12/,/29/. In our case we did not observe this effect even after several hours of exposure to X-rays.

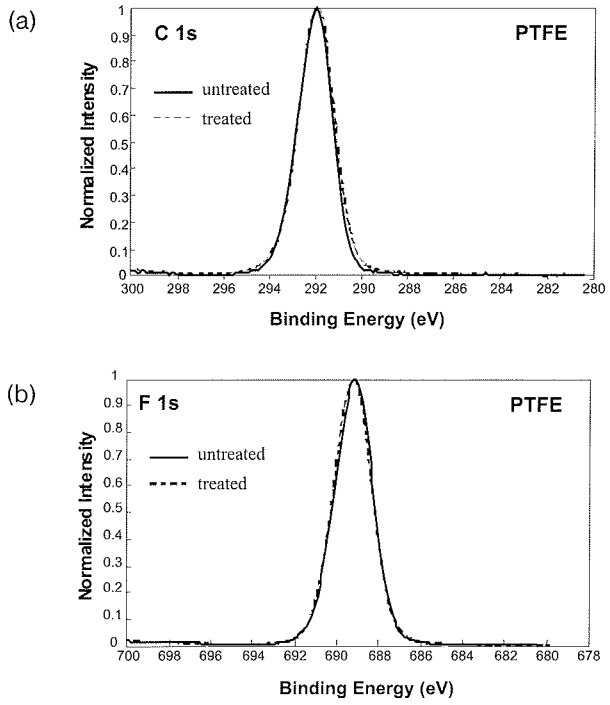

Fig. 12: High-resolution C 1s peak of (a) untreated and (b) treated PTFE surface.

Table 2: Comparison of oxygen uptake for different polymers.

Sample	$(O/C)_{before}$	$(O/C)_{after}$	O uptake
PS	0	0.36	
PP	0	0.23	
PPS	0.06	0.41	583%
$CELL_{paper}$	0.31	0.92	197%
PES	0.27	0.66	144%
PA6	0.17	0.41	141%
PET	0.26	0.61	135%
$CELL_{textile}$+AKD	0.56	1.02	82%

4 Conclusions

Oxygen plasma was found as an effective method for surface modification of different polymers. The only exception was PTFE, which is known as chemically very inert material and it was not possible to functionalize it even by plasma treatment. On all other samples a higher oxygen concentration was detected on the surface after the plasma treatment (Table 1, Table 2).

Plasma treatment did not produce one unique functionality on a polymer surface but usually a distribution of different functional groups was produced. On all polymers except PTFE new groups like C-O, C=O and O=C-O were observed; only their concentration was different depending on the polymer type (Table 3). For example, the rate of incorporation of new species after oxygen plasma treatment at identical conditions was found to be greater for PS than for PP. For polymers that do not contain only carbon and hydrogen, the amount of incorporation of new species via plasma treatment is reduced considerably (Table 2). The surface incorporation of new species depends on the number of available carbon atoms that can bond with the reactive species in the plasma. The primary available carbon atoms are those that are only bonded to other carbon atoms or hydrogen. Secondary sites would be carbon atoms with only a single bond to oxygen or nitrogen /2/,/26/. Oxidation of sulphur containing polymers resulted in oxidation of sulphur atoms as well, while this is not the case for oxidation of nitrogen containing polymers, where no groups with nitrogen bounded to oxygen were found.

Table 3: Comparison of concentration of different functional groups for different polymers.

	C-C ^{3}C-S	C-O ^{4}C-N	C=O ^{4}O=C-N	O=C-O	^{1}-C(=O)-O-C(=O)- $^2CO_3^{2-}$
PP untreated	100%	/	/	/	/
PP treated 3s	78.2%	12.1%	5.3%	4.5%	/
PS untreated	100%	/	/	/	/
PS treated 3s	70.7%	8.9%	8.6%	4.1%	7.8%[1]
PET untreated	75.8%	13.0%	/	11.2%	/
PET treated 3s	34.0%	30.4%	3.9%	31.7%	/
Paper untreated	16.3%	57.0%	22.0%	4.7%	/
Paper treated 3s	19.0%	54.9%	18.0%	8.2%	/
Paper treated 200s	8.9%	48.3%	7.1%	11.1%	24.6%[2]
Textile untreated	30.7%	60.0%	9.3%	/	/
Textile treated 3s	12.2%	57.7%	17.7%	12.4%	/
PES[3] untreated	82.1%	17.9%	/	/	/
PES[3] treated 3s	52.4%	22.3%	9.8%	15.6%	/
PPS[3] untreated	100%	/	/	/	/
PPS[3] treated 3s	78.9%	9.0%	6.4%	5.7%	/
PA[4] untreated	70.2%	16.5%	13.3%	/	/
PA[4] treated 3s	55.8%	17.7%	19.0%	7.5%	/

The surface chemistry of plasma-treated polymers containing carbon-oxygen or carbon-nitrogen functionalities is more complex and is significantly different from polymers containing only carbon-carbon species. Characterization of plasma-induced changes on oxygen- or nitrogen-containing polymers is more difficult due to the more complex chemical structure of the polymer and the number of possible chemical species that can be produced.

Not only oxygen plasma is used for surface modification. Other gasses can be used for plasma modification of polymers surfaces as well like N_2, NH_3, H_2O, CO_2, air and noble gases. The rate and amount of incorporation of new species into a polymer surface via plasma treatment is gas dependent /2/. According to incorporation rate of new species into the surface, the oxygen plasma gives the best results. Noble gas plasma treatments do usually not incorporate new species into the surface. If small amounts of reactive gas (impurities) are present we can still end-up

with incorporation of small amounts of new species at the surface. The real mechanism of surface activation by noble gas plasmas is bond breakage and desorption of various short chain species. Free radicals interact and form crosslinks. Therefore, one of the main effects typical of noble gas plasma treatment is crosslinking of polymer. We must be also aware that if a virgin polymer already contains some functional groups, we can end-up with surface reorganization producing new functionalities without incorporation of new species from plasma.

References

/1/ A. Meyer-Plath, K. Schröder, B. Finke, A. Ohl. Vacuum, 2003, vol. 71, pp. 391.

/2/ L. J. Gerenser. Surface Chemistry of Plasma-Treated Polymers, in Handbook of Thin Film Process Technology, Ed. D.A Glocker, S.I. Shah, IOP, Bristol, 1996.

/3/ M. Strobel, C. S. Lyons, K. L. Mittal. Plasma Surface Modification of Polymers: Relevance to Adhesion, VSP, Utrecht, 1994.

/4/ G. Borcia, C. A. Anderson, N. M. D. Brown. Plasma Sources Sci. Technol., 2003, vol. 12, pp. 335.

/5/ G. Borcia, C. A. Anderson, N. M. D. Brown. Appl. Surf. Sci., 2004, vol. 225, pp. 186.

/6/ J. Feng, G. Wen, W. Huang, E. Kang, K. G. Neoh. Polym. Degrad. Stabil., 2005, vol. 91, pp. 12.

/7/ R. Morent, N. De Geyter, C. Leys, L. Gengembre, E. Payen. Surf. Coat. Technol., 2007, vol. 201, pp. 7847.

/8/ C.-M. Chan, T.-M. Ko, H. Hiraoka. Surf. Sci. Rep., 1996, vol. 24, pp. 1.

/9/ D. Briggs, J. T. Grant. Surface Analysis by Auger and X-ray Photoelectron Spectroscopy, IMP & Surface Spectra, Trowbridge, 2003.

/10/ D. Briggs. Surface Analysis of Polymers by XPS and static SIMS, Cambridge University Press, Cambridge, 2005.

/11/ D. Briggs, M. P. Seah. Practical surface Analysis, Auger and X-rays Photoelectron Spectroscopy, Wiley, Chichester, 1994.

/12/ G. Beamson, D. Briggs. High Resolution XPS of Organic Polymers - The Scienta ESCA300 Database, Wiley, Chichester, 1992.

/13/ N. Krstulović, I. Labazan, S. Milošević, U. Cvelbar, A. Vesel, M. Mozetič. J. Phys. D: Appl. Phys., 2006, vol. 39, pp. 3799.

/14/ A. Vesel, M. Mozetič, A. Zalar. Vacuum, 2008, vol. 82, pp. 248.

/15/ A. Vesel, M. Mozetič. J. Phys. Conf. Ser., 2008, vol. 100, pp. 012027-1.

/16/ A. Vesel, I. Junkar, U. Cvelbar, M. Mozetič, J. Kovač. Surf. Interface Anal., 2008 (in press).

/17/ A. Vesel, M. Mozetič, A. Hladnik, J. Dolenc, J. Zule, S. Milošević, N. Krstulović, M. Klanjšek-Gunde, N. Hauptman. J. Phys. D: Appl. Phys. 2007, vol. 40, pp. 3689.

/18/ J. Feng, G. Wen, W. Huang, E. Kang, K. G. Neoh. Polym. Degrad. Stabil., 2005, vol. 91, pp. 12.

/19/ T. Vrlinič, A. Vesel, U. Cvelbar, M. Krajnc, M. Mozetič. Surf. Interface Anal., 2007, vol. 39, pp. 476.

/20/ U. Cvelbar, M. Mozetič, I. Junkar, A. Vesel, J. Kovač, A. Drenik, T. Vrlinič, N. Hauptman, M. Klanjšek-Gunde, B. Markoli, N. Krstulović, S. Milošević, F. Gaboriau, T. Belmonte. Appl. Surf. Sci., 2007, vol. 253, pp. 8669.

/21/ J. Larrieu, F. Clement, B. Held, N. Soulem, F. Luthon, C. Guimon, H. Martinez. Surf. Interface Anal., 2005, vol. 37, pp. 544.

/22/ P. A. Charpentier, A. Maguire, W.-K. Wan. Appl. Surf. Sci., 2006, vol. 252, pp. 6360.

/23/ Y. Deslandes, G. Pleizier, E. Poiré, S. Sapieha, M. R. Wertheimer, E. Sacher. Plasmas Polym., 1998, vol. 3, pp. 61.

/24/ D. J. Wilson, R. L. Williams, R. C. Pond. Surf. Interface Anal., 2001, vol. 31, pp. 385.

/25/ M. J. Wang, Y. I. Chang, F. Poncin-Epaillard. Surf. Interface Anal., 2005, vol. 37, pp. 348.

/26/ J. M. Grace, L. J. Gerenser. J. Disp. Sci. Technol., 2003, vol. 24, pp. 305.

/27/ R. Morent, N. De Geyter, L. Gengembre, C. Leys, E. Payen, S. Van Vlierberghe, E. Schacht. Eur. Phys. J. Appl. Phys., 2008 (in press).

/28/ A. Vesel, M. Mozetič, A. Zalar. Surf. Interface Anal., 2008, vol. 40, pp. 661.

/29/ K. Artyushkova, J. E. Fulghum. Surf. Interface Anal., 2001, vol. 31, pp. 352.

Alenka Vesel
Jozef Stefan Institute, Jamova cesta 39,
Ljubljana, Slovenia

Prispelo (Arrived): 17.09.2008 *Sprejeto (Accepted): 15.12.2008*

SURFACE MODIFICATION OF GRAPHITE BY OXYGEN PLASMA

Ita Junkar[1], Nina Hauptman[2], Ksenija Rener-Sitar [3],
Marta Klanjšek-Gunde[2], Uroš Cvelbar[1]

[1]Jožef Stefan Institute, Ljubljana, Slovenia
[2]National Institute of Chemistry, Ljubljana, Slovenia
[3]University of Ljubljana, Ljubljana, Slovenia

Key words: plasma, oxygen, etching, graphite, nanostructure, cone

Abstract: The technology of plasma etching of graphite by highly reactive oxygen plasma is presented. Etching was performed with low pressure cold weakly ionised oxygen plasma created in a glass plasma reactor by an inductively coupled RF generator. The density of charged particles, density of neutral oxygen atoms and the electron temperature was about $2x10^{16}$ m^{-3}, $6x10^{21}$ m^{-3}, and 4 eV, respectively. The effects of etching were observed by scanning electron microscopy. It was found that the surface roughness was increased dramatically after plasma treatment. The roughness increased with increasing plasma exposure time. The technology allows for pretty good control of the surface morphology of the samples and thus improved adhesion of different coatings.

Modifikacija površine grafita s kisikovo plazmo

Kjučne besede: plazma, kisik, jedkanje, grafit, nanostructure, stožec

Izvleček: Prikazujemo tehnološki postopek za jedkanje grafita z visoko reaktivno kisikovo plazmo. Za jedkanje uporabimo nizkotlačno hladno kisikovo plazmo, ki jo ustvarimo v steklenem plazemskem reaktorju z induktivno sklopljeno radiofrekvenčno razelektritvijo. Gostota nabitih delcev v naši plazmi je $2x10^{16}$ m^{-3}, gostota nevtralnih kisikovih atomov $6x10^{21}$ m^{-3}, temperature elektronov pa okoli 4 eV. Vpliv jedkanja smo spremljali z vrstičnim elektronskim mikroskopom. Ugotovili smo, da kisikova plazmo povzroči zelo močan porast hrapavosti grafita. Hrapavost narašča z naraščajočim časom obdelave. Opisani tehnološki postopek omogoča precej natančno določeno hrapavost materiala, ki je potrebna za izboljšanje adhezivnosti različnih prevlek.

1 Introduction

Advanced methods for the modification of surface properties of different materials often include treatment by gaseous plasma. Gaseous plasma is created in a suitable discharge. It can be created at atmospheric pressure or under vacuum conditions. Atmospheric pressure plasma is often characterized by a pretty high density of charged particles and a moderate, if not high kinetic temperature of neutral gas. /1-7/ Electron temperature is rather low: the typical electron temperature in atmospheric plasma is close to 1eV. Atmospheric plasma is usually limited to a rather small volume inside the discharge chamber. This is due to a high collision frequency of gaseous particles as the mean free path is extremely low. The high collision frequency allows for rapid de-excitation of plasma particles. On the other hand, low pressure plasma can spread far from the discharge region due to a rather small collision frequency./8-12/ Rather homogeneous plasma can be created in large chambers, often of the order of a m^3, if not more. This unique property makes low pressure plasma particularly suitable for treatment of materials and components on the industrial scale. Not surprisingly, low pressure plasma is nowadays widely used in various technologies from the synthesis of nanoparticles to automotive industry. /13-22/ Such plasma if created in oxygen or a mixture of oxygen, is extremely suitable for treatment of organic materials. /23-29/. The plasma parameters vary enormously depending on particular conditions, but as a general rule, the gas usually remains close to the room temperature, the electron temperature easily reaches several eV, while the density of charged particles can be anywhere between about 10^{15} and 10^{18} m^3 /30-33/. Low pressure oxygen plasma is often characterized by a huge density of neutral oxygen atoms /34-37/.

A modern technology based on interaction of oxygen plasma with carbon containing materials is selective etching. /38,39/ Plasma radicals that interact with the surface of materials can cause a surface functionalization with polar functional groups as well as slow etching. /40-42/ Although the flux of plasma radicals onto the surface is usually pretty uniform, the etching is often anisotropic and sometimes also not homogeneous. /43,44/ Plasma treatment often also causes increased surface roughness or even new structures. /38,45-50/ The features formed spontaneously on the surface of carbon containing material depend on the characteristics of specific material as well as on plasma parameters. /51,52/ In the current paper we address the possibility of increasing roughness of pure highly oriented electrolytic graphite.

2 Experimental

Samples were used as received from the NT-MDT producer. No cleaning (degreasing) was performed since oxygen

plasma effectively removes any possible organic impurities from surfaces of materials. The samples were pieces of highly oriented electrolytic graphite (HOPG-ZYH). Samples with the thickness of 1.7 mm were in quadratic pieces with the surface of 1x1 cm^2. Samples were mounted into the discharge chamber of a vacuum system schematically presented in Figure 1. The discharge vessel was a cylindrical tube with inner diameter of 36 mm and the length of 600 mm. The tube was made of a borosilicate glass (Schott 8250) with the recombination coefficient for oxygen atoms at the room temperature of less than $2x10^{-3}$. At both ends it was joined to kovar rings, which were welded to standard KF 40 flanges. The glass-to-metal joint was bakeble up to 400°C. On one side, the tube was connected to the vacuum system. The system was pumped with a two-stage oil rotary pump with the pumping speed of 4.4 l s^{-1} and the base pressure of 0.1 Pa. All connections between the pump and the discharge vessel were made of components with the conductance of approximately two orders of magnitude higher than the pumping speed of the pump, so the effective pumping speed in the discharge vessel was nearly as high as that of the pump. The pressure in the system was measured with a Pirani gauge. Prior to experiments the gauge was calibrated for oxygen with a precise baratron. A recombinator for O atoms was placed in front of the gauge in order to prevent its degradation

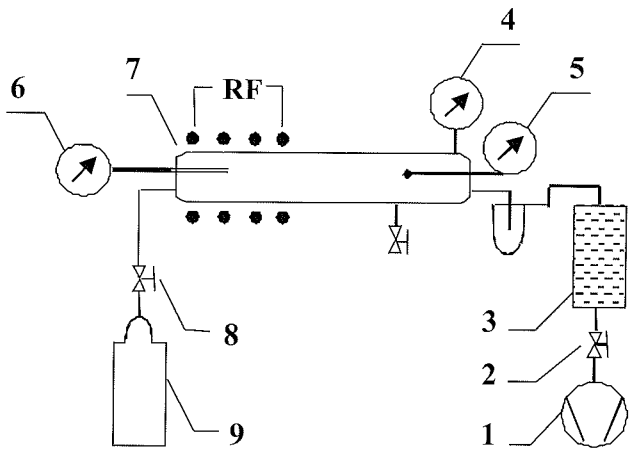

Fig. 1. Schematic of the experimental system. 1 - rotary pump, 2 - valve, 3 – trap with molecular sieves, 4 - vacuum gauge, 5 - catalytic probe, 6 – Langmuir probe, 7 – optical fibre catalytic probe, 8 - discharge chamber, 9 - leak valve, 10 - oxygen flask

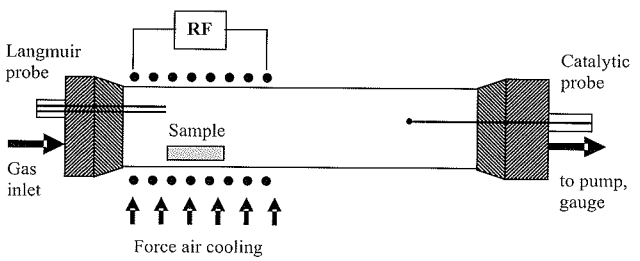

Fg. 2. The plasma reactor.

during plasma experiments. The discharge vessel was placed in a coil connected to a RF generator as shown in Figure 2. The frequency of the generator was 27.12 MHz and the output power approximately 250 W. The other side of the discharge vessel was connected to a gas inlet system. Commercially available oxygen was leaked to the system trough a leak valve. The discharge vessel was forced air-cooled.

The parameters of plasma in the discharge vessel were measured with a double Langmuir probe and a nickel catalytic probe. Measurements with Langmuir and catalytic probes were performed prior to experiments with samples. The position of the two probes is shown in Figure 2. The Langmuir probe is placed in the plasma region (to allow for proper reading of the electron temperature and plasma density) while the catalytic probe was mounted into afterglow, about 20 cm away from the glowing plasma region. The reasons for that were explained to details in /35,53,54/. Due to the completeness of this paper let us briefly repeat them here. Catalytic probes are based on measuring power released on the catalyst surface due to heterogeneous surface recombination of oxygen atoms. While they make give accurate results in afterglows, they are less accurate in plasma itself where other heating mechanisms have to be taken into account. Since other mechanisms (relaxation of metastables, recombination of charged particles, bombardment by positive ions, absorption of light quanta) are generally difficult to estimate, the probes are better placed in the afterglow, where they give accurate atom density in their vicinity. The oxygen atom density in the plasma itself is then calculated by taking into account the known oxygen atom decay along a continuously pumped glass tube (as explained in /35,53,55/). The density of charged particles was about $2x10^{16}$ m^{-3} and the electron temperature about 4 eV. The density of neutral oxygen atoms was $6x10^{21}$ m^{-3}.

The surface of the samples was imaged after the plasma treatment with a Scanning Electron Microscope (SEM) The SEM images obtained using a field emission microscope Carl Zeiss Supra 35 VP at accelerating voltage of 1 keV.

3 Results and discussion

The SEM images of plasma treated samples are presented in Figures 3 - 12. The original material is extremely flat so the SEM image does not reveal any measurable feature and is therefore not presented in this paper. After 10s of plasma treatment the surface of graphite remains practically intact as demonstrated by Fig. 3. The dose of oxygen atoms is calculated using equation (1)

$$D = 1/4\, n\, v\, t \qquad (1)$$

Where n is the atom density, v the average thermal velocity of oxygen atoms and t the treatment time. In 10s, the dose is $9x10^{24}$ m^{-2}. From this calculation it is possible to conclude that doses below $10^{25}m^{-2}$ are pretty benign to highly oriented graphite.

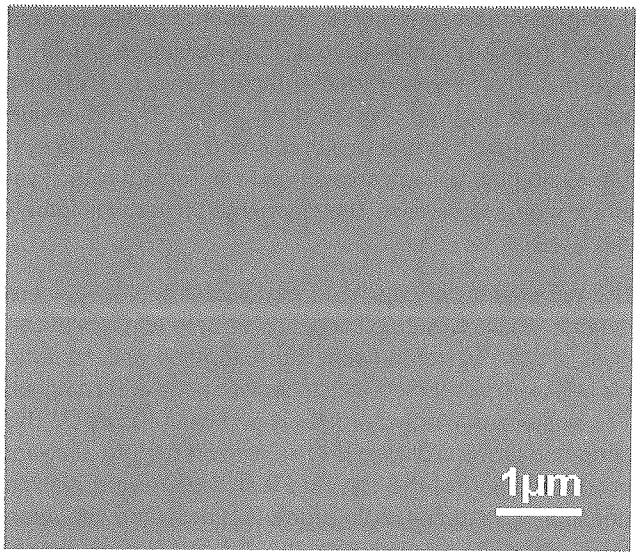

Fig. 3. SEM image of a sample exposed to plasma for 10s.

Interesting features are observed after 90s of plasma treatment. The corresponding SEM images are presented in Figures 4-6. The surface is far from being smooth. It is rather covered with small and almost spherical features with the typical diameter of few micrometers. The appearance of these features is definitely due to etching of graphite by oxygen atoms. Namely, positively charged oxygen ions that are other possible plasma particles capable of etching graphite are found at minor concentrations. Since the ion density in our plasma is more than 5 orders of magnitude smaller than the neutral atom density, they cannot cause such intensive etching even if all ions would remove a carbon atom from the surface of the samples. The flux of oxygen atoms onto the surface of graphite is homogeneous and isotropic so the formation of such structures is rather surprising. The anisotropic etching can be explained by localized inhomogeneity of the samples. Namely, any defect, even at atomic

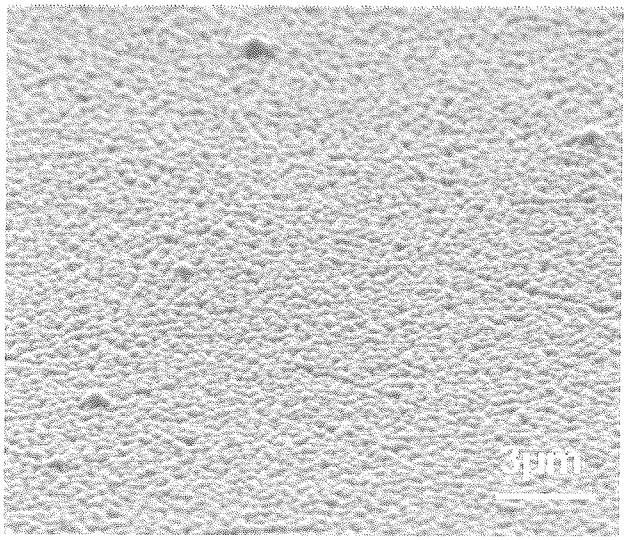

Fig. 4. SEM image of a sample exposed to plasma for 90s at low magnification

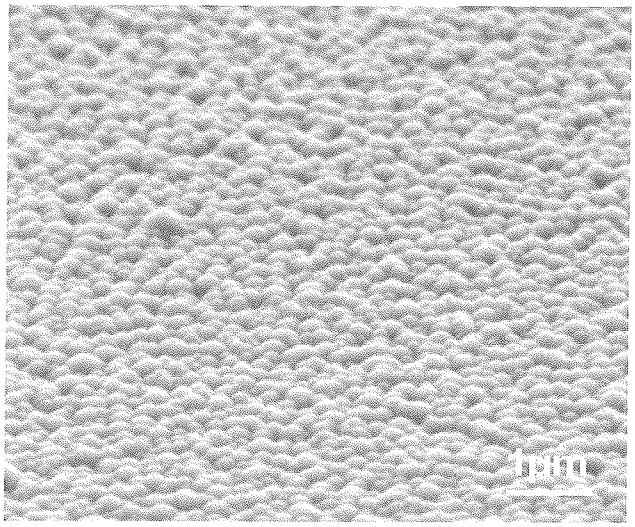

Fig. 5. SEM image of a sample exposed to plasma for 90s at medium magnification

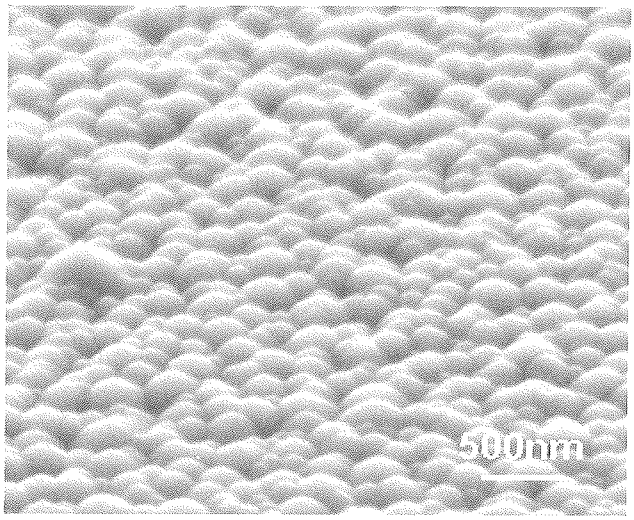

Fig. 6. SEM image of a sample exposed to plasma for 90s at high magnification.

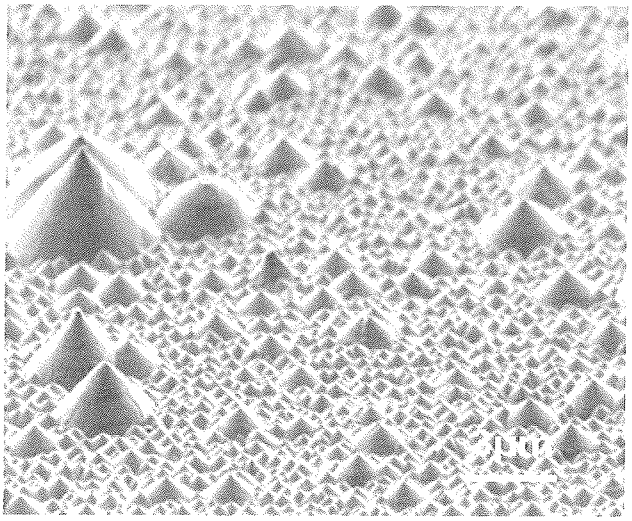

Fig. 7. SEM image of a sample exposed to plasma for 180s at low magnification.

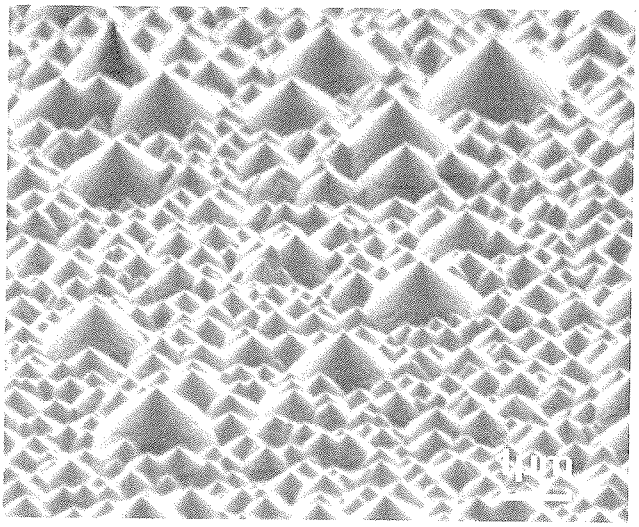

Fig. 8. SEM image of a sample exposed to plasma for 180s at medium magnification.

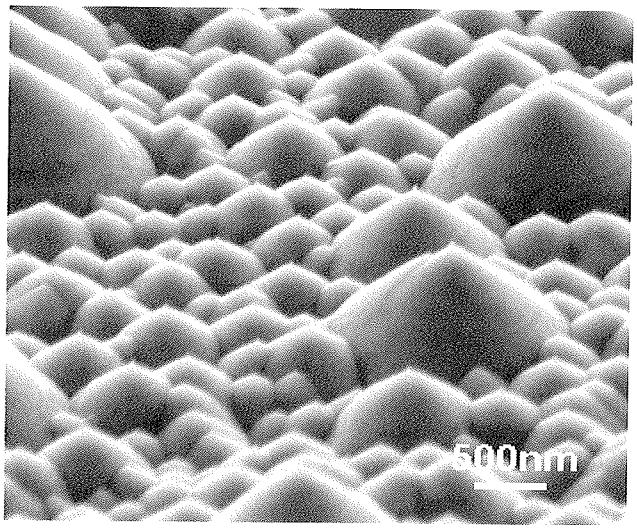

Fig. 9. SEM image of a sample exposed to plasma for 180s at high magnification.

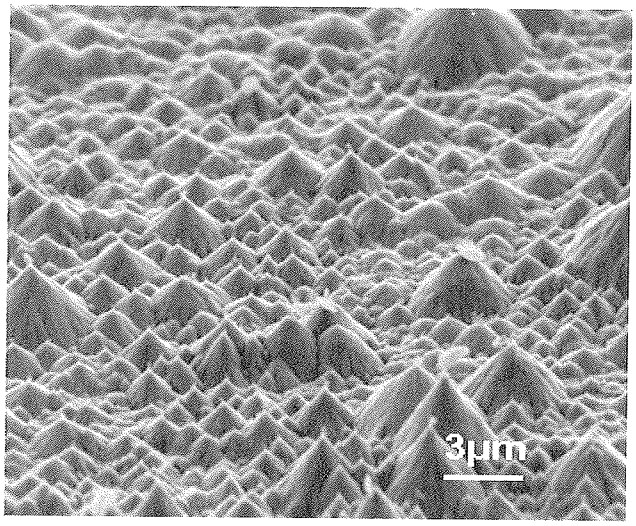

Fig. 10. SEM image of a sample exposed to plasma for 600s at low magnification

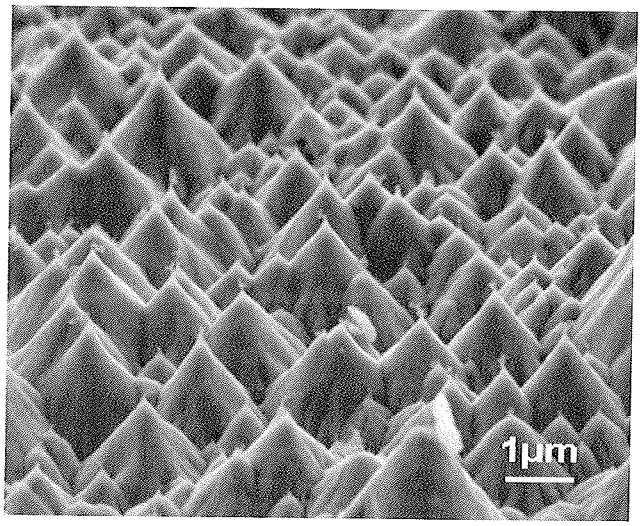

Fig. 11. SEM image of a sample exposed to plasma for 600s at medium magnification

scale, would lead to somewhat different reaction probability. Since the received dose is huge (after 90s of plasma treatment the dose is about $8x10^{25}m^{-2}$) the atoms can be extremely selective and still capable of removal carbon atoms. It is well known that any selectivity of etching causes the so-called orange skin effect: the etching un-isotropy keeps increasing with increasing dose of reactant.

The next step in etching is formation of conical features on the surface of our samples as demonstrated from Figures 7-9. The lateral size of the features remains the same as after treatment for 90s, but the shape is definitely more conical. This effect could be explained by taking into account original crystalline structure of our graphite. Our samples, however, are made from highly oriented graphite so it is not probable that the crystallites would be of observed shape. The formation of the cones is rather explained by another effect. One of them is self - organization of atoms on the surface of plasma - exposed samples. /44, 56-60/.

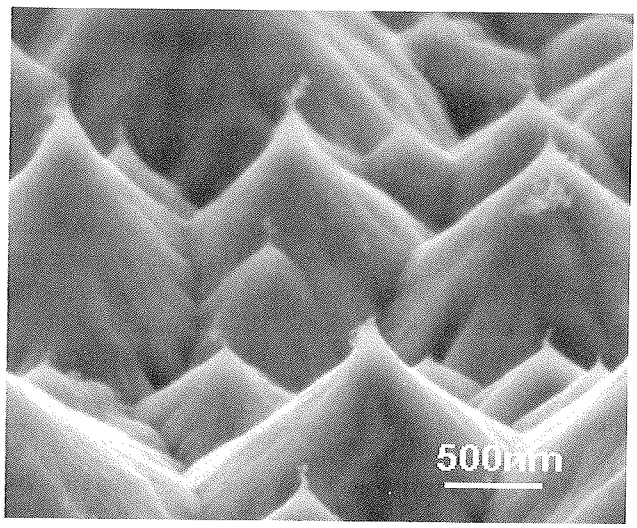

Fig. 12. SEM image of a sample exposed to plasma for 600s at high magnification

Namely, the surface mobility of atoms on the surface of samples under treatment with highly reactive plasma is huge comparing to the value calculated from the sample temperature assuming thermodynamic equilibrium. Our experiments may represent just another proof of the recent theory by Ostikov who predicted self-assembly and self-organization of material under extreme non-equilibrium conditions. Carbon atoms can have so high surface mobility that they move on the surface at the nanometer scale until they reach a thermodynamically more favourable position. /61, 62/ This position is definitely in the crystalline structure. The conical shape of the surface features may therefore be small crystals formed due to increased surface mobility of carbon atoms.

Prolonged plasma treatment does not influence the shape of surface features much, apart from the fact that the height of the features is much bigger. SEM images of samples treated for 600s are presented in Figures 10-12. Oxygen atoms obviously cause side etching of the features. The height of highest cones obtained after plasma treatment for 600s is several micrometers. This fact allows for (extremely rough) estimation of the etching rate. If the effective thickness of the removed layer is 3000 nm, then the etching rate will be

$$dx/dt = 3000\text{nm}/600\text{s} = 5\text{nm/s} \quad (2)$$

Let us finally calculate the probability that an atom reaching the surface would remove a carbon atom. The probability is proportional to the etching rate and treatment time as well as the density of our material, and inversely proportional to the received dose of oxygen atoms:

$$\eta = dx/dt\ \rho\ t\ /\ 12u\ D \quad (3)$$

Taking into account numerical values, i.e. $dx/dt = 5\text{x}10^{-9}$ m/s, $\rho = 2200$ kg/m^3, $t = 600$s, $u = 1.7\text{x}10^{-27}$ kg and $D = 5\text{x}10^{26}$ m^{-2} the probability is estimated to $\eta = 8\text{x}10^{-3}$.

4 Conclusion

The change in morphology of graphite can result in better performance of graphite based devices like gas sensing, energy conversion and others./63,64/ Therefore, highly oriented graphite was exposed to highly reactive oxygen plasma with the atom density of $6\text{x}10^{21}$ m^{-3}. The samples were kept in plasma for different time up to 600s. After plasma treatment, the samples were characterized by scanning electron microscopy. The SEM images revealed formation of surface features whose shape depended on the received dose of oxygen atoms. Up to the dose of about $1\text{x}10^{25}$m^{-2} no visible changes in surface morphology was observed. With increasing dose the surface becomes rough revealing orange-like skin morphology. The features were initially rather spherical and with increasing dose of atoms they became conical. The critical dose for transformation from the spherical to conical shape was almost $1\text{x}10^{26}$ m^{-2}. The transformation was explained by self-organization of atoms on the surface of the samples under extremely non-equilibrium conditions. Prolonged treatment of samples with oxygen plasma causes an extremely rough surface with well pronounced conical shape of surface features. The height of the highest cones allowed for estimation of the etching rate which was found to be about 5 nm/s. Since the oxygen atom density was measured it was possible to estimate also the reaction probability which was found to be almost 1%.

Acknowledgements

This work was partially supported by the Slovenian Research Agency, NATO Coll. Grant and the 6th FP EU.

References

/1/ G. Arnoult, R.P. Cardoso, T. Belmonte, and G. Henrion, Appl. Phys. Lett., vol. 93, no. 19, 191507, 2008.

/2/ R.P. Cardoso, T. Belmonte, P. Keravac, F. Kosior, and G. Henrion, J. Phys. D: Appl. Phys., vol. 40, no.5, 012, pp. 1394-1400, 2007.

/3/ D. Mariotti, H. Lindstrom, A.C. Bose et al., Nanotechnology, vol. 49, no. 49, 495302, 2008.

/4/ I. Levchenko, K. Ostrikov and D. Mariotti, Carbon, vol. 47, no. 1, pp. 344-347, 2009.

/5/ V. Kumar, J.H. Kim, C. Pendyala, B. Chernomordik, and MK Sunkara, J. Phys. Chem. C, vol. 112, no. 46, pp. 17750-17754, 2008.

/6/ N.A. Dyatko, A.P. Napartovich, S. Sakadzis, Z. Petrovic, and Z. Raspopovic, J. Phys.D: Appl. Phys., vol. 33, no. 4, pp. 375-380, 2000.

/7/ T. Belmonte, R.P. Cardoso, C. Noel, G. Henrion, and F. Kosior, Eur. Phys. J.: Appl. Phys., vol. 42, no. 1, pp. 41-46, 2008.

/8/ K.N. Ostrikov, S. Xu, and M.Y. Yu, J. Appl. Phys., vol. 88, no. 5, pp. 2268-2271, 2000.

/9/ Z.Lj. Petrović, M. Šuvakov, Ž. Nikitović, S. Dujko, O. Šašić, J. Jovanović, G. Malović and V. Stojanović, Plasma Sources Sci. Technol., vol. 16, pp. S1-S12, 2007.

/10/ K.N. Ostrikov, S. Kumar, and H. Sugai, Phys. Plasm., vol. 8, no. 7, pp. 3490-3497, 2001.

/11/ C. Canal, S. Villeger, S. Cousty, B. Rouffet, J.P. Sarrette, P. Erra and A. Ricard, Appl. Surf. Sci., vol. 254, no. 18, pp. 5959-5966, 2008.

/12/ A. Ricard, C. Canal, S. Villeger and J. Durand, Plasma Process. Poly., vo.5, no. 9, pp. 867-873, 2008.

/13/ J. Thangala et al., Small, vol. 3, no. 5, pp. 890-896, 2007.

/14/ S. Vaddiraju et al., Nano Lett., vol. 5, no. 8, pp. 1625-1631, 2005.

/15/ K. Ostrikov, Rev. Mod. Phys., vol. 77, no.2, pp. 489-511, 2005.

/16/ U.M. Graham, S. Sharma, M.K. Sunkara and B.H. Davis, Adv. Func. Mater., vol. 13, no. 7, pp. 576-581, 2008.

/17/ I. Levchenko, A.E. Rider, K. Ostrikov, Appl. Phys. Lett., vol. 90, no. 19, pp. 2713-2724, 2004.

/18/ C. Canal, R. Molina and P. Erra, Eur. Phys. J. Appl. Phys., vol. 36, pp. 35-41, 2006.

/19/ C. Canal, F. Gaboriau, S. Villeger, U. Cvelbar, and A. Ricard, Int. J. Pharm., vol. 367, no. 1/2, pp. 155, 2009.

/20/ K. Ostrikov and T. Murphy, J. Phys. D: Appl. Phys., vol. 40, no. 8, pp. 2223-2241, 2007.

/21/ U. Cvelbar et al., Appl. Surf. Sci., vol. 253, no. 21, pp. 8669-8673, 2007.

/22/ M. Mafra et al., Key Eng. Mater., vol. 373-374, pp. 421-425, 2008.

/23/ C. Canal, F. Gaboriau, A. Ricard, M. Mozetic, U. Cvelbar, A. Drenik, Plasma Chem. Plasma Process., vol. 27, no.4, pp. 404-413, 2007.

/24/ T. Vrlninič et al., Surf. Interface Anal., vol. 39,, no. 6, pp. 476-481, 2007.

/25/ A. Vesel, M. Mozetič, A. Hladnik, J. Dolenc, J. Zule, S. Milošević, N. Krstulović, M. Klanjšek Gunde, N. Hauptman, J. Phys. D: Appl. Phys., vol. 40, pp. 3689-2696, 2007.

/26/ U. Cvelbar, D. Vujošević, Z. Vratnica and M. Mozetic, J. Phys. D: Appl. Phys., vol. 36, pp. 3487-3493, 2006.

/27/ F. Rossi, O. Kylian, H. Rauscher, D. Gilliland and L. Sirgh, Pure Appl. Chem., vol. 80, no. 9, pp. 1939-19-51, 2008.

/28/ K. Stapelmann, O. Kylian, B. Denis and F. Rossi, J. Phys.D: Appl. Phys., vol, 41, no. 19, 192005, 2008.

/29/ T. Belmonte et al., Surf. Coat. Tech.., vol. 200, no. 1-4, pp. 26-30, 2005.

/30/ I. Levchenko and K. Ostrikov, J. Phys. D: Appl. Phys., vol. 40, no. 8, pp. 2308-2319, 2007.

/31/ K.N. Ostrikov et al., Phys. Plasmas, vol. 6, no. 3, pp.737-740, 1999.

/32/ R.E. Robson, R.D. White and Z. Lj. Petrović, Rev. Mod. Phys., vol. 77, no.4, pp.1303-1320, 2005.

/33/ T. Kitajima, Y. Takeo, Z. Lj. Petrović and T. Makabe, Appl. Phys. Lett., vol. 77, pp. 489-491, 2000.

/34/ A. Drenik et al., J. Phys.D. Appl. Phys., vol. 41, no. 11, 115201, 2008.

/35/ A. Drenik, U. Cvelbar, A. Vesel and M. Mozetič, Inf. Midem, vol. 35, pp. 85-41, 2005.

/36/ U. Cvelbar, K. Ostrikov, A. Drenik and M. Mozetic, Appl. Phys. Lett., vol. 92, no. 13, art. no. 133505, 2008.

/37/ M. Mozetič et al, J. Vac. Sci. Technol. A: Vac. Surf. Films, vol. 21, pp. 369-374, 2003.

/38/ U. Cvelbar, S. Pejovnik, M. Mozetič and A. Zalar, Appl. Surf. Sci., vol. 210, pp. 255-261, 2003.

/39/ M. Klanjšek Gunde et al, Vacuum, vol. 80, no. 1/3, pp. 189-192, 2005.

/40/ M. Mafra, T. Belmonte, F. Poncin-Epaillard, A.S.D.S. Sobrinho and A. Maliska, Plasma Chem. Plasma Proces., vol. 28, no.4, pp. 495-509, 2008.

/41/ V. Hody et al., Plasma Chem. Plasma Proces., vol. 26, no.3, pp. 251-266, 2006.

/42/ V. Hody et al., Thin Solid Films, vol. 506, pp. 212-216, 2006.

/43/ I.B. Denysenko al., J. Appl. Phys., vol. 95, no.19, pp. 2713-2724, 2004.

/44/ E. Tam, I. Levchenko and K. Ostrikov, J. Appl. Phys., vol. 100, no. 3, art.no. 036104, 2006.

/45/ U. Cvelbar, Z.Q. Chen, M.K. Sunkara and M. Mozetic, Small, vol.4, no.10, pp. 1610-1614, 2008.

/46/ M. Mozetic, U. Cvelbar, M.K. Sunkara and S. Vaddiraju, Adv. Mater., vol. 17, no. 17, pp. 2138-2142, 2005.

/47/ H. Chandrasekaran, G.U. Sumanasekara, J. Phys. Chem. B, vol. 110, no. 37, pp. 18351-18357, 2006.

/48/ M.K. Sunkara et al., J. Mater. Chem., vol. 14, no. 4, pp. 590-594, 2004.

/49/ Z.Q. Chen at al., Chem. Mater., vol. 20, no. 9, pp. 3224-3228, 2008.

/50/ U. Cvelbar, K. Ostrikov and M. Mozetic, Nanotechnology, vol. 19, no. 40, art.no. 405605, 2008.

/51/ G. Bhimarasetti, M.K. Sunkara, U.M. Graham, B.H. Davis, C. Suh and K. Rajan, Adv. Mater., vol. 15, no. 19, pp. 1629-1633, 2003.

/52/ G.D. Lian, E.C. Dickey, M. Ueno and M.K. Sunkara, Diamond Related Mater., vol. 11, no. 12, pp. 1890-1896, 2002.

/53/ M. Mozetic et al., J. Appl. Phys., vol. 97, no. 10, art.no. 103308, 2005.

/54/ A. Ricard, F. Gaboriau and C. Canal, Surf. Coat. Technol., vol. 202, no. 22-23, pp. 5220-5224, 2008.

/55/ U. Cvelbar and M. Mozetic, J.Phys. D: Appl. Phys., vol. 40, no. 8, pp. 2300-2303, 2007.

/56/ I. Levchenko, K. Ostrikov, U. Cvelbar, IEEE Trans. Plasm. Sci., vol. 36, no.4, pp. 866-867, 2008.

/57/ I. Levchenko, K. Ostrikov, M. Keidar and S. Xu, J. Appl. Phys., vol. 98, no.6, art.no. 064304, 2005.

/58/ I. Levchenko, K. Ostrikov, J.D. Long and S. Xu, Appl. Phys. Lett., vol. 91, no.11, art.no.113115, 2007.

/59/ Z.L. Tsakadze et al, Carbon, vol. 45, no. 10, pp. 2022-2030, 2007.

/60/ K. Ostrikov, Z. Tsakadze, P.P. Rutkevych, J.D. Long, S. Xu and I . Denysenko, Contr. Plasma Phys., vol. 45, no.7, pp. 514-521, 2005.

/61/ I. Levchenko, K. Ostrikov, M. Keidar and U. Cvelbar, J. Phys. D: Appl. Phys., vol. 41, no. 13, art.no. 132004, 2008.

/62/ I. Denysenko et al., J. Appl. Phys., vol. 104, no. 7, art.no. 073301, 2008.

/63/ R.C. Mani, M.K. Sunkara, R.P. Baldwin, J. Gullapalli, J.A. Chaney, G. Bhimarasetti, J.M. Cowley, A.M. Rao and R.H. Rao, J. Electrochem. Soc., vol. 152, no.4, pp. E154-159, 2005.

/64/ R.C. Mani et al., Electrochem Solid State Lett., vol. 5, no. 6, pp. E32-E35, 2002.

Uroš Cvelbar, Ita Junkar,*
Jožef Stefan Institute, Jamova cesta 39,
SI-1000 Ljubljana, Slovenia

Nina Hauptman, Marta Klanjšek-Gunde,
National Institute of Chemistry, Hajdrihova 19,
SI-1000 Ljubljana, Slovenia

Ksenija Rener-Sitar ,
University of Ljubljana, Hrvatski trg 6,
SI-1000 Ljubljana, Slovenia

** Corresponding author: uros.cvelbar@ijs.si*

Prispelo (Arrived): 17.09.2008 *Sprejeto (Accepted): 15.12.2008*

MICROWAVE PLASMAS AT ATMOSPHERIC PRESSURE: NEW THEORETICAL DEVELOPMENTS AND APPLICATIONS IN SURFACE SCIENCE

T. Belmonte*, G. Henrion, R.P. Cardoso, C. Noël, G. Arnoult, F. Kosior

Laboratoire de Science et Génie des Surfaces, Nancy-Université, CNRS, Ecole des Mines, Nancy Cedex, France.

Key words: plasma, atmospheric pressure, microwave, filaments, argon, oxygen

Abstract: Specificity of microwave plasmas created at atmospheric pressure is presented. Plasma is created in a quartz tube placed in a microwave cavity. The cavity is powered with a MW generator at the frequency of 2.45 GHz. Interesting results are obtained using a pulsed discharge with the frequency of few kHz. New phenomena such as filamentation are presented and described together with possible applications of such sources of reactive plasma particles.

Mikrovalovna plazma pri atmosferskem tlaku: sodobni teoretični pristopi in uporaba za modifikacijo površin

Kjučne besede: plazma, atmosferski tlak, mikrovalovi, niti, argon, kisik

Izvleček: Prikazujemo specifične značilnosti mikrovalovne plazme, ki jo vzbujamo pri atmosferskem tlaku. Plazmo ustvarimo v kvarčni cevi, ki je nameščena v mikrovalovni resonator. Resonator vzbujamo z MW generatorjem s frekvenco 2.45 GHz. Zanimive rezultate dobimo predvsem pri uporabi pulzne razelektritve s frekvenco nekaj kHz. Prikazujemo nekatere nove pojave, kot je na primer pojav drobnih razelektritvenih niti. Poleg razlage tega pojave predstavljamo tudi možnost uporabe tovrstne plazme kot izvira reaktivnih plazemskih radikalov.

1 Introduction

Microwave plasmas at atmospheric pressure can be easily implemented to get sources of active species for surface treatment. Contrary to the Dielectric Barrier Discharges, radiofrequency discharges /1-2/ and other microwave surfatrons /3-6/ which operate at low temperature, typically even at lower pressures, microwave plasmas in continuous mode make it possible to reach very high treatment temperatures /7-9/.

In this paper, we will situate the microwave plasmas among other sources at atmospheric pressure and describe the different aspects, both theoretical and applied, of microwave plasmas, including the micro-microwave plasmas newly proposed.

2 Design of sources

Several possibilities have been used to design microwave sources operating at atmospheric pressure (see Fig. 1). Sources like surface wave excited plasmas /11-15/, waveguide-based microwave torches /8, 16-21/ and resonant cavities /9, 22-26/ are widely used. Even split-ring resonator microplasma were recently proposed /27/ to create small-scale plasmas (the gap size can be as low as 45 µm). The choice of the microwave frequency (433, 915 or 2450 MHz among others) affects not only the size of the plasma, but also its mean electron density, leading to steeper gradients when the frequency increases. Of course, this choice strongly modifies the plasma properties. For example, it is possible to observe filamentation of a neon plasma at 2450 MHz but not at 433 MHz /28/.

Attention has been paid recently to the linear extension of these sources /29/ in order to obtain a plasma "curtain" that could be used over large dimension in continuous flow process but current solutions only apply under reduced pressure. A simpler solution would consist in multiplying the number of sources. However, such an approach would suffer from the lack of inhomogeneity in concentration at the boundary between two adjacent sources.

3 Theoretical study

New phenonema, like filamentation and contraction, have been recently studied using microwaves sources. In the first case, a reduction of the plasma diameter is observed in surface wave driven plasmas. The origin of this contraction is yet controversial. In the second case, the filamentation process is shown to depend on different time scales. The wave propagation conditions are defined by the dispersion equation and the boundary conditions of the problem.

3.1 Contraction

Contraction is defined as the compression of a plasma into a filament located at the discharge axis. This compression is due to a weaker ionization rate. According to /15/, it

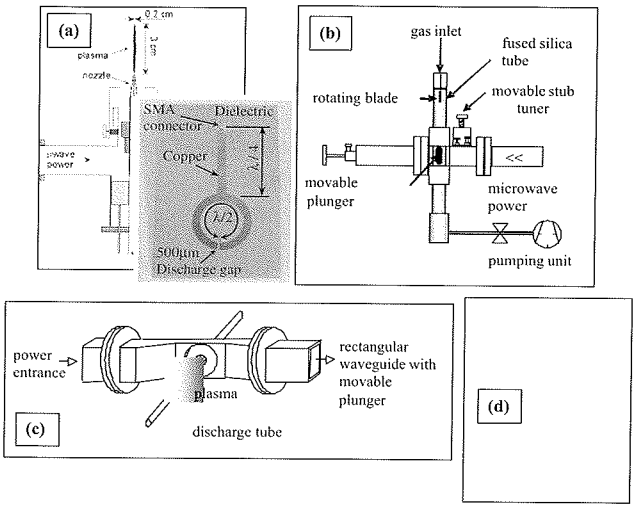

Fig. 1: Some possible designs of microwave sources operating at atmospheric pressure. (a) The "Torche à Injection Axiale" /7/, (b) resonant cavity /22/, (c) surfaguide wave launcher /11/ and (d) the split-ring resonator microplasma /27/.

could be due to a lower electron density caused by a decrease in the reduced electric field (E/N) due to a radial non-uniform heating of the gas. The decrease of the gas temperature changes the nature of the main dominating ion, since at high temperature, atomic ions prevail whereas dimmer ions are dominant at low temperature. Different works /30-31/ suggest that this lower electron density could result from a weak heating of the tail of the electron energy distribution function by electron-electron collisions.

3.2 Filamentation

When the discharge is sustained by a high frequency electric field, for certain operating conditions, another effect appears in addition to radial contraction - the breaking of the single plasma filament into two or more filaments of smaller diameters. We refer to this to as filamentation. The discharge filamentation is strongly connected to the contraction phenomenon. In these discharges that are controlled by ambipolar diffusion, we can think that the origin of filamentation is due to an inhomogeneity in the electron density or, but to a lesser extent, in the temperature. In Fig. 2, we observe a more intense light emission at the junction between the two filaments, suggesting a higher electron density as the possible source of the initial instability.

The filamentation process appears when the skin effect becomes important, i.e. at high electron density (typically ~10^{15} cm^{-3} in argon). The appearance of a second filament enables the better absorption of the power and a decrease in the mean electron density per filament. The presence of several filaments requires new microwave modes to satisfy the dispersion equations of the microwaves /32/.

We also showed recently that in pulsed mode, the growth of a filament could happen over different time scales. This is clearly evidenced in Fig. 3.

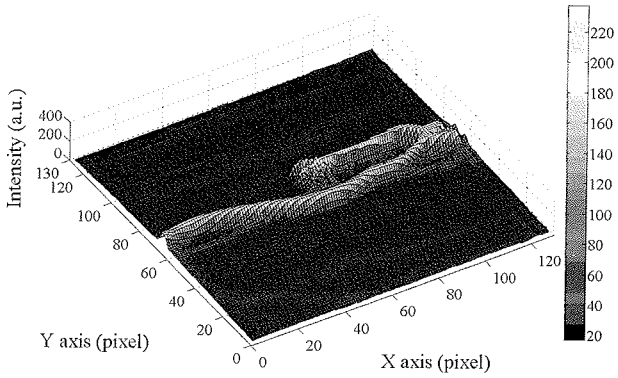

Fig. 2: Light intensity emitted by an argon plasma during the filamentation process. Two visible filaments are present in this image. Discharge sustained with a pulse frequency of 2 kHz. The pulse has a rectangular shape and the operation duty cycle is 41%. The absorbed power is ~70 W.

This memory effect is likely due to a post-discharge that remains active when the plasma is turned off.

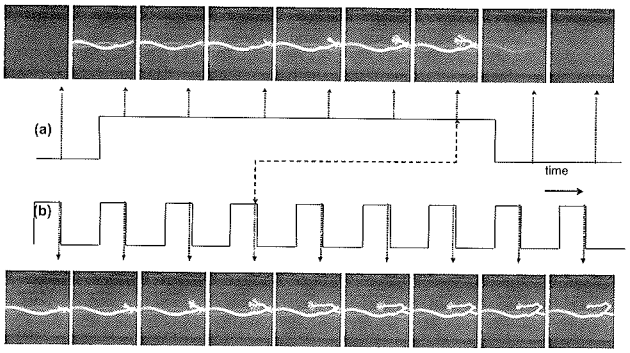

Fig. 3: Photographic sequence of atmospheric pressure discharges for a pulse frequency of 2 kHz. The pulse has a rectangular shape and the operation duty cycle is 41%. The absorbed power is ~70W. The resonant cavity is set up to resonate without plasma to ensure maximum electrical field, making the breakdown possible at each pulse. The integration time is 10 µs. (a): Selection of photographs taken every 31 µs during one period. (b): set of photographs taken at the end of each pulse after 9 pulses.

3.3 Modelling

Obviously, the lack of data on kinetic schemes occurring at high temperature requires specific works to improve the quality of the models /24, 33/ describing the behavior of these non-thermal plasmas. For example, the question of the dimmer ions dissociation rate as a function of the temperature is not solved yet since commonly used data only rely on estimation and not on measurements. This important question is essential to confirm the recent theory on contraction where the relative importance of atomic and molecular ions must be known accurately.

Another important aspect deals with the non-locality of the electron energy dissipation. Indeed, we have shown in /24/ that if the Boltzmann equation could be treated locally in helium, it is clearly not possible in argon, as it is yet commonly assumed. A more accurate treatment of the electron energy distribution function, as done for example in /13/, is necessary.

4 Surface treatments

Because of their high temperature (typically, above 1000 K and up to 5000 K), the microwave plasmas at atmospheric pressure can be use in many metallurgical applications like surface cleaning or Plasma Enhanced Chemical Vapor Depostion (PECVD). Micro-plasmas could also be used in small-scale materials processing or in micro chemical analysis systems /34,35/.

4.1 Surface preparation

Surface cleaning could be achieved with microwave sources at atmospheric pressure, by exploiting the high temperature of these sources, plasma processes being considered as environmental-friendly solutions. Many plasma processes (DBD, torches, corona discharges, etc.) are already proposed commercially to clean surfaces. However, a few is know on cleaning mechanisms. Two main problems arise: on the one hand, the oxidation of the surface can be enhanced in oxygen-containing plasma mixtures with respect to low pressure processes that usually operate at low temperature /36/. On the other hand, the cross-linking of radicals synthesized by the interaction of active species coming from the plasma with the contaminants can lead to the synthesis of a passive film that cannot be removed by the plasma. Under reduced pressure, this passive layer can be removed by sputtering. At atmospheric pressure, this step is no longer possible and a better understanding of the cleaning mechanisms is then required /37/.

4.2 PECVD

The main task to deal with in atmospheric PECVD is the control of the precursor flux with respect to the flux of active species from the plasma. Precursor dissociation and subsequent formation of intermediates must occur in the vicinity of the surface of the substrate. Diffusion being strongly limited at high pressure, one can only play on the convective flows of the precursors. The important time scale to be controlled is the residence time required for active species to reach the surface. For a long time scale, homogeneous nucleation leads to powder formation and deposition rates decrease. Transport of species through the boundary layer requires a minimum time that depends on the temperature and concentration. For shorter times, deposition rates decrease.

V. Hopfe and collaborators made huge progress in this field recently /38/. They succeeded in reaching deposition rates in the range 15-100 nm s^{-1} (static) and 0.3-2.0 nm m s-1 (dynamic) with properties of the silica thin films close to those of bulk silica. These very high values of the deposition rate make it possible to deposit thin films in continuous flow processes with moving substrate past the plasma source at several meters per minute.

However, deposition over large area with a high homogeneity in thickness and composition is still a difficult task to reach.

4.3 Other applications

Other possible applications deal with the development of small-scale microwave plasmas operating at high temperature. In general, microplasma sources capable of creating controlled small-sized discharges are desirable for applications such as bio-MEM sterilization, small-scale materials processing, micro chemical analysis systems, displays and micropropulsion. These microplasma sources can be integrated into small-scale portable devices that offer the same advantages of size, cost and reliability of microfabricated integrated circuits.

At high temperature, only some of these applications can be considered. We have developed recently a remote micro-plasma based on a resonant cavity by simply drilling a small hole (600 µm in diameter) on one side of the cavity. The microjet obtained like this can be a straight beam of active species over a relatively long distance (more than 10 cm - see Fig. 4).

This situation can only be reached at low flow rate to keep a laminar flow downstream the discharge which reaches ~2000 K /39/. The flow of this jet is controlled by the total

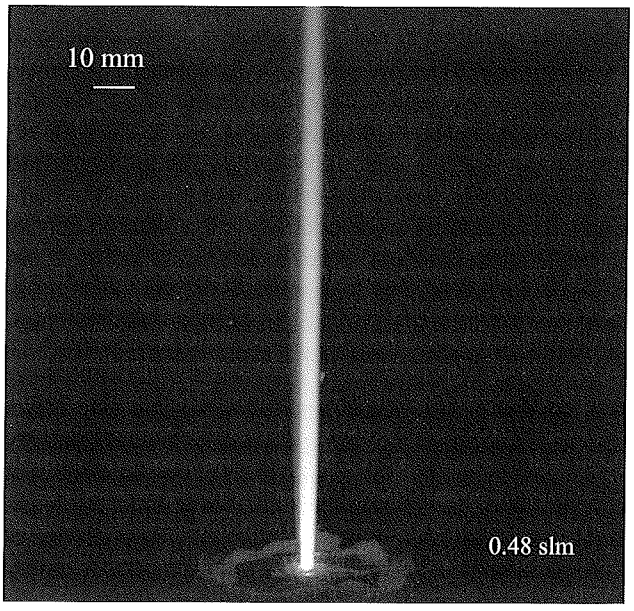

Fig. 4: Photograph of the atmospheric jet (Ar-20vol.%O_2) through a hole (600 µm in diameter) for a total flow rate of 0.48 slm. Power: 70 W.

flow rate of an Ar-20vol.%O_2 gas mixture. Three flow regimes are observed: one at low flow rates where the flow is laminar, one at intermediate flow rates where the flow is turbulent and transonic, and one at high flow rate where the flow is turbulent and supersonic.

With such a jet, thin film deposition by PECVD could be localized over a region as small as 1 mm^2. And more, such devices can be directly employed for the nanostructuring metals with oxygen plasma, where plasma radicals and surface heating is needed /40-46/. This will enable faster processing of materials and the growth of different nanostructures.

5 Conclusions

Atmospheric microwave plasmas are high-temperature non-equilibrium media where complex phenomena occur that are still under study. Resorting to atmospheric microwave plasmas can provide industrial solutions in the field of surface treatment. However, a lot must yet be done to improve the homogeneity of the surface treatments performed with such small-scale plasmas. We can hope also to be able to reach nanoscale using a top-down CVD approach as already performed under vacuum /47-55/. One difficulty to overcome will have to be the development of new plasma characterization diagnostics based on existing techniques in order to analyze these small-scale plasmas and their interactions with surfaces /56-65/.

References

/1/ K.N. Ostrikov, S. Xu, and M.Y. Yu, J. Appl. Phys., vol. 88, no. 5, pp.2268, 1999.

/2/ I.B. Denysenko, S. Xu., J.D. Long et al., J. Appl. Phys., vol. 95, is. 5, pp.2713, 2004.

/3/ C. Canal, F. Gaboriau, R. Molina, P. Erra, and A. Ricard, Plasma Process. Poly., vol. 4, pp. 445, 2007. A.

/4/ Ricard et al., Plasma Process. Poly., vol. 5, no. 9, pp.867, 2008.

/5/ C. Canal et al., Plasma Chem. Plasma Process., vol. 27, no. 4, pp. 404, 2007.

/6/ C. Canal et al., Int. J. Pharm., vol. 367, no. 1/2, pp. 155, 2009.

/7/ M. Moisan, G. Sauvé, J. Zakrzewski and J. Hubert, Plasma Sources Sci. Technol., vol. 3, pp. 584, 1994.

/8/ C. Tendero, C. Tixier, P. Tristant, J. Desmaison and P. Leprince, Spectrochim. Act. B, vol. 61, pp. 2, 2006

/9/ R. P. Cardoso, T. Belmonte, P. Keravec, F. Kosior and G. Henrion, J. Phys. D: Appl. Phys., vol. 40, pp. 1394, 2007.

/10/ K.N. Ostrikov, M.Y. Yu, N.A. Azarenkov, J. Appl. Phys., vol. 84, no. 8, pp. 4176, 1998.

/11/ M. Moisan and Z. Zakrzewski, J. Phys. D: Appl. Phys., vol. 24, pp. 1025, 1991

/12/ K.N. Ostrikov, M.Y. Yu, IEEE Trans. Plasma Sci., vol. 26, no.1, pp. 100, 1998.

/13/ U. Kortshagen, H. Schlüter and A. V. Maximov, Phys. Scr., vol. 46, pp. 450, 1992

/14/ K.N. Ostrikov, M.Y. Yu, L. Stenflo, Phys. Rev. E, vol. 61, no. 1, pp. 782, 2000.

/15/ Y. Kabouzi, D. B. Graves, E. Castaños-Martínez and M Moisan, Phys. Rev. E, vol. 75, 016402, 2007.

/16/ J. Jonkers, M. van de Sande, A. Sola, A. Gamero and J. van der Mullen, Plasma Sources Sci. Technol., vol. 12, pp. 30, 2003.

/17/ J. Jonkers, M. van de Sande, A. Sola, A. Gamero, A. Rodero A and J. van der Mullen, Plasma Sources Sci. Technol., vol. 12, pp. 464, 2003.

/18/ R. Alvarez, M. C. Quintero and A. Rodero, J. Phys. D: Appl. Phys., vol. 38, pp. 3768, 2005.

/19/ S. Y. Moon and W. Choe, Spectrochim. Act. B, vol. 58, pp. 249, 2003.

/20/ R. Stonies, S. Schermer, E. Voges and J. A. C. Broekaert, Plasma Sources Sci. Technol., vol. 13, pp. 604, 2004.

/21/ A. I. Al-Shamma'a, S. R. Wylie, J. Lucas and C. F. Pau, J. Phys. D: Appl. Phys., vol. 34 , pp. 2734, 2001.

/22/ R. P. Cardoso, T. Belmonte, G. Henrion and N. Sadeghi, J. Phys. D: Appl. Phys., vol. 39, pp. 4178, 2006.

/23/ R. P. Cardoso, T. Belmonte, P. Keravec, F. Kosior and G. Henrion, J. Phys. D: Appl. Phys., vol. 40, pp. 1394, 2007.

/24/ T. Belmonte, R.P. Cardoso, C. Noël, G. Henrion and F. Kosior, Eur. Phys. J. Appl. Phys., vol. 42, pp. 41, 2008.

/25/ A. A. Skovoroda and A. V. Zvonkov, J. Exp. Theoret. Phys.,vol. 92, pp. 78, 2001.

/26/ H. Potts and J. Hugill, Plasma Sources Sci. Technol., vol. 9, pp. 18, 2000.

/27/ F. Iza and J. Hopwood, Plasma Sources Sci. Technol., vol. 14, pp. 397, 2005.

/28/ E. Castaños Martinez, K. Makasheva and M. Moisan, "Study of the wave field azimuthal variation in surface wave discharges sustained at atmospheric pressure", XIX Escampig (07-2008), Granada, Spain, 2008.

/29/ J. Pollak, M. Moisan, Z. Zakrzewski, Plasma Sources Sci. Tehnol., vol. 16, pp. 310, 2007.

/30/ G. M. Petrov and C. M. Ferreira, Phys. Rev. E, vol. 59, pp. 3571, 1999.

/31/ Yu B Golubovskii, H Lange, V A Maiorov, I A Porokhova and V P Sushkov J. Phys. D: Appl. Phys., vol. 36, pp. 694, 2003.

/32/ H. Schlüter and A. Shivarova, Phys. Reports, vol.443, pp. 121, 2007.

/33/ T. Belmonte, R. P. Cardoso, G. Henrion and F. Kosior, J. Phys. D: Appl. Phys., vol. 40, pp. 7343, 2007.

/34/ I. Levchenko, K. Ostrikov, M. Keidar et al., J. Phys. D: Appl. Phys., vol. 41, no. 13, 132004, 2008.

/35/ I. Denysenko et al., J. Phys. D: Appl. Phys., vol. 104, no. 7, 115201, 2008.

/36/ M. Mafra et al., Key Eng. Mater., vol. 373-374, pp. 421, 2008.

/37/ M. Mafra, T. Belmonte, F. Poncin-Epaillard, A. S. da Silva Sobrinho, A. Maliska, Plasma Chem. Plasma Proces., vol. 28, no.4, pp. 495, 2008.

/38/ V. Hopfe, R. Spitzl, I. Dani, G. Maeder, L. Roch, D. Rogler, B. Leupolt, B. Schoeneich, Chemical Vapor Deposition, vol.11, no. 11-12, pp. 497, 2005.

/39/ G. Arnoult, R.P.Cardoso, T. Belmonte, G. Henrion, Appl. Phys. Lett., 93 (2008) 191507

/40/ U. Cvelbar, K. Ostrikov and M. Mozetic, Nanotechnology, vol. 19, no. 7, 073301, 2008.

/41/ U. Cvelbar, Z.Q. Chen, et al., Small, vol. 4, no. 10, pp. 1610, 2008.

/42/ S. Gubbala, V. Chakrapani, V. Kumar et al., Adv. Func. Mater., vol. 18, no. 16, pp. 2411, 2008.

/43/ A.H. Chin, T.S. Ahn, H.W. Li et al., Nano Lett., vol.7, no.3, pp. 626, 2007.

/44/ U. Cvelbar and K. Ostrikov, Cryst. Growth Design, vol. 8, no. 12, pp. 4347, 2008.

/45/ Z.Q. Chen et al., Chem. Mater., vol. 20, no. 9, pp. 3224, 2008.

/46/ M. Mozetic et al., Adv. Mater., vol. 17, no. 17, pp. 2138, 2005.

/47/ H.W. Li, A.H. Chin and M.K. Sunkara, Adv. Mat., vol. 18, no.2, pp. 216, 2006.

/48/ K.C. Krogman, T. Druffel, M.K. Sunkara, Nanotechnology, vol. 16, no.7, pp. S338, 2005.

/49/ M.K. Sunkara, S. Sharma , H. Chandrasekaran et al., J. Mat. Chem., vol. 14, no. 4, pp. 590, 2004.

/50/ J. Thangala, S. Vaddiraju, R. Bogale et al., Small, vol. 3, no. 5, pp. 890, 2007.

/51/ I. Levchenko, K. Ostrikov, J. Phys. D: Appl. Phys., vol. 40, no. 8, pp. 2308, 2007.

/52/ E. Tam et al., J. Appl. Phys., vol. 100, no. 3, 036104, 2006.

/53/ K. Ostrikov, A.B. Murphy, J. Phys. D: Appl. Phys., vol. 40, pp. 2223, 2007.

/54/ K. Ostrikov, S. Xu, A.B.M.S. Azam, J. Vac. Sci. Technol. A, vol. 20, pp. 251, 2002.

/55/ N.A. Azarenkov, I.B. Denisenko, K. Ostrikov, J. Appl. Phys., vol. 28, pp. 2465, 1995.

/56/ U. Cvelbar, M. Mozetic, J. Phys. D: Appl. Phys., vol. 40, pp. 2300, 2007.

/57/ M. Mozetic et al., Plasma Chem. Plasma Proc., vol. 26, pp. 103, 2006.

/58/ M. Mozetic et al., J. Appl. Phys., vol. 97, no. 10, 103308, 2005.

/59/ U. Cvelbar et al., Appl. Surf. Sci., vol. 210, no. 3-4, pp. 255, 2003.

/60/ U. Cvelbar, K. Ostrikov, A. Drenik, and M. Mozetic, Appl. Phys. Lett.,vol. 92, no. 13, 133505, 2008.

/61/ M. Mozetic et al., Appl. Surf. Sci., vol. 211, no. 1-4, pp. 96, 2003.

/62/ U. Cvelbar et al., Thin Solid Films, vol. 475, no. 1-2, pp. 12, 2007.

/63/ T. Vrlinic et.al , Surf. Interf. Anal., vol. 39, pp. 476, 2007

/64/ A. Drenik et al., J. Phys. D : Appl. Phys., vol. 41, no. 11, 115201, 2008.

/65/ F. Gaboriau et al., J. Phys.D : Appl. Phys., vol. 42, no. 5, 055204, 2009.

T. Belmonte, G. Henrion, R.P. Cardoso,*
C. Noël, G. Arnoult, F. Kosior
Laboratoire de Science et Génie des Surfaces, Nancy-Université, CNRS, Ecole des Mines, Parc de Saurupt - CS 14234 - 54042 Nancy Cedex, France.
Email : Thierry.Belmonte@mines.inpl-nancy.fr

Prispelo (Arrived): 17.09.2008 *Sprejeto (Accepted): 15.12.2008*

ENERGY AND MASS SPECTROSCOPY OF IONS AND NEUTRALS IN COLD PLASMA

Marijan Maček[1,2*] Miha Čekada[2]

[1]University of Ljubljana, Faculty of Electrical Engineering, Ljubljana, Slovenia
[2]Jožef Stefan Institute, Ljubljana, Slovenia

Key words: polymer; PES; PET; PPS; PS; PP; PA6; PTFE; cellulose; oxygen; plasma; functionalization; surface activation; surface modification, XPS

Abstract: A very versatile method for plasma characterization is plasma energy and energy-resolved mass spectroscopy. By this method energy and mass distributions of ions and neutrals can be analyzed. Results obtained on two different triode ion plating systems with different magnetic confinement show a good correlation between the average energy of the particles bombarding the surface and the properties of the layer (texture, stress-free lattice parameter and in minor extend others such as microhardness and internal stress).

In both systems single and multiply charged ions of Ar and N_2 gas and the evaporated Ti were detected. The system with a strong magnetic field confinement exhibits higher plasma potential (Up = 55 V) under the standard deposition conditions, the peak ion energy is higher and the energy distribution is narrower than in the system without magnetic confinement (Up = 12 to 35 V). Mass-spectroscopic studies reveal, that the electron impact ionization of titanium, $Ti^{n+} + e^- \rightarrow Ti^{(n+1)+} + 2e^-$, n = 0–3, within the electron beam with an energy above 27.5 eV is very effective. The probability for the multiple charged ions in this system is much higher than in the system without the magnetic confinement, so the population of Ti^{++} in this system is higher than that of Ti^+. Even the presence of Ti^{3+} and Ti^{4+} ions was confirmed experimentally.

An additional promising technique is also so called multiple ion detection (MID) which is very suitable for monitoring of different plasma assisted processes like etching and cleaning.

Energijsko ločljiva masna spektroskopija ioniziranih in nevtralnih delcev v hladni plazmi

Kjučne besede: energijsko ločljiva spektroskopija plazme, ionsko nanašanje, TiC; TiN;TiCN

Izvleček: Za okaratkterizacijo plazme je zelo primerna metoda energijsko ločljive masne spektroskopije. Z njo lahko pridobimo podatke o energijski in masni porazdelitvi ionov in nevtralnih delcev. Rezultati dobljeni v dveh sistemih za ionsko nanašanje z različnima magnetnima poljema pokažejo na dobro ujemanje med povprečno energijo delcev, ki zadevajo površino in lastnostmi nanesenih plasti (tekstura, mrežni parametri v stanju brez notranjih napetosti in v manjši meri trdota in notranje napetosti).

V obeh sistemih so bili zaznani enojno in večkratno nabiti ioni Ar, N_2 in naparjevanega Ti. Sistem z močnim magnetnim poljem ima med standardnimi pogoji nanašanja višji plazemski potencial (Up = 55 V), kar se odraža v energijski porazdelitvi ionov z vrhom pri višjih energijah, sama porazdelitev pa je ožja kot v sistemu z šibkim magnetnim poljem (Up = 12 to 35 V). Masna spektroskopija pokaže, da je ionizacija titana, $Ti^{n+} + e^- \rightarrow Ti^{(n+1)+} + 2e^-$, n = 0–3, znotraj elektronskega curka z energijo nad 27.5 eV zelo učinkovita. Verjetnost za večkratno ionizacijo je v sistemu z močnim magnetnim poljem mnogo večja kot v sistemu s šibkim magnetnim poljem. Zato je populacija ionov Ti^{++} mnogo višja kot enkrat nabitih ionov Ti^+. Zaznana je bila celo prisotnost ionov Ti^{3+} in Ti^{4+}.

Zelo obetavna tehnika za spremljanje plazemskih postopkov (jedkanje, čiščenje) pa je metoda MID (multiple ion detection), pri kateri spremljamo populacijo različnih ionov tekom samega procesa.

1 Introduction

Plasma assisted processes are gaining more and more attention due to its benefits. The temperatures involved in the process are lower; lower is also environmental pollution in some cleaning processes, and there is a greater possibility to tailor the process according to technology demands due to wider range of parameters involved in the reaction.

However, for a successful implementation of plasma assisted processes, the thorough knowledge of plasma status is of the crucial importance. The main methods, suitable for its characterization are:

- *electrostatic (Langmuire) probe* /1, 2/, which gives a valuable information about the plasma parameters such as: electron temperature (T_e) and its energy distribution, plasma potential (U_{pl}) and densities of electrons and ions (n_e, n_i),
- *optical emission spectroscopy*, OES /1, 3/. The method is very suitable to monitor the plasma assisted processes "ex-situ". But it can provide the information on the light emitting species only.
- *energy resolved mass spectroscopy* /1, 4/. This is the only method which can give information about the energy and mass distribution of ions (positive and negative) as well as neutrals from the plasma. On the

* This work was done during my stay at Jožef Stefan Institute

other hand, the method is a rather complicated and invasive one, since the spectrometer sampling orifice is protruding into the vacuum chamber.

In this paper, the applications of energy resolved mass spectroscopy during the all steps of a hard coating process based on Ti(C,N) in an triode ion plating system are given.

The hard coatings can be deposited by different PVD and CVD techniques, but ion plating, especially triode one, is a very common method. The advantage are high deposition rate and good mechanical properties of deposited films due to high ionization rate accompanied by high ion energy as it was shown also in our previous investigations /5, 6/.

The coatings properties are related to the chemical composition and to the microstructure, and depend on the state of the surface before the deposition (heating and etching) as well on the deposition conditions which affect the state of the plasma during ion plating process. There are many studies depicting the influence of the bombardment by energetic particles (especially ions and also radicals) on to the film microstructure and consequently on to the film properties /5, 7, 10/, but the understanding of plasma during a typical ion plating processes is not so clear, due to the complicated nature of interactions between hot electrons and reactive gas molecules even in a case of a relatively simple binary gas mixture of Ar + N_2, not to mention a more complicated systems involving also a (hydro)carbon precursor (CH_4, C_2H_2,...).

2 Experimental

2.1 Energy resolved mass spectroscopy

The energy-resolved mass spectrometer, such as Balzers PPM421, schematically shown in Fig. 1, is a differentially pumped device. The entry orifice (100 mm) is usually at the floating potential, or it can be biased or grounded if desired. The ions from the plasma are focused by the ion optics in the ion measuring mode, or they are deflected in the neutral measuring mode applying the appropriate potential.

Neutrals from the plasma are ionised in the crossed-beam electron ionisation chamber. The electron beam current equals about 0.20 mA at the pre-selected acceleration voltage up to 70 V. In the neutral-measuring mode the chamber is grounded, but its potentials follow the energy scan in the ion mode.

Ions from the plasma or from the ionisation chamber are subsequently filtered by the cylindrical mirror energy analyser with the resolution ~ 0.3 eV and then pass through the quadrupole mass analyser with the resolution[1] m/Dm = 100. In the present set-up the ions are deflected for

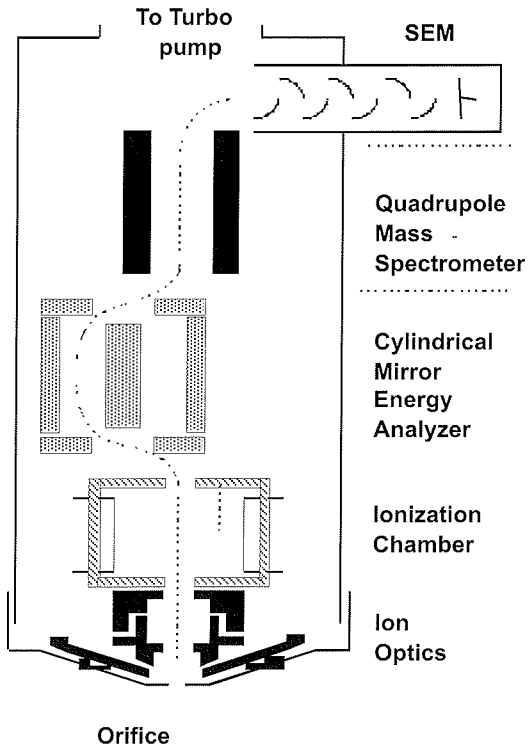

Fig. 1: Scheme of PPM421 energy and mass analyzer.

90° before they enter the secondary electron multiplier, where avalanche electrons are generated. In this way the sensitivity is greatly improved. It can give readings from 10^{-1} to 10^7 counts per second (CPS).

The analyser can perform a mass scan at selected ion energy (mass spectrum), multiple ion detection (MID) at selected energy, or it can perform an energy scan at selected mass number m/q. The measured energy spectrum is actually a spectrum of stopping potential. Therefore, the real ion energy is the product of the measured stopping potential and the ion charge.

Under some conditions, especially when the mean free paths for charge-exchange and/or other collisions are comparable with the plasma sheath thickness, the measured energy distributions depend on the voltage applied on the extraction electrode. But for the most of experiments at relatively low pressures (below 0.5 Pa) the plasma has collision-free sheaths (sheath thickness d" 1mm, mean free path H" 20-40 mm) and the measured distribution corresponds to the distribution in the plasma at least for the ions coming from the direction of the highest ion optics transmission.

An important problem arises since the spectrometer is partially immersed in the vessel with relatively strong magnetic field. Since it is very difficult to protect the whole spectrometer (inside and outside of the vacuum chamber with appropriate m-metal shield) from the effect of the magnetic field, we performed calibration measuring the effect of

1 Dm is defined as the peak width at 10% of the maximum intensity

magnetic field on the spectra of neutrals. As to be expected only light ions (m/q < 12 amu) are strongly affected. All our results for the integrals of ion intensities and energy distributions are corrected for the effect of the magnetic field. Mass spectra are as measured, therefore hydrogen ions (m/q = 1-3 amu) are relatively underestimated for about 5-10 times regarding the peaks with m/q ≥ 12 amu.

2.2 Description of the system

Energy resolved mass spectrometry studies were performed in the commercial Balzers BAI 730 triode ion plating system. This system uses a filament-based ionisation chamber, which forms a low voltage (LV) arc expanding into the reaction chamber. The power supply is electrically floating with respect to the chamber walls

Its negative pole is connected to the arc cathode, while the positive one can be connected to different anodes, depending on the operation mode (heating, etching, and evaporation, /6/).

The standard deposition process for M(C,N) hard coatings in this system consists of 3 steps:

- *heating* with electrons in Ar plasma for about 60 min up to above 350°C
- *etching* of the substrate surfaces with Ar ions for 15 min to improve adhesion
- *deposition.*

The standard prescribed conditions for TiN ion plating are: arc current I_{arc} = 200 A, substrate voltage U_B = -125 V, argon pressure p_{Ar} = 0.15 Pa (argon flow F_{Ar} ~ 90 cm^3/min), total pressure measured by ionisation gauge p_{tot} = 0.2 Pa (F_{N2} ~ 120 cm^3/min) and current in both coils I_C = 15 A which corresponds to magnetic field of 7 mT measured at the centre of the vessel. A more detailed description of the system, effects of process parameters on to the plasma parameters deduced from the electrostatic probe measurements and energy resolved mass spectroscopy are given in /6, 11, 12/.

3 Results and discussion

3.1 Energy spectra of positive ions

The main advantage of the energy resolved mass spectroscopy is its ability to measure energy distribution of ions and neutrals. In Fig. 2a the energy spectrum of selected positive ions during TiN deposition under the standard conditions in the above described system is shown. The peak of the distribution at 55 eV corresponds to the measured plasma potential, U_{pl}. For comparison in Fig 2b the energy spectrum in a very similar ion plating system, but without magnetic confinement /5/, is shown. In this case the energy distribution is a wide one, spreading from 12 to about 35 eV, with Ar distribution centred at about 12 eV and Ti spread over the whole energy interval. Peaks of the energy distribution for this system correspond to the measured potentials in the system (U_{pl} = 15 - 35 V) and are positioned at a considerably lower energy than in the system with magnetic confinement, (U_{pl} = 55 eV). Consequently the average energy <*E*> and effective bias U_{eff} are lower than in the previous system.

Calculations in /5/ show that a difference of some -75 V in U_{bias} is necessary to get the same average particle energy in the system without magnetic confinement. The difference in the effective bias was confirmed by the relationship between the film properties (texture, stress-free lattice parameter and in minor extend others such as microhardness and internal stress).

3.2 Analysis of ion flux by mass spectroscopy

In Fig. 3 mass spectra measured during the deposition of Ti, TiN and TiC, i.e. in the working gas composed of Ar, Ar/N_2 and Ar/C_2H_2 mixtures, respectively, are compared. Other parameters, the Ar pressure, corrected partial reactant pressure and arc current were the standard ones for TiN deposition.

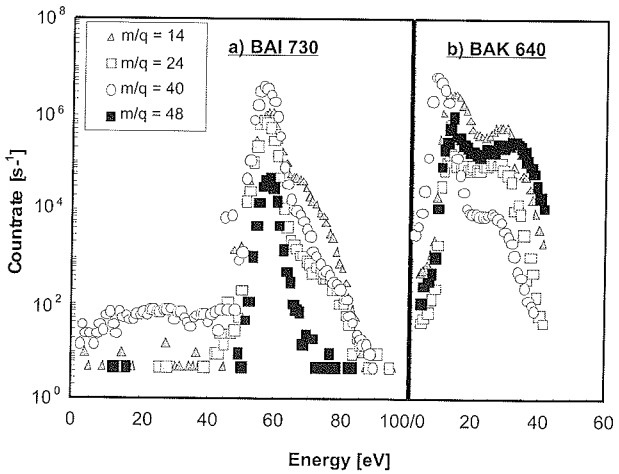

Fig. 2: Typical energy spectra of selected ions during deposition of TiN in two ion plating systems, a) with magnetic confinement, b) without magnetic confinement /5/

The mass spectrum for the Ti evaporation in pure Ar in Fig 3a reveals typical features of the plasma in the BAI 730 ion-plating apparatus /13/. A high degree of ionisation is notable for the evaporated Ti, highlighted by the fact that the intensities of the ndoubly charged Ti^{2+} ions observed at the mass-to-charge ratios from 23-25 are of the same order of magnitude as that of the singly charged Ti^+ ions (peaks at m/q 46-50 amu). There is even a well-defined peak of the triply charged Ti^{3+} ions centred at m/q = 16 amu (not the oxygen O^+!), as shown in the insert, measured at higher resolution m/Dm. It is worth to note that we reported even on the presence of the ions Ti^{4+} with peaks centred at m/q = 12 amu, but the intensity was about 100 times lower than that of Ti^{3+}. The Ar ions constitute the peaks at m/q = 40 amu (Ar^+) and 20 amu (Ar^{++}). The peak

at m/q = 41 amu (ArH^+) is due to the contamination of the system with hydrogen during previous depositions.

When 110-130 cm^3/min of nitrogen is added to the argon (equilibrium partial pressure p_{N2} = 0.08 Pa) strong peaks appear in the spectrum (Fig. 3b), in addition to those peaks discussed above. There are peaks at m/q = 14 amu (N^+ and/or N_2^{2+}), at m/q = 28 amu (N_2^+), and at m/q = 7 amu (N^{2+}). The peak at 14 amu belongs, most probably, to N^+ rather than N_2^{2+}, since the ratio of the intensities of the peaks at 14 amu and 28 amu is about 50. This is just the opposite to the ratio of about 0.02 between the doubly and the singly charged Ar ions at m/q = 20 and 40 amu, respectively. In the spectrum one can also see some hydrogen and hydrocarbon contamination. The peaks at m/q = 15 amu and 29 amu are hydrogenated nitrogen and argon, respectively, while the peak at m/q = 15 amu could be NH^+ and/or more probably CH_3^+, since it is accompanied by weaker peaks of the $CH_{n=0-4}^+$ ion family.

Much more pronounced changes in mass spectrum (Fig. 3c) resulted after the addition of C_2H_2 (85-90 cm^3/min, the same corrected partial pressure 0.08 Pa) to argon. In the previous case of ion plating in the Ar/N_2 mixture only peaks belonging to N and N_2 molecule appear. But now the spectrum contains many additional peaks as expected due to the complicated cracking pattern of the C_2H_2 molecule. The most intense additional peak is at the mass number m/q = 41 amu, which belongs to the hydrogenated argon ion ArH^+, followed by the hydrogen peaks at m/q = 1-3 amu. The hydro-carbon ion intensities are relatively low, compared with nitrogen in the Fig. 3b. The most intense peak is the carbon peak at m/q = 12 amu (C^+ or C_2^{2+}), while the hydrocarbon peaks $CH_{n=1-4}^+$ and $C_2H_{n=1-4}^+$ have an order of magnitude lower intensities, with the parent ion $C_2H_2^+$ (m/q = 26 amu) being the most intense of these.

However, it must be noted that the possibly present peaks at m/q = 24 and 25 amu (C_2^+, C_2H^+, respectively), could not be distinguished because of the strong contribution of the $^{48,50}Ti^{2+}$ isotope ions at these mass numbers. But on the basis of our previous spectroscopic studies performed during CrC ion plating /14/ we believe that they are of lower intensity than the parent $C_2H_2^+$ ion.

It is necessary to point out that the mass spectra are not corrected for the effect of magnetic field. It was already mentioned that hydrogen peaks are underestimated for about 5-10 times regarding the peaks with mass number m/q > 12 amu, which are more or less insensitive to the magnetic field. Consequently, the intensity of the hydrogen peaks with m/q = 1-3 amu is comparable to the intensity of the hydrogenated argon ion. The parent C_2H_2 molecules are dissociated under the standard condition for the Ti evaporation (I_{arc} = 200 A) almost to its single constituents, hydrogen and carbon. This is in agreement with observations in a hollow cathode arc deposition system /15/, where at the magnetic field comparable to that in our system the C^+ ions appear to be the most abundant.

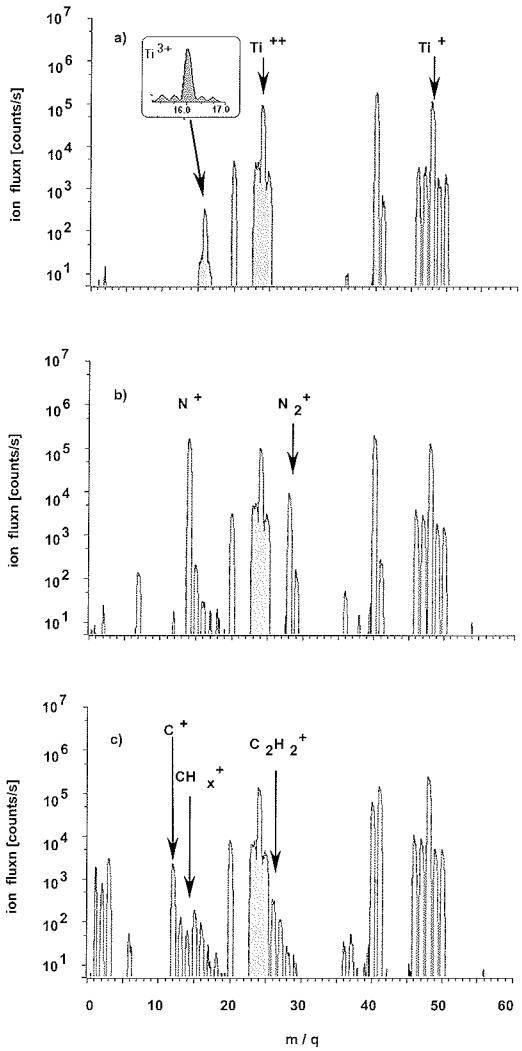

Fig. 3: Ion mass spectra measured during Ti evaporation at I_{arc} = 200 A in pure argon (a), mixture of argon and 120 cm^3/min nitrogen (b) and mixture of Ar and 87 cm^3/min acetylene (c).

3.3 Mass spectra of the neutrals

The mass spectra of neutrals with near zero energy were measured using the ionisation source of the spectrometer (U = 70 V) before ignition of the discharge and during the discharge with moderate I_{arc} = 175 A. The mass spectrum in Fig. 4a is an example for the Ar/C_2H_2 working gas mixture at low acetylene partial pressure, $p_{C2H2,corr}$ = 0.04 Pa, F_{C2H2} = 14 cm^3/min at I_{arc} = 0 A. Besides the usual peaks of the background gas in an analyser belonging to water (m/q = 17-18 amu), nitrogen (m/q = 28 amu) and CO_2 (m/q = 44 amu), the spectrum taken before ignition of the discharge contains strong peaks of argon (m/q = 40 and 20 amu) and of parent and fragment ions of C_2H_2 (m/q = 24-27 and 13 amu). The source of hydrogen at m/q = 1 and 2 amu may be either C_2H_2 and/or water.

After ignition of the discharge (the same pressure, F_{C2H2} = 34 cm^3/min), the spectrum in Fig. 4 b. is greatly changed in the C_2H_2-related peaks, while the intensity of the other

peaks remains basically unchanged. Namely, the peak at the mass number 26 amu (C_2H_2) decreases by a factor of about 100 while the hydrogen H_2 peak increases by the same factor. The peaks of CH (m/q = 13 amu), C_2 (m/q = 24 amu) and C_2H (m/q = 25 amu) fall below the detection limit. In spite of problems with accurate quantitative interpretation of such measurements, (e.g. the signal of radicals with high sticking coefficient is much suppressed in comparison with, say, argon), the large change in the relation between H_2 and C_2H_2 signal after ignition of the discharge allows to conclude that even during the discharge at moderate arc currents the atmosphere is composed mainly of argon and hydrogen, as a product of acetylene dissociation with some traces of hydrocarbon radicals, CH_3 and CH_4. As a consequence of the high hydrogen concentration during the discharge, the pressure measured by ion gauge is greatly overestimated. Therefore, the small increase in the acetylene flow with the increasing arc current is due to the decrease in the real pressure.

The acetylene dissociation is proportional to the arc current. The degree of dissociation is very high under the standard evaporation conditions. The hydrocarbons are almost completely stripped of hydrogen leaving mostly C^+, some radicals CH_x^+ and hydrogen. A high degree of acetylene dissociation in the system can not be explained by one-step electron impact dissociation. The acetylene–related spectra of positive ions are substantially different

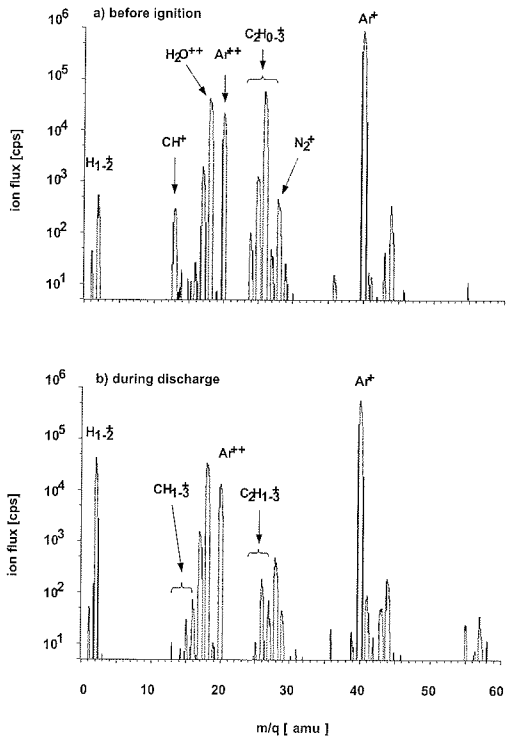

Fig. 4: The mass spectra of neutrals (i.e. using the spectrometer ionisation source) before (a, F_{C2H2} = 14 cm^3/min) and during discharge (b, F_{C2H2} = 34 cm^3/min) in an Ar/C_2H_2 working gas mixture.

from the mass spectra of C_2H_2 gas without discharge. Note that even the peak at m/q = 6 amu (C^{++}) is present and that the peak at m/q = 12 amu (C^+) is the most intense of all hydro-carbon peaks in the spectra of positive ions. It seems quite reasonable, that other reactions within the volume of the plasma, like charge transfer and Penning ionisation/dissociation, also play an important role.

On the other hand the high degree of Ti ionisation into doubly, triply and even higher charged states can be explained by electron impact ionisation, Ti^{n+} + e ! $Ti^{(n+1)+}$ + 2e, n = 0-3, within the electron beam of a few centimetre and with an electron energy slightly above the threshold for the ionisation of the triply charged Ti ion, i.e. about 27.5 V.

3.4 Multiple ion detection

Energy resolved mass spectroscopy is also a viable tool for process monitoring. For this purpose MID technique is used. A very important step before the deposition of any thin film is the cleanness of the substrates. Therefore, a typical deposition process includes a preheating step, as well as ion etching of the substrates without opening of the vacuum chamber.

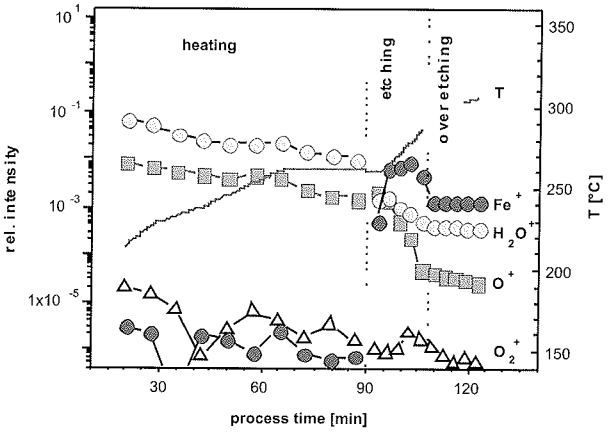

Fig. 5: Relative intensities of significant ions during the heating and etching steps, prior to the ion plating of hard coating

The question is when to terminate etching? An excessively long etching step increases the roughness of the substrates, while inadequately etched substrates suffer on poor adhesion. In Fig. 5 typical example of MID spectra normalized to Ar ions density for heating and etching step is shown. It has to be noted, that the etching time was longer than necessary to show the effect of over-etching. The break in spectra between both steps is due to the change in MID parameters as a result in different energy distributions. As already shown in /6/ the energy distribution of ions has peaks (E_p) at different values, corresponding to plasma potential. E_p equals to 15 V for heating, 12 V for etching and 52 V for deposition

From Fig. 5 it is clearly seen that during heating the intensities of O^+, H_2O^+ and O_2^+ ions slowly decrease, for less

than one decade per hour. This rate is independent on temperature of dummy stainless steel substrates, which rose to 250°C as measured by TC. During etching, the intensities of O^+ and H_2O^+ ions drop in 15 min for almost two decades. The intensity of O_2^+ ion decreases with the same rate as before. The increase in intensity of Fe^+ ion for 4 decades in first minutes of etching indicates the cleaning of the surface oxide. The native oxide is removed after app. 15 min. This was indicated by the fact that the intensities of O^+, H_2O^+ and Fe^+ ions become stable, while the temperature of the substrates gradually rises to above 300°C. Any additional etching increases the surface roughness, and should be avoided.

4. conclusions

Energy resolved mass spectroscopy is a very versatile method for the plasma characterisation. It enables the analysis of *ion energy* distributions of selected ions (and neutrals). Previously published /5/ results show a good correlation between the average energy of the particles bombarding the surface and the properties of the layer (texture, stress free lattice parameter and in minor extend others, like microhardness and internal stress).

Knowing the ion energy, *mass spectra* can be measured. On this way the composition of charged plasma particles and their degree of ionisation can be analysed. Using the ionisation cell the thermal and energetic neutrals can be analysed as well.

MID techniques provide real-time information on the process. Substrate cleaning/etching can be terminated exactly at the point, when the surface is clean, without unnecessary over-etching by monitoring O^+, H_2O^+ and Fe^+ (substrate) ions. It can be applied to the other plasma assisted processes like etching and plasma cleaning.

Acknowledgment

This work was done during my stay at Jožef Stefan Institute and was supported by the Ministry of Higher Education, Sciences and Technology of the Republic of Slovenia.

References

/1/ A. Grill, Cold Plasma in Materials and Fabrication, IEEE Press, NY, 1994

/2/ N. Herskowitz, Langmuir probe diagnostics, in D.A. Glocker, S.Ismath Shah, (Eds.), Handbook of Thin Film Process Technology, Institute of Physics Publising, Bristol, 1995, p. D3.0:1.

/3/ G. Baravian, G. Sultan, E. Damon, H. Detour, C. Hayaud, P. Jacquot, Surf. Coat. Technol., **76-77** (1995) 678-693

/4/ M. Nesládek, C. Quaeyhaegens, S. Wouters, L.M. Stals, E. Bergmann, G. Rettinghaus, Surf. Coat. Technol., **68-69** (1994) 339-343

/5/ S. Kadlec, M. Maček, S. Kadlec, M. Maček, S. Wouters, B. Meert, B. Navinšek, P. Panjan, C. Quaeyhaegens, L. M. Stals, Surf. Coat. Technol., **116-119** (1999) 1211-1218

/6/ M. Maček, B. Navinšek, P. Panjan, S. Kadlec, Surf. Coat. Technol., **135** (2001) 208-220

/7/ K.S. Fancey, A. Matthews, Appl. Phys. Lett., **55(9)** (1989) 834-836

/8/ S. Wouters, S. Kadlec, C. Quaeyhaegens, L.M. Stals, Surf. Coat. Technol., **97**, (1997) 114-121

/9/ S. Wouters, S. Kadlec, C. Quaeyhaegens, L.M. Stals, J. Vac. Sci. Technol., **A 16(5)** (1998) 2816-2826

/10/ S. Wouters, S. Kadlec, M. Nesládek, C. Quaeyhaegens, L.M. Stals, Surf. Coat. Technol., **76-77** (1995) 135-141

/11/ M. Maček , M. Čekada, *Surf. Coat. Technol.*, **180-181** (2004) 2-8

/12/ M. Maček, M. Mišina, M. Čekada, P. Panjan, *Vacuum*, **80** (2005) 184-188

/13/ M. Maček, B. Navinšek, P. Panjan, S. Kadlec, S. Wouters, C. Quaeyhaegens, L.M. Stals, Surf. Coat. Technol., **113** (1999) 149-156

/14/ M. Maček, M. Čekada, M. Mišina, Czechoslovak Journal of Physics, Vol **50**, Suppl. S3 (2000) 403-408

/15/ A. Buuron, F. Koch, M. Nöthe, H. Bolt, Surf. Coat. Technol., **116** (1999) 755-765

Marijan Maček
University of Ljubljana, Faculty of Electrical Engineering, Tržaška 25, 1000 Ljubljana, Slovenia

Miha Čekada
Jožef Stefan Institute, Jamova 39, 1000 Ljubljana, Slovenia

Prispelo (Arrived): 17.09.2008 *Sprejeto (Accepted): 15.12.2008*

SELF-ORGANIZED WORLD OF PLASMA NANOSCIENCE: APPROACHES TO NUMERICAL SIMULATION OF COMPLEX PROCESSES ON LOW TEMPERATURE PLASMA EXPOSED SURFACES

Igor Levchenko

School of Physics, The University of Sydney, NSW 2006, Australia.
Plasma Nanoscience Centre Australia (PNCA), CSIRO Materials Science and Engineering, Lindfield, NSW 2070, Australia

Key words: plasma, magnetron, microwave, arc, nanoscience, nanostructure, self-assemby

Abstract: In this paper we consider several general questions and problems related to self-assembly and self-organization on plasma-exposed surfaces. We are dealing here mainly with the case of low temperature plasma that can be produced in magnetrons, vacuum arcs and microwave sources. Such kind of plasma is very promising environment for the advanced nanotechnology, and its potential in promoting and controlling self-assembly and self-organization on plasma exposed surfaces is very large. Recent investigations, referenced in this work, have shown that the self-assembly and self-organization in low-temperature plasmas can be very effective and versatile tool for the production of complex nanostructures on surfaces. We discuss here several problems and possible features of self-organization in low-temperature plasmas, and indicate some possible ways for the future development and investigations.

Spontana organizacija v svetu plazemske nanoznanosti: pristopi k numerični simulaciji procesov na površini materialov, ki so izpostavljeni nizkotemperaturni plazmi

Kjučne besede: plazma, magnetron, mikrovalovi, oblok, nanoznanost, nanostrukture, spontana organizacija

Izvleček: V prispevku obravnavamo nekatera splošna vprašanja, ki se pojavljajo pri razumevanju procesov spontane organizacije atomov na površini materialov, ki so izpostavljeni nizkotemperaturni plazmi. Osredotočimo se na plazmo, ki jo ustvarimo z naslednjimi razelektritvami: magnetronsko, mikrovalovno in obločno. Takšna plazma predstavlja obetavno okolje za sodobne nanotehnologije, saj omogoča širok izbor parametrov, ki so potrebni za vzpodbujanje rasti nanostruktur in spontano organizacijo atomov na površini različnih materialov. V prispevku povzemamo rezultate najnovejših raziskav, ki jasno kažejo, da je s tovrstno plazmo mogoče vzpodbuditi rast dobro orientiranih nanostruktur, ki imajo lahko zelo zapleteno strukturo. V prispevku tudi komentiramo navajamo in komentiramo nekatere težave, s katerimi se soočamo pri sintezi tovrstnih materialov in nakazujemo možne prihodnje poti raziskav na tem področju.

1 Introduction

The methods of synthesizing complex large-scale nanodevices and extra-large arrays of nanostructures /1, 2/, large arrays of carbon nanotubes /3, 4/ and nanowires /5, 6, 7, 8/, nanoparticles /9/, various other nanostructures /10, 11, 12/, nanofiber /13/, nanotips /14/ and nanobelts /15, 16/ based on self-organization and self-assembly of complex nanosystems on low temperature plasma-exposed surfaces is one of the most promising ways for synthesizing complex surface-based nanosystems. This technology may be also affectively applied to synthesizing various coatings /17, 18/, nanowire-based probes /19, 20/ and sensors /21, 22, 23/, for bacteria degradation and other biology-related issues /24, 25/. The low-temperature plasma and plasma-based processes are very suitable for various techniques of nano-synthesis /26, 27, 28, 29/, for functionalization /30, 31/ and treatment /32, 33/ of various structured materials and systems /34/, including textile /35, 36/, fabrics /37, 38/, nanomembrane systems /39/ and various materials such as polyolefines /40/, polyamides /41/, graphite-polymer composite /42/, nanocomposite diamonds /43/ and nanotubes /44/. The microwave plasma and microwave plasma - based equipment /45, 46/, as well as magnetrons /47, 48/, setups with radio-frequency inductively coupled plasmas /49, 50/ and vacuum arc setups /51/ appeared to be the most promising environment and setups for these processes /52, 53/. Precise control of self-organization is very important for all processes and all techniques, but some applications such as those based on complex-shape nanowires /54/, as well as nanowires for solar cells /55, 56/ require especial attention to the controllability; as a result, researchers pay a great attention to the characteristics, regimes, and properties of the plasma-generating equipment /57, 58/.

In this situation, the studies on general question of self-assembly and self-organization on plasma-exposed surfaces are of greatest interest /59, 60/. The complex sophis-

ticated methods of numerical simulation allowing detailed investigation of the entire process of self-organization are particularly promising and should be extensively developed /61, 62, 63/. The progress in this direction is significant / 64, 65/, but a need in designing new complex numerical methods is pressing. Taking this into account, we have developed several numerical approaches and techniques able to simulate self-organizational and self-assemble processes on plasma-exposed surfaces. This approach allows modeling the whole system consisting of plasma bulk and surface.

The paper is organized as follows. In Section 2, we introduce several typical groups of nanostructures that can be produced by self-organization and self-assembly on plasma-exposed surfaces, and point out some major difficulties that appear in modeling self-organization. In Section 3, we describe an approach and complex model that can be used for numerical simulation of the self-organization and self-assembly in nano-world; in Section 4, we consider briefly the main numerical approaches, boundary conditions and some typical results obtained by numerical simulation of the self-organization and self-assembly on plasma-exposed surfaces.

2 Typical self-assembled and self-organized structures on plasma-exposed surfaces

In general, all self-assembled and self-organized nanostructures may be conditionally divided to the five main types: vertical and vertically-aligned nanostructures such as vertical nanotubes, nanorods, nanotips /66, 67, 68/; one-dimensional nanostructures (nanodots, quantum dots) / 69, 70/; two-dimensional nanostructures such as nanowalls /71/; complex self-assembled nanosystems and nanomaterials such as nanowires formed between surface-grown nanodots /72, 73/; nanostructures of complex internal structure, for example, nanodots with core-shell structure and partially-saturated nanoparticles /74, 75, 76/ . All these types are very important for the present day nanotechnology, and all of them represent significant difficulties in modeling, especially in cases when the self-organization processes are involved. It is important to note that modeling of low-dimension nanostructures (one- and two-dimensional, i.e. nanodots and nanowalls) cannot be considered as easier task, since in any self-organization process the number of objects involved is very large, and thus the complex (actually, 3D) systems should be modeled, even in cases when it consists of 1D nanodots. Besides, the models capable of describing the self-organization on surface should involve sub-models of several levels and hence several different scales; all this makes this problem very complex.

3 Approach to model self-assembled and self-organized nanostructures

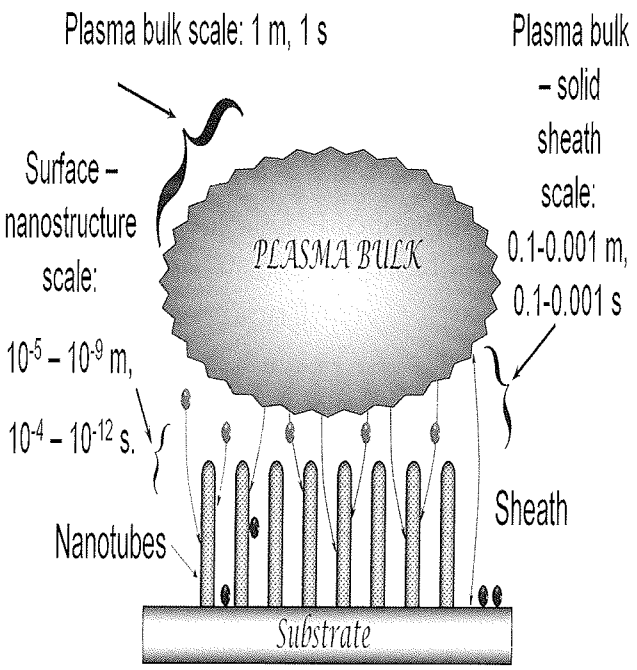

Fig. 1: Three levels of processes in self-assembly on plasma-exposed surface

To build an approach and model for simulation of the self-organization on plasma-exposed surface, one should consider at least three scale levels (Fig. 1). In general, they can be characterized as Plasma bulk level (1), Sheath level (2) and Nanostructure level (3); the characteristic sizes are shown in the figure. Thus, the complex model should involve processes and comprise equations for all three levels.

At the first level, the ion current extraction from the plasma bulk is the main process that determines the ion current density to the nanostructures and substrate surfaces, and hence it determines the kinetics of the self–organization and self-assembly, as well as temperature and other macro-parameters.

When the surface is biased, it is separated from the plasma bulk with a sheath, and the electric field is mainly concentrated in this sheath. In the models, it is often assumed that the ions enter the sheath with Bohm velocity that is calculated as *Vb=(Te/mi)1/2*, where *Te* is the electron temperature, and *mi* is the ion mass. Depending on the parameters, the two main cases can be considered, with respect to the relation between the surface potential *US* and the electron temperature *Te*. When the electron temperature is small, the sheath width is calculated:

$$\lambda_S = \frac{\sqrt{3}}{2}\lambda_D\left(\frac{2U_S}{T_e}\right) \qquad (1)$$

where $\lambda_D = (\varepsilon_0 T_e / ne)^{1/2}$ is the Debye length, ε_0 is the die-

lectric constant, *n* is the plasma density, and *e* is the electron charge.

In opposite case, i.e. when the surface bias is low, the sheath width can be calculated by the relation for Debye lengths:

$$\lambda_S = k_\lambda \lambda_D = k_\lambda \sqrt{\frac{\varepsilon_0 T_e}{ne}}, \qquad (2)$$

where *kl* is a constant of 1-5.

In the sheath, i.e. at the second scale level, the ions move under effect of the electric field created by the biased (charged) nanostructures and biased substrate surface. This electric field has a complex structure, and thus the trajectories of the ions are complex curves, with the ions being deposited onto side surfaces of the growing substrate. In general approximation, the electric field may be calculated as

$$\mathbf{E}(r) = \sum_1^N \left[\int_{S_i} \frac{\rho_i dS}{4\pi\varepsilon_0 r^3} \mathbf{r} \right] + U_S \left(\frac{z}{\lambda_S} \right)^{\frac{1}{3}}, \qquad (3)$$

where *N* is the number of nanostructures, *z* is the distance to the substrate surface, *ri* is the surface density of electric charges on nanostructure surfaces, and *Si* is the surface area of the *i*th nanostructure. The ion trajectory can be calculated by integration of the equation of ion motion in the electric field. With the density of ion current calculated, the flux of ions and atoms to each specific nanostructure can be obtained, and thus the growth kinetics can be calculated.

At the third scale level, i.e. on the substrate and nanostructure surfaces, the equations based on surface and bulk diffusion should be used. Namely, The two-dimensional flux of adsorbed atoms from the substrate surface to the nanostructure can be calculated from the diffusion equation

$$\frac{\partial \eta}{\partial t} = D_S \left(\frac{\partial^2 \eta}{\partial x^2} + \frac{\partial^2 \eta}{\partial y^2} \right) + \psi_{in} - \psi_{vp}, \qquad (4)$$

for adatom density field *h(x, y, t)* on the substrate surface, where *yin* is the external (from sheath) flux of atoms and ions to the substrate surface, and *yvp* is the flux of atom evaporation from the substrate surface. With the diffusion equation solved (in general, only numerical solution is possible due to very large number of boundary conditions involved), the total flux of adsorbed atoms at the border of an individual nanostructure can be calculated from equation:

$$\varphi_i = -2\pi r_i m_a D / \rho \left(\partial \chi / \partial r \right), \qquad (5)$$

where *ri* is the radius of the *i*th nanostructure, *ma* is the adatom mass, and *r* is the density of carbon material. In this case, the surface diffusion coefficient *D* can be calculated as *D = (l2´n)exp(-ed/kT)*, where *k* is Boltzmann's constant, *ed* is the surface diffusion activation energy, *l* a is the lattice constant of the substrate, and *T* is the surface temperature.

At the third (nanostructure) scale level, the equations for nanostructure growth and reshaping should be added which have the following general appearance:

$$\frac{\partial V_n}{\partial r_{on}} dr_{on} = J_{Sn} dt, \qquad (6)$$

$$\frac{\partial V_n}{\partial h_n} dh_n = J_{en} dt. \qquad (7)$$

Here, *ron, hn*, and *Vn* are the base radius, height and volume of *n*th nanostructure; *Jen* is the total flux of ions and atoms to surface of *n*th nanostructure; *Jsn* is the total surface flux of adatoms to the nanostructure from surface, and, finally, *∂V/∂r* and *∂V/∂l* are the nanostructure growth functions (shape- and size-dependent).

The above described model can be used for numerical simulation of the self-assembly processes on plasma-exposed surfaces. However, the three different scale levels of this system represent a very hard problem, which can be solved by involving different numerical techniques at different levels.

4 Numerical approach, boundary conditions and typical results

4.1 Numerical approach and boundary conditions

We have implemented the following numerical techniques for the different levels: at level 1 (plasma bulk), the traditional methods used for the plasma parameters calculation; at level 2 (sheath - surface), the Monte-Carlo (MC) method was used to trace the ions in the electric field created by charged nanostructures; and at level 3 (nanostructure level), depending on the types of nanostructures to be described, the diffusion or Kinetic Monte Carlo techniques.

The total model uses *N+1* boundary conditions, where *N* is the number of nanostructures on surface. Besides, additional boundary conditions should be set at the boundary of simulation domain which is restricted in the numerical process. An initial condition for the ion motion consists in setting the initial ion velocity at sheath border, which can be assumed as Bohm velocity. The initial shapes of the nanostructures can be set as representative for each specific type.

4.2 Typical results

Now, we consider several typical results obtained by the above described model. We recall that our main aim is to demonstrate that the complex multi-scale numerical ap-

proach is capable of simulating self-assembly and self-organization processes on plasma-exposed surfaces.

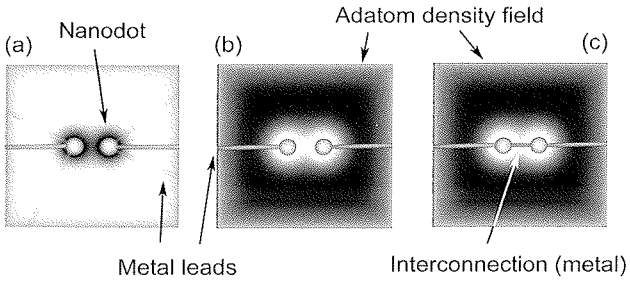

Fig. 2: Formation of metal leads to nanodots and interconnection between nanodots on surface: (a) – formation of external leads to the nanodots; (b) – formation of final leads; (c): formation of metal interconnection between nanodots. The correct growth of leads and interconnections is due to proper selection of the growth conditions.

In Fig. 2 we show the simulated process of the self-organized formation of metal leads (long nanowires shown in green in the figure) to nanodots on surface, and then – formation of metal interconnection (red nanowire) between the nanodots; thus, with the material correctly chosen, this self-assembled system may represent a base for semiconductor nano-diode and nano-transistor.

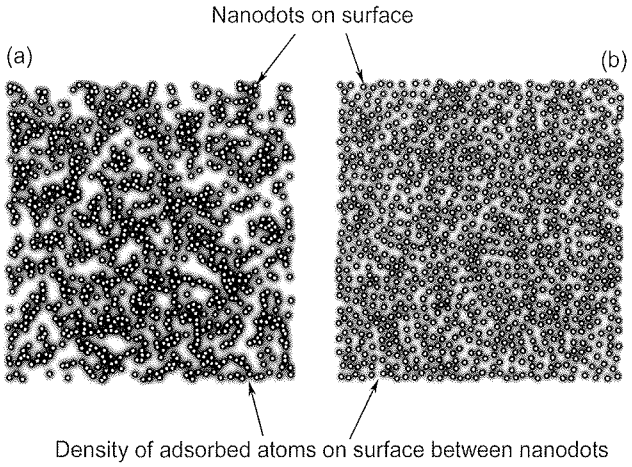

Fig. 3: Self-organization in large arrays of nanodots: formation of ordered pattern: (a) – initial pattern of very low ordering; (b) – final pattern of higher ordering, the nanodots were re-arranged due to self-organizational processes on surface.

In the figure, the first fragment (a) illustrates the formation of leads; the dimmed green leads are not preferable by the conditions of growth, and eventually the process results in the perfect oppositely directed leads (b). Then, with the density of adsorbed atoms on surface increased (as seen from darker color), the interconnections of other metal can be formed directly between the nanodots. The correct growth of leads and interconnections is due to proper selection of the growth conditions and correct guidance of the self-organization.

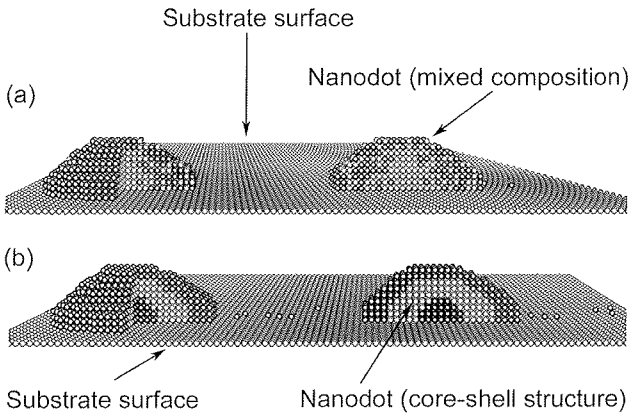

Fig. 4: Self-assembled core-shell nanodots on plasma-exposed surface: (a) – Nanodot of mixed composition, i.e. with the external layer enriched with the dopant, but perfect core-shell structure was not formed; (b) – perfect core-shell structure was formed due to correctly guided self-assembly processes.

The experimental investigation of the interconnection formation on plasma-exposed surface is described elsewhere /lxxiii/.

In Fig. 3 we show the simulated process of the self-organized formation of large array of nanodot on plasma-exposed surface. At the first stage (a), the array of nanodots is completely disordered; at the final stage (b), the pattern is much more ordered. The self-organization processes triggered by the presence of electric field on surface (the nanodots were formed from plasma on biased surface) caused rearrangement of the nanodots and finally resulted in better pattern. The experimental investigation of the ordered nanodot pattern formation on plasma-exposed surface is described elsewhere /lxix/.

In Fig. 4 we show the simulated process of self-assembling the core-shell nanodots on plasma-exposed surface. In the first case (a), the nanodot of mixed composition, i.e. with the external layer enriched with the dopant, was formed; but perfect core-shell structure was not formed; in the second case (b), the perfect core-shell structure was formed on the nanodot due to correctly guided self-assembly processes.

In Fig. 5 we show the results of numerical simulation of self-assembling process that leads to the formation of complex nano-structure consisting of three metal nanodots, interconnected with metal nanowires.

This structure, which can be a prototype of the nano-circuit, was successfully simulated by the above described model.

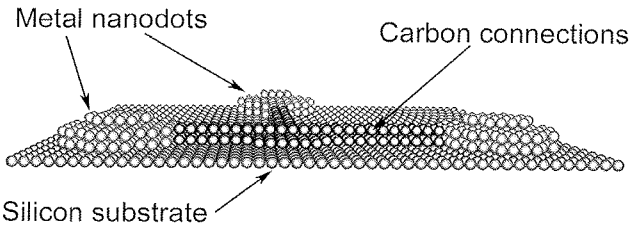

Fig. 5: numerical simulation of self-assembling complex nano-structure consisting of three metal nanodots, interconnected with metal nanowires.

5 Conclusions

In this paper we have discussed some important questions related to the self-organization and self-assembly of nanostructures on plasma-exposed surfaces. We have demonstrated that the proper selection of the structure of model, as well as numerical methods ensures effective modeling and simulation of the complex process of self-assembly and self-organization on low temperature plasma exposed surfaces.

Acknowledgments

This work was partially supported by the Australian Research Council, CSIRO, the University of Sydney, and the International Research Network for Deterministic Plasma-Aided Nanofabrication.

References

/1/ K. Ostrikov, Rev. Mod. Phys., vol. 77, no. 2, pp. 489-511, 2005.

/2/ U. Cvelbar, Z.Q. Chen, M.K. Sunkara et al., Small, vol. 4, no. 10, pp. 1610-1614, 2008.

/3/ U.M. Graham, S. Sharma, M.K. Sunkara et al., Adv. Funct. Mater., vol. 13, no. 7, pp. 576-581, 2003.

/4/ I. Levchenko, K. Ostrikov, M. Keidar et al., J. Phys. D. Appl. Phys., vol. 41, no. 13, art. no. 132004, 2008.

/5/ M.K. Sunkara, S. Sharma, R. Miranda et al., Appl. Phys. Lett., vol. 79, no. 10, pp. 1546-1548, 2001.

/6/ S. Vaddiraju, A. Mohite, A. Chin et al., Nano Lett., vol. 5, no. 8, pp. 1625-1631, 2005.

/7/ M. Mozetic et al., Adv. Mater., vol. 17, pp. 2138-2142, 2005.

/8/ H.W. Li, A.H. Chin, M.K. Sunkara, Adv. Mater., vol. 18., no. 2, pp. 216-224, 2006.

/9/ K.C. Krogman, T. Druffel, M.K. Sunkara, Nanotechnology, vol. 16., no. 7, pp. S338-S343, 2005.

/10/ J. Thangala, S. Vaddiraju, R. Bogale et al., Small, vol. 3, no. 5, pp. 890-896, 2007.

/11/ H. Chandrasekaran, G.U. Sumanasekara, M.K. Sunkara, J. Phys. Chem. B, vol. 110, no. 37, pp. 18351-18357, 2006.

/12/ A.H. Chin, T.S. Ahn, H.W. Li et al., Nano Lett., vol. 7, no. 3, pp. 626-631, 2007.

/13/ I. Denysenko, K. Ostrikov, et al., J. Appl. Phys., vol. 104, no. 7, 073301, 2008.

/14/ E. Tam, I. Levchenko, K. Ostrikov, J. Appl. Phys., vol. 100, no. 3, 036104, 2006.

/15/ Z.Q. Chen et al., Chem. Mater., vol. 20, no. 9, pp. 3224-3228, 2008.

/16/ U. Cvelbar, M. Mozetic, J. Phys. D. Appl. Phys., vol. 40, no. 8, pp. 2300-2303, 2007.

/17/ U. Cvelbar, M. Mozetic, M. Klanjsek-Gunde, IEEE Trans. Plasma Sci., vol. 33, no. 2, pp. 236-237, 2005.

/18/ M.K. Gunde, M. Kunaver, et al., Vacuum, vol. 80, no. 1-3, pp. 189-192, 2005.

/19/ M. Mozetic, et al., J. Appl. Phys., vol. 97, no. 10, art. no. 103308, 2005.

/20/ M. Mozetic, et al., Plasma Chem. Plasma Proc., vol. 26, no. 2, pp. 103-117, 2006.

/21/ U. Cvelbar, K. Ostrikov, A. Drenik et al., Appl. Phys. Lett., vol. 92, no. 13, art. no. 133505. 2008.

/22/ U. Cvelbar, M. Mozetic, I. Poberaj et al., Thin Solid Films, vol. 475, no. 1-2, pp. 12-16, 2005.

/23/ A. Drenik et al., J. Phys. D: Appl. Phys., vol. 41, no. 11, art. no. 115201, 2008.

/24/ Z. Vratnica, D. Vujosevic, et al., IEEE Trans. Plasma Sci., vol. 36, no. 4, pp. 1300-1301, 2008.

/25/ C. Canal, F. Gaboriau, S. Villeger, et al., Int. J. Pharmaceutics, vol. 367, no.1-2, pp. 155-161, 2009.

/26/ V. Hody, T. Belmonte, T. Czerwiec et al., Thin Solid Films, vol. 506-507, pp. 212-216, 2006.

/27/ M. Mafra, T. Belmonte, A. Maliska, et. al, Key Eng. Mat., vol. 373-374, pp. 421-425, 2008.

/28/ V. Hody, T. Belmonte, C. Pintassilgo et. al., Plasma Chem. Plasma Process., vol. 26, pp. 251-266, 2006.

/29/ M. Mafra, T. Belmonte, F. Poncin-Epaillard, A. S. da Silva Sobrinho, A. Maliska, Plasma Chem. Plasma Process., vol. 28, no. 4, pp. 495-509, 2008.

/30/ U. Cvelbar, M. Mozetič, I. Junkar, et al., Appl. Surf. Sci., vol. 253, no. 21, pp. 8669-8673, 2007.

/31/ T. Vrlinic et al., Surf. Interface Anal., vol. 39, no. 6, pp. 476-481, 2007.

/32/ S. Xu, K. Ostrikov, J. D. Long, S. Y. Huang, Vacuum, vol. 80, no. 6, pp. 621-630, 2006.

/33/ A. Ricard, F. Gaboriau, C. Canal, Surf. Coat. Technol., vol. 202, no. 22-23, pp. 5220-5224, 2008.

/34/ A.E. Rider, I. Levchenko, K. Ostrikov, J. Appl. Phys., vol. 101, 044306, 2007.

/35/ C. Canal, S. Villeger, S. Cousty, B. Rouffet, J.P. Sarrette, P. Erra, A. Ricard, Appl. Surf. Sci., vol. 254, no. 18, pp. 5959-5966, 2008.

/36/ C. Canal, F. Gaboriau, R. Molina, P. Erra, A. Ricard, Plasma Proc. Polym., vol. 4, pp. 445-454, 2007.

/37/ C.Canal, R.Molina, P.Erra, A.Ricard, Eur. Phys. J. Appl. Phys., vol. 36, pp. 35-41, 2006.

/38/ C. Canal, F. Gaboriau, A. Ricard et al., Plasma Chem. Plasma Process., vol. 27, no. 4, pp. 404-413, 2007.

/39/ A. Ricard, C. Canal, S. Villeger, J. Durand, Plasma Proc. Polym., vol.5, no. 9, pp. 867-873, 2008.

/40/ T. Belmonte, C.D. Pintassilgo, T. Czerwiec et al., Surf. Coat. Technol., vol. 200, no. 1-4, pp. 26-30, 2005.

/41/ C. Canal, R. Molina, E. Bertrán, P. Erra, J. Adhesion Sci. Technol., vol. 13, pp. 1077-1089, 2004.

/42/ U. Cvelbar, S. Pejovnik, M. Mozetič et al., Appl. Surf. Sci., vol. 210, no. 3-4, pp. 255-261, 2003.

/43/ R.C. Mani, S. Sharma, M.K. Sunkara et al., Electrochem. Solid State Lett., vol. 5, no. 6, pp. E32-E35, 2002.

/44/ M. Keidar, A. M. Waas, Nanotechnology, vol. 15, pp. 1571-1575, 2004.

/45/ R.P. Cardoso et al., J. Phys. D.: Appl. Phys., vol. 40, no. 5, pp. 1394-1400, 2007.

/46/ G. Arnoult, R.P. Cardoso, T. Belmonte, G. Henrion, Appl. Phys. Lett., vol. 93, no. 19, art. no. 191507, 2008.

/47/ I. Levchenko, M. Romanov, M. Keidar, J. Appl. Phys., vol. 94, 1408, 2003.

/48/ I. Levchenko, M. Romanov, M. Keidar, I. I. Beilis, Appl. Phys. Lett., vol. 85, 2202, 2004.

/49/ K. N. Ostrikov, S. Xu, M. Y. Yu, J. Appl. Phys., vol. 88, no. 5, pp. 2268-2271, 2000.

/50/ K. N. Ostrikov, S. Kumar, H. Sugai, Phys. Plasmas, vol. 8, no. 7, pp. 3490-3497, 2001.

/51/ M. Keidar, I. Levchenko, T. Arbel, M. Alexander, A. M. Waas, and K. Ostrikov, Appl. Phys. Lett., 92, 043129, 2008.

/52/ T. Belmonte, R.P. Cardoso, G. Henrion, F. Kosior, J. Phys.D.: Appl. Phys., 40, pp. 7343-7356, 2007.

/53/ K. Ostrikov, J. D. Long, P. P. Rutkevych, S. Xu, Vacuum, Vol. 80, no. 11-12, pp. 1126-1131, 2006.

/54/ M.K. Sunkara, S. Sharma, H. Chandrasekaran et al., J. Mater. Chem., vol. 14, no. 4, 590-594, 2004.

/55/ S. Gubbala, V. Chakrapani, V. Kumar et al., , Adv. Funct. Mater., vol. 18, pp. 2411-2418, 2008.

/56/ U. Cvelbar, K. Ostrikov, M. Mozetic, Nanotechnology, vol. 19, no. 40, art. no. 405605, 2008.

/57/ U. Cvelbar, M. Mozetic, D. Babic et al., Vacuum, vol. 80, no. 8, pp. 904-907, 2006.

/58/ M. Mozetic, A. Zalar et al., Appl. Surf. Sci., vol. 211, no. 1-4, pp. 96-101, 2003.

/59/ K. Ostrikov, Vacuum, vol. 83, pp. 4-10, 2008.

/60/ K. Ostrikov, I. Levchenko, S. Xu, Pure Appl. Chem., vol. 80, pp. 1909-18, 2008.

/61/ I. Levchenko, K. Ostrikov, J. Phys. D.: Appl. Phys., vol. 40, no. 8, pp. 2308-2319, 2007.

/62/ I. Levchenko, K. Ostrikov, U. Cvelbar, IEEE Trans. Plasma Sci., vol. 36, no. 4, pp. 866-867, 2008.

/63/ I. Levchenko, K. Ostrikov, A.B. Murphy, J. Phys. D: Appl. Phys., 41, no. 9, art. no. 092001, 2008.

/64/ K. Ostrikov, A. B. Murphy, J. Phys. D: Appl. Phys., vol. 40, no. 8, pp. 2223-2241, 2007.

/65/ Z. L. Tsakadze, I. Levchenko, K. Ostrikov, S. Xu, Carbon, vol. 45, no. 10, pp. 2022-2030, 2007.

/66/ I. Levchenko, K. Ostrikov, J. D. Long, S. Xu, Appl. Phys. Lett., vol. 91, art. no. 113115, 2007.

/67/ I. Levchenko, K. Ostrikov, M. Keidar, and S. Xu, Appl. Phys. Lett., vol. 89, art. no. 033109, 2006.

/68/ I. Levchenko, K. Ostrikov, E. Tam, Appl. Phys. Lett., vol. 89, art. no. 223108, 2006.

/69/ I. Levchenko, K. Ostrikov, K. Diwan, K. Winkler, and D. Mariotti, Appl. Phys. Lett., vol. 93, art. no. 183102, 2008.

/70/ I. Levchenko, K. Ostrikov, Nanotechnology, vol. 19, art. no. 335703, 2008.

/71/ I. Levchenko, K. Ostrikov, A. E. Rider, E. Tam, S. V. Vladimirov, and S. Xu, Phys. Plasmas, vol. 14, art. no. 063502, 2007.

/72/ K. Ostrikov et al., Thin Solid Films, vol. 516, no. 19, pp. 6609-6615, 2008.

/73/ I. Levchenko, K. Ostrikov, D. Mariotti, Carbon, vol. 47, no. 1, pp. 344-347, 2009.

/74/ I. Levchenko, A.E. Rider, K. Ostrikov, Appl. Phys. Lett., vol. 90, art. no. 193110, 2007.

/75/ I. Levchenko, K. Ostrikov, Appl. Phys. Lett., vol. 92, art. no. 063108, 2008.

/76/ I. Levchenko, K. Ostrikov, D. Mariotti, A. B. Murphy, J. Appl. Phys., vol. 104, art. no. 073308, 2008.

Igor Levchenko
School of Physics, The University of Sydney, NSW 2006, Australia.
**Email: I.Levchenko@physics.usyd.edu.au*

Prispelo (Arrived): 17.09.2008 *Sprejeto (Accepted): 15.12.2008*

INNOVATIONS IN SLOVENIAN ELECTRONICS INDUSTRY

Mojca Marc[1*], Uroš Cvelbar[2], Ljubica Knežević Cvelbar[1]

[1]Faculty of Economics, University of Ljubljana, Ljubljana, Slovenia
[2] Jožef Stefan Institute, Ljubljana, Slovenia

Key words: Innovations, patents, electronics industry, Slovenia

Abstract: We conducted a survey-type research of innovation activity and the use of intellectual property instruments in Slovenian manufacturing companies in the period 2004-2006. The results show that companies in electronics industry have slightly more active innovation policy than companies in other industries. The electronic industry companies typically have larger R&D departments, are larger companies, and have on average more new patents and products then other companies in Slovenian economy. Other aspects of innovation characteristics and behavior of Slovene electronics companies are presented and put into broader perspective by comparison to other Slovenian companies.

Inovacije v slovenski elektronski industriji

Kjučne besede: inovacije, patenti, elektronska industrija, Slovenija

Izvleček: Opravili smo raziskavo o inovativni dejavnosti in uporabi instrumentov intelektualne lastnine v slovenskih podjetjih med leti 2004-2006. Rezultati so pokazali, da imajo podjetja, ki proizvajajo elektroniko značilno več aktivne inovacijske politike kot ostala podjetja. Podjetja, ki proizvajajo elektroniko imajo značilno večje RR oddelke, so večja podjetja in imajo v povprečju več novih patentov in produktov kot ostala podjetja v slovenski ekonomiji. V članku so predstavljene tudi ostale inovacijske značilnosti in obnašanje slovenskih podjetij, ki proizvajajo elektroniko v primerjavi z ostalimi slovenskimi proizvodnimi podjetji.

1 Introduction

Innovation is widely recognized as an important factor of firm profitability and long-term success. Innovation can be implemented in a new product or a new process. In the first case, the gains for an innovative firm come from a higher quality product (in terms of value added to consumers) for which a higher price can be charged. In the second case, gains come from input cost savings, which permit higher price-cost margins.

However, new scientific or technological knowledge embedded in innovations can easily spill out and end up in someone else's R&D effort. In economics, this property of new knowledge is called non-excludability and is typical for public goods. Arrow /1/ was the first to show that when it is not possible to exclude the use of a good with this property by individuals who did not pay for the good, the incentive to produce such a good is reduced. Without protection offered by intellectual property rights (IPR), new knowledge is very much like public good: it can be used by people or companies who did not originate (or pay) for it and the incentive to create new knowledge (in other words, to engage in R&D effort) is therefore undermined.

Legal instruments like patents, trademarks and licences (IPR) serve to protect the benefits arising from innovative products and processes. For example, Greenhalgh and Longland /2/ find empirical evidence for positive returns from doing R&D and also from registering patents and trademarks in UK. Also, Varsakelis (2001) /3/, Lederman and Maloney (2003) /4/, Kanwar and Evanson (2003) /5/, Basanini and Ernst (2002) /6/, Bebczuk (2002) /7/, and Falk (2006) /8/ empirically investigate the effect of patent protection on business R&D intensity and generally find some evidence that a stronger patent protection indeed has a positive effect on business R&D intensity. However, patents do not protect most of innovations and some of the reasons why firms decide not to patent are the following: innovations are not novel enough to be eligible for patent protection, too much information must be disclosed in a patent application, the cost of applying and defending a patent in court is too high, it is easy to legally invent around the patent, technology is moving so fast that patents are irrelevant.

Besides preventing unauthorized imitation, patents are used also to secure royalty income. Licensing is a common method of awarding the right to use a patent to other parties and earn additional revenue from innovation. Furthermore, it is also used for more "strategic" reasons such as deterring entry of potential competitors /9/, enhancing demand /10/, and facilitating collusion /11/. Kim and Vonortas /12/ find that licensing is more extensively used if a company has more technological knowledge, has used licensing before, the growth rate of its sector is higher, IPR protection is stronger, and the nature of technology is more "complex"[1]. However, Levin et al. /13/ find empirical evidence that patents are regarded less as a way to gain additional revenue through licensing than they are as a way to prevent imitation. Their study also revealed two other possible reasons to use patents which are not related to protecting returns from innovations: i) patents can be used as a measure of performance for R&D employees and ii) patents can open access to certain foreign markets which require the licensing of technology to domestic industry as a condition to enter the market. In addition, Hall and

Ziedonis /14/ found out that companies in US Semiconductor Industry were aggressively patenting since the early 1980's, but not so much to protect the returns to their innovation as to build patent portfolios which were aimed at reducing the danger of being held up by external patent owner and were later also used for cross-licensing, patent exchange and other negotiations.

Then again, a patent is not the only instrument of protecting innovation and the benefits arising from them. In fact, Cohen et al. /15/ and Levin et al. /13/ study U.S. manufacturing companies and empirically find that no industry, even pharmaceutical, relies exclusively on patents or see them as the most effective mechanism of protection. In spite of the existence of IPR, which do alleviate the problem of non-excludability, we can still observe practices of reverse engineering and industrial espionage resulting in imitation and inventing around legally protected products and processes. The existence and large magnitude of knowledge spillover has been documented by a number of empirical studies (for a review see /16,17/). Therefore, companies must use also other mechanisms that can protect the returns to their R&D effort more effectively. Among other mechanisms of protection secrecy, lead time (i.e. first mover advantage), complementary sales and service, and complementary manufacturing facilities and know how are the most general. Different mechanisms can be appropriate for effective protection in different industries and also in different stages of the innovation process. In the initial stages of innovation, prior to commercialization, companies can rely on secrecy, but later when the new product is introduced in the market, they may protect their competitive advantage by obtaining a patent or invest in aggressive marketing and increased lead time /15/.

Empirical studies find that companies typically use a combination of mechanisms to protect their inventions /13,15/ , where Cohen identified three common combination strategies employed by U.S. manufacturing companies: 1) they exploit complementary capabilities and lead time, 2) they use legal instruments (notably patents) or 3) they keep their innovations secret. Besides, their study has shown considerable differences in mechanisms deemed most effective among industries. For example, companies from drugs and medical equipment industries found all mechanisms highly effective in protecting their innovation, while companies from semiconductor, machine tools and aerospace industries believed that secrecy and lead time were most effective to protect benefits from product innovation, and companies from communications equipment, computer, steel, and car and truck industries thought lead time gave most protection. Interestingly, companies from electrical equipment industry indicated that none of these mechanisms is effective in protecting their innovation.

The effectiveness of a particular mechanism in a particular industry depends on a number of factors: the technology itself, the complexity of the product, the nature of the innovation (e.g. secrecy is more appropriate for process innovations), the nature of the production process (e.g. complex, capital-intensive production can rely on manufacturing capabilities as a mechanism of protection), the nature and intensity of competition within an industry (e.g. the importance of price versus other product characteristics), the organization and size of R&D department, and the financial resources and limitations of the company.

In this paper we investigate the protection mechanisms that are used by Slovenian electronics companies in order to protect and benefit from their innovations. Electronics industry is a high-tech industry with a complex technology that creates high value-added /18/. It is becoming evermore important for the growth of Slovenian economy and the effective protection of the knowledge it creates, develops and employs is crucial for its success. We claim that because of specific industry level characteristics, such as the ones in the above paragraph, electronics companies use different mechanisms than companies in other manufacturing sectors. Theory and existing empirical studies suggest that since the technology embodied in electronics industry products is complex, patents should not be seen as important and effective mechanisms of protecting innovation. Because of the nature of production process, complementary manufacturing facilities should be seen as more important in this respect. Nevertheless, patents are important not only as an instrument of IPR, but are used by companies also for other reasons (e.g. strategic reasons). Thus, our second aim is also to identify the reasons that hinder the use of patents and licences as means of commercial exploitation of innovations in Slovenian electronics companies. To answer our research questions, we employ statistical analysis and survey data on innovation activity and protection of intellectual property in Slovenian manufacturing companies that were collected for the first time by RCEF (Research Centre of the Faculty of Economics, University of Ljubljana) in 2007. To the best of our knowledge our paper is the first attempt to analyze the use of different mechanisms of intellectual property protection in Slovenian companies (and specifically electronics companies) by means of a survey carried out on a national level. Our findings give important insights into the nature of intellectual property protection of electronics companies and by pointing out major obstacles for not patenting and licensing provide an additional orientation to the policy-maker. We present data and methodology in more detail in the next section, followed by the results and discussion.

1 Following Cohen et al. (2000), a complex technology is a technology that consists of many parts that are (or can be) separately patented; e.g. electronics products are typically considered as complex products. A simple technology is one which is comprised of only a few parts that are (or can be) patented under one patent; drugs or chemicals are typical examples of simple (or discrete) products.

2 Data and methodology

Data on innovation activities and protection of intellectual property in Slovenian companies were collected in a primary research performed by the RCEF from February to September 2007.

A survey questionnaire was constructed largely on the basis of questionnaires used by the Carnegie Mellon Study /15/ and Yale Study /13/ in order to ensure comparability of results; OECD's Oslo Manual for measuring scientific and technological activities was considered for measurement methodology /19/. Questionnaires were mailed to 716 Slovenian manufacturing companies: 272 (38%) were large companies, 302 (42%) were medium companies and 142 (20%) were small companies.[2] All large and medium manufacturing companies in Slovenia and a sample of small manufacturing companies [3]were included in the mailing list. The response rate was 23 percent, meaning that 166 questionnaires were returned.

In order to test the differences in innovation activities and protection of intellectual property in Slovenian electronics companies, the sample was divided in two sub-samples. In the first sub-sample are classified companies engaged in the industrial manufacturing of electrical, electronic and optical products. Those companies, in compliance with the Companies Act (1990), can be members of the Electronics and Electrical Industry Association of Slovenia and are classified under the activities: DL30, DL 31, DL32, DL 33 and DK 29.71. of the SKD[4] 2002 classification. The second sub-sample is composed from other manufacturing companies. In the first sub-sample we have 24 companies and in the second sub-sample the rest of 142 companies. Secondary data sources available from the Agency of the Republic of Slovenia for Public Legal Records and Related Services were used in order to obtain financial data. We used ROA (return on assets), DTS (total sales growth), VA/E (value added per employee) and DA (debt to assets) as financial measures of firm performance.

Methodology used is based on methods of statistical analysis. Differences in innovation activities and protection of intellectual property between electronics companies and other companies in Slovene economy were tested with independence sample t-tests.

3 Results

The existence of an R&D department in the company is the sign that company has innovation activities. As presented in Table 1 only 75 percent of Slovenian electronics companies have an R&D department. Those companies have on average 55 employees in R&D departments, which is significantly higher than in other manufacturing companies in Slovene economy. Other manufacturing companies on the other hand have a higher *relative* R&D budget in comparison to electronics companies. One very important difference between Slovenian electronics and other manufacturing industry is the size of the average company in electronics industry, which is twice as large as the average company from all other manufacturing industries. This fact must be taken into consideration when explaining results since it is well documented that firm size has important influences on R&D activity.

Table 1: *R&D departments in Slovenian electronics and other manufacturing companies in 2004 - 2006*

				T-test for equality of means	
		N	Mean	T	Sig.
R&D department	Electronics	24	75%	0.702	0.488
	Other	141	68%		
Number of employees in R&D department	Electronics	18	55	1.500	**0.101**[c]
	Other	95	26		
R&D costs in 2004 (in % of total sales)	Electronics	17	6.67%	-0.225	0.822
	Other	94	7.39%		
R&D costs in 2005(in % of total sales)	Electronics	17	6.83%	-0.498	0.619
	Other	94	8.88%		
R&D costs in 2006 (in % of total sales)	Electronics	17	6.59%	-1.731	**0.087**[c]
	Other	94	10.19%		
Total employees	Electronics	24	534	1.818	**0.07 1**[c]
	Other	137	281		

Note: (a). (b) and (c) represent statistical significant of coefficients for the level of risk of 1%. 5% and 10%.

Innovation activity of the company can go in the direction of development of new products or processes. New products in Slovenian electronics companies represent on average one quarter of the total company sales, while new processes represent one third of the total company sales. As expected, companies from electronic industry have a

2 We divide companies into large, medium and small according to the criteria in the Slovenian Companiess Act. Large companies are those satisfying at least two of the following three criteria: more than 250 employees, more than 29.2 million EUR in total sales, and more than 14.6 million EUR in total assets. Medium companies have two of the following: more than 50 employees, more than 7.3 million EUR in total sales, and more than 3.65 million EUR in total assets. Other companies are categorized as small.

3 The sample of small manufacturing firms was constructed by randomly selecting small companies from the register of companies. The industry structure of this sample was matched to the industry structure of the population of slovenian small manufacturing companies.

4 SDK is short for Standard Classification of Activities (Industries) which is used in Slovenia, the version from 2002 is harmonized with NACE rev 1.1.

significantly higher share of new products as percentage of their total sales than other manufacturing companies (Table 2).

Table 2: *Share of new products and processes in Slovenian electronics and other manufacturing companies in 2006*

				T-test for equality of means	
		N	Mean	T	Sig.
Share of new products (in % of total sales)	Electronics	24	25.88%	1.917	**0.057**[c]
	Other	142	17.21%		
Share of new processes (in % of total sales)	Electronics	24	33.42%	0.825	0.416
	Other	142	28.08%		

Note: (a). (b) and (c) represent statistical significance of coefficients for the level of risk of 1%. 5% and 10%.

So far the data showed that electronics industry in comparison to other manufacturing industries has a higher number of employees and a higher share of new products in their total sales, which can indicate a slightly more active innovation policy in those companies. In order to get a further understanding of their innovation activities, we analyzed how electronics companies protect their innovations.

We asked the respondents to estimate the percentage of innovations for which each of the following mechanisms has been effective in protecting the company's competitive advantage from those innovations: i) secrecy, ii) patents, iii) lead time, iv) complementary marketing capabilities, v) complementary manufacturing capabilities, and vi) know-how. The five point response scale was: 1) less than 10%, 2) 10% through 40%, 3) 41% through 60%, 4) 61% through 90%, and 5) more than 90%.[5] The particular response scale reflects how important a mechanism is to companies in terms of *frequency* and *effectiveness* of its use and was selected in order to obtain comparable results with the Carnegie Mellon Study (Cohen et al., 2000). The results are demonstrated in Table 3.

Overall, the specific know-how, which cannot be transferred, is regarded as the most important mechanism to protect innovations in both groups of companies; on average 10 to 40 percent of innovations is effectively protected by this mechanism. Besides know-how, other manufacturing companies see also secrecy as an equally important mechanism. The least important mechanism in both groups of companies are patents, but there is a statistically significant difference between electronics and other manufacturing companies. Electronics companies on average consider patents to be effective protection for less

Table 3: *Mechanisms for protection of innovations in Slovenian electronics and other manufacturing companies in 2006*

				T-test for equality of means	
		N	Mean	T	Sig.
Secrecy	Electronics	12	1,75	-2,339	**0,035**[b]
	Other	154	2,37		
Patent	Electronics	12	1,25	-2,440	**0,027**[b]
	Other	154	1,73		
Lead time	Electronics	12	1,33	-2,430	**0,028**[b]
	Other	154	1,83		
Complementary marketing capabilities	Electronics	12	2,00	-0,518	0,613
	Other	154	2,16		
Complementary manufacturing capabilities	Electronics	12	1,92	-1,298	0,217
	Other	154	2,34		
Know How	Electronics	12	2,08	-0,878	0,396
	Other	154	2,37		

Note: (a). (b) and (c) represent statistical significance of coefficients for the level of risk of 1%. 5% and 10%.

than 10% of their innovation, while other manufacturing companies on average estimate that more than 10% (but less than 40%) of their innovations are effectively protected by patents. This finding suggests that patents are less important mechanisms in electronics industry than in other manufacturing industries and it is consistent with the findings of most empirical studies /13,15/ and our theoretical prediction based on the specific characteristics of the industry (complexity, production process).

Despite the supposed unimportance of patenting as a protection mechanism for electronics industry, our survey data show that electronics industry in fact has more patents than other manufacturing industries. As it can be seen from Table 4 electronics companies have on average 2.88 patents per company, which is significantly higher that the average for other manufacturing companies (0.93 patent per company). The share of international patents in electronics companies is the same as the average in the other manufacturing companies, which is very low (2.31 percent of all patents are international). Other manufacturing companies are investing a larger share of their sales in patents applications than electronics companies, even if they have on average twice as less patents. Furthermore, other manufacturing companies have on average more patent application in procedure than electronics companies (differences are not statistically significant), which could indicate that patents can generally be obtained faster in electronics industry.

5 To ensure that our respondents understand correctly each of the mechanisms of protection, a description of the way it is used to protect competitive advantages from innovations was used instead of just a list of mechanisms (as in Table 3). Also, an example of the response was provided: »If you believe secrecy (as a protection mechanism) effectively protects competitive advantages from around 20% of your innovations, mark response 2) 10% through 40%«.

Table 4: *Patents in Slovenian electronics and other manufacturing companies in 2006*

				T-test for equality of means	
		N	Mean	T	Sig.
Number of patents	Electronics	24	2.88	2.515	**0.013[b]**
	Other	142	0.93		
Share of international patents	Electronics	9	2.56%	0.413	0.682
	Other	32	2.31%		
Share of RD costs for patents	Electronics	9	1.40%	-2.205	**0.033[b]**
	Other	32	6.07%		
Number of patent applications in procedure	Electronics	9	5.89	-0.467	0.643
	Other	32	9.66		

Note: (a). (b) and (c) represent statistical significance of coefficients for the level of risk of 1%. 5% and 10%.

Although these results imply that companies in electronics industry could be more efficient in their patenting activity, we must be careful with the interpretation of absolute numbers. The average number of patents of patents per employee or per R&D employee is actually (significantly) lower for electronics industry, as well as the ratio of number of patents to % of R&D in sales.

In order to investigate the reasons that prevent companies from patenting, we asked the respondents to estimate the importance of the following reasons for not patenting in the last three years for their companies: i) no innovation, ii) innovation is not novel enough, iii) information disclosed in patent, iv) cost of patent application, v) cost of defending the patent in court, and vi) ease of legally inventing around the patent (patent is not an efficient mechanism of protection). The respondents were asked to estimate the reasons on a five-point subjective Likert response scale where 1 was "not important at all" and 5 was "very important".

Table 5 shows that the most important reason for not patenting in both groups of companies was the fact that innovation was not novel enough to be eligible for patent protection. Both groups of companies on average think that the quantity of information disclosed in patents is not very problematic. The only significant difference between electronics industry and other manufacturing industries with respect to reasons for not patenting is the ease of legally inventing around the patent. Electronics companies on average believe this was not an important reason for not patenting, while other manufacturing companies on average believe it was. This last result suggests that patents offer a better protection from imitation in electronics industry than in other manufacturing industries, which is somewhat contradictory to the previous finding about the unimportance of patents as means of protecting innovation. However, this could indicate that patents do offer a reasonably effective protection from imitation in electronics industry, but because of the high cost involved in obtaining them and enforcing them in court, they are not used as much as the companies would want to and are consequently a less important mechanism for protection in terms of the frequency of use.

Table 5: *Reasons for not patenting innovations*

				T-test for equality of means	
		N	Mean	T	Sig.
We do not have innovative products	Electronics	12	2,92	-0,197	0,844
	Other	151	3,01		
Innovation is not novel for the market	Electronics	12	3,42	0,026	0,980
	Other	153	3,41		
Too much information is disclosed	Electronics	12	2,83	0,021	0,984
	Other	153	2,82		
The costs of patent application	Electronics	12	3,08	-0,449	0,661
	Other	153	3,31		
The cost of defending a patent in court	Electronics	12	3,00	-0,345	0,736
	Other	153	3,17		
Easy to invent legally around the patent	Electronics	12	2,58	-1,751	**0,101[c]**
	Other	153	3,24		

Note: (a). (b) and (c) represent statistical significance of coefficients for the level of risk of 1%. 5% and 10%.

Patents are not used only for protection; they can be also a source of additional revenue. Licensing is related to the use of patents as revenue generators. Slovenian companies on average have very low number of licences agreement for their products or processes (Table 6). On average only 8 percent of other manufacturing companies in our survey have licence agreements for their products. On the other hand, 17 percent of electronics companies have licence agreements for their products, which is significantly higher than the average for other industries. Only 4 percent of companies from both sub-groups have the licence agreements for their processes.

Table 6: *Licences in Slovenian electronics companies and in all Slovenian companies in year 2006*

				T-test for equality of means	
		N	Mean	T	Sig.
Licences for products	Electronics	24	17%	1.610	**0.10 1[c]**
	Other	131	8%		
Licences for processes	Electronics	23	4%	-0.013	0.990
	Other	136	4%		

Note: (a). (b) and (c) represent statistical significance of coefficients for the level of risk of 1%. 5% and 10%.

To understand better what keeps companies from not using licences, we asked the respondents about the importance of the following possible reasons: i) no innovations that can be licensed, ii) additional competition, iii) disclosure of important information, iv) reputation damage by bad practising of the licensee, v) unappealing legislation on licensing, vi) no demand for licenses, and vii) failed negotiations for licensing. A five-point subjective Likert response scale was used to measure the importance of these reasons where 1 was "not important at all" and 5 was "very important".

Table 7: *Reasons for not licensing innovations.*

				T-test for equality of means	
		N	Mean	T	Sig.
We do not have innovations that can be licensed	Electronics	12	3,83	1,152	0,251
	Other	154	3,27		
We would create additional competition	Electronics	12	2,17	-0,819	0,414
	Other	154	2,51		
We would loose the control over the important information	Electronics	12	2,50	-0,030	0,977
	Other	154	2,51		
The licence buyer could ruin the reputation of our products	Electronics	12	2,92	0,772	0,455
	Other	154	2,53		
The unappealing legislation in that field	Electronics	12	2,92	1,802	**0,073**[c]
	Other	154	2,19		
There is no demand for licencing our products	Electronics	12	2,58	-0,692	0,501
	Other	154	2,90		
The negotiation on licensing our products have failed	Electronics	12	1,67	-0,194	0,849
	Other	153	1,74		

Note: (a). (b) and (c) represent statistical significance of coefficients for the level of risk of 1%. 5% and 10%.

The responses indicate that the most important reason for not licensing in both groups of companies was the fact that companies did not have innovations that could be licensed (Table 7). The least important reason was therefore failed negotiations in both groups of companies. The main difference between electronics companies and others is with respect to legislation. For electronics industry legislation was more important as a reason for not licensing their innovations as for other manufacturing industries.

To exclude financial reasons for differences in innovation activities between electronics industry and other manufacturing industries, we further tested the differences in financial performance of electronics and other manufacturing companies. The results presented in Table 8 confirmed that there are no statistically significant differences between electronics and other manufacturing industries in this respect.

4 Discussion

This paper investigates the nature of innovative activity in Slovenian electronics industry. Specifically, our hypothesis was that companies in this industry use different mechanisms of protection for their innovations than companies in other manufacturing industries. Based on questionnaire survey results we find enough evidence to support this hypothesis. The study exposed a seemingly paradoxical behaviour of electronics companies. Even though patents are not the most important mechanism of protection in this industry and are also deemed as less important than in

Table 8: *Performance indicators in Slovenian electronics and other manufacturing companies in 2006*

				T-test for equality of means	
		N	Mean	T	Sig.
ROA	Electronics	24	3.99%	0.046	0.964
	Other	137	3.88%		
DTS	Electronics	24	9.35%	-0.053	0.958
	Other	136	9.69%		
VA/E	Electronics	23	8.954 EUR	-0.441	0.660
	Other	140	10.659 EUR		
DA	Electronics	24	0.53	-0.616	0.539
	Other	137	0.57		

Note: (a). (b) and (c) represent statistical significance of coefficients for the level of risk of 1%. 5% and 10%. ROA is return on assets, DTS is total sales growth, VA/E is value added per employee, DA is debt to assets ratio.

other manufacturing industries, electronics companies have significantly more patents and are also more active in patenting and licensing their intellectual property than other manufacturing industries. Electronics companies think that complementary marketing and manufacturing capabilities with know-how protect their innovations most effectively. We believe there are three reasons for such results: 1) the nature of technology and products in electronics industry is complex, 2) the average company in electronics industry as well as R&D departments are considerably larger than in other manufacturing industries, and 3) the nature of competition in electronics industry requires fast technological change.

Electronics technology and products consist of numerous parts that come from several suppliers, also from other industries, and many of them can be patented individually. Besides, the technological change in this industry has a rapid pace and the innovation process is cumulative, meaning that innovations typically overlap with existing technologies /14/. Complete patenting is extremely costly and the novelty of innovation is easily questioned in such complex circumstances. Indeed, Slovenian electronics companies named the lack of novelty and cost of patent application and defence in court as most important obstacles to patenting. The build-up of specific manufacturing or marketing capabilities and know-how therefore protects innovations better as these capabilities are not easy to copy because they have high fixed costs and are typically non-transferable.

In spite of this, electronics industry has a considerably larger number of patents than other manufacturing industries. We can explain this by considering several facts about companies in Slovenian electronics industry. Firstly, they rely more on R&D departments to carry out their innovative activities than companies in other manufacturing industries. This makes the process of innovation more systematic and productive as opposed to spurious innovation attempts in companies without R&D departments. Second-

ly, because they are on average larger than companies in other manufacturing industry, they can exploit economies of scale related to R&D costs better and have a lower cost per patent than other manufacturing industries. Furthermore, their R&D departments are also proportionally larger than departments in other manufacturing industries and more people are working on activities leading to more patents and licenses. Thirdly, the above average complexity of the technology involves more patentable components (related to one product or process) than in a simpler technology. Lastly, the considerably higher share of new products and processes in electronics industry could be interpreted as a sign that companies in this industry are also forced to be more innovative because market and competitive pressures demand constant technological change. Consequently, more innovations lead to more patents.

At this point we would like to stress that one of the most important reasons for not patenting and licensing in both groups of companies was the fact that companies do not have innovations. This is particularly worrying in the light of globalization processes that move production facilities to more favourable locations in terms of costs, but increasingly also in terms of technological knowledge. It is not uncommon anymore for firms to move R&D departments in India, Taiwan or other countries, known for cheaper but technologically skilled labour. If it was once possible for Slovenian companies to rely on higher value-added and better technological skill as competitive advantage vis-à-vis cheaper, mass-production rivals, our survey reveals this could not be possible anymore already in the near future.

5 Conclusions

On average Slovenian electronic companies have more employees in R&D department than other Slovenian manufacturing companies. Even if their R&D budget is lower, they have more patents and new products than other companies in Slovene economy. In general, we concluded that electronic companies in Slovenia conduct slightly more active innovation policy than other manufacturing companies. In spite of a larger number of patents, electronic companies consider them as a less important and less effective mechanism for protecting innovations than companies in other manufacturing companies. Electronic companies think that complementary manufacturing and marketing capabilities or know-how are more effective mechanisms for protecting innovations than patents. We believe this inconsistency arises because of greater firm (and R&D department) size, technological complexity and pressure for fast technological change.

Acknowledgments

This work was done under Slovenian Ministry of Economy (Slovenian Intellectual Property Office - SIPO) and Slovenian Agency for Research and Development CRP research grant.

References

/1/ K. Arrow, "Economic Welfare and the Allocation of Resources for Invention", R. R. Nelson, London, NBER/Princeton University Press, 1962.

/2/ C. Greenhalgh and M. Longland, "Running to Stand Still?-The Value of R&D, Patents and Trade Marks in Innovating Manufacturing Firms", Int. J. Econ. Bus., vol. 12, no. 13, pp. 307-328., 2005.

/3/ N. C. Varsakelis, "The Impact of Patent Protection, Economy Openness, and National Culture on R&D investment: A Cross-country Empirical Investigation", Research Policy, vol. 30, pp. 1059-1068, 2001.

/4/ D. Lederman and W. F. Maloney, "R&D and Development", World Bank mimeo, 2003.

/5/ S. Kanwar and R. Evenson, "Does Intellectual Property Protection Spur Technological Change?", Oxford Economics Papers, vol. 55, pp. 235-264, 2003.

/6/ A. Bassaniani and E. Ernst, "Labor Market Regulatio, Industrial Relation and Technological Change: A Tale of Comparative Advantages", Industrial Corporate Change, vol. 11, pp. 391-426, 2002.

/7/ R.N. Bebczuk, "R&D Expenditures and the Role of Government", Estud. Econ., vol. 29, pp. 101-121, 2002.

/8/ M. Falk, "What drives business R&D intensity across OECD countries", Appl. Econ., vol. 38, pp. 533-547, 2006.

/9/ N.T. Gallini, "Deterrence through Market Sharing: A Strategic Incentive for Licensing", Am. Econ. Rev., vol. 74, pp. 931-941, 1984.

/10/ A. Shepard, "Licensing to Enhance Demand for New Technology." RAND J. Econ., vol. 18, pp. 360-368, 1987.

/11/ P. Lin, "Fixed-fee Licensing of Innovations and Collusion", J. Ind. Econ., vol. 44, pp. 443-449, 1996.

/12/ Y. Kim and N.S. Vonortas, "Determinants of technology licensing: The case of licensors", Managing Decision in Economics, vol. 27, pp. 235-249.

/13/ R.C. Levin et al., "Appropriating the returns from industrial research and development", Brookings Papers on Economic Activity, vol. 3, pp. 783-831, 1987.

/14/ B. Hall and R. Ziedonis, "The patent paradox revisited: An empirical study of patenting in US semiconductor industry", RAND J. Econ., vol. 32, no.1, pp. 101-128, 2001.

/15/ W.M. Cohen et al., "Protecting their intellectual assets: Appropriability conditions and why US manufacturing firms patent (or not)", NBER Working papers, 2000.

/16/ Z. Griliches, "R&D and productivity", Handbook of the Economics and Innovation and Technological Change, P. Stoneman (ed.), Oxford, Basil Blackwell, 1995.

/17/ W.M. Cohen, "Empirical studies of innovative activity", Handbook of the Economics and Innovation and Technological Change, P. Stoneman (ed.), Oxford, Basil Blackwell, 1995.

/18/ P. Domadenik and M. Koman, "The energy efficiency of firms in electronic industry in Slovenia", Info. Midem, vol. 4, pp. 279-304, 2008.

/19/ Oslo Manual: The Measurement of Scientific and Technological Activities, Paris, OECD, 2007.

Mojca Marc, Ljubica Knežević Cvelbar*
Faculty of Economics, University of Ljubljana,
Kardeljeva ploščad 17, SI-1000 Ljubljana, Slovenia

Uroš Cvelbar
Jožef Stefan Institute, Jamova cesta 39, SI-1000, Slovenia
**Corresponding author: mojca.marc@ef.uni-lj.si*

Prispelo (Arrived): 17.09.2008 *Sprejeto (Accepted): 15.12.2008*

THE ENERGY EFFICIENCY OF FIRMS IN ELECTRONICS INDUSTRY IN SLOVENIA: DO THEY PERFORM BETTER THAN AVERAGE MANUFACTURING FIRMS?

Polona Domadenik* and Matjaž Koman

Faculty of Economics, University of Ljubljana, Ljubljana, Slovenia

Key words: Energy efficiency, electronic companies, Slovenian companies

Abstract: The article analyses the energy efficiency of Slovenian firms from the demand for energy perspective. Special emphasis is put on analyzing firms in electronics industry that manufacture electronics and small electrical devices, in comparison with other firms in manufacturing. The sample consists of 100 firms operating in different industries in the period of 2005-2007. The results show that Slovenian manufacturing firms are becoming more energy efficient indicating that possible energy efficient investment and innovations were made in the period under study. Moreover, firms operating in electronics industry exhibit above average energy efficiency in terms of energy per output and price elasticity of energy demand. Increasing energy-efficiency of consumption should become a goal of both firms and households. Firms need to restructure and invest in energy-efficient technologies, while households need to build energy-efficient houses and use energy-efficient house appliances. In the absence of a level playing field (e.g., global emissions trading or border adjustment taxes) we propose that regulatory and supportive policy instruments should be used much more extensively and actively than today.

Energijska učinkovitost podjetji v elektronski industriji v Sloveniji: Ali so ta podjetja boljša od povprečja v predelovalni industriji?

Kjučne besede: energijska učinkovitost, elektronika, slovenska podjetja

Izvleček: Članek analizira energijsko učinkovitost slovenskih podjetij z vidika povpraševanja po energiji. Poseben poudarek je na analizi podjetij, ki proizvajajo elektroniko in manjše električne naprave ter njihovi primerjavi s podjetji v predelovalni industriji. Vzorec sestavlja 100 podjetij, ki delujejo v različnih panogah predelovalne industrije v obdobju od leta 2005 do 2007. Rezultati prikazujejo, da postajajo slovenska podjetja energijsko bolj učinkovita, kar nakazuje, da so v preteklosti izvedla energetsko učinkovite investicije in inovacije. Podjetja, ki proizvajajo elektroniko izkazujejo nadpovprečno energetsko učinkovitost, če jo merimo v količini energije, porabljene na enoto proizvoda in cenovne elastičnosti povpraševanja po energiji. Povečevanje učinkovite rabe energije mora postati cilj tako podjetij kot gospodinjstev. Podjetja se morajo prestrukturirati in investirati v energetsko učinkovite tehnologije, medtem ko se morajo gospodinjstva v večji meri odločati za gradnjo energetsko učinkovitih hiš in uporabo učinkovitih gospodinjskih aparatov. V odsotnosti ukrepov ekonomske politike (kot na primer globalni sistem trgovanja z emisijami ali davčne izravnave med državami) predlagamo, da se uporabijo regulatorni in pomožni ukrepi za stimuliranje energetsko učinkovitega obnašanja.

1 Introduction

There is now a widespread consensus that man-made climate change is occurring, that it will continue into a foreseeable future, and that the climate change is a global externality /1/. The main GHGs emitted by human activity are carbon dioxide, (CO_2) contributing about 77% of total GHG emissions, followed by methane and nitrous oxide, each contributing about 14% and 8% respectively. A substantial part of GHG arises largely from the energy sector which, given its factors of internal dynamics, represents a special challenge. Due to a soaring demand, energy prices have continued to increase sharply. Moreover, given the continuous political instability and political interference in energy supply, energy markets have become more volatile. In order to avoid future energy crisis, the exposure to external factors must be decreased and the right incentives to consume less energy, to start consuming a renewable energy, and to improve energy efficiency should be developed.

In the past few years, the economic analysis of sustainable development gained new impetus by the merger of environmental economics and new (endogenous) growth theory, focusing on the issue of conditions under which sustainable growth within an endogenous growth model with environmental concern is feasible. Early economic growth models incorporating technical change as an exogenous factor /17/ attempt to explain the role of technical change for sustainable growth by "manna from heaven". A commonly found argument in standard growth theory literature is that technical change and factor substitution can effectively de-couple economic growth from the demand for resources and environmental services /6/. Energy efficiency, as part of the technical progress in neoclassical growth theory, is conventionally seen as a driver of economic growth. Depletion of finite energy and other resources and environmental degradation is not seen as a significant barrier to economic growth, since there will always be more abundant substitutes (either natural resources or human-made capital). In the 1990s, endogenous growth theorists have started to formally include concerns

about environmental and resource factors limiting growth in standard growth models /2, 16/. Doing so, endogenous growth theory enables new insights about the relationships between resource scarcity, technical change, and economic growth, and hence constitutes a great leap forward compared to standard neoclassical growth theory. A further development of endogenous growth models to also account for rebound effects renders hope that in the future the relationship between economic growth, technical change and resource use (and eventually the size of various rebound effects on the macroeconomic level) can be better modeled and understood

Within the position of climate change paradigm in economic science the most important topic is to analyze environmental behavior, related to energy consumption at the macroeconomic and microeconomic levels. Industry accounts for about one-third of the energy used in Slovenia and is a major emitter of greenhouse gasses. Energy wastefulness in production is part of the socialist legacy of Central and Eastern European countries. In 1989, the energy consumption per unit of product in the Eastern bloc was four times greater than the average in the EU-15, whereas in 2000 it was twice as much. With 1.5 times as much energy per unit of output, Slovenia was the closest to the EU-15 average, while the worst was Lithuania which in 2000 still spent about five times as much energy per unit of output than the EU-15 average /9/. Data for 2006 show that Slovenia is still lagging behind the EU since it uses about 1.5 times more energy per unit of output than the EU. The question of energy efficiency is strongly associated with restructuring. Companies that achieved greater energy efficiency in the past are likely to invest more in capital goods that enable energy savings.

The literature shows many different barriers to energy efficiency such as inadequate pricing and lack of information. Internalising the environmental costs of energy would seem an evident solution to the first problem but it may be difficult to implement in a single country. In small open economy as the Slovene one, the basic industry is export oriented and sensitive to changes in its relative prices. In past years the introduction of emission trading system has contributed to significant energy price increase that spurred a new interest for energy efficiency in industry.

In the paper we summarize the energy efficiency of firms in Slovenian firms with special emphasis on electronics industry. The overall objective is to take stock of the current situation and discuss implications for future policy measures. Significant increase of energy prices since year 2000 considerably increased interest in energy efficiency and associated fields. The purpose of the article is to analyse energy consumption patterns in Slovenian companies and notably to establish whether their energy intensity is falling, especially among the largest users, with special emphasis on firms in electronics industry.

The paper contributes to the existing literature in at least three significant ways. First, the understanding about necessity of fulfilling environmental demands and efficient energy use is not yet developed in former socialist and communist economies. Therefore, the paper presents empirical microeconomic evidence on energy efficiency in the most developed former socialist economy, Slovenia. Second. From the microeconomic perspective it is urgent to scan the current situation and identify the factors that determine the energy demand at the firm level with respect to the profit maximizing behavior and imposed regulations. In this context we introduce dynamic components into the modeling of energy consumption because the effects of explicative factors are not totally instantaneous and lagged effects continue to act over more periods of time. Energy demand is derived demand on one hand since the needs expressed for the various energy sources result from the operation of a plant, and conditional demand on the other, a function of equipment stock. If we model the production decision at the firm level as profit maximizing behavior with respect to several factors of production including non-renewable factor - energy, we are able to identify energy demand and potential significance of particular factors that affect it. By our knowledge energy demand has not been studied in this context so far. Third, with special emphasis on electronics industry the paper brings new evidence and comparison of electronics with other manufacturing sectors within economy.

In the first part of the paper energy consumption data for Slovenia are presented, followed by a presentation of a model of energy efficiency. Third part introduces a theoretical and empirical framework, while in the fourth part the results are presented. Based on the findings, at the end some guidelines for the formulation of economic policy are suggested.

2 Energy efficiency in Slovenia

The efficiency of energy consumption at the level of a whole economy is monitored by the indicator of energy intensity calculated as the ratio between the amount of energy (expressed in kilograms of oil equivalent - kgoe) and gross domestic product expressed in constant prices of 1995. The indicator measures both energy consumption as well as overall efficiency.[1] Energy intensity (GJ per unit of GDP) and unit consumption ratio (GJ/t of product, GJ/Sq.m) in new EU member states are, despite clear progress during the last decade, still much higher than the average in Western Europe. For instance, energy intensity in the Czech Republic is 1.6 times higher. The comparison of energy efficiency in Slovenia and the EU shows that, despite this improvement, Slovenia still very much lags behind EU member states. Based on energy intensity data for the 1995 to 2006 period for the EU and Slovenia, it may be

1 Total energy spent is calculated as the sum of the following energy sources: coal, electricity, oil, natural gas and renewable energy sources. Sources are calculated as the equivalent of oil consumed.

concluded that the average energy consumption in both the Eurozone and the EU-27 is becoming increasingly efficient. According to Eurostat, in 2003 the European Union used energy more efficiently than the United States of America and less efficiently than Japan: an indicator of energy intensity for Japan amounted to 119 million kgoe/1000, in the EU-25 it amounted to 209 million kgoe/1000 and 313 kgoe/1000 million in the United States. With 128 kgoe/1000, Denmark had the lowest energy intensity in the European Union followed by Austria (151) and Germany (160). The least effective in its energy use were Estonia with 1208 kgoe/1000 million, Lithuania (1204) and Slovakia (937). In 2003 Slovenia spent 338 kgoe energy for EUR 1000 of generated GDP, which exceeds the average of both the EU-25 as well as the United States.In Slovenia, since 1995 energy intensity has on average decreased, with the exception of 1996 and 2001 when it rose slightly. In 2001 it amounted to 350 million kgoe/1000, and in 2003 to 338 kgoe/1000 million. In 2006 and 2007 the energy intensity again dropped significantly at both the primary level and with regard to final consumption[2]. Part of the decrease can be attributed to the growth of GDP, but another part can be attributed to the overall decrease in final energy consumption. In 2007 the share of electricity from renewable energy sources in total electricity generation amounted to 23 percent[3]. Based on statistical data it can be assumed that Slovenian energy consumers are becoming more energy efficient. The estimates of the economic potential for energy saving in Central Europe are estimated to exceed 20% of the total current final consumption. In South East Europe and CIS, this potential is even higher, in the range of 30-50%.

In year 2007 final energy consumption in Slovenia grew by five percent. The largest share is attributed to electricity (41 percent) followed by natural gas (36 percent), oil products (5 percent), renewable resources (5 percent), heat [4] (4 percent) and others as reported in figure 1.

The final consumption of energy is biggest in transport (29 percent), followed by manufacturing and construction (28 percent) and households that use a quarter of all energy consumed in Slovenia /15/. Comparing energy consumption by industry sectors we figure out that 93% of all consumption in 2006 and 95% in 2007 are in manufacturing.

When comparing the energy consumption by different manufacturing sectors we can see that manufacturing of basic metals and fabricated products accounts to 27 percent of all manufacturing consumption in 2007, manufacturing of other non-metal and mineral products 17 percent and manufacturing of textile and textile products to almost 15 percent. Manufacturing of electronics and electrical devices contributed less than 3 percent of all energy consumption in total manufacturing in 2007.

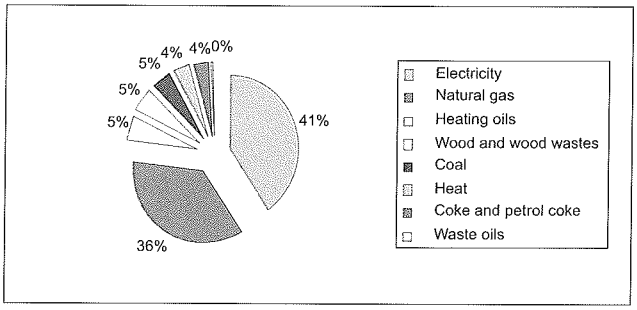

Fig. 1: Energy consumption of fuels, electricity and heat in manufacturing sector in Slovenia, 2007 Source: SI-STAT database, Statistical Office of Slovenia.

The energy consumptions by all manufacturing as well as electronics industry show upward trends in the period of 2003 - 2007 as reported by figure 2. However, when interpreting figure 2 we have to be careful as energy consumption is correlated with production. Therefore, the energy increase captures two effects: increase in total production in the industry and potential energy inefficiencies in production-

The prices of all sources of energy have shown sharp increase especially after year 2000. The prices of natural gas increased by almost 100 percent in the period of 2000-2007 for the smallest industry users while increased by 244 percent for the biggest ones. The prices of electrical energy increased from 0,145 EUR/kWh in 2000 to 0,195 in 2009 for the small consumers and from 0,050 to 0,094 EUR/kWh for the biggest ones.

A comparison of energy prices in Slovenia with those in other EU member states shows that the price of electricity for households in Slovenia is 25 percent lower than the average price in the European Union. In the Czech Republic, Malta, Poland, Estonia, Greece, Latvia and Lithuania the prices of electricity for households are below the Slovenian ones. The highest price is found in Denmark. In Slovenia the price of natural gas for households that use gas for heating is about the same as the average price in

2 In 2006 we reported a decrease in energy intensity (by 5 percent for the primary level and 4 percent for the final level). This trend was also present in 2007 when energy intensity on the primary level again dropped by 5 percent and by 7 percent for final level of consumption (Source: Statistical Office of Slovenia).

3 The biggest share of energy was produced by hydroelectric power stations - producers by main activity (89 percent), followed by small hydroelectric power plants (5 percent) and hydroelectric power plant self-producers. (2 percent), while the remaining electrical energy from renewable resources was produced from wood, wooden waste and bone meal (2 percent) and photovoltaic, deposited gas, gas from treatment plants, other biogas and formalin gas (2 percent).

4 Heated sanitary water meant for remote heating purposes.

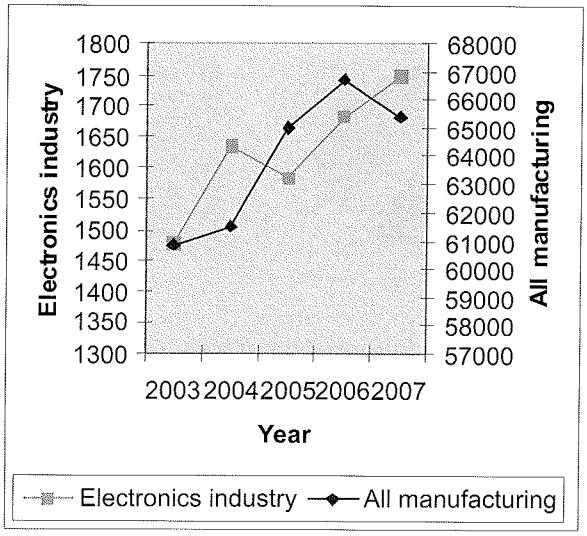

Fig. 2: Energy consumption by manufacturing and electronics in Slovenia in 2007 (measured in TJ) Source: SI-STAT database, Statistical Office of Slovenia.

the European Union. In the European Union the maximum price of natural gas for households has been recorded in Denmark and Sweden and the lowest in Estonia and Latvia /15/.

3 Model of energy efficiency

A model of energy efficiency can be derived from neoclassical factor demand. It is similar to the models used in the empirical studies by /20/, /3/ and /4/ to study the investment behaviour of firms. Based on similar models, also /8/ studied the factor demand of Slovenian companies in the 1996-2000 period.

Neoclassical factor demand is based on the assumption that a company in any period of time maximises the value of shareholders' assets[5]. The company operates in competitive markets and demands three types of production factors: capital ($K = (K_1, K_2, \ldots, K_E, K_N)$), which offers productive services in several periods of time, work ($L = (L_1, L_2, \ldots L_R)$) that is according to economic theory a variable production factor, as well as production factors purchased and entirely spent in the current manufacturing process ($M = (M_1, M_2, \ldots M_S)$). In the context of capital goods, more energy-efficient capital goods (K_E) are an important part because after the investment period they allow lower energy intensity and consequently significant cost savings. Therefore, the enterprise encounters the problem of the maximisation of shareholders' value, which can be illustrated as follows:

$$V_t(s_{t-1}) = \max_{K,L,I,M}\{\Pi_t(s_t, M_t, I_t, H_t) + \beta_{t+1} E_t[V_{t+1}(s_t)]\} \quad (1),$$

with V_t being the maximised value of the company at time t $\Pi_t(.)$ is a profit function in time t, $s_t = (L_t, K_t)'$ is a vector of labour stock and capital at the end of time period t. H_t measures the gross employment rate of workers and I_t the permanent investment in the capital stock, while investment in energy-efficient capital goods are an important part. Et indicates the expected value, $\beta_{t+1} = 1/(1+\theta_{t+1})$ the discount factor, where θ_{t+1} is the nominal required rate of return between t and t + 1. The company in each period t invests in various types of capital goods I, even in energy-efficient ones. The amount of capital operating in the company at any time can be defined as the sum of capital goods in the past period and the current investment period (I_t).

The profit function can be expressed as:

$$\Pi_t(K_t, L_t, M_t, I_t, H_t) = p_t * Y_t(K_t, L_t, M_t) - p^I_t I_t - w_t L_t - p^M_t M_t , \quad (2)$$

where $Y_t(K_t, L_t, M_t)$ represents a company's total product, p_t the price of the company's product, $p^I_t = (p^1_t, \ldots, p^N_t)$ is the price vector for each type of capital good, $w_t = (w^1_t, \ldots, w^R_t)$ is the wages vector for each type of work, $p^M_t = (p^{M,1}_t, \ldots, p^{M,S}_t)$ is the factors vector of material production prices.

Based on a static model of the factor demand the reduced demand for labour and capital goods can be derived. Assuming the CES form of production function and a constant coefficient of demand elasticity for the finished product (η^D), and if the company has no impact on establishment of the final price, then the optimal amount of capital is:

$$K_t = \alpha_K^{\sigma} Y_t \left(\frac{p^I_t}{p_t\left(1 - \frac{1}{\eta_D}\right)}\right)^{-\sigma} \quad (3)$$

The optimal amount of capital may represent a long-term equilibrium level of the employment of capital. Using logs, we can rewrite (3) as follows:

$$k_t = \mu_K + y_t - \sigma(p_i - p)_t , \quad (3a)$$

where k_t denotes the logarithm of the volume of capital goods, y_t is the logarithm of the total product, $(p_i-p)_t$ is the costs of the capital production factor in the production process, and μ_K is constant.

The energy-efficient type of capital is one of the types of capital in which the company invests. Therefore, equation (3a) provides the framework for an empirical model that we now examine.

4 Sample description and empirical model

The population of companies targeted in this research was made up of all companies registered in Slovenia, operat-

5 It is assumed that shareholders are risk-neutral, companies do not issue debt security and do not pay taxes.

ing in the manufacturing industry and which had more than 50 employees in 2007. According to AJPES' data there were 434 such enterprises. The data were collected through a questionnaire which was distributed via ordinary mail and e-mail from July to September 2008. The questionnaires were addressed to presidents of companies or executive directors[6]. The data gathered were supplemented with financial information from the balance sheets and income statements of companies (AJPES database).

On average, companies in the sample[7] had 251 employees at the end of 2005. Two years later, the number of employees had on average risen to 265. The average total revenues in 2005 were EUR 24.8 million and EUR 35.4 million two years later. The volume of total assets in 2005 amounted to an average of EUR 8.78 million and EUR 10.6 million two years later. Firms in electronics industry included in the sample were, on average, bigger than the average sampled firms. They reported 345 employees in 2005 and 353 in 2007. The average total revenues in 2005 were EUR 37.3 million and EUR 47.2 million two years later. The labour productivity in the electronics industry in the period of 2005-2007 was at 98 percent of average value.

Companies in the sample spent an average of 8.5 million kilowatt-hours of electricity in 2005 (0.5 kilowatt-hour for EUR 1 of revenue), 1.16 million cubic meters of gas and 46,000 tonnes of fossil fuels, where only 24 companies used gas and 60 companies fossil fuels. The consumption of electricity increased and was 10 million kilowatt-hours in 2007, while gas consumption dropped to 1.12 million tonnes, along with the consumption of fossil fuels to 43,000 tonnes. The observed trend is positive in terms of cost efficiency (electricity is the cheapest energy). Greater efficiency can also be detected in the consumption of electricity for every euro created. On average in 2005, firms spent 0.5 of a kilowatt-hour of electricity per EUR 1 of revenue, in 2006 0.42 kilowatt-hour and in 2007 only 0.37 kilowatt-hour, representing a 26-percent reduction over 2005. A company can primarily achieve such savings by investing in new energy-efficient technology and to a smaller extent by raising the prices of its finished products[8].

The real costs of energy used by an average company in 2005 amounted to EUR 651,000 and EUR 876,000 two years later. When comparing the cost of energy to generated revenues, we see that the share fell slightly from EUR 0.028 (cost of energy) per generated EUR 1 of revenue in 2005 to 0.026 in 2007 (Table 1).

An analysis of the average consumption of electricity per EUR 1 of revenue by industry reveals that this share declined on average in all sectors, with the most obvious reduction seen in the chemical and rubber industry (from 0.48 kilowatt-hour per EUR 1 of revenue in 2005 to 0.34 kilowatt-hour per EUR 1 of revenue in 2007), and the smallest reduction in the production of food and drinks (from 0.17 kilowatt-hour per EUR 1 of revenue in 2005 to 0.16 kilowatt-hour per EUR 1 of revenue in 2007). Electronics sector exhibits the lowest average consumption of electricity by revenue. However, a comparison of energy costs with revenue generated by different industries shows that the share slightly rose in the industry of wood processing, paper production and publishing (from EUR 0.030 of energy costs per EUR 1 of generated revenue in 2005 to 0.035 in 2007) and in the industry of machinery, appliances and vehicles production (from EUR 0.016 of energy costs per EUR 1 of generated revenue in 2005 to 0.017 in 2007). The share remained unchanged during the observed period in the production of textiles, apparel and leather (EUR 0.036 of energy costs per EUR 1 of generated revenue), while it slightly decreased in all other sectors including electronics (Table 1).

The empirical model of the desired volume of energy-saving capital is derived from equation (3a) as:

$$k^E_{it} = \beta_0 + \beta_1 y_{it} + \beta_2 (p^i - p)_{it} + \nu_{it} \quad (4)$$

where β_1 represents the elasticity of the use of energy-saving capital according to the company's sales, β_2 is the elasticity of capital according to the cost of usage, i indicates companies and t the time period (year). Since companies have difficulties assessing the level of energy-saving capital in the production process, instead of the volume of capital we used a "proxy" variable which measures the consumption of electricity in companies in given years, while the costs of usage are measured as the real costs of energy for electricity consumed at the company level.

5 Results

Based on a regression analysis of the model (4), estimates of elasticity over the years were obtained (Table 2). The

6 According to /7/ 39.5 percent of the questionnaires were completed by presidents of the company or executive directors. 35.4 percent of the questionnaires were completed by middle management (e.g. directors of business units), in 25.2 percent of the companies respondents to the questionnaire were other groups of employees (e.g. representatives of the management responsible for protecting the environment, or heads of various other business units). Of the 434 companies that were suitable for research, the questionnaires were collected from 153 companies, representing a 35.3-percent response rate.

7 Companies included in the sample were only those that stated information on energy consumption in the examined period (2005-2007).

8 The sample mainly includes companies which have a larger part of their sales in foreign markets, where they act as niche suppliers.

Table 1: Average values of electricity consumption, energy costs, consumption of electricity per revenues created and energy costs per revenue created by industry

Industry	Year	No. of firms	Average consumption of electricity (in kilowatt hours)	Average costs of energy (in EUR)	Average consumption of electricity per revenues created (in kilowatt hours per EUR)	Average energy costs per revenue created
Industry 1 (manufacturing of food, beverages and tobacco)	2005	12	4,179,736	532,736	0.17	0.034
	2006	12	4,437,948	602,135	0.17	0.034
	2007	12	4,564,269	666,534	0.16	0.032
Industry 2 (manufacturing of textile and textile products)	2005	8	5,588,478	483,686	0.35	0.036
	2006	8	5,537,949	521,170	0.32	0.036
	2007	8	5,140,179	586,870	0.28	0.036
Industry 3 (manufacturing of wood and wood products)	2005	9	50,195,608	126,917	2.5	0.030
	2006	9	62,059,460	154,417	2.5	0.033
	2007	9	63,452,348	180,695	2.3	0.035
Industry 4 (Manufacturing of chemicals and rubber)	2005	16	4,414,245	655,860	0.48	0.038
	2006	16	4,815,720	691,528	0.44	0.028
	2007	16	4,975,775	811,537	0.34	0.029
Industry 5 (manufacturing of electronics and electrical devices)	**2005**	**14**	**3,158,328**	**365,228**	**0.12**	**0.015**
	2006	**14**	**3,362,148**	**408,574**	**0.10**	**0.014**
	2007	**14**	**3,509,351**	**479,464**	**0.09**	**0.014**
Industry 6 (manufacturing of machinery and equipment)	2005	25	4,280,374	432,849	0.13	0.016
	2006	25	4,555,109	519,027	0.11	0.017
	2007	25	4,717,132	584,338	0.096	0.017
Industry 7 (manufacturing of basic metals and fabricated metal products)	2005	16	5,148,617	1,704,450	0.31	0.039
	2006	16	4,984,370	2,225,614	0.27	0.039
	2007	16	5,640,602	2,439,610	0.24	0.036
Sample (all companies)	**2005**	**100**	**8,508,568**	**651,039**	**0.50**	**0.028**
	2006	**100**	**9,738,433**	**781,547**	**0.42**	**0.027**
	2007	**100**	**10,038,850**	**876,589**	**0.37**	**0.026**

Source: Own calculations based on the survey questionnaires and the AJPES database

results show that, on average, 1 percent growth in sales recorded by the sample companies led to 0.88 percent growth in electricity consumption in the period from 2005 to 2007. A comparison by years indicates that the elasticity of consumption relative to total sales declined throughout the whole period, indicating that the manufacturing process is becoming more efficient in terms of electricity consumption[9]. When looking at prices we see that the demand for electricity is almost constantly elastic - an increase in energy prices by 1 percent leads to a reduction of consumption on average by 0.93 percent with unchanged sales. A comparison over the years suggests that companies are becoming increasingly sensitive to the price of electricity, which is leading to increasing the absolute value of the coefficient of the price elasticity of demand.

A comparison of energy efficiency by industry, reported in Table 3, shows that the highest electricity consumption per unit of revenue generated was used in industry 4 (chemical and rubber) and 7 (production of metals and fabricated metal products), where the increase in revenue for each percent increases the energy consumption by more than 1 percent. This is followed by the industries of the production of food, beverages and tobacco (industry 1), manufacturing of wood and wood products (industry 3), production of electronics and electrical devices (industry 5) and production of machinery and equipment (industry 6). It is interesting that in the case of the production of textiles and textile products (industry 2) there is no distinct connection between the product and energy consumption, even though it has an extremely high coefficient of the price elasticity of demand for electricity.

A comparison of industries by the size of the coefficient of the price elasticity of demand shows that industry 2 (production of textiles and textile products) is the most sensitive to electricity price changes, whereas the least sensitive to price changes is industry 4 (chemical products), which on average consumes 10 times more electricity than the rest of the industries. Obviously, this industry is primarily related to the use of technology which does not allow for significant savings if the price of electricity rises. A price-elastic demand for energy during the observed period is also seen in industry 5 (production of electronics and electrical devices) and 7 (production of metals and fabricated metal products). In the other industries the demand is constantly elastic.

9 This conclusion is derived from the assumption that the prices of finished products in the analysed companies remained unchanged in real terms. Given that the sample companies operate mainly in foreign markets as niche suppliers, it can be concluded that during the observed period there were no major changes regarding prices.

Table 2: Estimates of regression coefficients of model 4 for the period from 2005 to 2007

Model (4)	Year			
	2005 OLS method	2006 OLS method	2007 OLS method	2005-2007 XT on groups' averages
y_{it}	0.893*** (0.075)	0.889*** (0.075)	0.866*** (0.070)	0.885*** (0.072)
$(p^i\text{-}p)_{it}$	-0.931*** (0.042)	-0.911*** (0.041)	-0.941*** (0.041)	-0.935*** (0.040)
Constant	-2.099* (1.241)	-2.056 (1.252)	-1.722 (1.77)	-2.005* (1.196)
Adjusted R^2	0.854	0.860	0.870	0.864
Number of observations	100	100	100	100

Note: the standard error is shown in brackets

*** Coefficient is significant with a level of risk of less than 1 percent

** Coefficient is significant with a level of risk of less than 5 percent and more than 1 percent

* Coefficient is significant with a level of risk of less than 10 and more than 5 percent

Source: Own calculations based on the survey questionnaires and AJPES database

A comparison of effective electric power consumption by industry and by years shows that efficiency in the observed period only grew in industry 6 (production of machinery, appliances and vehicles)[10]. In the other industries there are no significant changes. It should be noted that these results could be significantly affected by the lower number of observations in certain years and certain industries.

6. Conclusions

Strict environmental regulations could stimulate innovations and advancement of sustainable technologies by which companies by itself find out that the final effect is often a process which does not only pollute less but also lowers costs and raises quality /14/. The survey presents the energy efficiency in Slovenian firms. We can conclude that, on average, Slovene firms became more energy efficient in the period under study in terms of decreasing ratio of energy consumed per unit of output and energy costs. Therefore we can conclude that firms most likely invested in advanced technology that enabled energy efficient production. Some industries, also electronics industry, performed significantly better comparing to others. However, the changes are not big, especially when compared to the extent to which Slovenian industrial companies are lagging behind their counterparts in more developed countries. There are still significant reserves. An important task for businesses is that they must invest in the introduction of energy-efficient practices and related technologies, yet it is also a significant task of the government. The government should therefore create appropriate incentives, promote the benefits of these technologies to businesses and provide support. Based on the paper we can highlight some possibilities of regulations for purposes of stimulating progress and innovation in technologies aligned with the sustainable development paradigm /13/.

The International Energy Agency stressed the need to encourage investment to boost the efficiency of energy consumption. The current subsidy scheme should be revised, while precise standards for measuring energy efficiency should be determined and benefits at the company level

Table 3: Estimates of regression coefficients of model 4 after sectors for the period from 2005 to 2007

Model (4)OLS method	Industry						
	Industry 1 (manufacturing of food, beverages and tobacco)	Industry 2 (manufacturing of textiles and textile products)	Industry 3 (manufacturing of wood and wood products)	Industry 4 (manufacturing of chemical products)	**Industry 5 (manufacturing of electronics and electrical devices)**	Industry 6 (manufacturing of machinery and equipment)	Industry 7 (manufacturing of metals and fabricated metal products)
y_{it}	0.837*** (0.068)	0.319 (0.252)	0.763*** (0.225)	1.257*** (0.103)	**0.759*** (0.085)**	0.849*** (0.061)	1.096*** (0.103)
$(p^i\text{-}p)_{it}$	-0.972*** (0.051)	-1.241*** (0.109)	-0.942*** (0.064)	-0.733*** (0.045)	**-1.067*** (0.042)**	-0.933*** (0.035)	-1.018*** (0.164)
Constant	-0.851* (1.101)	-6.790 (4.032)	-0.027 (3.380)	-7.785*** (1.715)	**-0.445 (1.471)**	-1.671 (1.027)	-5.191*** (1.741)
Adjusted R^2	0.953	0.891	0.944	0.889	**0.943**	0.921	0.741
Number of observations	36	24	27	48	**42**	75	48

Note: the standard error is shown in brackets

*** Coefficient is significant with a level of risk of less than 1 percent

** Coefficient is significant with a level of risk of less than 5 percent and more than 1 percent

** Coefficient is significant with a level of risk of less than 10 and more than 5 percent*

Source: Own calculations based on the survey questionnaires and AJPES database

10 These results are not specifically shown in the article in the form of a table and are available from the authors.

resulting from reduced energy consumption should be represented. Since the biggest problems with such investments are adequate resources (also due to the uncertainty and long periods of reimbursement), creating the appropriate funding schemes should be considered.

Another of the proposed measures is the creation of minimum energy-efficient standards for machines, which are the most important consumers of energy. Some 10 percent of all energy could be saved by ensuring the greater efficiency of power consumption involved in such mechanisation.

Tapping the energy-saving potential of electricity is an opportunity custom-made for today, as the issues of a sustainable energy future and a clean and safe environment become more urgent. In addition to addressing these needs, electro technologies offer a host of non- energy benefits, including improved manufacturing precision and control, enhanced product quality, increased worker productivity, and reduced environmental impacts. While efficient electro technologies are used throughout industry today, the potential for broader application remains, as does the potential for greater energy-efficient processes.

References

/1/ C. Alonso-Borrego, "Demand for labor inputs and adjustment costs: Evidence from Spanish manufacturing firms", Labor Economics, Vol. 5, pp. 475-497, 1998.

/2/ F. J. André, S. Smulders, "Energy use, endogenous technical change and economic growth", (unpub-lished mimeo, version as of 13 Jan 2006), 2006.

/3/ S. Bond, J. Van Reenen, "Microeconometric Models of Investment and Employment", Mimeo. The Institute for Fiscal Studies, London, 2002.

/4/ S. Bond, C. Meghir, "Dynamic Investment Models and the Firm's Financial Policy", Review of Economic Studies, Vol. 61, No. 2, pp. 197-222, 1994.

/5/ G. Bresson, F. Kramarz, P. Sevestre, "Heterogeneous labor and the dynamics of aggregate labor demand: some estimations using panel data". Empirical Economics , Vol. 17, pp. 153-168, 1992.

/6/ C. J. Cleveland, "Biophysical constraints to economic growth". In. D. Al Gobaisi (Ed.), Encyclopedia of Life Support Systems, EOLSS Publishers, Oxford, UK, 2003.

/7/ B. Čater, T. Čater, J. Prašnikar, "Okoljske strategije ter njihovi motivi in rezultati v slovenski poslovni praksi", In Prašnikar, J. in Cirman, A., eds. Globalna finančna kriza in eko strategije podjetij: dopolnjevanje ali nasprotovanje? Ljubljana: Časnik Finance, pp. 221-234, 2008.

/8/ P. Domadenik, J. Prašnikar, J. Svejnar, "Restructuring of firms in transition: ownership, institutions and openness to trade", Journal of International Business Studies, Vol. 39, pp. 725-746, 2008.

/9/ A. Froggatt, G. Canzi, "Ending wasteful energy use in Central and Eastern Europe", WWF European Policy Office, Belgium, 2004. /URL: http://assets.panda.org/downloads/endingwastefulenergyincentraleasterne urope.pdf/.

/10/ Intergovernmental Panel on Climate Change. (2007), "Synthesis Report. Summary for Policymakers", /URL: http://www.ipcc.ch/pdf/assessment-report/ar4/syr/ar4_syr_spm.pdf/.

/11/ International Energy Agency, "Efficiency: Policy recommendations", 2008. /URL: http://www.iea.org/G8/2008/G8_EE_recommendations.pdf/.

/12/ E. Jochem, "Energy end-use efficiency", In World energy assessment: Energy and the challenge of sustainability New York: United Nations Development Programme, 2000. /URL: http://www.undp.org/energy/activities/wea/drafts-frame.html/.

/13/ M. Marc, U. Cvelbar, L. Knežević Cvelbar, "Innovations in Slovenian Electronic Industry", Inf. Midem, vol.38, no.4, pp. 289-296, 2008.

/14/ M. Porter, "The Competitive Advantage of Nations", Harvard Business Review, March-April, pp. 73-100, 1990.

/15/ N. M. Razinger, "Učinkovita raba energije v Sloveniji", SURS, 2006. /URL: http://www.stat.si/novice_poglej.asp?ID=914/.

/16/ S. Smulders, M. de Nooij, "The impact of energy conservation on technology and economic growth", Resource and Energy Economics, Vol. 25, No.1 , pp. 59-79, 2003.

/17/ R. Solow, "A contribution to the theory of economic growth", Quarterly Journal of Economics, Vol. 70, No. 1, pp. 65-94, 1956.

/18/ N. Stern, "The Economics of climate change: The Stern Review." London, HM Treasury, 2007.

/19/ SURS, "Letna energetska statistika, Slovenija, 2007", SURS, 2008. /URL: http://www.stat.si/novica_prikazi.aspx?ID=1888/

/20/ T. M. Whited, "Debt, Liquidity Constraints and Corporate Investments: Evidence from Panel Data", The Journal of Finance, Vol. 53, No. 4, 1425-1460, 1992.

Polona Domadenik and Matjaž Koman*
Faculty of Economics, University of Ljubljana,
Kardeljeva ploscad 17, 1000 Ljubljana, Slovenia
Email: polona.domadenik@ef.uni-lj.si

Prispelo (Arrived): 17.09.2008 *Sprejeto (Accepted): 15.12.2008*

44. Mednarodna konferenca o mikroelektroniki, elektronskih sestavnih delih in materialih - MIDEM 2008
ZAKLJUČNO POROČILO
44nd International Conference on Microelectronics, Devices and Materials - MIDEM 2008
CONFERENCE REPORT

17.09. 2008 - 19.09. 2008, Hotel BARBARA , Fiesa, Slovenija

Štiriinštirideseta mednarodna konferenca o mikroelektroniki, elektronskih sestavnih delih in materialih - MIDEM 2008 (44th International Conference on Microelectronics, Devices and Materials) nadaljuje uspešno tradicijo mednarodnih konferenc MIDEM, ki jih vsako leto prireja MIDEM-Strokovno društvo za mikroelektroniko, elektronske sestavne dele in materiale.

Na konferenci je bilo predstavljeno 42 rednih in 8 vabljenih predavanj v petih sekcijah in delavnici na temo Napredne plazemske tehnologije.

Na konferenci so bili predstavljeni najnovejši dosežki na naslednjih področjih:

- Fizika elektronskih elementov, modeliranje in tehnologija
- Debeli in tanki filmi
- Elektronika
- Testiranje v elektroniki
- Senzorji
- Integrirana vezja

To leto je bila v okviru konference že enajstič zapored organizirana enodnevna delavnica, tokrat na temo Napredne plazemske tehnologije. Predstavljeni so bili najnovejši dosežki na področju plazemske nanoznanosti, obdelavi biokompatibilnih materialov v plazmi, uporabi plazemske tehnologije v elektronski industriji ter plazemski fuziji.

Pred konferenco je bil izdelan zbornik referatov v obsegu 19 ap (približno 310 strani), ki je podobno urejen kot prejšnja leta.

Nekaj statističnih podatkov:

Število udeležencev: 59, iz tujine 14

Število referatov v zborniku: 62, iz tujine 16

Dr.Iztok Šorli

CD ROM - dvajset letnikov revije Informacije MIDEM

Revija Informacije MIDEM je krepko vstopila v svoje tretje desetletje.
Ob tem jubileju smo pripravili posebno izdajo zadnjih dvajsetih letnikov v elektronski obliki.

Izkoristite svojevrstno priložnost, da izpopolnite svojo strokovno knjižnico.

Naročite svoj osebni izvod.

Za člane društva MIDEM je cena CD ROMa 50,00EUR, za ostale pa 60,00EUR.

Naročila sprejema uredništvo revije.

Pišite na: iztok.sorli@guest.arnes.si

UDK621.3:(53+54+621+66), ISSN0352-9045 Informacije MIDEM 38(2008)1, Ljubljana

UDK621.3:(53+54+621+66), ISSN0352-9045 Informacije MIDEM 38(2008)2, Ljubljana

VSEBINA CONTENT

UDK621.3:(53+54+621+66), ISSN0352-9045 Informacije MIDEM 38(2008)3, Ljubljana

VSEBINA CONTENT

UDK621.3:(53+54+621+66), ISSN0352-9045 Informacije MIDEM 38(2008)4, Ljubljana

VSEBINA CONTENT